Assessing the biodiversity crisis within the Triassic - Jurassic boundary interval using redox sensitive trace metals and stable carbon isotope geochemistry

Halla Margrét Viðarsdóttir

Dissertations in Geology at Lund University,
Master's thesis, no 605
(45 hp/ECTS credits)

Department of Geology
Lund University
2020

Assessing the biodiversity crisis within the Triassic - Jurassic boundary interval using redox sensitive trace metals and stable carbon isotope geochemistry

Master's thesis

Halla Margrét Viðarsdóttir

Department of Geology
Lund University

2020

Contents

Cover Picture: Core boxes belonging to Stenlille, well nr. 4 coming from storage at GEUS in Copenhagen

Contents, continuation

Assessing the biodiversity crisis within the Triassic-Jurassic boundary interval using redox sensitive trace metals and stable carbon isotope geochemistry

HALLA M. VIÐARSDÓTTIR

Viðarsdóttir, H.M., 2020: Assessing the biodiversity crisis within the Triassic-Jurassic boundary interval using redox sensitive trace metals and stable carbon isotope geochemistry. *Dissertation in Geology at Lund University*, No. 605, 80 pp. 45 hp (45 ECTS credits).

Abstract: Around the Triassic-Jurassic-Boundary time interval, a severe mass extinction event occurred, which has been associated to volcanism of the Central Atlantic Magmatic Province (CAMP). Significant amounts of greenhouse gases as carbon dioxide (CO_2) or methane (CH_4) and other volatiles are suggested to have been released into the atmosphere, leading to global warming with subsequent impact on the biosphere. The marine realm was affected to a greater extent than observed from the terrestrial record and there, the biotic recovery was slow and prolonged. The causes of this severe extinction and protracted recovery in the oceans are still not well understood. One recurring hypotheses is the presence of extended anoxic conditions in neritic shallow seas.

The aim of this study was to address redox conditions of the European epicontinental sea during this time interval. Two cores from the Triassic-Jurassic boundary sedimentary successions were sampled with the target to gain further knowledge on the oxygen conditions that prevailed during time of deposition. One core comes from Stenlille, well nr. 4 from the Danish Basin (Denmark) and the other one, from Schandelah. Schandelah is located within the north German Lower Saxony Basin. Successions from both localities constitute shallow marine to coastal sandstones, mudstones and shales. Variations in oxygen grades of these successions was addressed with elemental analysis, evaluating enrichments of V, Mo, U, Zn, Cr, Co, Cu, Mn and their covariation with Al and TOC. The results indicate that anoxic conditions where generally not met in the seas at those localities during this time interval. Hg and Ni were used as markers of volcanic activities. In Stenlille, one level of anomalous concentrations of Hg and Ni is present, and in Schandelah two anomalous levels are present. At both localities, abnormal accumulation of both Hg and Ni coincide with a negative δ^{13}Corg excursion associated to CAMP, which may indicate that the enrichment of these elements was due to volcanic activity. $\delta^{13}C_{org}$ values are presented here for Stenlille 4, and serve as a tool for stratigraphic correlation between TJB successions.

Keywords: Stenlille, Schandelah, redox conditions, C-isotopes, marine sediments, trace elements, enrichment factors, mass extinction, Triassic – Jurassic boundary

Supervisor(s): Sylvain Richoz (LU), Sofie Lindström (GEUS)

Subject: Bedrock Geology

Halla Margrét Viðarsdóttir, Department of Geology, Lund University, Sölvegatan 12, SE-223 62 Lund, Sweden. E-mail: hallamagga@gmail.com

Utvärdering av den biologiska krisen runt det triassiska-jurassiska tidsintervallet genom analyser av redoxkänsliga spårmetaller och stabila kolisotoper

HALLA M. VIÐARSDÓTTIR

Viðarsdóttir, H.M., 2020: Utvärdering av den biologiska krisen runt det triassiska-jurassiska tidsintervallet genom analyser av redoxkänsliga spårmetaller och stabila kolisotoper. *Examensarbeten i geologi vid Lunds Universitet, in Geology at Lund University,* Nr. 605, 80 sid. 45 hp (45 ECTS credits).

Sammanfattning: I övergången mellan de triassiska och jurassiska perioderna, för ca 200 miljoner år sedan, inträffade ett massutdöende som bedöms ha koppling till vulkanism i den Centralatlantiska magmatiska provinsen (CAMP). En signifikant ökning av växthusgaser som koldioxid (CO_2) eller metan (CH_4) och andra flyktiga ämnen, med efterföljande global uppvärmning som följd, föreslås vara den viktigaste drivkrafterna för påverkan på biosfären under detta tidsintervall. Den grundmarina miljön påverkades speciellt mycket och där var den biotiska återhämtningen långsam och långvarig. De direkta orsakerna till massutdöendet och den utdragna återhämtningen i haven är fortfarande inte väl förstådda. En hypotes är att syrefattiga eller syrefria miljöer uppstod i grundhaven.

Syftet med denna studie är att undersöka detta ämne genom analys av samtida, idag fossila, sediment dokumentera redoxförhållandena i det europeiska grundhavet. Två borrkärnor med sedimentära bergarter från övergången mellan trias och jura undersöktes med målet för att få ytterligare kunskap om syreförhållandena som rådde under tiden för deposition. En kärna kommer från Stenlille, brunn nr. 4, från Danska bassängen (Danmark) och den andra från Schandelah i den nordtyska Niedersachsenbassängen. Bergarterna i Stenlille- och Schandelahkärnorna är sandsten, siltsten, skiffer och lersten som avlagrats i kust- eller grundmarina miljöer. För att utvärdera under vilka syreförhållanden som rådde i havet när sedimenten avsattes, analyserades koncentrationerna av V, Mo, U, Zn, Cr, Co, Cu och Mn samt deras förhållande till Al och halten organiskt kol (TOC). Resultaten indikerar att syrefria (anoxiska) förhållanden i allmänhet inte existerade och att miljön normalt var syresatt till svagt syresatt. Hg och Ni användes som markörer för vulkanisk aktivitet. Analys av dessa element påvisar en (1) nivå av avvikande ackumulering i Stenlillekärnan, och två i Schandelahkärnan. De höjda nivåerna av både Hg och Ni inträffar samtidigt som det sker negativa avvikelser i relationen mellan ^{12}C och ^{13}C ($\delta^{13}Corg$, dvs. i kolcykeln) i såväl Stenlillekärnan som Schandelahkärnan och korrelarar därför dessa händelser till utvecklingen i CAMP. Värden för $\delta^{13}Corg$ presenteras här för Stenlille 4, och dessa fungerar som verktyg för stratigrafisk korrelation till andra områden och sedimentära successioner där den triassiska-jurassiska gränsen är känd.

Nyckelord: Stenlille, Schandelah, redox, spårmetaller, organiskt kol, massutdöende, Centralatlantiska magmatiska provinsen, triassiska-jurassiska gränsen, stratigrafisk korrelation

Handledare: Sylvain Richoz (LU), Sofie Lindström (GEUS)

Ämnesinriktning: Berggrundsgeologi

Halla Margrét Viðarsdóttir, Department of Geology, Lund University, Sölvegatan 12, SE-223 62 Lund, Sweden. E-mail: hallamagga@gmail.com

1 Introduction

A significant biodiversity crisis is associated to the Triassic–Jurassic boundary, with great impact on Earths biosphere (Raup & Sepkoski 1982; Stanley 2007). The impact of the crisis is mostly observed within the Rhaetian Triassic stage, often termed as the end-Triassic crisis. This crisis led to mass extinctions both amongst terrestrial and marine organisms (McElwain et al. 1999, 2007; Olsen et al. 2002; Whiteside et al. 2007). To a greater extent was the impact on the marine realm (Hallam & Wignall 1999; Hautmann 2004; van de Schootbrugge et al. 2007). Primary producers such as dinoflagellates and coccolithophorids, which had during the Late Triassic time the opportunity to radiate rapidly experienced high extinction rates (Falkowski 2004). Species that were hit especially hard were benthic organisms such as bivalves, scleractinian corals and calcareous algae. In addition, nektonic predators, among them ammonites, suffered from high diversity losses as well (Kiessling et al. 2007). It has been suggested that this biotic crisis is attributed to climate change associated with extensive volcanic episodes and consequent degassing of great volumes of SO_2 and CO_2 from the Central Atlantic Magmatic Province (CAMP). The CAMP resulted from the separation of the African and European tectonic plates, away from the North American plate with subsequent tectonisms and sea-level oscillations (Lindström et al. 2019). CAMP is one of the world‘s most expansive large igneous province (LIP) recognized on Earth.

Atmospheric emissions of volatile gases from CAMP have been estimated to a range from $1{,}11 \times 10^{12}$ and $5{,}19 \times 10^{12}$ metric tons (McHone 2003). The areal distribution of extrusive volcanics of CAMP is estimated to be about 10^7 km^2 and distributed within four continents (McHone 2003; Davies et al. 2017). The oldest age that has been reported from the CAMP is of 201,635 ± 0,029 Myr from intrusives in Guinea and preceeds extrusive basalts of North America by 150 ± 38 kyr (Davies et al. 2017). This suggests that magmatic activity was already ongoing before the extrusive volcanic episodes, supporting a possible early impact on changes in climatic and biotic records (Davies et al. 2017). Untill recently all stratigraphic sections which preserved lava flows, post-dated the end-Triassic extinction event (ETE), questioning the correlations between the CAMP and the ETE (Heimdal et al. 2018). Radioisotope ages of the CAMP volcanic rocks show that it was initiated approximately 100,000 years before the ETE (Davies et al. 2017) and continued for c. 700,000 years in pulses (Blackburn et al. 2013).

How exactly the mass extinction operated following CAMP, has been debated and proposed hypotheses include impact from the sea-level changes (Hallam 1981), anoxic conditions in the marine realm (Hallam 1981; Hallam & Wignall 2000), release of methane into the atmosphere and ocean acidification (McHone 2003; van de Schootbrugge et al. 2009; Hautmann 2012). Other hypothesis have followed as of an extraterrestrial origin (Olsen et al. 2002), but that theory has been dismissed as it has been shown that around the T-J boundary, modest Ir-anomalies have been described which were recognized of volcanic origin and not extraterrestrial (Tanner et al. 2016; Tegner et al. 2020). These observations dismiss the impact theory (see further review in Tegner et al. 2020). The repeated release of carbon dioxide (CO_2) and possibly methane (CH_4) due to the CAMP activity is suggested as causal effect on enrichment of light carbon isotopes in the atmosphere. It is generally held responsible for major negative shifts in carbon isotope records registered across the T-J boundary interval in marine and terrestrial successions worldwide (Hesselbo et al. 2002; Ruhl et al. 2011). There are still some uncertainties included in the response of the interaction between the lithosphere-ocean-atmosphere to considerable injections of CO_2, HS and other volatiles following such a major volcanic event as the CAMP.

The largest uncertainty during the Triassic-Jurassic boundary interval involves how climate forcing would have impacted the oceans. Schootbrugge et al. (2007) mentioned that as oceans are a major sink for CO_2, its increase must have led to subsequent acidification of the upper oceans, with corresponding calcification crisis. An other expected response to increased amounts of CO_2 is the likely enhanced hydrological cycle leading to increased rates of weathering on global scales. It would also drive to rising temperatures both on land and in the oceans. Globally, an expected response in the oceans would be 1) a decreased ability to retain dissolved oxygen concentrations in solution and 2) enhanced density differences promoting vertical stratification of water masses. This last one would impact the carbon sink with a slow down of the deep ocean ventilation. On continental shelf areas, seas are more susceptical for developing anoxic situations especially in enclosed basins. These basins are prone to stagnant waters masses, low renewal rates and limitations for mixing, which can result in an establishment of a chemocline. Increased freshwater input can also contribute to stratification in the water column. Short term anoxic conditions can also happen in those situation when sudden nutrient supply provokes strong increase in primary production.

The recovery of the marine ecosystem as been delayed in comparison to the recovery of terrestrial ecosystem and ocean anoxia in epicontinental seas has been inferred as the main mechanisms with delaying the biotic recovery in the earliest Jurassic (Lindström et al. 2012; Richoz et al. 2012; Jaraula et al. 2013; Luo et al. 2018). A study with biomarkers linked to green sulphur bacteria in early Jurassic successions, indicate euxinic conditions in the photic zone on the epicontinental shelves (Richoz et al. 2012), the UK and Nevada (Ruhl et al. 2011, Jaraula et al. 2013). Anoxic indicators from lithological observations on paper shales have been made across the European Epicontinental Seaway (EES) (van de Schootbrugge et al. 2009). Other localities within the EES, from northwest Germany have shown evidence for euxinic conditions prior to the end-Triassic extinction in the epicontinental sea (Blumenberg et al. 2016). Localities from South Germany have shown high levels of enrichments of redox sensitive trace elements, above lithogenic background values (Quan et al. 2008), indicating that euxinic conditions developed shortly

after the extinction event. But despite these studies, the timing and expansion of such post-extinction anoxia is still not well understood.

For this study drillcores were studied from the Danish and Lower Saxony basins. The Danish Basin has previously been studied on the basis of high-resolution palynology, organic $\delta^{13}C$-isotope measurements and sedimentological data in different cores (Nielsen 2003; Lindström et al. 2006, 2012, 2017). The basin has good preservation potential and has experienced low levels of diagenesis in terms of preservation of fossil indexes and good temporal resolution based on preceding work, emphasising the terrestrial and marine ecosystem changes occurring during the Triassic-Jurassic interval. Therefore, these cores could serve as good candidates for addressing redox conditions in the basin. Earlier work has demonstrated widespread deforestation, proliferation of opportunistic ferns and other spore-producing plants, negative organic $\delta^{13}C$ isotope excursions, episodes of intense earthquake activity and wildfire frequency (Petersen & Lindström 2012; Lindström et al. 2015; Lindström et al. 2017). In addition, the Schandelah core from the Lower Saxony Basin has a mean to provide good constraints for the Triassic-Jurassic interval with a complete succession of Upper Triassic (Rhaetian) to Lower Jurassic (Hettangian) shallow marine deposits, with good biostratigraphic and lithostratigraphic foundation (van de Schootbrugge et al. 2018)

The aim of the following research was to focus on analysing elemental redox proxies from two cores; the one derived from the Danish Basin comes from Stenlille, well nr 4 and the one from the Lower Saxony Basin comes from Schandelah. An attempt will be made to determine the oxygen conditions that prevailed in the basins, prior, during and after the mass extinction. This could aid in increasing the knowledge of the extent and intensity of bottom water anoxia/ euxinia during this interval, and aid in understanding if it could be a factor promoting the extinction itself or rather delaying the recovery. Alongside looking into the concentrations and distribution of redox sensitive trace elements from those two cores, a $\delta^{13}C$ isotopic signature of the organic fraction of samples of the Stenlille 4 core was also determined to see if it has a good correspondence to the signatures that have already been obtained at other localities and to further constrain stratigraphic correlations between sections. Configuration of Stenlille 4 and Schandelah around the TJB boundary is demonstrated in Fig. 5.

2 Geological setting

2.1 The Danish Basin

The Danish Basin is an intracratonic structure that trends WNW-ESE and was formed during the Late Carboniferous – Early Permian, after crustal extension, thermal cooling and local faulting (Nielsen 2003). The basin is enclosed by the Ringkøbing – Fyn High to the S and by the Fennoscandian Border Zone to the NE (Nielsen 2003). The interior of Pangea that consists of present days central and northern Europe had already before the Rhaetian established a epeiric shallow sea that covered most of northern Europe (Manspeizer 1994; Veevers 1994; Lindström & Erlström 2006). The Upper Triassic-Jurassic succession is close to 1 km thick and includes Skagerrak, Vinding, Gassum, Fjerritslev, Haldager Sand, Flyvbjerg, Børglum and Fredrikshavn formations (Nielsen 2003). During this interval great changes are recorded in terms of tectonics, areal extent and sea level (Nielsen 2003). A shallow, low-gradient marine embayment without a shelf-slope was established in late-Triassic times. Due to the gentle physiography of the basin, fourth-order sea level changes exerted a strong controlling factor on the distribution and architecture of the depositional facies (Nielsen 2003). Progradation of coasts occurred during sea-level fall, with regressive shoreface sandstones deposited wastly, resting on regressive surfaces of marine erosion. Subsequently sea-level rose resulting in widespread floodings and formations of ravinement surfaces overlain by marine mudstones (Nielsen 2003). The stacking patterns emphasize variations of progradation and retrogradation of estuarine and shoreface deposits, typical of shallow basins, and a widespread marine maximum flooding surface (Nielsen 2003). This shallow basin received high continuous sediment influx from the basin margins on three sides and with high sediment distribution longshore (Nielsen 2003). Fluvial transport of sand into the basin was effective and is proposed to be a result of poorly developed vegetation cover (Nielsen 2003).

The Jurassic had a deeper and more fully marine setting compared to the Triassic. A low-gradient shelf was established as a consequence of a steady state subsidence as well as of a overall eustatic/regional sea-level rise (Nielsen 2003). Fine grained sediments accumulated with high concentration rates from the landmasses to the east and north as a result of extensive weathering characterized by humid, warm-temperate to subtropical climate with well-established and widespread vegetation on land (Nielsen 2003). The Triassic was characterized in general with dry and arid climate. At the end of the Triassic, warm and humid greenhouse conditions were established (Preto et al. 2010). In particular an increase in the abundance of fern spores occurred during and after the extinction level (Lindström 2016). A similar increase in spores over the extinction interval occurred on both hemispheres, indicating a global scale changes in environmental conditions that affected pollen-producing plants (Lindström 2015). Along the coast of the Danish basin, the end-Triassic greenhouse conditions can be recognized with peat (coal) Rhaetian deposits (Lindström 2016). Kaolinite rich mudstones at the Triassic-Jurassic boundary (Ahlberg et al. 2003) and occurrences of tropical climate soils in lowermost Jurassic strata (Arndorff 1993).

2.2 Stenlille

The Stenlille cores were drilled in 1980, on the Danish island Sjælland (Zealand) (Fig. 1). It was a possible potential site for hydrocarbon gas storage for the populated Copenhagen area, located approximately 60 km to the NE of Stenlille (Laier & Øbro 2009). For that reason, multiple cores were drilled around the Stenlille area. Most published studies have been done on Sten-

lille 1 core (Lindström et al. 2012; Lindström et al. 2015; Lindström et al. 2017; Lindström et al. 2019) whereas the dataset in this study was obtained from the Stenlille 4 core. The Stenlille cores penetrates the Gassum and Fjerritslev formations (Nielsen 2003; Lindström et al. 2017) and these formations span the TJB. The distance between the Stenlille 1 and 4 wells is about 3 km. The Stenlille 1 and 4 cores show some typical lithological variations. The grain size varies more within the Stenlille 4, with more frequent sandyer intervals, compared to Stenlille 1. This indicates that the former is accumulating in shallower environment than Stenlille 1. Most notable differences, when comparing between the cores, is that Stenlille 4 shows to have more soft sediment deformation observed within the gray siltstone interval (Fig. 3). In regards to sedimentology and biostratigraphy, the Stenlille 4 core shows to be more compacted in comparison to the Stenlille 1, that indicates some variations concerning sedimentation rates between the Stenlille 1 and 4 wells (Lindström et al. 2019).

In Stenlille 1, the Triassic Gassum Formation comprises interbedded, fine to medium grained, occasionally coarse-grained pebbly sandstones, mudstones, heteroliths and few thinly coastal shallow-marine coaly beds (Bertelsen 1978; Bertelsen & Nielsen 1991). It has been interpreted as formed in a shallow marine to coastal environment (Bertelsen 1978; Michelsen & Nielsen 1991). Within the upper parts of the Gassum Formation, dark grey shale unit follows that was deposited during the late Rhaetian transgression (Fig. 3). Within this unit a maximum flooding surface (MFS7) is observed (Nielsen 2003). On top of the dark gray shales, greenish gray siltstones and fine-grained sandstones succeed (denoted as the gray siltstone interval (Lindström et al. 2012) in Fig. 3). Then, succeeding this unit, is the Jurassic Fjerritslev Formation that comprises of marine claystones, mudstones and fine-grained sand intervals, deposited following another transgressive event (Lindström et al 2017).

From Stenlille, the main fossils analysed and recovered from the cores are spores and pollen. Based on palynological assemblages, Lindström et al. (2017) subdivided the Stenlille 1 (and 2) into six zones (Fig 3.): the *Granuloperculatipollis-Classopollis-Perinopollenites* zone (GCP) that consists of succession that belongs to the Gassum Formation upwards to the gray silstone interval. The GCP zone is dominated by the presence of conifer pollens. During the early Mesozoic era, conifers were amongst the dominating land plants. The palynozone *Polypodiisporites Ricciisporites- Deltoidospora* zone (PRD) has been assigned within the gray siltstone interval (recognized as well as the stratigraphic marker of the *Polypodissporites polymicroforatus*

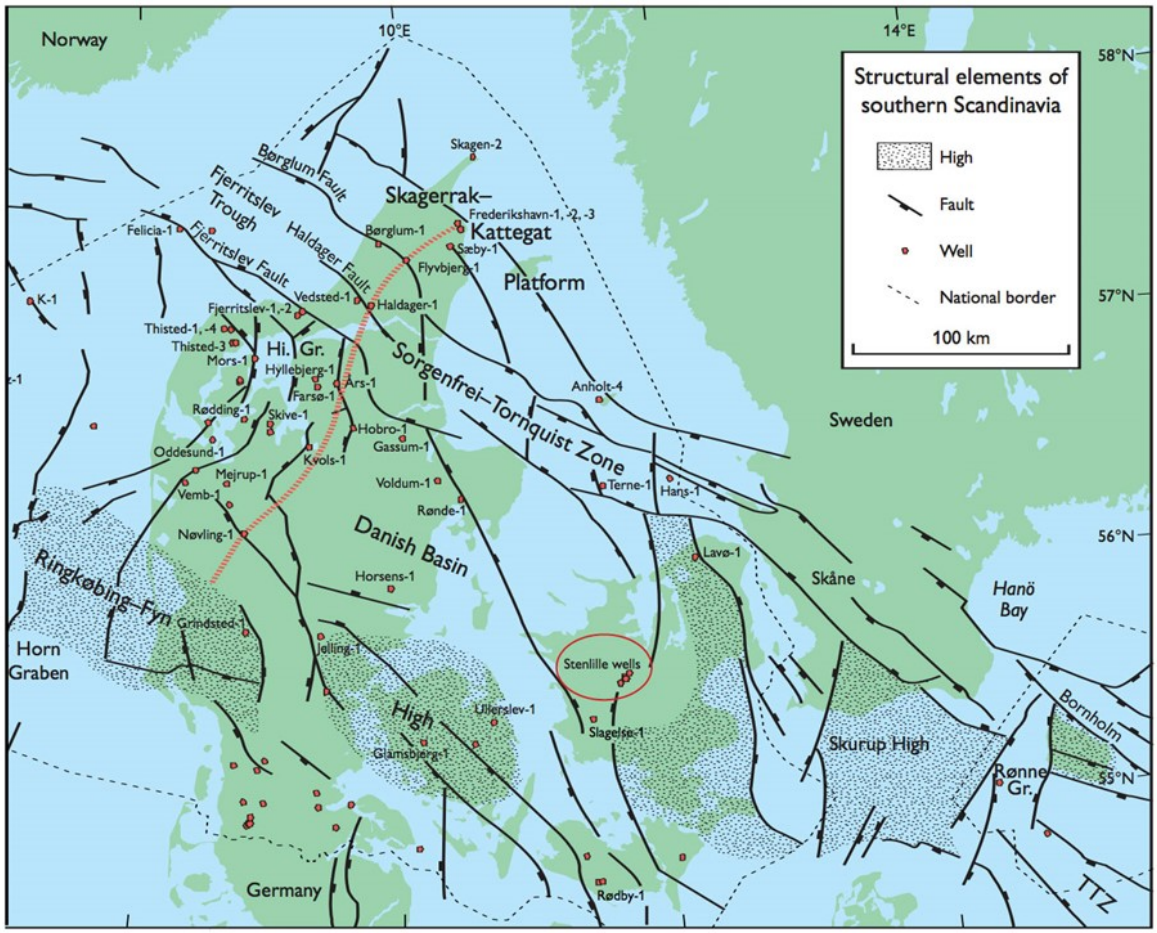

Fig. 1. Map showing locations of the Stenlille wells and main structural features of the Danish Basin from Nielsen, 2003 (after modifications from Michelsen & Nielsen (1991) and Vejbæk (1997).

palynoflora). In this zone, the abundance of conifer pollen decreases substantially and becomes near absent towards the upper parts. The PRD zone is dominated by fern spore species. Ferns most commonly inhabit warm damp areas. The zone has been described over large areas in terrestrial and marine successions (Lindström et al. 2017; 2019). Following is the *Conbaculatisporites-Calamospora-Monosulcites* zone (CCM), that converges with a negative carbon isotope excursion, called the Speale CIE. In the uppermost part of the gray siltstone interval, the biostratigraphical marker *Cerebropollenites thiergartii* is first noted. Above the CCM palynozone, *Perinopollenites-Deltoidospora-Stereisporites* zone (PDS) is followed by the *Deltoidospora-Perinopollenites-Pinuspollenites* zone (DPPi*)* and lastly, the *Perinopollenites-Pinuspollenites* zone (PPi). Within the CCM and PDS zones a palynofloral recovery is recognized. Through the lowermost parts of the PDS zone, the dinoflagellate cyst *R. Rhaetica* disappears, and a severe reduction in numbers occurs within the black shales around the MFS7. Interestingly the palynofossils of the PRD zone, are near restrictive around the gray siltstone interval (Fig. 3) and become near absent in the succeeding zone. At this greenish-gray siltstone interval, fossils become near devoid and soft-sediment deformation structures are observed, typical of seismites (Lindström et al. 2017). The First Common Occurrence (FCO) of *Pinuspollenites minimus* marks a lower boundary of a post-extinction phase zone of *Perinopollenites-Pinuspollenites* (PPi) (Lindström et al. 2017). According to palynomorpic distribution (Fig. 11) Lindström et al. (in prep) classified the palynomorphs by abundance of terrestrial versus marine species for Stenlille 4 (Fig. 11). Throughout the Gassum Formation until the lowest part of the the *PRD* zone, the palynomorps show to be more equally distributed amongst terrestrial versus marine palynomorphs, with some exeptions, especially around depth of 1515 m. Then a significant drop in appearances of marine dinoflagellate cysts is apparent. Towards the top of the PRD Zone a slight increase in abundances of freshwater microalgae is observed, especially around 1502 m, and indicates more freshwater input into the basin. Around 1504 m depth, the marine dinoflagellate cysts are again more abundant. The marine acritarchs have an apparent relatively low abundance interval from c. 1493 – 1498 m depth.

The Jurassic GSSP (Global Stratotype Section and Point) has been established at Kuhjoch, a locality in the Karwendel Mountains in the Northern Calcareous Alps, Austria (Hillebrandt et al 2013). It is based on the first occurrence of the Jurassic ammonoid *Psiloceras spelae tirolicum* (Hillebrandt and Krystyn 2009). However, not all sections, terrestrial or marine could be correlated by ammonoids (Lindström et al. 2017). In consequence, an accessory marker was made for the base of the Jurassic, the pollen taxon *Cerebropollenites thiergartii*, with its First Occurrence (FO) about 3 m below the FO of *P.spelae* in the Kuhjoch section (Hillebrandt et al. 2013). Further stratigraphic temporal framework has been made using C-isotope excursions. Around the Triassic-Jurassic boundary, three negative C_{org} excursions (CIEs) have been described from Stenlille 1 by Lindström et al (2012), named the Marshi, the Spelae and top-Tilmanni CIEs. The Marshi CIE fits close to the Last Occurrence (LO) of a typical Triassic ammonoid *Choristoceras marshi* or closely related *Choristoceras crickmayi* and represents the onset of the end-Triassic mass extinction in marine successions (Lindström et al. 2017). The Marshi CIE is succeeded by the latest Rhaetian transgression with a maximum flooding event (MFS7). Then succeeded by the prementioned *Polypodissporites polymicroforatus* abundance interval (PRD zone) associated with a regressive event with shallow marine environment and more positive $d^{13}C_{org}$ values (Lindström et al. 2017). This time interval is also encompassed by periods of maximum extinction of the marine biota, along with major terrestrial ecosystem changes and deforestation (Lindström et al. 2019). The Spelae CIE, is located before the first occurrence of the marker taxon for the base of the Jurassic, the ammonite *Psiloceras spalae tirolicum,* and is associated with event of transgression and a depauperate benthic marine faunas, while on land, evidence exist of the recovery of plant communities dominated by spore producing plants (Lindström et al. 2019).

2.3 The Western Lower Saxony Basin, Germany

The Lower Saxony Basin (LSB) belongs to one of several sedimentary basins within the Central European Basin System that formed as a result of the Variscan orogeny in the late Carboniferous to early Permian. The LSB formed during a tectonically active period of extension and moderate subsidence during Late-Triassic times with downwards displacement of the northern part of the basin (Adriasola-Muñoz et al. 2007). There is a large difference within the basin in the thickness of the lower Triassic sediments that results of contemporaneous syn-sedimentary faulting and salt diapirism (van de Schootbrugge et al. 2018). The basin is 300 km long and 65 km wide, strikes in E -W direction and parallels to the northern margin of the Rhenish Massif (Betz et al. 1987). The basin became inverted during the late Cretaceous and earliest Tertiary (Ziegler 1982; 1987).

2.4 Schandelah

A 338 m core was obtained from the North German Basin, close to the village of Schandelah (Fig. 2). Exact location of the drill site is 52°18'21.85"N and 10° 42'27.43"E, in an elevation of 84 m, in the municipality of Lehre, Landkreis Helmstedt, Lower Saxony (van de Schootbrugge et al. 2018). Extensive work has been done regarding this core in sense of geophysical borehole data, lithological and sedimentological descriptions, biostratigraphy (van de Schootbrugge et al. 2018). The Schandelah core consists of sediments that span the Rhaetian to Toarcian, which involve the transition from the Triassic to Jurassic period (Fig. 3). Concerning lithology, the lowermost part of the core is composed of the Rhaetian, Arnstadt Formation, a deltaic sand- and siltstone succession, with reddish-brown, gray and green claystones. Siderite concretions are present at the base and a relative increase in the

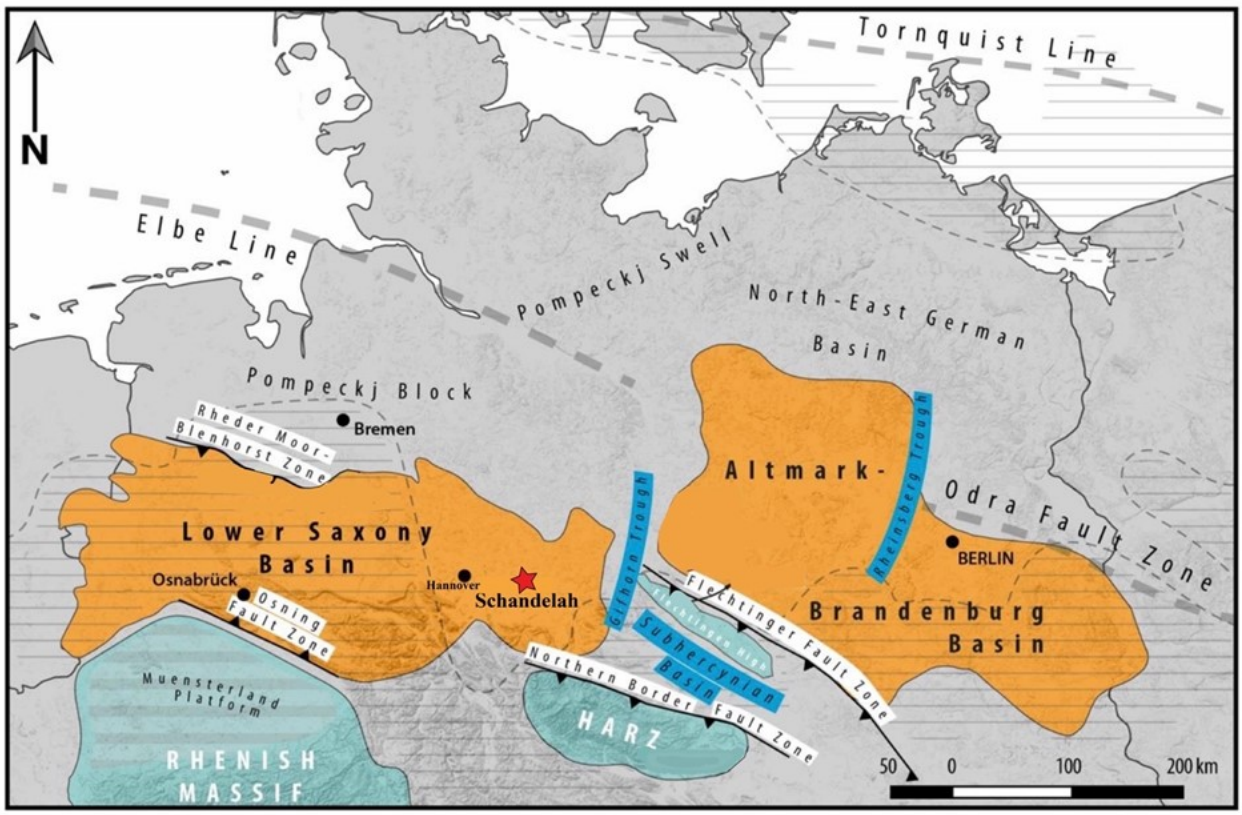

Figure 2. A map presenting the Schandelah locality and the Lower Saxony Basin (LSB) with major structural features of northern Germany. Modified from Nadoll et al. 2008.

amount of sand is observed towards the top (van de Schootbrugge et al. 2018). In terms of sedimentary structures, they show loading structures and flaser bedding. The presence of dinoflagellate cysts suggests that predominantly shallow marine environment prevailed during time of deposition (van de Schootbrugge et al. 2018). The Exter Formation (Rhaetian) overlies this unit, with medium grained, sharped based sandstones that are current rippled with thin mud partings, an abundancy of plant material is observed, amongst charcoals and a possible sequence boundary is located at the base of this unit (van de Schootbrugge et al. 2018). The Exter Formation has been subdivided into two informal members. The Contorta Beds, named after the bivalve *Rhaetavicula contorta* and the so called Triletes Beds, which correspond more or less to the gray siltstone interval in Stenlille. The Contorta beds are located above the Armstadt Formation and, succeed upwards with the Triletes beds towards the base of the Hettangian and the Angulatenton Formation. In general, the Rhaetian is consisting of fine-grained gray to dark grey sand and siltstone with indications of high sedimentary influx, evident in abundant small scale cross stratification with ripples featuring climbing sets (van de Schootbrugge et al. 2018).

In terms of biostratigraphy, both Rhaetian formations do not contain ammonites, foraminifera or ostracods, eliminating the possibility of utilizing biozonations in regards of macrofossils. However, using organic walled microfossils has been successful, especially in regards of correlating within the Triassic-Jurassic boundary (using the dinoflagellate cysts of *Lunnomidinum scaniense*) (van de Schootbrugge et al. 2018). Noteworthy is that within the Danish Basin, this dinoflagellate cyst occurrs only near around the lower-upper Rhaetian boundary (Lindström 2002; 2006). From the base of the core, two dinocyst marker species are also present, *Rhaetogonyaulax rhaetica* and *Dapcodinium priscum*, which culminate at a distinct level (332 m). *D. priscum* ranges into the Jurassic, but the LO of *R. rhaetica* is associated with the Triassic-Jurassic (Rhaetian-Hettangian) boundary (Lindström 2006). The lower Jurassic, Hettangian, Angulatenton Formation (318,6 - 233,3 m) succeeds the Exter Formation with laminated dark-gray mudstone with intervals that contain paper shales. The characterization of the remainder of the Hettangian succession is by most parts composed of silts- and sandstone lenses interspersed by organic-rich mudstones and shales (van de Schootbrugge et al. 2018). The sandstone layers show signs of reworking, bioturbation and crossbedding. Gutter casts are abundant, but generally the fossil content is low throughout the Hettangian, except from few crinoid stems occurring (van de Schootbrugge et al. 2018). Few distinct red-coloured laminated claystone intervals occur between the sandstone-mudstone alternations, showing similar lithology throughout, except for colour appearance (van de Schootbrugge et al. 2018). For biostratigraphic determination, ammonites, despite critically low in abundances, showed some useful species. The first benthic marine microfauna occurs at (302,0 mbs) with the foraminifers *Lenticulina* and the ostracod *Kinkelinella* but their bio-

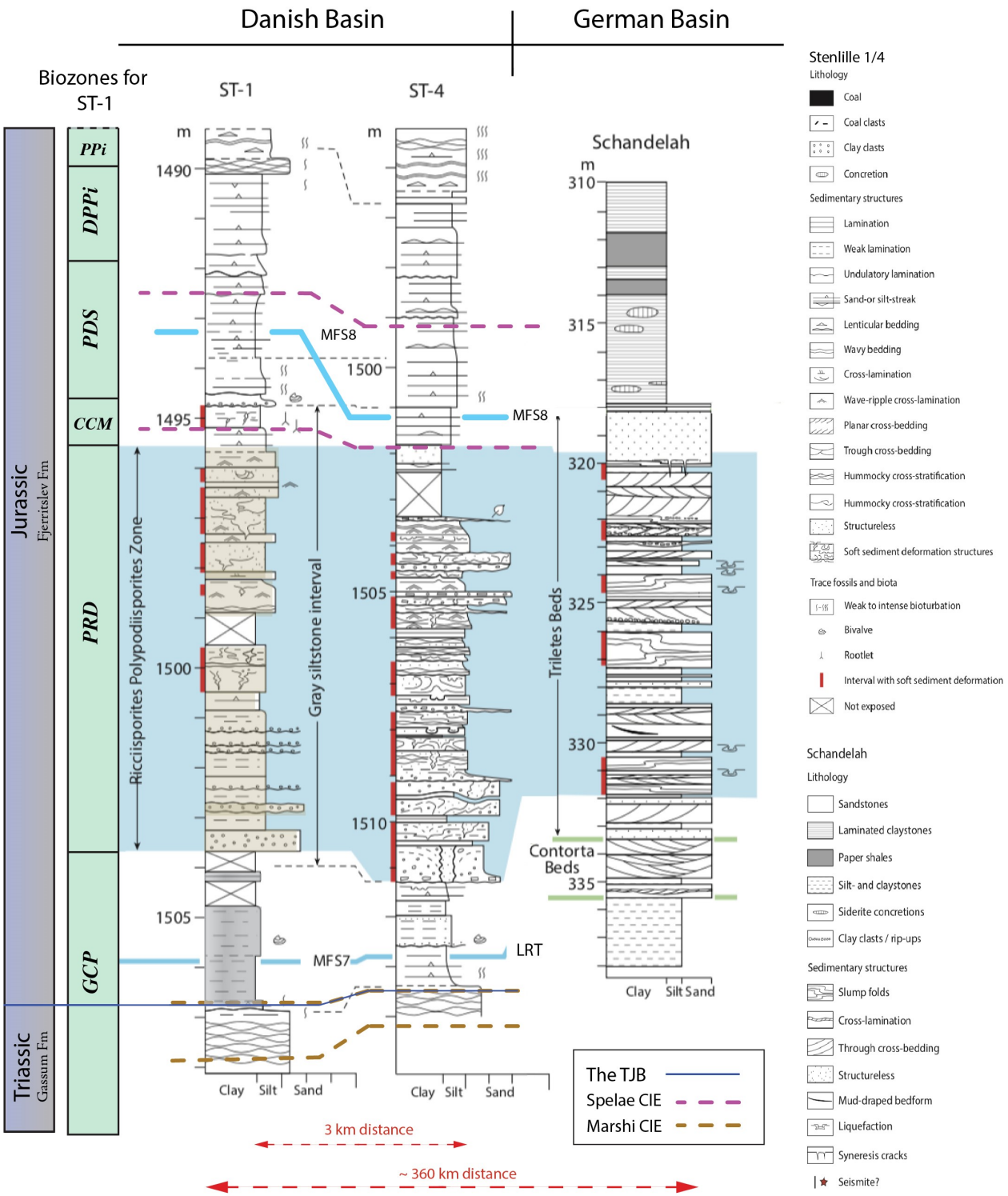

Figure 3. Correlation from the Danish Basin (Stenlille 1-4) to Schandelah and the TJB. Including overview of the palynostratigraphy of Stenlille 1, made by Lindström (2017). GCP = Granuloperculatispollis-Classopollis-Perinopollenites zone, PRD = Polypodissporites-Ricciisporites-Deltoidospora zone, CCM = Conbaculatisporites-Calamospora-Monosulcites zone, PDS =Perinopollenites-Deltoidospora-Stereisporites zone, DPPi = Deltoidospora-Perinopollenites-Pinuspollenites zone, PPi = Perinopollenites-Pinuspollenites zone. MFS = maximum flooding surfaces, LRT = Late Rhaetian Transgression. Note the coloured gray shale unit within the GCP in Stenlille 1 and succeeding greenish-gray siltstones and fine-grained sandstones in the PRD zone. Note aswell the range of the CIE excursions. Modified from Lindström et al. 2015, 2017 and 2019. The boundary between the Gassum and Fjerritslev Formations, are placed according to Nielsen (2003).

stratigraphic position was difficult to define due to the lack of index ostracods and foraminifers from other localities within Europe (van de Schootbrugge et al. 2018). A big change was noticed within palynofacies and palynomorphs assemblages, around 318,2 mbs, where typical Early-Jurassic species as *Pinusspollenites minimus, Kraeuselisporites reissingerii* and *Trachysporites fuscus* become abundant. Based on palynology the boundary can be emplaced at 318,6 mbs at a base of a grey-brown sandstone within the Psilonoten Sandstone (van de Schootbrugge, 2018). Noteworthy is a sharp negative $\delta^{13}C_{org}$ isotopic excursion at this point, which is as well correlatable to another locality, the Mariental core (van de Schootbrugge et al. 2018). This negative peak corresponds as well to the Spelae CIE in Stenlille and allow a good correlation between the two sites (Lindström et al. 2017).

3 Theoretical background

3.1 Minor and trace elements in marine sediments

To reconstruct paleo-conditions based on minor and trace elements in marine sediments, it is fundamental to reflect on the processes that operate in the water-column and in sediments, during the time of deposition and during early diagenesis. Concentrations of trace and minor elements in marine sediments are a result of range of chemical, oceanographic and sedimentary controls that govern how they are supplied to, distributed in, and removed from the oceans and sediments (Calvert & Pedersen 1993). Trace elements are present in abundance in seawater, either in soluble form or adsorbed onto particles (Tribovillard et al. 2006). Including controls are the composition of sedimentary input to the oceans, partitioning of individual elements between solid and solution phases, biogeochemical cycling of the elements in the oceans, their delivery to the sea-floor and lastly the post-depositional conditions that can lead further to diagenesis, with recycling of the elements or their preciptitation (Calvert and Pedersen 1993). Trace elements that end up in the oceans are derived from the ocean crust, mid-ocean ridges, seafloor sediments, hydrothermal vents, rivers, groundwater influxes, glacial meltwater and eolian particles (Martin et al. 1976; Martin and Whitfield 1983; Duce et al. 1991; Metz and Trefry 2000; Kim et al. 2015; Smrzka et al. 2019). A potentially important source of trace elements are hydrothermal fluxes that can be inferred by characteristic tectonic and mineralogic associations (Morford et al. 2005; Tribovillard et al. 2006). Cold seeps could also be an important source but harder to identify (Morford et al. 2005; Tribovillard et al. 2006). These occur on areas of the ocean floor, where hydrogen sulphide, methane and other hydrocarbon-rich fluid seeps through, over fissures in correlation with tectonic activity (Joseph 2017). Hydrothermal activity can also contribute to large quantities of manganese and iron, that can influence the sedimentary accumulation of other trace elements through their redox behaviour in oxygen-deficient environments (Morford et al. 2005; Tribovillard et al 2006). The residence time of the elements within the seawater plays as well an important role.

Processes that control the removal of dissolved trace elements from the water column to the sediments are either biotic or abiotic (Tribovillard et al. 2006). Biotic processes are when plankton (mainly phytoplankton) use trace elements as minor or micronutrients. Abiotic processes are limited in oxic environments but most effective in environments that are suboxic through diffusion of dissolved trace elements from the water column across the sediment-water interface or through remobilization and repartitioning along redox gradients within the sediments (Tribovillard et al. 2006). In reducing conditions, abiotic processes are particularly efficient with adsorption of metallic ions or ionic species onto organic or mineral substrates, formation of organometallic complexes and precipitation of (iron-) sulphides and/or insoluble oxyhydroxides (Tribovillard et al. 2006). Marine sediments are composed basically by three types of inorganic material: detrital material, biogenic material and authigenic material (Burdige 2006) (Schematic illustration for the main processes is presented in Fig. 4).

The detrital input (terrigenous) originates on land while the biogenic components (mainly calcium carbonate and opaline silica) are generally produced in the water column by living organisms (Burdige 2006). The authigenic material includes non-biogenic components that form *in situ* in the water column or at the sediment surface or within the sediments. The abiotic authigenic precipitate may be derived from the dissolution of the sediments or be supplied from outside the sediments (Berner 1980). In most marine sediments the detrital and biogenic material predominates. As a quantitative feature, the authigenic components are less important in terms of total sediment input, however they can play important roles in geochemical cycling of elements such as Fe, Mn, P and S and as indicators for biochemical processes occurring within sediments (Burdige 2006). It is the biogenic and authigenic fraction of the trace and minor elements that become responsive to variations within the bottom waters or sediments pore water conditions in a response to varying redox gradients. This process is mainly controlled by microbial degradation of organic matter (Calvert & Pedersen 1993). The system that controls the accumulation or depletion of trace metals in sedimentary rocks is controlled by many variants and can be complicated to access individually. It can be influenced by changes that occur within the water-column, within the sediments or at the sediment-water interface. Sedimentation rates can also play a significant role regarding the controls on accumulation of redox sensitive trace elements.

3.2 Redox control and the role of oxygen

The trace elements show variations in oxidation state and solubility as a function of changes in redox conditions in the environment. Estimating paleo-redox conditions in sediments involve reflecting if conditions were oxidizing or reducing. Redox gradation is generally parted in three stages: oxic – suboxic and anoxic.

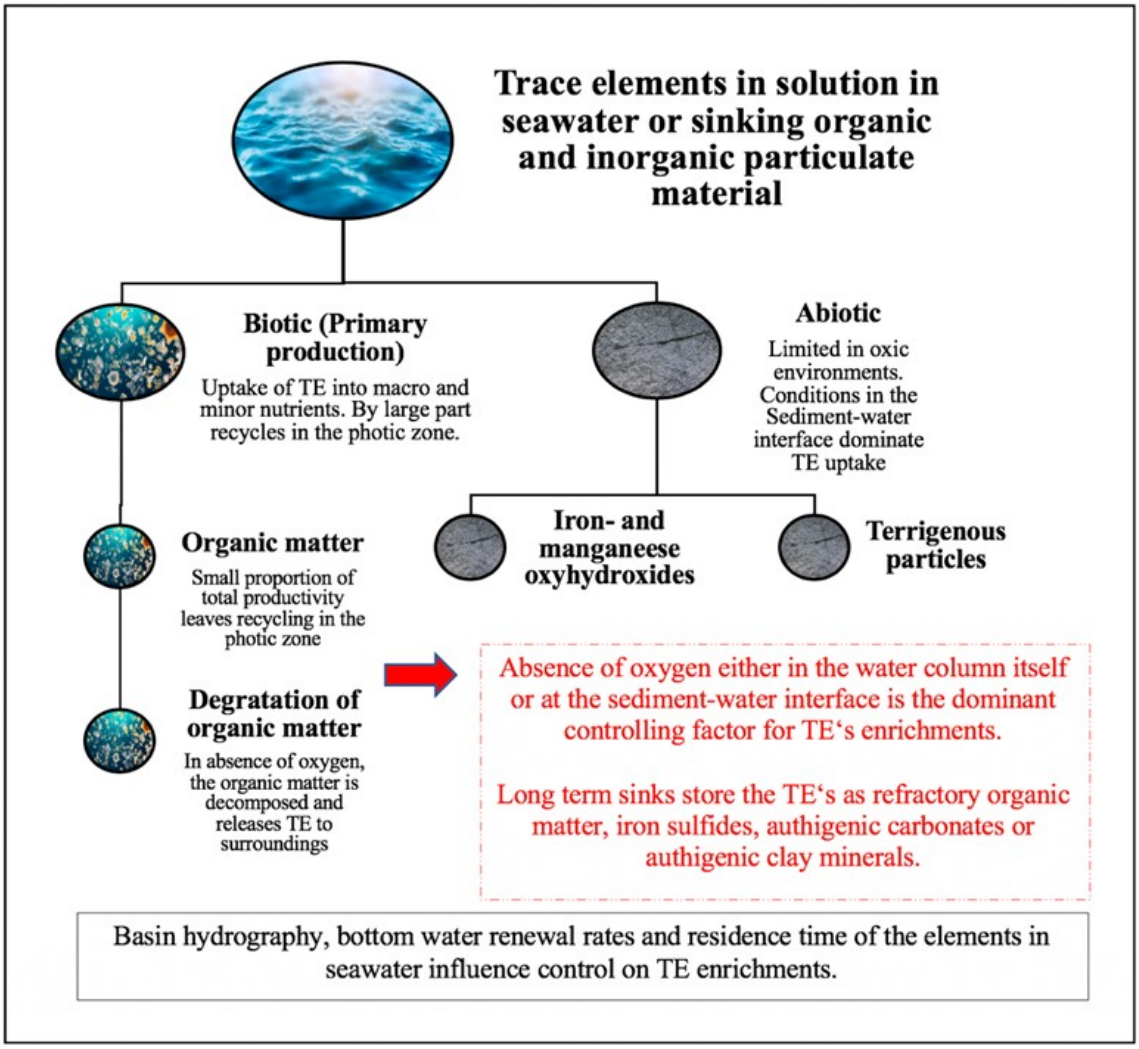

Figure 4. Illustration for the possible pathways for trace element enrichment from the ocean to the sediments, summarizing their most controlling factors.

Anoxic conditions can be sulfidic or nonsulfidic: when sulfidic, hydrogen sulphide is occurring in the water column, this condition is described as euxinic (Tribovillard et al. 2006). Oxic conditions occur when aerobic organisms can use dissolved O_2 from the overlying and interstitial waters for their metabolism (e.g. respiration and the degradation of organic matter). Suboxic conditions are characterized by extremely low to non-zero concentrations of oxygen in the water column where H_sS is limited to pore waters below the sediment-water interface (Tribovillard et al. 2006). At the sediment-water interface or within sediments, conditions can become oxygen-limiting and ultimately lead to anoxia if oxygen demand exceeds the supply (Tribovillard et al. 2006). Formations of organic-rich black shales in the geological record has been considered as a consequence of bottom water anoxia, with preferential preservation of deposited organic matter, formed in anoxic basins, or in intermediate-depth oxygen minima, on continental margins or on the margins of oceanic pedestals and plateaus (Calvert & Pedersen 1993). Another possible explanation could be provided as the result to increased primary plankton production in the surface waters of the ocean (Calvert & Pedersen 1993). Moving towards oxygen depletion, organisms use secondary oxidant sources as nitrate, manganese oxides, iron oxides, oxyhydroxides and sulfate (Tribovillard et al. 2006). H_2S is a catabolic byproduct of sulfate-reducing bacteria (Tribovillard et al. 2006). In the absence of available oxidants, degratation continues and methanogenic bacteria starts to break down organic matter with oxidative-reductive disproportionation of available carbon (Tribovillard et al. 2006). Developement of anoxia can occur in the water column of stagnant or confined waters. As well if insufficient circulation of O_2 occurs and renewal gets limited or in places with high intensity of degradation of organic matter that consumes O_2 faster than it is replenished (Tribovillard et al. 2006). For sediments, this scenario can also occur, provided that additionally O_2 replenishment is interlinked to sedimentary composition, texture and intensity of bioturbation (Tribovillard et al. 2006). Redox reactions are an important component in the biochemical cycle, and marine environments are of no exception. The cycles of carbon (C), nitrogen (N), sulfur (S), iron (Fe) and manganese (Mn) are all driven

by redox processes (Borch et al. 2010). The trace elements play a significant role amongst marine organisms, which utilize redox reactions for energy production and for aquiring essential elements. They mediate these reactions with enzymes that serve as potent catalysts (Libes 2009). In aerobic seawaters, reduction of O_2 and oxidation of organic matter is most thermodynamically stable, as both are the most abundant source of strongly oxidizing and reducing agents respectively (Libes 2009). Under oxidizing conditions, the redox-sensitive trace metals have a tendency to stay in solution in the water column, on the contrary, in reducing conditions they are less soluble and get enriched by authigenic processes (Tribovillard et al. 2006). When the redox conditions differ, it affects the elements by changing the configuration of the oxidation number of a molecule, atom or ion, by gain or loss of an electron. This affects the valance states that the trace elements can exhibit, and in the reduced form created under low-oxygen conditions, organic acids are more readily complexed, either as authigenic components or taken into solid solution by sulphides or precipitated as insoluble oxyhydroxides (Tribovillard et al. 2006). In the sediments, the trace elements exist in various phases: adsorbed onto minerals or organic surfaces, as organometallic complexes, within solid solutions of metal sulphides (as pyrite) or phosphates or as insoluble oxides and oxyhydroxides (Tribovillard et al. 2006). At the sediment-water interface or in the water column, prevailing low-oxygen to euxinic conditions cause all trace element enrichment processes to be more strongly affected. The redox-dependent cycle of iron and manganese are particularly effective in concentrating trace elements. Environments that have been euxinic, are commonly laminated, organic rich and enriched with trace elements. Little if any enrichments are exhibited in bioturbated, organic-poor facies (Algeo & Maynard 2004).

3.3 The trace elements and their implications

Trace element enrichments in sediments can be utilized to reconstruct paleo-depositional conditions despite the almost infinite varieties of processes that control their deposition and early diagenesis. A successful means of utilizing the concentrations and ratios of redox-sensitive trace elements for modern and ancient sedimentary system have been made possible by Algeo and Maynard (2004) and has been synthesised by Tribovillard et al. (2006). Reconstructing paleoenvironmental conditions with trace element concentrations is based on assessing relative enrichments or depletions referred to a standard. In case of sedimentary rocks, the most commonly used standard are the average shale, average crustal rocks or Post-Archean Australian Shales (PAAS) (Wedepohl 1971, 1991; McLennan 2001; Tribovillard et al. 2006). For reconstruction, ideal are fine-grained siliciclastic sediments rich in organic matter (Tribovillard et al. 2006). The bulk rock content of sediments consists of different proportions of mineral phases, mostly controlled by major and minor elements, with the role of trace elements as

Table 1. Average compositions of the Earth's upper continental crust, shale and marine sediments of Al, Fe, Ca, K, Mg, Na, Si and S. Data source: Li & Schoonmaker (2003). *Data souce from Wedepohl (1971, 1991) and McLennan (2001).

Element	Upper crust	Average Shale	Pelagic clay
Al %	7,83 (80400 ppm)*	8,8 (88900 ppm)*	8,4
Fe %	4,17	4,72	6,5
Ca %	3,15	1,6	1
K %	2,56	2,66	2,5
Mg %	1,64	1,5	2,1
Na %	2,54	0,59	2,8
Si %	30	27,5	25
S (ppm)	530	2400	2000

Table 2. Geochemical data of trace elements used in this study. Data source: Tribovillard et al. (2006). [a] McLennan (2001), [b] Wedepohl (1971, 1991).

Elements	Average concentration in seawater (nmol/kg)	Residence time in seawater (kyr)	Average upper crust abundance (ppm)[a]	Average shale (ppm)[b]
Mn	0,36	0,06	600	850
Co	0,02	0,34	17	19
Cr	4,04	8	83	90
Cu	2,36	5	25	45
Mo	105	800	1,5	1,3
Ni	8,18	6	44	68
U	13,4	400	2,8	3
V	39,3	50	107	130
Zn	5,35	50	71	95

substitutes within the present phases. In marine sediments it can be contributed by lithogenous, hydrogenous, biogenous and cosmogenous minerals. (See further overview in Li & Schoonmaker 2003). Which phases are present can influence elemental concentrations significantly, and it is thus important to account for the lithological components of the rock. The most common biogenic component are calcium carbonate and opal phases (Tribovillard et al. 2006). Aluminium can be referred as the aluminosilicate fraction of the sediments (mainly clay), and during diagenesis, the aluminium phase is relatively immobile (Brumsack 1989). When comparing trace-elemental proportions in samples, the best method would be normalize their concentrations to its aluminum content (titanium would also be useful) (Tribovillard et al. 2006). The redox sensitive behavior of the trace elements is applicable for U, V, and Mo and to a lesser extent Cr and Co. Some trace metals are delivered to the sediment mainly in association with organic matter (Ni, Cu, Zn and Cd) and are retained in association with pyrite in reducing environments (Tribovillard et al. 2006). In anoxic, organic-rich sediments, molybdenum, vanadium and uranium are strongly enriched, as waters depleted of oxygen are the most operational effective sinks for these metals (Holland 1984; Brumsack 1989; Koide et al. 1986; Emerson & Huested 1991). In this research, the redox trace elements, that will be in main focus, are vanadium, molybdenum and uranium, and thus, subsequent revision for each of them individually will follow. A brief discussion about pyrite formation and the role of Sulphur cycle will follow. Additionally a revision of nickel, mercury, total organic carbon (TOC) and short revision of C isotopes and their implications is included as well.

3.4 Vanadium

Vanadium is a mildly incompatible, refractory, lithophilic element. It is distributed in igneous and sedimentary rocks and minerals in variable concentrations, with crustal abundances similar as of Zn and Ni, but more dispersed through the crust (Huang et al. 2015). In seawater, (V) is an essential nutrient for phytoplankton in the photic zone and provides means of metal nucleus for numerous vital enzymes (Nalewajko et al. 1995; Moore et al. 1996). Eventually it leads to the element being depleted in the photic zone in the water column as a result of its biological cycling (Collier 1985). Then the resulting biomass created in the photic zone sinks and starts to degrade, releasing the element again in deeper waters, with small fraction of it eventually being deposited as sediments. The elemental distribution in oxygenated waters are controlled by physiochemical processes of sorption and particle scavenging (Smrzka et al. 2019). The oxygen state of (V) varies resulting in the possibility for the element to be used as a tracer for biogeochemical processes, both in the water column and sediments (Wanty & Goldhaber 1992). The controlling factors on the speciation of (V) are pH-levels and redox conditions (Smrzka et al. 2019). In oxic waters, such as surface waters or well mixed waters (V) stays present as V(V) in the form of vanadate oxyanions (HVO_4^{2-} and H_2VO^{4-}) (Sadiq 1988; Wehrli & Stumm 1989). For pelagic and hemipelagic sediments it is coupled with the redox cycle of Mn (Hastings et al. 1996; Tribovillard 2006). It adsorbs readily onto both Mn- and Fe-oxyhydroxides and it also shows a covariation trend with kaolinite (Tribovillard 2006). The most effective way to deliver vanadium to sediments is adsorption onto sinking particles alongside diffusion from seawater (Trefry & Metz 1989; Prange & Kremling 1985; Brumsack 1986). When conditions are mildly reducing, V(V) is reduced to V(IV) forming vanadyl ions (VO^{2-}), the hydroxyl species $VO(OH)^{3-}$ and insoluble hydroxides $VO(OH)_2$. These reactions are further favoured in the presence of humic and fulvic acids. V (IV) ionic species may be incorperated in sediments by surface adsorption processes or by the formation of organometallic ligands (Emerson & Huested 1991; Morford & Emerson 1999). In environments with reduced situations, the enrichment of vanadium is considerable over crustal contents (Emerson &Huested 1991; Thomson et al. 1998). In strongly reducing environments with the presence of free H_2S, vanadium is converted to V(III), where it could be taken up by geoporphyrins or precipitated as a solid oxide (V_2O_3) or hydroxide ($V(OH)_3$) (Algeo & Maynard 2004).

3.5 Molybdenum

The main source of Molybdenum (Mo) to the oceans is from rivers via weathering of rocks exposed at Earth‘s surface (Smrzka et al. 2019). In oxic seawater, molybdate (MoO_4^{2-}) is the most dominant species (Algeo & Maynard 2004). In the oceans, Mo has a concervative behaviour and holds near constant ratio to salinity (Bruland 1983; Collier 1985). In seawater it has relative high abundance, compared to other trace metals (Algeo & Maynard 2004). Thermodynamically, the oxidation state six of Mo (VI) is favoured in oxic seawater (Emerson & Huested 1991). When conditions become reducing, Mo is stable in the oxydation state of (IV) (Emerson & Huested 1991). With the presence of dissolved sulphide, it is efficiently reduced and subsequently enriched in sediments (Helz et al. 1996, 2011; Vorlicek et al. 2004) For the reasons that Mo is closely associated with sulphides, and that it does not accumulate under denitrifying conditions, as is the case for other redox sensitive trace elements, it can be useful to reflect on lower redox potentials and distinguish changes of sulphidic concentrations within pore waters (Algeo & Lyons 2006). If organic matter is present, it tends to act as an additional transfer agent for Mo to sediments, as being a phase for Mo enabling sulphide production alongside microbial oxidation with sulphate (Piper & Perkins 2004). Presence of humic substances in organic rich sediments can promote transfer of MoO_4^{2-} to the sediment-water interface (Brumsack 1989; Helz et al. 1996). Plankton do not concentrate molybdenum and natural particles do not adsorb them effectively. Mo has a limited affinity to be incorporated into clay mineral surfaces, as well $CaCO_3$ and to iron-oxyhydroxides at marine pH values (Brumsack 1989; Goldberg et al. 1998). Under oxic conditions, Mo concentrations are controlled by coprecipitation and adsorption onto oxyhydroxides, with manganese oxides being the strongest sink (Morford & Emerson 1999; Gobeil et al. 1997; Algeo & Rowe 2012). Mo accumulation is extremely favoured in euxinic basins, in which molybdate is

converted to tetrathiomolybdate (MoS_4^{2-}) within the water column (Neubert et al. 2008; Herrmann et al. 2012). Concentrations of Mo (and V as well) within the water column in anoxic basins are lower compared to oxic seawaters, a consequence of those elements being transferred to the sediments (Emerson & Huested 1991). If reduced further it can be incorporated into solid solution with iron-sulphides (Huerta-Diaz & Morse 1992; Helz et al. 1996; Morse & Luther 1999; Adelson et al. 2001). For effective long term storage of Mo in sediments, the presence of dissolved sulfides and formation of thiomolybdate complexes is a key factor (Scott & Lyons 2012).

There is a strong association in modern environments supporting that low or zero bottom water oxygen concentrations, are requisite for authigenic solid phase formation of molybdenum and vanadium as illustrated by Shaw et al. (1990), in a study of metals in the Californian Borderland basin. From other localities as the Saanich Inlet and the Black Sea, where anoxic waters are prominent, molybdenum and vanadium concentrations are greater than compared to oxygenated locations within these basins (Pilipchuk and Volkov 1974; Francois 1988). From the Baltic Sea, there has also been observed correlation between anoxia in the Baltic Sea bottom waters and Mo concentrations in underlying sediments during times of restricted circulations with the open ocean (Hallberg 1974). Observations from sediments in upwelling zones west of Peru and from West Africa, have shown high values of V and Mo in connection to rising old water masses, as these waters are depleted of oxygen (Bertine & Turekian 1973; Calvert 1983; Seralathan & Hartmann 1986).

3.6 Uranium

Being derived from rivers to the oceans, in oxic and suboxic waters, uranium (U) is predominantly present as the conservative uranyl ion U(VI) which bonds to carbonate ions forming the chemically unreactive uranyl tricarbonate complexes ($UO_2(CO_3)_3^{4-}$) (Langmuir 1978; Klinkhammer & Palmer 1991; Calvert & Pedersen 1993). The vertical distribution of it in the oceans, is conservative (Smrzka et al. 2019). Uranium is transported from the photic zone to bottom waters and sediments depending on the dissolved oxygen concentrations and flux of organic matter (McManus et al. 2005, 2006). In oxic marine environments, enrichments are limited, as dissolved U (VI) is neither reduced to more thermodynamically stable U(IV) nor is scavenged by particulates (Tribovillard et al. 2006). When conditions become anoxic, a reduction of U(VI) to U(IV) is favoured by the highly soluble uranyl ion UO^{2+} or uranous fluoride complexes which are less soluble (Algeo & Maynard 2004). The strongest controlling factor for removing U from the seawater to the sediments, is diffusion by biological or physicochemical reduction close to or at the sediment-water interface (Legeleux et al. 1994; Morford et al. 2009). In typical Eh conditions that are present at the sediment-water interface, the uranium gets reduced leading to accumulation being most effective in the upper few centimeters below the seafloor (McManus et al. 2005; Morford et al. 2009). Abiotic reduction of U(VI) is very slow in the absence of catalysts (Swarenski et al. 1999). However concominant oxidation with ferrous iron does occur abioticly. In addition, U(VI) reduction can be catalyzed by adsorption of anionic uranyl-carbonate complexes, given the terms that there is acess to positively charged surfaces of ferric hydroxides ($Fe(OH)_3$), given circumneutral pH conditions (Boland et al. 2004). Accumulation of U into sediments can be accelerated by humic acids under reducing conditions with formation of organic-metal ligands or by diffusion at the sediment-water interface as precipitation of crystalline uraninite (UO_2) or a metastable precursor (Algeo & Maynard 2004). U reduction is decoupled to the amount of free H_2S and is indirectly influenced by redox cycling of Fe and Mn in the water column (Algeo & Maynard 2004; McManus et al. 2005). It is suggested rather, that reduction of U (VI) is controlled by Fe-redox reactions at the Fe (II)-Fe(III) boundary (Algeo & Maynard 2004). Typical values for U in continental margin sediments is usually 1-10 ppm (Algeo & Maynard 2004). In modern euxinic environments, reduction of U (VI) in the water column has not been observed (Anderson et al 1989). That indictates that the process of reduction of U(VI) is not a simple inorganic reaction, and rather for reduction processes to proceed, it requires particle surfaces for catalysis or specific enzymes created by iron and sulfate-reducing bacteria in the sediments (Barnes & Cochran 1990; Zheng et al. 2002).

3.7 Iron sulphides and the link to the sulfur cycle in sediments

Iron sulphides can incorperate some trace element during their formation. An interconnected relationship exists between organic matter decomposition, sulphate reduction and iron sulphide formation and these three principal factors are the ultimate limits that control each other and how iron sulphides as of pyrite can be formed. Sulphur plays a key role in the oxygen and carbon cycle on this globe, essentially within the marine systems, mainly due to sulfate being more soluble in water and acts as an abundant electron acceptor aiding microbial respiration (Rickard & Luther 2007). Influencing factors for formation of iron sulphides, are the amount and reactivity of the organic matter towards sulphate reduction, availability of iron to react with H_2S and availability of dissolved sulphate (Berner 1985). Most or nearly 90% of all medium to fine grained sediments that become buried in marine sediments on continental margins (as well as deep sea sediments) become anoxic below the top few centimeters (Berner 1985). At the sediment-water interface, bacteria and other micro-organisms consume all dissolved oxygen from the surroundings leading to anoxic levels (Berner 1985). For organic matter to become decomposed further, anoxic communities are needed, with sulphate reduction as a principal process. Sulphate-reducing bacteria and fermentative micro-organism get their energy by oxidizing organic matter to CO_2 and reduce dissolved sulphate to H_2S (Berner 1985). This leads to that produced hydrogen sulphate can migrate upwards and/or laterally and can accumulate within oxygenated portions of the sediment where it can be oxidized back to sulphate or react with available detrital iron minerals to form iron

sulphides as of pyrite (FeS_2) (Berner 1985). The typical simplified sequence, given for conditions being undisturbed by physical processes, demonstrates that O_2 reaches depleted levels before reduced forms of Fe and S^{2-} are presented. This level is described as the suboxic zone. This sequence can vary in regards to scales. When levels of H_2S can build up and reaches maximum, sulphate levels drop, as sulphate does not diffuse to deeper depths in absence of oxygen (for comprehensive overview, see Rickard & Luther 2007).

3.8 The global carbon cycle and TOC

Marine productivity plays a key role in transferring carbon, nitrogen and phosphorous to the oceans and lastly to the sediments. The main primary producers that create organic matter in the modern ocean are single-celled phytoplankton that dwell in the photic zone (Levinton 2008). Via photosynthesis, primary producers in the photic zone take up CO_2 from the atmosphere, to form organic matter (Schoepfer et al. 2015). All the organic matter created by the photosynthesizers supports heterotrophic activity in the sea, as it gets transferred through the food web by the heterotrophs as of bacteria, protozoans and animals (Libes 2009). The final stage for the particules of organic matter, weather dissolved or not, eventually gets transferred to the sediments if it succeeds escaping the re-cycling in the water column. This transport is termed the biological pump and includes also sinking inorganic particles of biogenic origin, mostly composed of calcium carbonate and silicate shells (Libes 2009). An important consuming process for the organic matter is degration and bacterial activity, by heterotrophic microbes as bacteria, archaea and protists. Remaining carbon sinks into the thermocline and eventually to the deep oceans as necromass and fecal pellets (Schoepfer et al. 2015). The flux of organic carbon leaving the ocean-surface layer is described as export production and represents a fraction of total primary productivity or particle export (Dunne et al. 2005).

Total carbon includes both inorganic and organic carbon in a sample. The inorganic part is removed with acids from the sample, and the sediments are then dried to be analyzed for total organic carbon (TOC) and presented as TOC % wt (organic carbon (g), divided by W(g)). The TOC content hence represents the total productivity, excluding the effects of recycling before reaching to the sediment-water interface and excluding the effects of successive degradation by aerobic and anaerobic respiration (Libes 2009). The organic carbon content for marine sediments is usually less than 1% by mass, excluding coastal areas where values as high as 10% can occur (Libes 2009). The range of total organic carbon (TOC) in marine sediments ranges from < 2.5 mg C gdw^{-1} to > 20 mg C gdw^{-1} on a global scale and the concentrations are lower in open ocean (pelagic) sediments and higher for coastal and continental margin sediments (Premuzic et al. 1982; Romankevich 1984; Burdige 2006). The largest contributor to organic matter is organic carbon, and hence provides the most direct proxy for productivity (Pedersen & Calvert 1990; Canfield 1994; Tyson 2005; Zonneveld et al. 2010). Mineralized phytoplankton did not become common until the Triassic, and phytoplankton tests were not a dominant component of marine sediments until the Cretaceous (Martin 1995; Ridgwell 2005). Alongside organic material in sediments being produced in the surface ocean, there is also terrigenous component to consider in marginal marine settings (Goñi et al. 1997; Opsahl & Benner 1997). Before reaching to the sediments, the bulk of organic material exported from the surface ocean is decomposed by bacterial respiration (Deuser 1971; Opsahl & Benner 1997). A small fraction of primary production ends up being deposited at the sediment-water interface (Müller & Suess 1979; Canfield 1994; Hedges & Keil 1995), with a substantial portion of organic matter lost to anaerobic respiration via (i) denitrification, (ii) manganese, iron or sulphate reduction, or (iii) methanogenesis after burial in the sediments (Froelich et al. 1979).

In addition to the significance that organic matter plays in the marine realm to regulate carbon, it plays an important role in regulating oxygen. Locations that operate as a substantial large oxygen sink are the continental margins with organic carbon buried in sediments resulting from high primary productivity (Libes 2009). Factors that can enhance burial of organic matter and preserve it from oxidation are high sedimentation rates, shallow water depths, large flux of organic matter to create oxygen-deficient conditions and proximity to terrestrial source of clay minerals that form aggregates with organic matter (Libes 2009). For oxygen in the atmosphere and in the oceans, there is a continuous feedback mechanism operating in conjunction to climatic responses following rising temperatures as a response to accumulation of atmospheric greenhouse gases. Paleo-oceanographic records do demonstrate indications for ocean anoxia on a global scale (Libes 2009). These periods of oceanic anoxia events (OAE) coincide with mass extinction events and period of rapid climate change (Libes 2009).

3.9 C-isotopes

For sediments and aquatic systems, the isotopic composition of organic matter can be utilized for tracing the source of the organic matter to the sedimentary basin (Peters et al. 1978; Fry & Sherr 1984; Fogel & Cifuentes 1993). There are two stable isotopic compositions of carbon: ^{12}C (with 98,89% abundance rate) and ^{13}C (1,11%). The ratio of the stable isotopes is conventionally expressed as $\delta^{13}C$ value relative to a standard (Descolas-Gros & Fontugne 1990) (see further on theoretical applications in methods). The heavy isotopic fraction ^{13}C tends to get more concentrated in the oxidized form of carbon (as of CO_2) and the ^{12}C gets strongly partitioned into organic matter, hence a reduced low $\delta^{13}C$ reservoir (Sharp 2009). The $\delta^{13}C$ of marine particulate material ranges from -20 to -28‰. The $\delta^{13}C$ gradient varies within basins and a stronger $\delta^{13}C$ gradient is indicative of a stronger stratification. Autotrophic organisms (via photosynthesis mainly) integrate carbon with a specific isotope fractionation processes, favouring the lighter isotopes (Thomazo et al. 2009). This leads to (C_{org}) to become enriched in ^{12}C relative to the inorganic fraction (Thomazo et al. 2009). The isotopic

signature of organic matter that supplies heterotrophic organisms is reflected from the origin of the organic matter, from primary producers in the food chain (Thomazo et al. 2009), with an increase of around 1 per mil by trophic level (Schoeninger & DeNiro 1984). Carbon bearing compounds in sedimentary rocks are either (C_{org}) or (C_{carb}), and the carbonitic fraction is mainly composed of skeletal remains of animals that segregate calcite or aragonite and as well inorganically precipitated carbonate phases from the water column, on the sea floor or as intergrading cements (Thomazo et al. 2009) and reflects the isotopic composition of Dissolved Inorganic Carbon (DIC). The organic fraction in sediments, is originated as residues of living organisms, excluding biomineralization (Thomazo et al. 2009). The isotopic signature of organic carbon in seawater can be influenced by terrestrial organic matter, that would lead to less negative results than those derived further away from continental margins where the biomass is primarily derived from *in situ* production (Fogel & Cifuentes, 1993). For more recent times, reconstruction of stratification in the water column can be made by measuring differences in benthic versus planktonic shells of foraminifers, then however, the procedure needs to be very selective.

The possible changes that can be reflected on the carbon cycle from the isotopic fractionation processes, based on positive shifts in the isotopic signal include enhanced productivity rates and changes in burial rates of organic matter in the oceans. The positive shift results of relatively lighter carbon being removed from the seawater and stored into the sediments. Reduction of the pre-described conditions would shift them more negatively, putting more weight on the heavier isotope in terms of their isotopic ratio. Negative shifts would be a consequence of volcanisms or weathering of exposed, former reduced reoxygenated sedimentary sources that contain stored organic matter or other gas hydrates with introduction of external lighter carbon influencing the ratio of the isotopes. As much as the isotopic fractionation processes of organic carbon is beneficial in reflecting perturbations in the global carbon cycle, the C-isotopes can be useful for relative stratigraphic correlation (Lindström 2017). In order to be successful in accomplishing good correlations, time constraints need to be sufficiently established, and ideally events can be traced regionally or globally with biostratigraphic terms amongst other globally correlated events as of volcanic origin, meteors and more (Lindström 2017).

3.10 Consequences of major volcanic episodes with the example of the CAMP

One of the consequences of the CAMP large igneous province is the release during eruptions of great quantities of volatile materials into the atmosphere as gases and aerosols (Oppenheimer et al. 1998, Mather et al. 2003a; Mather & Pyle 2003). Substantial amounts of SO_2, CO_2 and halogens was degassed. For a shorter term scales, ejection of high concentrations of SO_2 into the stratosphere, might have produced volcanic winters and furthermore affected photosynthesis negatively by diminishing light sources (Saunders 2005). Accumulation of CO_2 in the long term might subsequently have induced global warming (Saunders, 2005). As natural source for many chemical species, eruptions emit substantial quantities of toxic volatile trace metals and metalloids into the atmosphere and oceans (Nriagu 1989; Rubin 1997). It has been demonstrated that across the TJB, vast quantities of greenhouse gasses CO_2 and SO_2 were ejected into the atmosphere (Hesselbo et al. 2002; Lindström 2012; Marzoli et al. 2018). Altered volcanic glass spherules, euhedral pyroxene and amphibole pseudomorphs and increased levels of iridium in marine sediments are indicators that have been correlated to the activity of the CAMP volcanism within the CAMP area (Tanner et al. 2016). Throughout the geological history of the Earth, there is a link between LIP's and mass extinctions, some that have been demonstrated by rapid shifts in carbon isotope records (Saunders 2005; Bond & Wignall 2014).

The end-Triassic extinction (ETE) event is associated with a 3-6‰ negative CIE recorded in both marine and terrestrial records (Heimdal et al. 2018 and references therein) and global warming of 3-4°C (McElwain et al. 1999). It has been suggested that the magnitude of the negative CIE excursion in correlation to CAMP needs further explanation for the extent of the negative amplitude that can be provided by a potential additional source for ^{12}C enriched carbon (Heimdal et al. 2018). This additional source is suggested to be a result of contact metamorphism with large scale sill emplacements in Brazil in association with CAMP with corresponding intrusion events through sedimentary basins containing carbonates and evaporites and contact source for organic-rich shales and large hydrobarbon resevoirs (Heimdal et al. 2018). Other possible causes could be methane hydrates or anomalously low volcanic $\delta^{13}C$ signature, but in general the release of CO_2 could have been sufficient as a cause for the ETE (Heimdal et al. 2018). High precision U-Pb geochronology suggests the following possible stratigraphic scenario: intrusive events commenced around the Marshi CIE and the extinction event. A secondary intrusive phase with high-Ti intrusives coincide with the Spelae CIE. Extrusive volcanic CAMP events in North America and Morocco occur after the Spelae CIE (Stenlille 4 CIE chronology is presented here in Fig. 11). An earlier example throughout geological history is provided at the end of the Permian period with an great extinction event, attributed to the formation of the Siberian Traps. Associated intrusions through organic-rich shales and petroleum bearing evaporites realeased significant amounts of greenhouse gases, with correspontant global warming and ozone depletion (Svensen et al. 2009). In addition, a global nickel anomaly has been associatied between the Siberian Trap eruptions and the Permian mass extinction events (Rampino et al. 2017). For Permian-Triassic successions, spikes of nickel abundances have been reported over conventional background values, coinciding with negative carbon-isotope shifts and mass extinction events (Rampino et al. 2017). Nickel anomalies in the Siberian Traps have been interpreted as resulting from magma chamber processes with

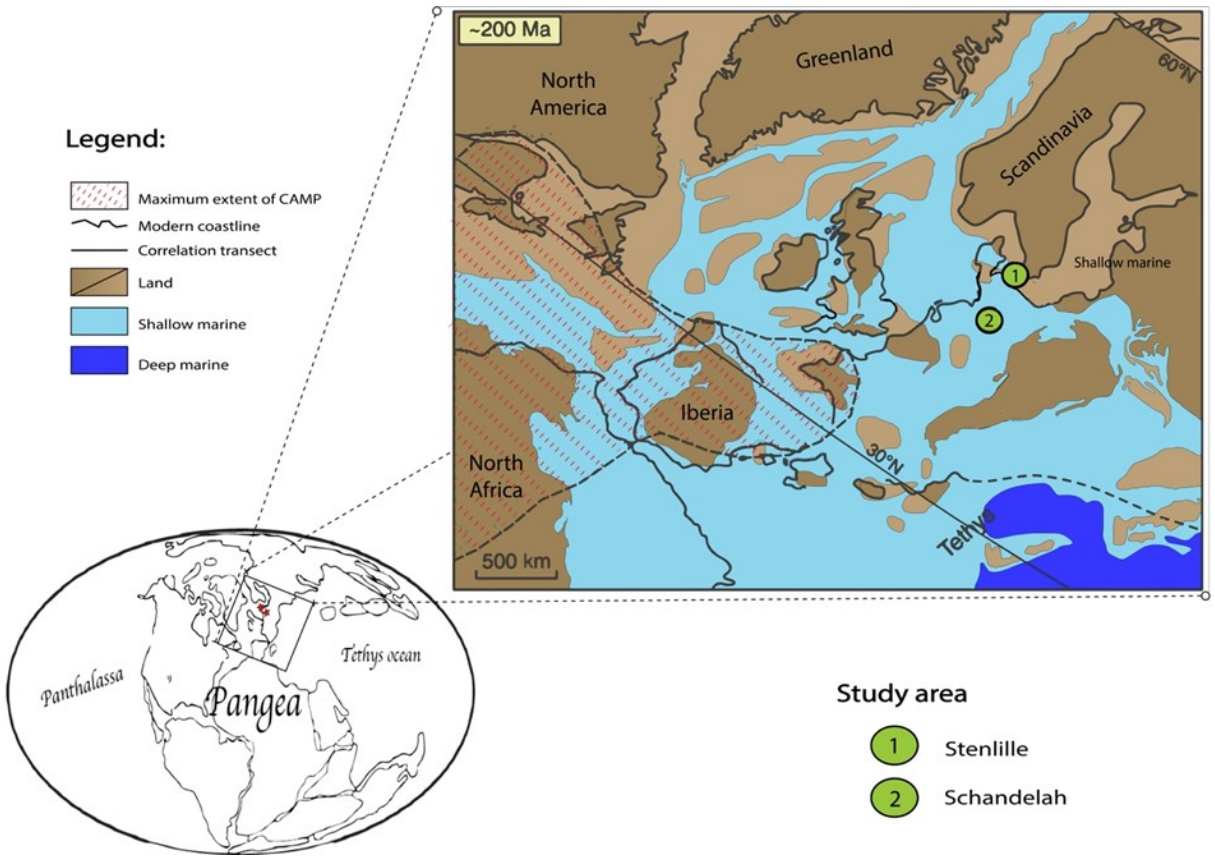

Figure 5. A simplified two-figure map providing the configuration of late Triassic Pangea, showing the Tethys ocean and the superocean Panthalassa (modified from Lucas & Tanner) And secondly a close up map of Europe's configuration around the Triassic-Jurassic boundary, also showing maximum extent of CAMP. In addition showing where Stenlille and Schandelah are respectively (modified from Blakey 2014; Lindström et al. 2015).

segregation of co-existing sulphide liquids. As Ni is highly compatible, it will become enriched in the metals of the sulphitic fraction and leave Ni-depleted silicate magma left (as well depleted in other platinum group elements) (Rampino et al. 2017). Volatile volcanic emissions of this magma could distribute these elements globally (Rampino et al. 2017). The presence of mercury as a product of coal cumbustion in Siberia in Permian-Triassic boundary sections have been desribed as well (Rampino et al. 2017). Lindström et al. (2019) reported elevated concentrations of mercury in terrestrial and marine sediments from southern Scandinavia and northern Germany. These studies needed further test for any correlation between the ETE events and the presence of Ni and Hg. Subsequently, I will review these elements and how they can be brought into marine sediments.

3.11 Nickel

In the crust, nickel (Ni) is the 24th most abundant element, by weight it is the 5th most abundant. It can exist in many various mineral forms, and as it belongs to the transition metal series, it has a high resistance for corrosion by air, water and alkali, but dissolves readily in dilute oxidizing acids (Cempel & Nikel 2006). Nickel is a chalcophile element and is concentrated within Earth's crust in sulphide deposits and enriched within sedimentary rocks, especially within black shales (Calvert & Pedersen 1993). In the oceans, Ni plays a role as being a micronutrient, mainly used up by phytoplankton for growth. In the water column, it gets recycled within the photic zone and remineralized. Eventually it partly sinks as organic particles in the water column (Calvert & Pedersen 1993; Dupont et al. 2010). Ni in seawater is present in the form of divalent Ni^{2+} ion, and manganese oxides sorbs it strongly via structural incorporation and replacement of Mn (Peacock & Sherman 2007). Ni is strongly enriched in ferromanganese deep-sea nodules (Smrzka et al. 2019). It is mostly present as soluble Ni carbonate ($NiCO_3$) or adsorbed onto humic and fulvic acids (Calvert & Pedersen 1993; Whitfield 2002; Algeo & Maynard 2004). Ni accumulation can be accelerated by complexing with organic matter, at or below the sediment-water interface (Algeo & Maynard 2004). In anoxic sediments, it tends to be co-enriched with Cd, Co, Zn and Cu and incorporated into pyrite in a solid solution (Huerta-Diaz & Morse 1992). In anoxic conditions Ni forms the sulfide NiS. Uptake of Ni is kinetically slow, resulting in its concentration in authigenic sulphides to be limited (Morse & Luther 1999). In pore waters the behavior of Ni is by large parts not influenced by redox variations despite showing some relations with Mn (Klinkhammer 1980; Sawlan & Murray 1983). Nickel may serve as indicator for microbial methane formation in the water column and in marine sediments as it is needed in the formation of key enzymes in methanogenic archaea (Hausinger 1997; Kida et al. 2001; Scheller et al. 2012).

3.12 Mercury

Mercury (Hg) has long residence time in the atmosphere of 6 months to 2 years, with global distribution expected by atmospheric circulations (Schroeder & Munthe 1998). It is strongly concentrated by biological processes following deposition (Pyle & Mather 2003). The most common species in natural samples is the organometallic cation methylmercury $[CH_3Hg]^+$ that is environmentally toxic and bioaccumulative (Bozke et al. 2003). Hg varies in concentrations in bottom sediments from 10 to 200 ng/g dry mass (or 10 – 200 ppb conventionally) (Bozke et al. 2003). The chalcofile behaviour of mercury, leads it to combine rather to sulphur than oxygen, resulting in sulphur playing a major role in controlling mercury chemistry in anaerobic sites (Bozke et al. 2003). In anaeorbic conditions, given low concentrations of sulphides, methylmercury binds with organic matter (Bozke et al. 2003). HgS gets deposited presumably by the presence of iron oxides or organic matter (Bozke et al. 2003). The solubility of HgS is aided by the presence of sulphide ions S^{2-} with formation of soluble sulphide and disulphide complexes, resulting in great concentrations of soluble mercury species accumulating in anaerobic zones of bottom sediments (Bozke et al. 2003). Distribution of Hg in preindustrial sedimentary records, could be useful as a proxy for volcanic activity (Sanei et al. 2013). Degassing from volcanic sites release gaseous Hg into the atmosphere, then atmospheric circulation and wind patterns control how far they get distributed, aided by the long residence time of the element in the atmosphere (Schroeder & Munthe 1998). Elevated concentrations of Hg have been described in marine sedimentary rocks around the TJB globally (Thibodeau et al. 2016; Percival et al. 2017). Lindström et al. (2019) presented evidence for increased levels of mercury in correlation to high occurrences of abnormalities in fern spores indicative of volcanogenic contribution from the Danish Basin (Stenlille 1 and 4) and from the North German Basin (Rødby) for the ETE event.

4 Methods

4.1 Sampling

50 samples were provided from the Stenlille 4 core section by the Geological Survey of Denmark and Greenland (GEUS). These samples span about 31,24 m, from 1492,54 – 1523,79 m of corrected depth. The interval between the samples varies between one to three samples per meter. This interval was chosen as it represents the transition from the Triassic - Gassum Formation to the Jurassic - Fjerritslev Formation and has a potential on supplementing information about the redox chemistry of the sediments before, during and after the extinction event that took place at this time interval. In addition, 154 samples were provided from Schandelah, Western Lower Saxony Basin. These samples span about 108 m, between 230 – 338 mbs and include the transition from the Triassic-Arnstadt Formation to the top-most Jurassic- Angulatenton Formation.

4.2 Analytical methods

There is a variety of techniques in order to obtain chemical compositions from rocks. For this project, major, minor and trace element concentrations were gathered using X-ray fluorescence (XRF) spectroscopy and inductively coupled plasma mass spectrometer (ICP-MS). The XRF irradiates a solid sample with x-rays, with sufficient energy to excite electron transitions amongst the valance electrons and the inner electron shells of atoms for varieties of elements in a sample (Winter 2010). The following return to the ground state results in emissions of fluorescent x-rays with its characteristic high-energy ranging x-ray spectra, which are eventually dispersed through an oriented crystal lattice that diffracts the spectrum. An x-ray detector can be tuned to a particular frequency and measures rate of emission corresponding to the energy of an particular element (Winter 2010). For many elements the XRF technique is reasonably accurate and precise and can reliably detect many elements in concentrations down to a few parts per million. However, if concentrations of certain elements are very low, the technique is limited by its detection limits.

The Inductively coupled plasma (ICP) technique, acquires samples to be dissolved and mixed with argon gas, as they are aspirated into a very small radio frequency generator, where a plasma is created that excites atoms effectively (Winter 2010). Each element has a corresponding emission line that gets isolated by a diffraction grating, detected by a series of photomultipliers, with separate channels for every specific element tuned to it (Winter 2010). In mass spectrometry (MS), after the heating and ionization of a sample, the ions are introduced into an evacuated chamber with a strong magnetic field where stream of charged ions follow a curved path in a magnetic field, as heavier ions with greater momentum follow a path with a larger radius of curvature (Winter 2010). The ions are counted on mass basis as they pass through slits in a charged detector, but this method does not rely on emissions or absorption, but physically dissociates the sample and counts the particles of a particular mass (Winter 2010). Trace element measurements were focused mainly on V, Mo, U, Cr, Co, Ni, Cu, Zn to be able to address paleoredox conditions and paleoproductivity.

The isotopic compositions of $\delta^{13}C$ (organic) was obtained using isotope-ratio mass spectrometry (IRMS), the technique consists of measuring isotopic compositions of samples, relative to an isotopic composition of a working gas. This analysis is mostly used to measure isotopic variations resulting from mass dependent isotopic fractionation in natural systems. The samples are introduced to the mass spectrometer as pure gases either with combustion, as was the case for this research, however other ways include using gas chromatographic feeds or chemical trapping (Paul et al. 2007). IRMS includes tight electron impact ion source, a magnetic sector and Faraday cup detectors that can simultaneously conduct measurements of two or more isotopes of a light gas (Zhang et al. 2012). A simple description of the procedure involves organic solvent being combusted at high temperatures into CO_2 and H_2O and the organic solvent is then back-

flushed into valves to divert the solvent from the reactor as it prevents the oxygen source of it to become completly depleted of oxygen. The solvent is then carefully vented before the analyte is introduced, following a flow of CO_2 through the IRMS through open split. Before the CO_2 enters, all H_2O is removed so it will not get converted to HCO_2^+ (see Zhang et al. 2012 for detailed information). The measured isotopic composition is then converted and reported (normalized) on an international stable isotope reference scale (VSMOW: Vienna Standard Mean Ocean Water, VPDB: Vieanna Peedee belemnite, and/ or VCDT: Vienna Canyon Diablo Troilite) (Paul et al, 2007).

4.3 Sampling and preparation

50 samples from Stenlille and 154 samples from Schandelah were collected for analysis of major, minor and trace metal concentrations using X-ray flurescence (XRF) instrument at the Department of Geology at Lund University. This method was chosen to get an overview of the general compositions of the samples at disposition. However, trace elements are typically in rather low concentrations and therefore this method has strong limitations. Some samples from Stenlille had previously gone through pulverization before we obtained them, rest of them were pulverized with a porcelain mortar. Samples coming from the Schandelah core were however, directly taken from the core. The samples were split, one part for keep and the other pulverized. Do to the Schandelah samples being rather competent, they were mechanically grinded and pulverized. The XRF instrument was a Niton XL3t XRF analyser. The mode used of the XRF-analyser was targeted for soils and mining, partially because then, there does not have to be any adjustment for a matrix. The elemental spectrum utilised in that mode gives wider range and more suitable elements, needed for the analysis of redox controlled trace metals. Each sample was placed in a small sample cup with a 4-micron thick polypropylene film and analysed for 240 sec per sample. The XRF analyses were made for the elements of Ba, Mo, Sr, Sb, Nb, U, Sn, Th, Cd, Zr Rb, Ag, Y, Bi, Au, Se, As, Pb, W, Zn, Cu, Ni, Co, Fe, Mn, Cr, V, Ti, Ca, K, Al, P, Si, Cl, S and Mg. The elements that had fairly low concentrations, and in general got limit of detection (LOD) signal amongst the sedimentary samples were the following elements: Mo, Sb, U, Sn, Th, Cd, Ag, Bi, Au, Se, Pb, Ni, Co, P and Mg. LOD is the lowest quantity of the analyte that can be detected reliably. The data reduction was performed with the program NDTREL-08 and concentrations presented in ppm. Generally, for element to be detected by the analyser in a given sample, the measured concentration of the sample must be at least three times the standard deviation of the measurement, and detection limits will depend on the composition of the sample, precision of each measurement is two times the standard deviation (sigma). To standardize the analytical procedure, a standard with known amounts of analyte, **2709a** was used. Reproductive analysis of a standard (n=32) of 2709a gave different results depending on the elements, relative error was for example for V ± 6,46% (% difference of standard deviation from the mean) and for Fe it was 0,60%, being significantly lower in general for the major elements (Appendix 1 - part III).

4.4 ICP-MS analysis

Following the results from the XRF, the intervals were evaluated to select samples for further analysis using an inductively coupled plasma mass spectrometer (ICPMS) to gain more precision and sensitivity for the concentrations of the trace elements from the cores. The intervals chosen were the ones that showed most variations within V, Mo and U after being normalized to Al. Including as well were low and middle ranging intervals chosen to use as a "baseline" for comparison. The controls on how many samples were possible to analyse, were cost dependant and therefore restricted to 34 samples, 18 samples from Stenlille 4 and 16 from Schandelah. The samples were sent to a laboratory in Canada, where they were analysed using Ultratrace 4acid Digest (Total Digestion ICP-OES/ ICPMS) method, that involves preparation of samples with vigorous digestion of acids, employing hydrochloric, nitric, perchloric and hydrofluoric acids. This suits adequately dissolve all type of sedimentary rocks. Sulphide sulphur and soluble sulphates are extracted. Detection limits and random error varies by element, for the majors Al and Fe it is 0,01%. For V, Cr and Mn it is 1 ppm. For Ni it is 0,5 ppm. For Cu and Zn it is 0,2 ppm. For Co and U it is 0,1 ppm. For Mo it is 0,05 ppm and for Hg it is 10 ppb.

4.4 Utilizing trace elements as redox proxies

In order to be useful for addressing paleoenvironmental conditions, trace elements have to be determined as relatively enriched or depleted compared to a standard. The standards commonly used are the average shale or average crustal rocks (Tribovillard 2006). For this research, average shale is chosen as a representative for fine-grained siliciclastic sedimentary rocks, fairly rich of organic matter. In order to exclude the effect of varying biogenic diluents (calcium carbonate and opal) within the sediments, concentrations are normalised with the aluminium content (representing the aluminosilicate fraction of the sediments). These elements have moreover the advantage to be unaffected by diagenic alterations (Tribovillard et al. 2006). For ease of interpretation, enrichment factors (EF) can be calculated by corresponding equation:

$$EF\ (element_x) = (X/Al)_{sample}) / (X/Al)_{average\ shale})$$

If $EF_{(x)} > 1$, then element X is enriched relative to the average shale, if $EF_x < 1$ it is depleted.

Next step is to cross-plot the trace elements to aluminium (or titanium), to examine if given content is controlled by detrital flux or not (Tribovillard et al. 2006). If a good correlation is observed, and no important deviation occurs from the average shale concentrations, then the source of the elements comes from detrital provenance and is thus not useful for paleoenvironmental analysis (Tribovillard et al. 2006). Further way to evaluate if trace elemental concentrations are of detrital or authigenic origin, is to estimate it, as a part

in excess of the average shale abundance. The clastic fraction of element X can be estimated as follows:

a) Detrital X = $(X/Al)_{\text{average shale}}$ x Al_{sample}

b) Authigenic fraction of X = total X– detrital X

The methods of Algeo and Maynard (2004) can be synthesized to access redox conditions, and it involves looking at the trace elemental concentration and their relations to total organic carbon (TOC). The method is based on results of comparison of two types of sediments (Pennsylvanian Kansas-type cyclothems). The two types of sediments represent different end-members of redox conditions, black shales that are highly enriched in redox-sensitive trace elements relative to overlying gray shales. Algeo and Maynard (2003) concluded that two patterns emerged from their results. The first pattern was exhibited by Mo, U, V, Zn and Pb to show moderate EF's and strong covariation with TOC in samples having < 10 wt% TOC. Secondly, Cu, Ni, Cr and Co exhibited low EF's and moderate to strong covariation with TOC in samples having > 10 wt% with TOC in all samples. They summarized that these results reflect different respones to benthic redox conditions. They also described the first pattern as characteristics of TEs of strong euxinic affinity, as they are taken up into solid solutions by Fe-sulfides or involved in H_2S catalysed reactions in authigenic phases. They described the second pattern as characteristic of trace elements of weak euxinic affinity, not being strongly influenced by the presence of free H_2S, but resident mainly in the organic carbon or detrital fractions of the sediments. They concluded that multi-proxy accessing procedure would best fit in addressing redox conditions. Based on their results in the black shale samples, euxinic conditions were considered to have existed if at least two of four „redox-indcator" showed enrichment at euxinic levels, and non-sulfidic conditions were inferred otherwise.

4.5 C-isotopes

Bulk organic $\delta^{13}C_{org}$ were determined for nearly all available samples from the Stenlille 4 core section, in total of 46 samples. They were dissolved in two steps in 10% HCL acid, until they stopped reacting, then they were washed with deionized water and set to dry for 24 hours. Then, 10 mg were weighted of each, and put into tin capsules and analysed on a Flash 2000 Elemental Analyser, coupled with a Delta V mass spectrometer via Conflo II interface at the Biology department of Lund University. Values of $\delta^{13}C$ are herein reported as per mille (‰) deviations from the ratio in the Vienna Defined Pee-Dee Belemnite (V-PDB). (Note further review of C-isotopes and analytical methods above).

The definition of $\delta^{13}C$ is:

$$\delta^{13}C = (((^{13}C/^{12}C) \text{ sample})/ (^{13}C/^{12}C)\text{standard}) - 1) \text{ x } 1000 ‰$$

The standard is an established reference material, such as the gas CO_2 referred on international standards of $\delta^{13}C_{VPDB.}$ Calibrations are made internally and externally. Internal calibration accounts for all sources in the system for isotopic fractionation. Preferably the standard undergoes similar chemical reactions and goes through the same passages as the analytes, and ideal is that they include similar isotopic range (Zhang et al. 2012). External calibration involves to analyze a compund of isotopic standard mixture efter every few samples to monitor and correct for any system drift and preferably that it involves partially similar compounds to mitigate effects of isotopic fractionation (Zhang et al. 2012). For external calibration in this study glycin, caffeine, acetanilide and sucrose was used. The standard deviation of the glycin standard is 0,1‰.

5 Results

5.1 XRF results

5.1.1 Summary

The XRF instrument reports concentrations of 36 identified elements. Bal stands for balance. It represents x-ray energy levels that the analyser does not attribute to a particular element. If elements are reported with limit of detection (LOD), then the instrument is limited as it represents the lowest quantity of a substance that can be detected, after being subtracted from the noise of a blank value. All concentrations are given in ppm. The accuracy of the results of the XRF instrument varies differently according to each element, as an effect of both the detection limits of the instrument and the error margins. The focus of this project was on elements that are redox sensitive and that are delivered to the sediments by authigenic processes, essentially controlled by oxygen availability. Additionally included were the evaluation of other proxies, which could help to reflect contributions of changes in sedimentary provenance or in biological activity. Elements that could infer a volcanogenic origin were also included. For the purpose of this research, main focus was on **V, Mo, U, Cr, Cu, Co, Mn, Zn, Ni, Fe, S** and **Hg**. Of those, the XRF showed to be useful, without major limitations for the major elements (Al, S, Fe) and the following minor and trace elements: V, Cr, and Mn. Regarding the trace elements, the XRF could therefore not be used to evaluate Mo, U, Cu, Co, Zn, Ni and Hg. Data is presented in table 3 and table 4, and concentration-depth profiles and histogram of the elemental distribution are presented in Appendix 1. Results of reproductive analysis of a standard (2709a) are presented as well in Appendix 1. A more detailed summary for Al, Fe, S, V, Mo, U are described subsequently, including how choosing samples for ICPMS was implemented and a brief conclusion of other anomalous observations.

5.1.2 Aluminium

Al has a conservative behaviour and depicts the silicate fraction of sediments. As mentioned before this element can be considered as a normalize

parameter in order to assess the relative degree of enrichment or depletion of given elements in a sample. It allows also to evaluate the background contribution from crustal sources. Average Al value for Stenlille 4 is 56.075 ppm and Schandelah is 66.400 ppm. Compared to average shale (88.900 ppm), both values are significantly lower. In Schandelah, it is noteworthy that Al stratigraphic distribution is reflected by a generally increased concentration in finer grained interval, from c.a. 300-318 m. This reflect proportionally more clays and feldspars (Appendix 1 (I and II). For Stenlille 4, on a stratigraphic appearance, there is no obvious distinction observed indicating a trend to lithology. In Stenlille more lithological variations are present throughout the core and the stratigraphic distribution of Al oscilliates more randomly with two of the lowest intervals at 1493,06 and 1514,91 m. The highest concentration is reported at 1511,26 m.

5.1.3 Iron and sulphur

At Stenlille 4 the average concentration of Fe is 2,912 % wt and S is 5.672 ppm. In Schandelah average Fe is 3,9469 % wt and S 4.496 ppm. Compared to average compositions of the Earth's upper continental crust, shale and marine sediments (pelagic clays), the average iron content of both Stenlille 4 and Schandelah is significantly lower (Table 1). Average Fe% in the upper continental crust is 4,17%, for shales it is 4,72% and for pelagic clays it is 6,5%. Average S content of the upper continental crust is 530 ppm, 2.400 for shales and 2.000 for pelagic clays, therefore the S content in both Stenlille 4 and Schandelah is considerably higher.

When looking at the stratigraphic distribution of Fe normalized to Al in Stenlille 4, there are few intervals where the ratio becomes significantly low, mainly due to very low concentrations of Fe, and occur at depth intervals of 1492,54 m, 1498,18 m and 1514,91 m. Stratigraphic distribution of Fe normalized to Al, and S/Fe ratio normalized to Al is presented in Appendix 1 (IV) for Stenlille and Schandelah. Additional information about the Fe and S concentration is given in tables 11 and 12 for intervals with EF's > 2 (further discussion about EF's is provided in chapter 5.3.1). When looking at S/Fe ratios normalized to Al, the stratigraphic distribution shows peak intervals at 1492,54 m. Including intervals at 1493,06 m, 1493,97 m, 1498,18 m, 1501,84 m and 1514,91 m, which are considerably higher then the general trend. In Schandelah, after normalizing Fe with Al, Fe has a distribution closer to near constant ratio, with some exeptions. The intervals with the highest values that are relatively high compared to the constant ratio, are at depts of 231,3 m, 233,4 m, 263,3 m 264,0 m, 266,1 m and 318,0 m. Three of the lowest intervals are at 233,0 m, 326,0 m and 330,0 m. A summary of the stratigraphic distribution of S/Fe normalized to Al, shows a significant high value peak at 241,8 m. Other smaller ones are present at 233,4 m, 318,0 m and 334,5 m, and even smaller ones are also present.

5.1.4 The redox sensitive elements: vanadium, molybdenum and uranium

Detection of vanadium (V) proved useful, however molybdenum and uranium are present in too low concentration for the the instruments abilities for detection. In Stenlille, V has only 3 values below limit of detection (LOD) amongst samples, U and Mo is detected as below LOD in all but 4 samples. In Schandelah, V results are in 5 samples below LOD, Mo results are in all but 5 below LOD, U results are in all but 4 below LOD (Figure 6 and 7). This limits the results of the XRF for Mo and U, and therefore those results can only be used as estimates with caution, since its accuracy could deviate far from the true value, and that the instrument itself has high error margins, affecting its precision. The average value in the upper crust for V is 107 ppm, and the average shale value is 130 ppm, in Stenlille 4 it is reported as 335 ppm and in Schandelah it is 155 ppm. Compared to average shale the difference is therefore 158% and 19% respectively for the Stenlille 4 and Schandelah core sections. The few reported non LOD values for Stenlille for Mo (counts of 4) and U (counts of 4) were 9 and 22 ppm, and in Schandelah 9 (counts of 5) and 31 (counts of 4) ppm respectively. The average upper crustal abundance value of Mo and U is 1,5 and 2,8 ppm and in average shale it is 1,3 and 3 ppm. That equals to a difference for Stenlille 4 of 592% for Mo and 633% for U compared to average shale, and in Schandelah of 592% and 933% respectively to the elements.

5.1.5 Stenlille 4 XRF summary

Subsequent tables show the range of the results for the XRF analysis (Table 3), in range of lowest to highest values, the average and the median for the distribution of the 50 samples. All concentrations are reported in ppm. NA's (LOD) are samples where concentration are reported below the limit of detection or (LOD) and excluded from statistical interpretation. Graphical presentation of the elements is presented in Appendix 1. Subsequent graphs show how the distribution of elements that have been emphasized are distributed with corresponding depth. Looking at V, Mo and U there is apparent high range values in concentrations at both 1492,54 m and 1498,04 m depth. For the interval 1501,79 – 1507,57 m. Noteable is that Cu shows an interesting plateau. At 1501,84 m, both S and additionally Pb have high ranged values.

5.1.6 Schandelah 4 XRF summary

As for Stenlille, subsequent tables (Table 4) show the range of the results for the XRF analysis for the distribution of the 154 samples. All concentrations are reported in ppm. NA's (LOD) are samples were concentration is reported below the limit of detection or (LOD) and excluded from statistical interpretation. Graphical presentation of the elements is presented in Appendix 1. At depths of 233,14 m and 317,7 – 318 m there is a large enrichment observed in Mo. V also shows enrichments from intervals of 230,4 - 233 m and a distinct plateau from 300 – 318,1 m depth. U also shows enrichments at intervals of 230,4 - 240,3 m, but only slight enrichment at those levels that Mo got enriched. Cr shows the plateu trend similar to V

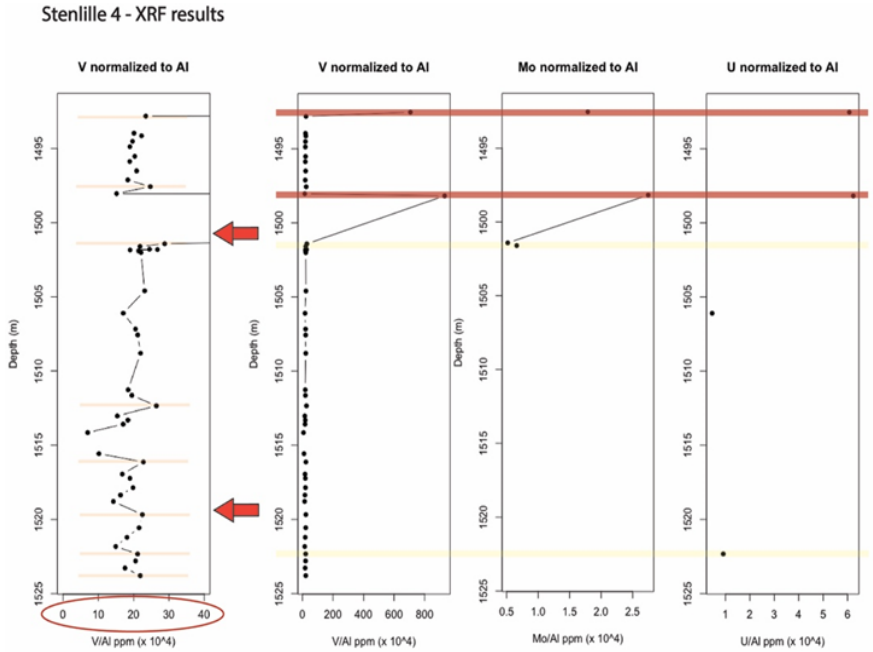

Figure 6. Stratigraphic variation of V, Mo and U normalized values from 50 XRF measurements in Stenlille. Two of the XRF results showed considerable high values in V, Mo and U. Note the scale´-up graph for V, where variatons can be observed amongst V. Additionally, detection of Mo and U is limited by the XRF detection limits. The dark red lines represent the intervals with the highest detected XRF values amongst V, Mo and U. The lighter shade represents individual elemental higher range values.

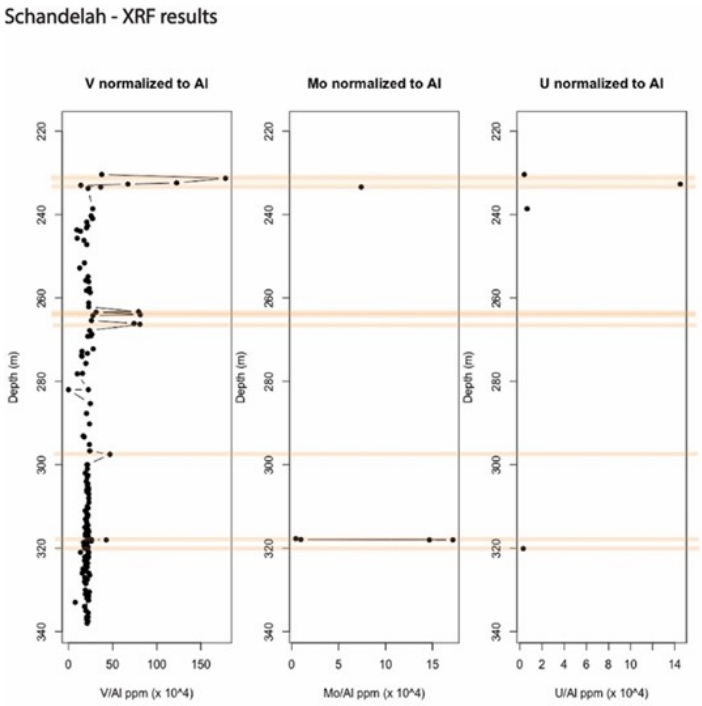

Figure 7. Stratigraphic variation of V, Mo and U normalized to Al values from 154 measurements. Here also, is the detection of Mo and U emphasized. Where higher range of individual element is detected, it has been highlighted. Those areas were targeted for ICP-MS analysis.

Table 3. XRF measurements from Stenlille 4, reported in ppm. n = 50

Element	*Min*	*1st qu.*	*Median*	*Mean*	*3rd qu.*	*Max*	*NA's (LOD)*
Al	*12414*	*47431*	*56866*	*56075*	*69.526*	*92049*	*-*
Si	*168172*	*243804*	*270085*	*273552*	*303.856*	*422.826*	*-*
Ti	*42,86*	*3571,44*	*4824,30*	*4364,45*	*5258,01*	*6709,66*	*1*
Fe	*50,31*	*19079,27*	*29955,72*	*29188,94*	*38828,85*	*65464,32*	*-*
S	*179,3*	*1325,8*	*2440,5*	*5671,6*	*7.250,8*	*24973,0*	*3*
V	*22,81*	*96,83*	*117,71*	*335,14*	*148,91*	*5268,98*	*3*
Cr	*35,76*	*94,24*	*120,84*	*124,24*	*157,79*	*226,59*	*4*
Cu	*13,07*	*18,67*	*23,07*	*23,72*	*29,01*	*36,46*	*20*
Mn	*70,59*	*139,14*	*301,02*	*386,71*	*490,66*	*1.123,47*	*15*
(Zn)	*12,52*	*35,28*	*55,41*	*51,76*	*68,29*	*126,11*	*5*
Zr	*18,52*	*263,26*	*360,04*	*391,25*	*547,22*	*982,02*	*-*
Nb	*2,68*	*10,76*	*13,80*	*12,81*	*15,43*	*19,56*	*2*
Y	*4,28*	*21,43*	*25,38*	*27,21*	*29,31*	*107,59*	*1*
Sr	*24,87*	*78,02*	*90,08*	*117,79*	*110,73*	*520,46*	*2*
Rb	*8,71*	*26,78*	*33,74*	*35,12*	*40,80*	*68,10*	*2*
As	*4,610*	*9,425*	*12,360*	*14,288*	*15,660*	*73,890*	*-*

Table 4. XRF measurements from Schandelah, reported in ppm. n = 154

Element	*Min*	*1st qu.*	*Median*	*Mean*	*3rd qu.*	*Max*	*NA's (LOD)*
Al	*10407*	*47275*	*65203*	*66400*	*92976*	*111965*	*-*
Si	*39891*	*216949*	*254949*	*259913*	*287021*	*434808*	*-*
Ti	*820,2*	*3513,7*	*4927,4*	*4531,4*	*5513,2*	*8069,9*	*2*
Fe	*4235*	*24926*	*34708*	*39469*	*47272*	*174729*	*-*
S	*89,63*	*478,55*	*1121,54*	*4495,58*	*3173,45*	*103607,11*	*13*
V	*21,62*	*97,53*	*162,63*	*154,59*	*203,27*	*657,55*	*5*
Cr	*27,77*	*92,90*	*170,47*	*158,14*	*204,71*	*519,96*	*16*
Cu	*13,02*	*18,95*	*26,43*	*42,33*	*33,30*	*1353,03*	*57*
Mn	*53,13*	*166,06*	*375,22*	*610,32*	*780,80*	*2418,90*	*27*
W	*35,91*	*122,64*	*521,67*	*698,75*	*901,13*	*4690,33*	*44*
Zr	*25,61*	*182,85*	*280,81*	*322,23*	*443,96*	*1169,54*	*-*
Nb	*1,82*	*9,82*	*13,35*	*12,66*	*15,77*	*22,98*	4
Y	*3,43*	*17,17*	*21,32*	*27,50*	*27,81*	*682,57*	*-*
Sr	*19,93*	*60,19*	*82,18*	*85,95*	*91,96*	*634,68*	*-*
Rb	*1,74*	*19,00*	*33,55*	*35,80*	*54,20*	*69,02*	*-*
As	*4,830*	*9,65*	*13,11*	*22,17*	*17,44*	*710,64*	2

and peaks at around 230,4 m. Cu shows discrete peaks at 230,4 - 233,4 as well as at 317,6 - 118,1 m.

5.1.7 Accessing intervals for ICP-MS analysis

The approach that was done was to evaluate how the distribution of mainly V was after being normalized to Al, was based on looking at variations amongst V, Mo and U at both localities (see fig 6 and 7). In Stenlille 4, V showed considerable high values at two depth intervals, at 1492,54 and 1498,18 m. Evaluating the difference between the highest value and the median value of V gives difference of 4479%. At same depth intervals, after being normalized with Al, Mo and U also showed high values that were well detected by the XRF. The difference between the highest value and the median for Mo is 79,39% and for U is 138%. The reason for the median value used here in comparison is based on the data-set being scewed and not normally distributed with few high ranging values for V. For that reason, the median value is more appropriate to evaluate distribution from the middle of a dataset. The comparison for Mo and U is however a result of only 4 values, since the rest of the samples fell below XRF limits. The covarying apparent enrichmentt of V, Mo and U at these depth intervals is therefore considerable. To access further wich intervals to choose for the ICPMS analyzes, the samples that showed higher concentrations in V were chosen, as well as low range values and intermediate values, to get some comparison-values. Including those were intervals that were detected by the XRF of Mo and U above its limitation range (Fig. 6 and 7). In Schandelah, the same procedure was obtained. The difference between the highest value and the median of V reported is 729%. Mo showed difference between values of 132%. For U the difference showed to be of 2658%. In total for ICPMS analysis, 18 samples were chosen for Stenlille 4 and 16 for Schandelah.

5.1.8 Other observations

The anionic species, chlorine (Cl) showed to be limited by LOD in Stenlille 4 from 1492,54 – 1498,18 m. The rest of the samples, ranging from 1501,42 – 1523,79 m showed however higher concentrations, with average of 7163,44 ppm in 36 samples. In Schandelah there is also a stratigraphic variation observed for Cl. From c. 338- 302,5 m Cl is mostly detected as LOD. Above these depths, in the younger sediments, it is mostly present in higher concentrations, with average value of 1291,82 ppm, in 68 samples. Cl has reported average values for the upper crust of 150 ppm, in shales it is reported as 180 ppm. In the cases for Stenlille 4 and Schandelah, where it is not limited by the XRF methodology, Cl shows considerably higher concentrations (graphs in Appendix 1). Observed was that tungsten (W) was not detected in significant concentrations in Stenlille, with LOD in all samples except for two. In Schandelah, it is present in all but 44 samples, and the average value is 698,75 ppm. Compared to the upper crusts average value of 1,3 ppm and average shale of 1,8 ppm, it is significantly higher. The stratigraphic trend of W shows a peculiar variation within the Schandelah samples, that corresponds to variations amongst Zr as well, and seems to be correlated to the litholgy. There seems to be a significant drop in concentration of W in Schandelah at around 300 – 317 m depth, aswell as in Zr. Notable is that concentration of Zr in Stenlille increases linearly with depth but oscillates with varying magnitude. On the other hand, zinc is present beyond LOD in 45 samples in Stenlille but limited by LOD in 55 samples in Schandelah (See stratigraphic variation in Appendix 1 and tables 3-4).

5.2 ICP-MS results

5.2.1 Summary

The ICPMS reports elemental concentration of 58 elements. The amount of samples analyzed was 34, 18 for Stenlille 4 and 16 for Schandelah. The elements that are reported are: B, Li, Na, Mg, Al, K, Ca, Cd, V, Cr, Mn, Fe, Hf, Ni, Er, Be, Ho, Hg, Ag, Cs, Co, Eu, Bi, Se, Zn, Ga, As, Rb, Y, Zr, Nb, Mo, In, Sn, Sb, Te, Ba, La, Ce, Pr, Nd, Sm, Gd, Tb, Dy, Cu, Ge, Tm, Yb, Lu, Ta, Sr, W, Re, Ti, Pb, Th and U. Elements that are limited by the detection limits of the ICP-MS, include Ba, In, and in many samples for Cd, Ag, As, Sn, Sb, Te, Ta, Re and in few samples for Tb, Ge and W. Those elements are excluded in further summary. Summary of 20 elements for both localities is presented in table 5 and 6 and the elements that are relevant for this research purpose are highlighted. Additional summary is included for the remaining elements in Appendix 2. When comparing the summarized elements in the table, between Stenlille and Schandelah by maximum values, there is a significant difference in some cases. Notably are higher concentrations in Schandelah in Fe, Ca, Ti, Mo, U, Co, Cu, Mn and Hg compared to Stenlille 4. In Stenlille 4 maximum values of Na, Zn and Ni are however relatively higher compared to Schandelah.

5.3 Addressing redox conditions

5.3.1 Normalization to Al

The normalization parameters were evaluated with comparison of aluminium and titanium. If both elements are contributed primarly by detrital flux, they should follow a similar trend. When analysing two variables, x and y with linear regression, the agreement between the variables can be tested. Then, the coefficient of determination (R^2) measures the proportion of variance between the variables. If there is a perfect linear agreement, with constant ratio between the x and y variables, it results in $R^2 = 1$. Any deviation between the agreements results in R^2 to decrease, and the lowest value $R^2 = 0$ implies that there is no agreement between the variables. Values that range between 0,7-1 are usually interpreted as a good correlation. However using R^2 can have problems when accessing datasets that are not normally distributed. Ti/Al ratios from the ICPMS results, show that there is a good linear relationship between the variables for Stenlille. Ti/Al coefficient of determination (R^2) for Stenlille yielded value of 0,7. For Schandelah, there are two intervals were Ti has significant “spikes above background levels” and are at depths 233,4 m and 318 m. That results in skews with the fit of linear regression. Removing those Ti samples from the dataset, as outliers, gives a high R^2

Table 5. ICP-MS measurements from Stenlille 4, reported in ppm (unless otherwise stated). n = 18 The elements labelled in bold are this study's main subject.

Element	***Min***	***1st qu.***	***Median***	***Mean***	***3rd qu.***	***Max***
Al (%)	*1,050*	*4,260*	*6,940*	*6,246*	*7,992*	*9,890*
Fe (%)	*1,330*	*2,195*	*3,525*	*3,220*	*4,013*	*5,940*
Na (%)	*0,2600*	*0,6500*	*0,8700*	*0,7889*	*1,0025*	*1,1200*
Mg (%)	*0,0400*	*0,5000*	*0,5950*	*0,6944*	*0,8975*	*2,0200*
K (%)	*0,670*	*1,145*	*1,545*	*1,578*	*1,873*	*3,110*
Ca (%)	*0,060*	*0,200*	*0,250*	*1,089*	*0,455*	*10,300*
Ti	*0,1600*	*0,3950*	*0,4350*	*0,4906*	*0,5700*	*0,8200*
V	*8,00*	*37,00*	*54,50*	*64,94*	*106,50*	*126,00*
Mo	*0,0800*	*0,2725*	*0,7450*	*1,0944*	*1,1675*	*3,8900*
U	*1,300*	*2,725*	*3,150*	*3,061*	*3,850*	*4,500*
Cr	*22,00*	*63,00*	*79,50*	*77,06*	*97,00*	*108,00*
Co	*2,60*	*13,65*	*16,00*	*16,72*	*19,43*	*31,20*
Cu	*7,40*	*19,82*	*24,65*	*25,12*	*32,35*	*41,20*
Mn	*139,0*	*174,2*	*284,5*	*422,9*	*501,2*	*1340,0*
Zn	*12,80*	*32,23*	*54,35*	*49,23*	*63,85*	*107,00*
Ni	*7,00*	*24,90*	*42,30*	*40,58*	*51,70*	*84,60*
Pb	*7,60*	*14,30*	*22,35*	*27,53*	*33,23*	*94,40*
Zr	*21,0*	*115,8*	*146,5*	*142,4*	*188,2*	*230,0*
Nb	*0,200*	*1,925*	*5,300*	*8,483*	*15,700*	*22,400*
Hg (ppb)	*10,00*	*50,00*	*70,00*	*64,44*	*77,50*	*110,00*

Table 6. ICP-MS measurements from Schandelah, reported in ppm (onless otherwise stated). n = 16 The elements labelled in bold are this study's main subject.

Element	***Min***	***1st qu.***	***Median***	***Mean***	***3rd qu.***	***Max***
Al (%)	*1,210*	*2,705*	*3,985*	*4,301*	*4,705*	*>10,000*
Fe (%)	*0,710*	*1,460*	*2,365*	*3,826*	*4,655*	*11,800*
Na (%)	*0,1800*	*0,2375*	*0,3150*	*0,3619*	*0,5100*	*0,6500*
Mg (%)	*0,100*	*0,1675*	*0,2800*	*0,6619*	*0,9450*	*1,9900*
K (%)	*0,100*	*0,6675*	*0,8550*	*0,9356*	*1,0325*	*2,2100*
Ca (%)	*0,050*	*0,305*	*2,860*	*5,236*	*4,277*	*25,00*
Ti	*0,1500*	*0,2325*	*0,3200*	*0,5544*	*0,4600*	*2,2200*
V	*23,00*	*27,00*	*50,00*	*68,38*	*99,25*	*170,00*
Mo	*0,120*	*0,390*	*0,665*	*5,134*	*1,075*	*53,200*
U	*0,2*	*1,5*	*2,3*	*4,8*	*3,0*	*41,6*
Cr	*18,00*	*39,50*	*60,00*	*60,69*	*80,00*	*100,00*
Co	*2,00*	*61,33*	*78,15*	*92,66*	*103,00*	*281,00*
Cu	*6,70*	*12,45*	*17,75*	*110,44*	*44,90*	*1400,00*
Mn	*47,0*	*193,0*	*589,5*	*864,9*	*1340,0*	*2380,0*
Zn	*8,30*	*12,12*	*21,55*	*21,99*	*26,55*	*54,50*
Ni	*0,300*	*0,600*	*1,500*	*3,119*	*2,325*	*16,200*
Pb	*5,40*	*8,60*	*12,20*	*35,82*	*19,52*	*171,00*
Zr	*2,0*	*36,75*	*78,0*	*90,19*	*130,25*	*207,00*
Nb	*0,300*	*0,600*	*1,500*	*3,119*	*2,325*	*16,200*
Hg (ppb)	*40,0*	*70,0*	*105,0*	*128,1*	*155,0*	*350,0*

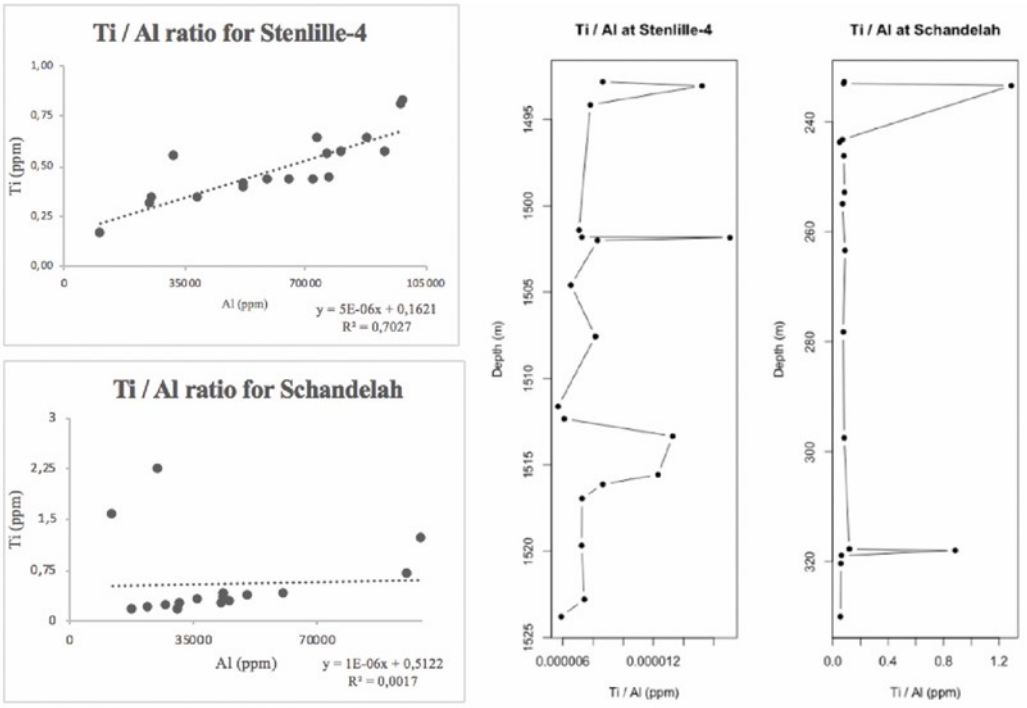

Figure 8. Evaluation of the normalization parameters, Ti and Al.

Table 7. Coefficient of variation (standard deviation / mean) of each of the following elements, Ratio to Al% is a relative difference of the coefficient of variation for the trace element divided to aluminium x 100, for relative comparison.

	V	Mo	U	Zn	Cr	Co	Ni	Cu	Al
Stenlille-4	*61%*	*107%*	*33%*	*50%*	*33%*	*36%*	*50%*	*36%*	*42%*
Ratio to Al %	*145%*	*255%*	*79%*	*119%*	*79%*	*86%*	*119%*	*86%*	-
Schandelah	*73%*	*261%*	*207%*	*56%*	*39%*	*66%*	*87%*	*312%*	*56%*
Ratio to Al %	*130%*	*466%*	*370%*	*100%*	*70%*	*118%*	*155%*	*557%*	-

of value of 0,8, that otherwise would result in 0,0017. Using Al is therefore preferred for normalization, as it suits better to depict the lithogenous fraction as it has no extreme values that deviate far from the rest of the values (see fig 8)

Another way to access if the normalization with Al is valid, is to compare the coefficient of variation of Al, to the coefficient of variation of other elements. This evaluation can be done for the trace elements addressed in this research. The coefficient of variation (relative standard deviation) is obtained by dividing the standard deviation (σ) of a variable with its mean (μ).

Coefficient of variaton = $(\sigma/\mu) \times 100\%$

This measures the dispersion of the data, and can be used for comparision between different series of data. To minimize the effect of spurious correlations, it is ideal to evaluate the value of the coefficient of variation of the common divisor (here Al) and to determine if its value is less than the coefficient values given for the trace elements (see table 7) for results of evaluation based on the coefficient of variation and comparison to coefficient of variation for Al. Comparing the ratios of the different coefficient of variation of trace elements (TE) with the coefficient of variation of Al for Stenlille 4, results are ranging < 200% except for Mo. In Schandelah, Mo, U and Cu range > 200%. The reason for these high ratios can be explained by a range of few max values that affect the distribution of the entire dataset. All high values are above the value for Al coefficient of variation, and validates the use of Al as a normalization parameter.

5.3.2 Trace elements enrichment factors (EF's)

Trace elements enrichment factors (EF's) were evaluated for V, Mo, U, Zn, Cr, Co, Ni, Cu and Mn and compared to average shale values reported by (Wedepohl 1971, 1991). The method is described in section 4.4. Mo, U, V, Zn are considered as trace elements of strong euxinic affinity and Cu, Ni, Cr and Co are considered to have weak euxinic affinity (Algeo & Maynard, 2004). The values are reported in table 8 for Stenlille 4 and in table 9 for Schandelah for each element and for each interval that was analysed in ICP-MS. The values that are enriched compared to values in average shale are marked in red. The values with very high EF are in bold (only in Schandelah). A

Table 8. Calculated EF¨s values for Stenlille 4, compared to average shale values. Showing subsequenct measured depth intervals from ICP-MS measured values. EF values > 1 are dashed with red colours.

Depth	V	Mo	U	Zn	Cr	Co	Ni	Cu	Mn	∑EF‘s
1492,82	0,94	0,93	1,24	0,57	1,37	1,02	0,72	0,80	0,40	3
1493,06	0,52	25,27	3,67	1,20	2,07	1,16	0,87	2,20	1,38	7
1494,15	0,56	0,10	1,58	1,04	1,77	1,59	0,81	0,67	1,16	5
1501,42	1,07	3,30	1,14	0,78	1,22	1,23	0,83	0,81	0,66	5
1501,81	0,62	0,16	1,40	0,84	1,64	1,54	0,81	0,78	1,19	4
1501,84	0,79	3,89	1,56	0,73	1,17	4,53	2,74	1,33	4,16	7
1502,01	0,84	0,62	0,81	0,65	0,93	0,94	1,12	0,66	0,52	1
1504,60	0,23	0,08	1,85	0,46	0,99	1,00	0,87	1,03	0,72	3
1507,57	0,57	0,15	1,06	0,57	0,72	0,91	0,84	0,83	0,31	1
1511,64	0,54	0,62	1,60	0,69	0,93	0,85	0,87	0,68	0,20	1
1512,34	0,81	1,64	1,17	1,07	0,65	0,74	0,72	0,78	0,18	3
1513,35	0,48	3,15	1,74	0,47	2,01	2,12	0,73	1,80	0,57	5
1515,57	0,60	1,82	1,76	0,72	2,16	2,51	0,68	1,51	0,98	5
1516,13	0,78	0,68	2,64	1,91	2,66	1,88	0,80	0,72	3,57	5
1516,95	0,96	1,00	1,23	0,79	0,95	1,57	0,77	0,56	0,31	3
1519,68	0,90	0,61	1,34	0,59	0,95	0,91	0,77	0,68	0,18	1
1522,8	0,48	0,34	2,20	0,57	1,61	1,16	0,60	0,97	0,58	3
1523,79	0,52	0,29	1,83	0,43	1,46	0,86	0,48	0,20	0,32	2
SUM	1	7	17	4	11	12	2	5	5	

Table 9. Calculated EF¨s values for Schandelah, compared to average shale values. Showing subsequenct measured depth intervals from ICP-MS measured values. EF values > 1 are dashed with red colours.

Depth	V	Mo	U	Zn	Cr	Co	Ni	Cu	Mn	∑EF‘s
232,7	3,78	2,985	**68,108**	0,54	3,165	16,674	1,5	**152,8**	0,76	**7**
233,0	1,01	0,343	1,755	0,42	1,710	10,978	0,7	0,3	0,31	4
233,4	1,41	**88,730**	0,490	0,70	1,469	31,245	11,0	7,3	4,64	7
243,2	0,89	1,070	1,760	0,46	1,956	7,894	0,9	0,8	0,84	4
243,7	0,55	1,434	1,147	0,36	1,275	15,546	0,7	1,1	1,39	4
246,2	1,05	1,481	1,699	0,51	1,730	10,982	0,9	1,1	4,23	6
252,8	0,83	1,472	1,595	0,51	1,462	**58,959**	0,7	2,1	3,01	5
254,9	1,00	0,313	1,973	0,38	0,915	2,580	0,8	0,2	1,12	3
263,4	1,55	1,346	1,627	0,57	1,808	14,561	0,7	0,7	1,98	6
278,2	0,72	4,246	1,177	0,43	1,355	12,753	0,7	0,9	0,59	4
297,5	3,19	0,451	1,465	0,69	2,442	6,761	0,9	1,0	6,84	5
317,7	1,06	3,782	1,215	0,51	0,790	2,962	1,4	0,9	0,21	5
318,0	1,42	**144,943**	1,889	0,87	1,417	28,707	4,4	5,0	9,17	8
318,9	0,30	0,135	1,465	0,45	1,025	4,270	0,6	0,2	2,67	4
320,3	0,63	0,223	1,679	0,53	1,334	10,153	0,7	2,3	4,35	4
330,0	0,36	0,900	1,506	0,18	1,209	0,216	0,2	0,3	0,11	2
SUM	9	10	15	0	14	15	4	7	10	

stratigraphic presentation of how the enrichments is distributed is presented in fig. 13 for Stenlille and fig. 15 for Schandelah.

5.3.3 TOC and comparison to TE's

The TOC concentrations reported from Stenlille 4 vary from 0,06 – 8,07 (wt %) (see fig 11). Amongst the set of samples analysed in this research by the ICPMS, the TOC concentration varies from 0,06 - 4,01 (wt %). For Schandelah samples, comparing with the TOC (wt %) reported by van de Schootbrugge (comm. Mail), involves problems for the reasons that the samples that have been analyzed for chemical composition do not correspond to depth intervals used for TOC concentration analysis. In best case an estimate can be made using the TOC (wt%) reported. The TOC levels from Schandelah range from TOC of 0,02 and 1,45 (wt %). Looking at the stratigraphic distribution of TOC in Stenlille, the values show a distinct interval with close to zero values ranging from 1501,84 m to 1511,26 m depths. At 1501,79 m in proximity to the TJB, it has a value that is considerably higher (8,07 % wt) than the background values. In the younger sediments (Jurassic) above the highest reported value, the average values of TOC is 1,55 (%wt) and in the older sediments (Triassic) it has an average of 1,02 (% wt). A lithological correlation is observed, with sediments composed of finer clay intervals seemingly having higher TOC content, compared to the coarser grained intervals. In Schandelah, a stratigraphic trend of this correlation is also observed, with more dynamic variation amongst bedding intervals of different grain sizes. Three intervals in Schandelah deviate from the „background" in TOC content. One around 334 m (Triassic) with the highest value of 4,16 (%wt), and from c. 330-336 m the values range considerarably higher. Another high range value is also reported around the TJB, at 318 m of 1,45 (%wt). A low value plateau is reported around c. 231-241 m (Jurassic). In sediments younger than 230 m there seems to be a general shift to a higher ranging values of TOC, falling closer around 1 (%wt) ranging around 0,4 (%wt) otherwise. The results of the comparison of trace elements to the TOC content for Stenlille 4 is presented in figures 9 and 10.

Algeo and Maynard (2004) proposed a scheme to evaluate redox conditions. They used comparison between two shale redox end-members (see further in section 4.4). The relative thresholds to define large EF's values and anoxic versus euxinic conditions considered here are based on their conclusion. They define an euxinic threshold of TOC values of ~ 10 wt% and an suboxic threshold of ~ 2,5 wt%. They also found an anoxic pattern manifested in samples with >10 wt% TOC and EF's values > 50-100 for V, Mo and Zn and EF's >1000 for U. In samples with TOC < 10 wt%, they observed moderate enrichments and strong TOC-TE relationship. For Cu, Ni, Cr and Co a different pattern was observed, with strong positive covariation at all TOC levels. The TOC content in the case for Stenlille 4 and Schandelah is below 10% wt in all cases. However, the intervals where enrichment occurs (EF's > 1), will be evaluated in comparison to those that are not enriched. Summary for each of the elements with the TOC-TE relationship is listed in section 3.4.4.

5.3.4 Summary of redox evaluation

A detailed summary of elemental concentration (table 11 and 12), evaluation of EF's (table 8 and 9) and comparison to TOC (Stenlille 4) (fig 8 and 9) was made for V, Mo, U and Ni. Their correlation and stratigraphic distribution are presented in Fig. 12 for Stenlille and Fig. 14 for Schandelah. Additionally Zn, Cr, Co, Ni, Cu and Mn are summarized, including evaluation of EF and comparison to TOC content. Stratigraphic overview is presented in Appendix 2 for the latter trace elements. A short summary of Hg also follows and stratigraphic presentation is included in Appendix.

5.3.4.1 Stenlille 4

Vanadium:

Elemental concentration of V range from 8 – 126 ppm, with average value of 65 ppm. Linear regression of V/ Al, results in a positive slope, and coefficient of determination (R^2) = 0,71. Compared to avarage shale, only one sample showed to be enriched, with EF > 1. Despite, the resulting value, it is very insignificant and equals 1,07. V has a weak correlation to TOC No samples fall within the criteria of having a Large EF's (EF's greater than 50-100). Given an anoxic threshold of TOC = 2,5 % wt, five samples reach beyond that threshold. The rest of them lie with the range of disoxic facies. The sample that shows EF's > 1 and falls beyond the threshold (TOC = 2,5 wt%) is at depth 1501,42 m. The samples that have TOC (wt %) > 2,5, with no relative enrichment are at depths of 1501,81 m, 1512,34 m, 1516,13 m and 1519,68 m. R^2 values between V normalized values with TOC, equals 0,19, indicating no correlation between the variables (see fig x.). Stratigraphic overview yields no distinct pattern, the highest peak is observed at 1501,42 m, and is not significantly higher than the other high-end intervals. The lowest value is located at depth of 1504,06 m (see fig.x).

Molybdenum:

Elemental concentration of Mo range from 0,08 – 3,89 ppm, with average value of 1,09 ppm. Linear regression of Mo/Al, gives R^2 value of 0,04 and a negative slope. Seven samples have EF value greater than 1. The highest EF value is 25,27 situated at depth of 1493,06 m. Of the five TOC values that exceeds beyond the 2,5 threshold, only two fall within the range of being enriched and are at depths of 1501,42 m and 1512,34 m. None would fall within the criteria of having a Large EF's (EF's greater than 50-100). Linear regression of Mo normalized values to TOC for samples with EF's > 1 equals R^2 = 0,23. For EF's < 1, R^2 = 0,01, thus meaning no significant correlation in both cases. When looking at the stratigraphic distribution of Mo/Al ratios a significant peak is observed at 1493,06 m relative to the overall distribution (see fig x). One sample at 1493,06 m depth is considerably higher than the rest of the samples with Mo/Al ratio value of 3,70. However at that interval the Al content is significantly low or 1,05

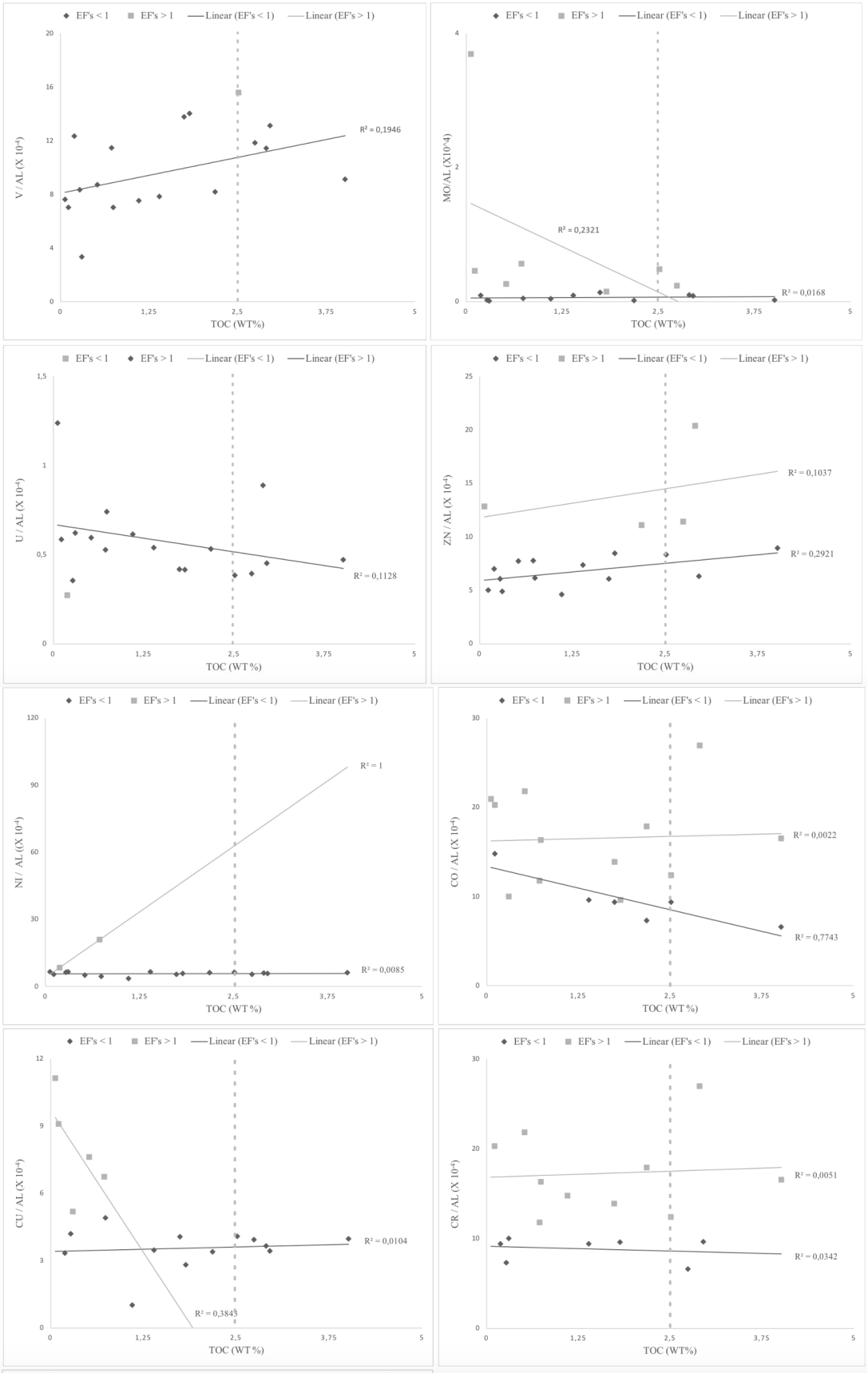

Fig 10. Correlation of Al normalized trace elements with TOC (wt %) for V, Mo, U, Zn, Ni, Co, Cu and Cr. For EF's < 1 and EF's > 1.

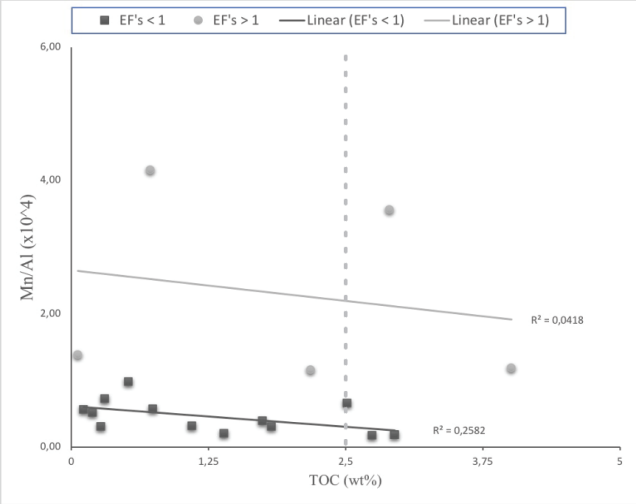

Fig 11. Correlation of Al normalized trace elements with TOC (wt %) for Mn. For EF's < 1 and EF's > 1.

%wt compared to the average of ICPMS Stenlille values that is 6,25 %wt. The Mo content, at this depth is 3,88 ppm and compared to the average shale content of Mo that is 1,3 ppm, it is 185% higher.

Uranium:
Elemental concentration of U range from 1,3 – 4,5 ppm, with average value of 3,06. Linear correlation when normalized to Al, gives R^2 = 0,49 with a positive slope. EF‘s relative to average shale over 1, are found amongst all samples except one. R^2 with normalized U to TOC equals 0,11, or no correlation. Highest observed U/Al peak is observed at 1493,06 m, that peak does not deviate to far from the other ratio values. The highest EF value is at 1493,06 m and equals 3,67, the reported U concentration value for that interval is 1,3 ppm. The highest U concentration is reported at depth of 1523,79 m as 4,5 ppm, compared to the average shale value of 3 ppm, makes a difference of 50%.

Zinc:
Concentration of Zinc range from 13,5 – 107 ppm, with average value of 49,2 ppm. When normalized to Al, linear regression gives R^2 value of 0,48 and a positive slope. Four samples have EF > 1. Samples with EF‘s > 1 and TOC > 2,5 are at depths of 1512,34 m and 1516,13 m. R^2 of normalized Zn values with TOC and EF‘s > 1 is 0,10 and EF‘s < 1 equals to 0,29, resulting in no correlation with TOC content. Stratigraphic distribution of Zn normalized to Al, show one considerable high peak at 1516,13 m (20,41), there the reported concentration value is 80,2 ppm, compared to an average shale value of 95 results in a negative 18,85 % difference. The highest Zn value reported is 107 ppm at depth of 1512,34 m or 12,6% higher then in average shale.

Chromium:
Chromium ranges in concentration of 22 – 108 ppm, and average value of 77 ppm. Linear regression to Al gives R^2 value of 0,27 and a positive slope. Of the samples, 11 show EF‘s > 1. Samples with EF‘s > 1, and TOC > 2,5 are situated at 1501,81 m, 1512,34 m and 1516,13 m. R^2 for Cr normalized values to TOC show no correlation, given values of EF‘s < 1 = 0,03 and EF‘s > 1 = 0,01. Stratigraphic overview yields one relatively higher peak, located at 1516,13 m depth with value of 106 ppm, compared to average shale is 17,8% difference.

Cobalt:
Concentrations of cobalt range from 2,6-31,2 ppm with average value of 16,9 ppm. When normalized to Al, linear regression yields R^2 value of 0,39 and a positive slope. Correlation to TOC gives coefficient of determinaton for EF‘s > 1 equalling 0,01 and for EF‘s < 1 equals to 0,77. Of the samples, 12 have EF‘s values > 1, and 6 samples < 1 relative to average shale. Cobalt seems to be a negative relationship of EF‘s < 1, not seen amongst the samples with EF < 1. Caution should be with interpretation, since the result is based on population of six values for the EF´s < 1. In a stratigraphic overview, of Co/Al, it shows to have a distinctive high peak at 1501,84 m with ratio of 9,69. At that point, the concentration of Co is ~31 ppm. Compared to average shale‘s value of 19 ppm, leads to a difference of a 63,2%.

Nickel:
Nickel ranges from 7,0 - 84,6 ppm, with average value of 40,6 ppm. When normalized to Al, linear regression yields R^2 value of 0,55 and a positive slope. Two samples have EF‘s > 1. Sample depths of the EF values above 1 are located at depths of 1501,84 m and 1502,01 m. Amongst the values with EF‘s < 1, no linear relationship exists with TOC (R^2 = 0,01). The population of EF‘s > 1 is made up of two sample values and no correlation test can be made . Noticeable is that stratigraphic distribution of Ni/Al ratios show a distinct very stable curve except at depth of 1501,84 m where the EF value is 2,74 (and highest EF value). There, the Ni concentration value is 67,5 ppm equivalent to average shale (68 ppm), resulting in a small difference of 0,74%. The mean value for Ni in Stenlille is however 40,58 ppm andrel-atively low in comparison.

Copper:
Copper ranges in concentration from 7,4-41,2 ppm, with an average value of 25,1 ppm. When normalized to Al, linear regression yields R^2 value of 0,43 and a positive slope. Five samples give EF‘s result of > 1. None of the EF‘s > 1 falls beyond the 2,5% TOC threshold. Very weak negative correlation is apparent for samples with EF‘s > 1, one should be cautius with drawing conclusions from it, since it is based on 5 points. Normalized to Al, and set in correlation with TOC for R^2 value of the EF‘s > 1 equals to 0,38, which is weak and unsignificant correlation, with a negative slope. EF‘s < 1 gave value of 0,01. Cu is distributed rather randomly in a stratigraphic overview. The three highest peaks are located at 1493,06 m, 1501,84 m and 1513,35 m. One distinctively low value is reported at 1523,79 m.

Manganese
Manganese (Mn) ranges from 139,0 ppm to 1.340 ppm with average of 422,9 ppm. In average shale, the Mn trace elemental concentration is reported as 850 ppm. When normalized to Al, it shows a R^2 value of 0,07. For Mn, five values have EF‘s > 1, with highest value of 4,16 at depth of 1501,84 m. There the elemental concentration is 1280 ppm, and compared to average shale value of 850 ppm shows to be 50,6% higher. Overview of Mn normalized to Al, shows two „high peaks“ , firstly the pre-mentioned, with the high EF value at 1501,84 m and another one at 1516,13 m.

Mercury
Mercury (Hg) concentrations range from 10 – 110 ppb, with average value of 64 ppb. When normalized to Al, gives R^2 value of 0,04 with a negative slope. When normalized to the TOC content, it also displays an insignificantly low correlation or R^2 that equals 0,25 and a positive slope.. In stratigraphic overview of Hg/ Al, it shows a relatively high peak interval at 1493,06 m. Smaller peaks are found at 1501,81 m, 1504,06 m and higher range is observed between 1513,35 – 1516,13 m (see appendix).

Iron
Iron (Fe) concentration from ICP-MS in Stenlille range from 1,330 – 5,940 %, with average value of 3,220%. When regressed to Al it gives an R^2 value of 0,244 and a positive slope. In a stratigraphic overview there are three distinctive high peaks observed at 1493,06 m, 1501,84 m and 1516,13 m. Comparison can be made between Fe normalized to Al XRF results (Appendix 1(IV)) and the ICP-MS results (Appendix 2).

Stratigraphic trend for Stenlille
The EF‘s values were summarized in a stratigraphic overview (Fig. 13). This figure deomonstrates the intervals that have co-occurring enrichments. The highest enrichment is observed in Mo, at depth of 1493,06 m and at that interval, enrichment is shown in 7 of 8 elements used for estimation. Another depth interval, where enrichment is observed in more than 7 elements is at 1501,84 m, with Mo being most enriched. Other intervals show considerably lower levels of enrichment.

5.3.4.2 Schandelah

Vanadium:
Elemental concentration of vanadium (V) ranges from 23 – 170 ppm, with average value of 65 ppm. Weak positive linear correlation is present when normalized to Al, and R^2 = 0,31. Highest observed values are in two relatively higher peaks at intervals of 232,7 m and 297,5 m. Compared to average shale, nine samples classify as being enriched, with EF’s > 1. Most range with EF values between 1-2. At the pre-mentioned depth intervals, the EF‘s value is 3,78 and 3,19 respetively. The highest V concentration is reported as 170 ppm (at 297,5 m depth), and the difference compared to average shale (value of 130 ppm) is 30,8%.

Molybdenum:
Molybdenum (Mo) ranges from 0,12 to 53,2 ppm with average value of 5,13 ppm. When normalized to Al, it gives R^2 = 0,31 and a slightly negative slope. Two values deviate considerably from the linear trendline, with values that are three to tenfold higher than the average, and are observed at depths of 233,4 m (EFs = 88,7) and the highest at 318,0 m (Efs = 144,9). The two peaking values can be classified as having a „Large enrichment value“ (EF value between 50-100). Eight samples have EF‘s values ranging from > 1 to 4,2. Comparing the highest observed value of Mo that is 53,2 ppm, to average shale that is reported as 1,3 ppm gives relative difference of 3990%, which is significantly higher. The lesser prominent peak has relative difference to average shale value for Mo of 1108%.

Uranium:
Uranium (U) ranges from 0,2 to 41,6 ppm with average value of 4,8 ppm. When normalized to Al, one sample deviates greatly from the sample data set, R^2 = 0,05 and a slight negative slope . Slight enrichment is apparent (EF‘s > 1) compared to average shale within all samples except for one, and are all under EF = 2, except for one that has EF‘s = 68,1 at 232,7 m depth. For U that is not considered as a „Large enrichment“ as it must exceed EF‘s > 1000 for that, however that enrichment is significant.

Zinc:
Zinc (Zn) ranges from 8,3 – 54,5 ppm, with average value of 22,0 ppm. When normalized to Al, a relatively strong positive linear relationship exists as R^2 = 0,70 , indicating that it is controlled dominantly by detrital flux. Compared to average shale, all samples are depleted, to an average of EF = 0,50, and is Zn the only element remarkedly depleted in all samples in comparison to the average shale, given value of 95 ppm. Thus on average, the depletion equals 332%. Stratigraphic trend for Zn, displays 3 gradually high intervals, that do not deviate from the trendline in general. Three highest intervals are present at 232,7 m, 233,4 m, and 252,8 m.

Chromium:
Chromium (Cr) ranges from 18 – 100 ppm, with

average value of 61 ppm. When normalized to Al a poor linear fit exists between the variables, with R^2 = 0,43 and a positive slope. In stratigraphic overview, there are no great outlying values, indicating that the elemental accumulation is not entirely controlled by the detrital fraction. There are 14 out of 16 samples with EF‘s > 1, none with large enrichments. The EF‘s value are mostly ranging between 1-2, and the highest EF‘s values of 3,2 and 2,4 are located at depths of 297,5 m and 232,7 m respectively. Compared to average shale, the highest Cr value observed in Schandelah is 11,1 % higher.

Cobalt:
Cobalt (Co) ranges from 2,0 – 281,0 ppm with an average value of 92,7 ppm When normalized to Al, there is no linear trend aparent, R^2 = 0,11, the slope of the trend-line is negative. Compared to average shale, all samples show enrichment, except for one sample. One fits the criteria of having a large EF of 59,0 at 258,2 m, with reported value of 281, compared to average shale (19 ppm) makes a difference of 1379% higher. Stratigraphic distribution show two other not as pronounced peaks at 233,4 m and 318,0 m.

Nickel:
Nickel (Ni) ranges from 6,8 – 137,3 ppm with an average value of 37,3 ppm. When normalized to Al, R^2 = 0,10 with a positive slope. Only 4 samples have EF‘s > 1, The highest EF value is 11,0 (depth of 233,4 m) and following the second highest, EF‘s = 4,4 (at 318 m) and then there is slight enrichment observed with EF‘s of 1,5 and 1,4 (at depths of 232,7 and 317,7 m respectively). The enrichment distribution with depth covaries with the enrichment observed for Mo. Looking at the stratigraphic distributions, shows a generally low value, evenly distributed ratio, except at the two observed peaks. Compared to average shale the value at the highest EF level, is 102 ppm, and in the second highest peak is 108 ppm. Compared to average shale (68 ppm), those value differentiate as 50% and ~ 59%.

Copper:
Copper (Cu) ranges from 6,7 – 1400,0 ppm with average of 110,4 ppm and median value of 17,75 ppm. When normalized to Al, no correlation is aparent. No correlation is further seen after removal of the highest value. The highest value is significantly greater than the second highest (by two orders of magnitude). The highest value (1400 ppm) is located at depth of 232,7 m. Comparing to the average shale (45 ppm) results in 3010% difference. When compared to average shale, seven samples show EF‘s > 1. The value that was significantly highest, is enriched to an EF‘s of a 152,8 (at depth of 232,7 m) which is classified beyond being a large enrichment (EF‘s 50-100). Six other samples show enrichment with EF‘s = 1,1 – 7,3.

Manganese
Manganese (Mn) ranges from 47,0-2380 ppm with average value of 864,9 ppm (median of 589,5). When normalized to Al, linear regression yields R^2 = 0,01. Highest EF‘s value for Mn is 9,17, located at depth of 318,0 m. The highest concentration of Mn is reported at depth of 297,5 m and equals 2380 ppm. Comparing to average shale (850), leads to a difference of 180%. Mn/Al stratigraphic trend shows that higher peak intervals seem to be more condensed in older sediments, below 297,5 m, however the sample population is not great (n=16).

Mercury
Mercury (Hg) ranges from 40 – 350 ppb, with average value of 128,1 ppm. When normalized to Al, linear regression yields R^2 = 0,11 and a negative slope. Stratigraphic overview shows two pronounced peaks at two depth intervals, that range beyond the trendline, located at 231,4 m and 318 m.

Iron
Iron (Fe) ranges from 0,710 – 11,8%, with average value of 3,826%. When normalized to Al, R^2= 0,01. Removing the two highest values, considered as outliers, results in R^2= 0,63 and a positive slope. Fe/ Al, stratigraphic overview shows two higher range intervals, located at depths of 233,3 m and relatively lower one at 318 m.

Stratigraphic trend for Schandelah
The EF‘s values were summarized in a stratigraphic overview (Fig. 15). Compared to Stenlille, there are more high EF‘s apparent in Schandelah, and they also range considerably higher. The highest enrichment is observed in Cu at 232,7 m, U is also considerably enriched at that interval. Cu is generally not enriched, expect at two interwals, and the second interval is just a slight insignificant enrichment. Zn is depleted in all samples compared to average shale, resulting in all Efs values ranging below 1. At depth of 318,0 m, enrichments occurs in in most frequency, or within 8 elements. 232,7 m and 234,4 m

5.4 Further assessment on EF’s

All the analysed intervals from XRF and ICP-MS that included enrichments > 2 compared to average shale were summarized for each locality (tables 11 and 12). If there were overlapping values, the ICP-MS values were preferred as they are provided with more precision and accuracy. The reason for setting a EF‘s values > 2 threshold is to allow relative assessment between Stenlille 4 and Schandelah and also to exclude values provided from XRF that are not significantly enriched or amplified by the larger error range of the XRF. If the EF‘s value reach the criteria proposed by Algeo and Maynard (2004), they are highlighted with bold capitals. The major elements from those corresponding intervals, Al, Ca, Fe and S were normalized to 100% of total concentrations. This is a normative approach for getting an overview of the bulk geochemistry confined by those specific elements. However, for sedimentary rocks, it comes with many problems as sediments are usually consisting of different minerals from different sources, as of quartz, feldspars, clays, carbonates, oxides, sulphides and organic matter. To differentiate the different phases present, a close up investigation has to be made including spot analysis to look at which phases are present and which incorperate trace

Table 10. Results of a normative approach for accessing the major elements Si, Al, Ca, Fe, S for Stenlille 4 and Schandelah.

Average values normalized to 100%	% Si (wt)	% Al (wt)	% Ca (wt)	% Fe (wt)	% S (wt)
Stenlille 4 (n~50)	72,2	14,8	3,2	7,9	2,0
Schandelah (n~154)	66,8	17,1	4,8	10,1	1,2

Table 11. Depth intervals with reported EF´s values > 2, compared to average shale for V, Mo, U and Ni and the concentrations of the major elements norm to 100% of bulk concentration for each depth interval. XRF values are used in calculations for majors, as Si concentrations are not reported by the ICP-MS. LOD represents values limited by XRF.

Stenlille 4	Depth (m)	EF's V	EF's Mo	EF's U	EF's Ni	% Si (wt)	%Al (wt)	%Ca (wt)	%Fe (wt)	%S (wt)
XRF	**1492,54**	**48,3**	**12,2**	**17,99**		74,7	22,7	0,7	LOD	1,9
	1498,18	**63,6**	**18,8**	**18,47**		79,2	15,0	5,2	0,2	0,3
	1501,60		4,5			74,5	16,0	2,2	6,5	0,8
	1522,33			2,71		88,0	8,6	0,2	2,8	0,3
ICP-MS	**1493,06**		**25,3**	3,7		95,9	2,8	0,1	1,0	0,2
	1501,42		3,3			68,1	18,9	1,2	10,5	1,3
	1501,84		3,9		2,7	50,2	8,0	26,9	8,8	6,1
	1513,35		3,2			87,0	8,1	0,6	2,9	1,3
	1516,13			2,6		76,0	10,9	0,8	12,0	0,3
	1522,80			2,2		81,9	12,3	0,5	5,0	0,4

Table 12. Depth intervals with reported EF´s values > 2, compared to average shale for V, Mo, U and Ni and the concentrations of the major elements norm to 100% of bulk concentration for each depth interval. XRF values are used in calculations for majors, as Si concentrations are not reported by the ICP-MS. LOD represents values limited by XRF.

Schandelah	Depth (m)	EF's V	EF's Mo	EF's U	EFs Ni	% Si (wt)	%Al (wt)	%Ca (wt)	%Fe (wt)	%S (wt)
XRF	**230,4**	2,6				37,7	19,2	7,8	34,8	0,6
	231,3	**12,2**				36,1	8,2	16,8	38,8	0,1
	232,4	8,4				68,2	5,4	7,0	19,1	0,2
	263,3	5,4				40,7	5,4	20,1	33,5	0,4
	264,0	5,5				59,4	3,5	22,8	12,4	1,9
	266,1	5,1				81,9	3,5	1,9	12,3	0,3
	266,3	5,5				90,1	3,3	0,9	5,7	LOD
	317,9		6,63			51,4	23,8	0,8	15,4	8,6
ICP-MS	**232,7**	3,8	3,0	**68,1**		26,4	5,0	62,0	4,9	1,6
	233,4		**88,7**		**11,4**	7,4	4,4	51,5	19,7	16,9
	263,4	2,1				69,2	11,9	8,7	9,5	0,7
	278,2		4,2			85,3	8,6	0,3	4,0	1,8
	297,5	3,2				38,5	11,9	36,5	12,0	1,1
	317,7		3,0			54,0	25,2	0,6	13,8	6,4
	318,0		**144,9**		4,4	45,5	6,5	9,9	20,1	18,0

Table 13. Estimation of the relative authigenic enrichments in samples with EF's > 2 in reference to average shale composition. Detrital part = $(TE_{av.sh.}/Al_{av.sh})*TE_{sample}$. Authigenic = Detrital part - TE_{sample}. Authigenic partition can include sulphides, oxides, carbonates or organic matter. (Note that after TOC analysis, Ni, could reside in the organic fraction).

Stenlille 4		**U**		**Mo**		**V**		**Ni**	
	Depths (m)	**% detr.**	**% auth.**	**% det.**	**% auth.**	**% detr.**	**% auth.**	**% detr.**	**% org..**
XRF	1492,54	**5,6**	**94,4**	**8,2**	**91,8**	**8,2**	**97,9**	x	x
	1498,18	**5,4**	**94,6**	**5,3**	**94,7**	**5,3**	**98,4**	x	x
	1501,60	x	x	22,2	77,8	x	x	x	x
	1522,33	36,9	63,1	x	x	x	x	x	x
	Depths (m)								
ICP-MS	1493,06	27,3	72,7	4,0	96,0	x	x	x	x
	1501,42	x	x	30,3	69,7	x	x	x	x
	1501,84	x	x	25,7	74,3	x	x	36,5	63,5
	1513,35	x	x	31,7	68,3	x	x	x	x
	1516,13	x	x	x	x	x	x	x	x
	1522,80	x	x	x	x	x	x	x	x

Table 14. Estimation of the relative authigenic enrichments in samples with EF's > 2 in reference to average shale composition. Detrital part = $(TE_{av.sh.}/Al_{av.sh})*TE_{sample}$. Authigenic = Detrital part - TE_{sample}. Authigenic partition can include sulphides, oxides and carbonates. (Note that after TOC analysis, Ni, could reside in the organic fraction).

Schandelah		**U**		**Mo**		**V**		**Ni**	
	Depth (m)	**% detr.**	**% auth.**	**% detr.**	**% auth.**	**% detr.**	**% auth.**	**% detr.**	**% org..**
XRF	230,4	84,4	15,6	x	x	38,8	61,2	x	x
	231,3	x	x	x	x	**8,2**	**91,8**	35,3	64,7
	232,4	x	x	x	x	11,9	88,1	x	x
	263,3	x	x	x	x	18,4	81,6	x	x
	263,4	x	x	x	x	46,7	53,3	x	x
	264,0	x	x	x	x	18,0	82,0	x	x
	266,1	x	x	x	x	19,7	80,3	x	x
	266,3	x	x	x	x	18,1	81,9	x	x
	317,9	x	x	15,1	84,9	x	x	x	x
	Depth								
ICP-MS	232,7	1,5	98,5	33,5	66,5	26,5	73,5	x	x
	233,4	x	x	1,1	98,9	x	x	9,1	90,9
	278,2	x	x	23,6	76,4	x	x	x	x
	297,5	x	x	x	x	31,3	68,7	x	x
	317,7	x	x	26,4	73,6	x	x	x	x
	318,0	x	x	0,7	99,3	x	x	22,9	77,1

elements and how. These observations could be observed in pyrite and in carbonate minerals. The effects of changes in oxygen availability on those phases need to be well constrained additionally. Without any constrains, the overlaps of the elements as the chemical constituents for each phase cannot be determined. The reason for this comparison here, is to see if there is any general trend in the concentrations of the majors chosen, linked with the level of EF's. All average values from XRF of Al, Ca, Fe and S were normalized to 100% for comparison in each locality. There seems to be a good agreement between the average compositions for these elements in Stenlille 4 and Schandelah except for slight difference with S, which is relatively higher in Stenlille 4 (looking at median values in tables 3 and 4). However the differenece is not so apparent looking at the values from Table 10. In Stenlille 4, two opposing situations occur where enrichment in V, Mo and U is detected. At depth 1492,54 m a depletion in Fe and relatively high Al concentration could indicate that the enrichment follow an increased clay or feldspar concentration. At 1498,18 m, Fe and S are relatively low, but Ca is high, indicating enrichment in carbonates. In Schandelah, where the highest U and Mo enrichment occurs, the Ca content is relatively high at depths of 232,7 m and 233,4 m. In the former S and Fe are relatively low and that is the level where enrichments in all V, Mo and U are observed above EF's > 2. Concluding that enrichment is rather linked with carbonates, So in both cores, enrichments is rather linked with carbonates.

For those depth intervals with EF's > 2, including both XRF and ICP-MS measurements, the detrital versus authigenic part was evaluated in each locality. The stepwise procedure can be viewed in table in Appendix 4. The percential fraction of each corresponding element is summarized in table 13 and 14. Average shale ratio of trace elements versus Al

were used as reference material. It must be noted that average shale values do not necessary represent the environment for the Stenlille 4 and Schandelah samples as it has been shown in this study that the averaged Al values at both localities are lower than in average shales. It could be possible to use median or mean values as well from the results herein. Additionally, it should be noted that the concentrations reported from the XRF do include more uncertainties compared to the ICP-MS results, and careful approach should be made when evaluating thoese intervals except in cases that are well beyond the instruments limitations. EF's > 10 from XRF analysis are marked with bold capitals (see tables 11 and 12).

5.5 Analytical comparison of XRF and ICP-MS

Comparison between the two analytical teqniques of X-ray fluorescence (XRF) and inductively coupled plasma mass spectrometry (ICP-MS) were made, for comparison of measurements of elements in major concentrations Al and Fe. Including concentrations of minor trace elements V, Mo, Zn, Cu, Ni, Mn, Cr, and additionally for U in Schandelah (Appendix 6). Both are powerful analytical technique for applications in geosciences, but as for precision goes, the ICP-MS method has more significance. The results from the ICPMS and XRF were analysed with linear regression and X-axis representing the ICPMS results and Y-axis the XRF results. The ICPMS results were used for reference, on the premises that they should represent more accuracy to the actual value. The results are based on 18 samples for Stenlille, and 16 for Schandelah. All LOD values in XRF were excluded from comparison, which explains the variance in population size. The XRF method provided excellent correlation (R2 > 0,91) when analysing the major elements Al and Fe. It is important to keep in mind the population number representing each element as there is more uncertainity in estimating small populations. An increase in variance also adds additional uncertainty. One way to evaluate spread of variables is to look at the values given by the coefficient of variation (standard deviation/mean). The relative difference of the average shows weather the analytical method under (in red) or overestimates (in blue) the reported values relative to XRF. In Stenlille, samples with population > 10 and R2 > 0,85 are reported for Al, Fe, Zn and Mn. In Schandelah there are reported for Al, Fe, Cu. However the coefficient of variation for Cu is considerably high (245% in XRF and 255% in ICP-MS). In Stenlille 4, elements with sample population > 10 and moderate linear correlation R2 > 0,75 is V and in Schandelah V and Mn.

5.6 $\delta^{13}C_{org}$ results of Stenlille 4

Table (Appendix 5) lists all the measurements of the bulk $\delta^{13}C_{org}$ values from Stenlille 4 study section, combined with previously collected data of bulk $\delta^{13}C_{org}$ values. The total population of samples is 88. Of those values 43 are reported for the first time herein with 45 values previously measured and reported by GEUS. Fig. 11 shows the stratigraphic profile of the $\delta^{13}C_{org}$ content, when these values have been combined together in a graph. A separate profile from values reported here can be viewed in fig. 12. The $\delta^{13}C_{org}$ values range from -43,1 to -24,4 ‰ (VPDB). The lowest value of -43,1 ‰ is out of normal range for organic matter and therefore is considered as an outlier. The reason why it has so low values could be due to the limited concentration of carbon in the sample or contamination of the original signal, following diagenesis. The second lowest value is at -34,3 ‰ and is also excluded as it does as well deviate from typical values. Looking at the values reported in terms of stratigraphic distribution, the most apparent major negative shifts, are three and are concentrated between 1501,6 m, 1507,6 m and 1519,68 m. Two lesser ones are observed at 1514,15 m and 1516,95 m. A relative great positive excursion (-24,43‰) is observed at 1519,12 m. The magnitude of the value difference from that more positive value to the following greater negative one, given from that interval is 3,96‰. From 1492,54 -1501,42 m, the variations of the values are more subtle (with average of -25,5‰) and magnitude difference of 1,2‰. The interval from 1507,17 - 1523,79 m (average of -26,8‰), shows more prominent shifts with more regularity compared to the one with the subtle variations, and has a magnitude difference of 3,0‰, and probably reflects variations in lithology or composition. A second relative large negative excursion of magnitude of 4,0‰ is at depth of 1506,1 m. Except those two, negative excursions of greater magnitude than 2‰ , are not detected. After combining the pre-existing values that had already been obtained by GEUS, a more complete profile could be made, with sum of 88 values. The relative difference of the averaged values of each population reported here and GEUS equals 2,4%. Overall the trend for Triassic sediments shows to have greater deviations, compared to the more „fixed" and smooth trend for Jurassic sediments. Three large negatives excursions occur at three intervals before the greatest one that seems to be correlated to the TJB (figure with values reported herein are presented in fig 12).

6 Discussion

6.1 Additional observations and the role of diagenesis

Important is to evaluate the geochemical observations with other indicators within the sediments, that could provide siginificant supplementary information. That includes observations of fossils and biofaces within, or post diagenic processes that can remobilize the sediments. Observing changes in colour, lithology and ichnofabric (laminated versus bioturbated) are all useful indicators for different environmental conditions. The behaviour of elements that have been authigenecly enriched varies throughout diagenesis, and can be influenced by range of constraints, like different pH and Eh conditions. They also accumulate to a different degree in varying phases, as of metal sulfides, solid solution in pyrite, within insoluble oxides and oxyhydroxides, phosphate, sulfate, organometallic complexes and adsorbed on organic or mineral surfaces (Tribovillard et al, 2006). Immobility of many trace elements depends on oxygen availability

Stenlille 4

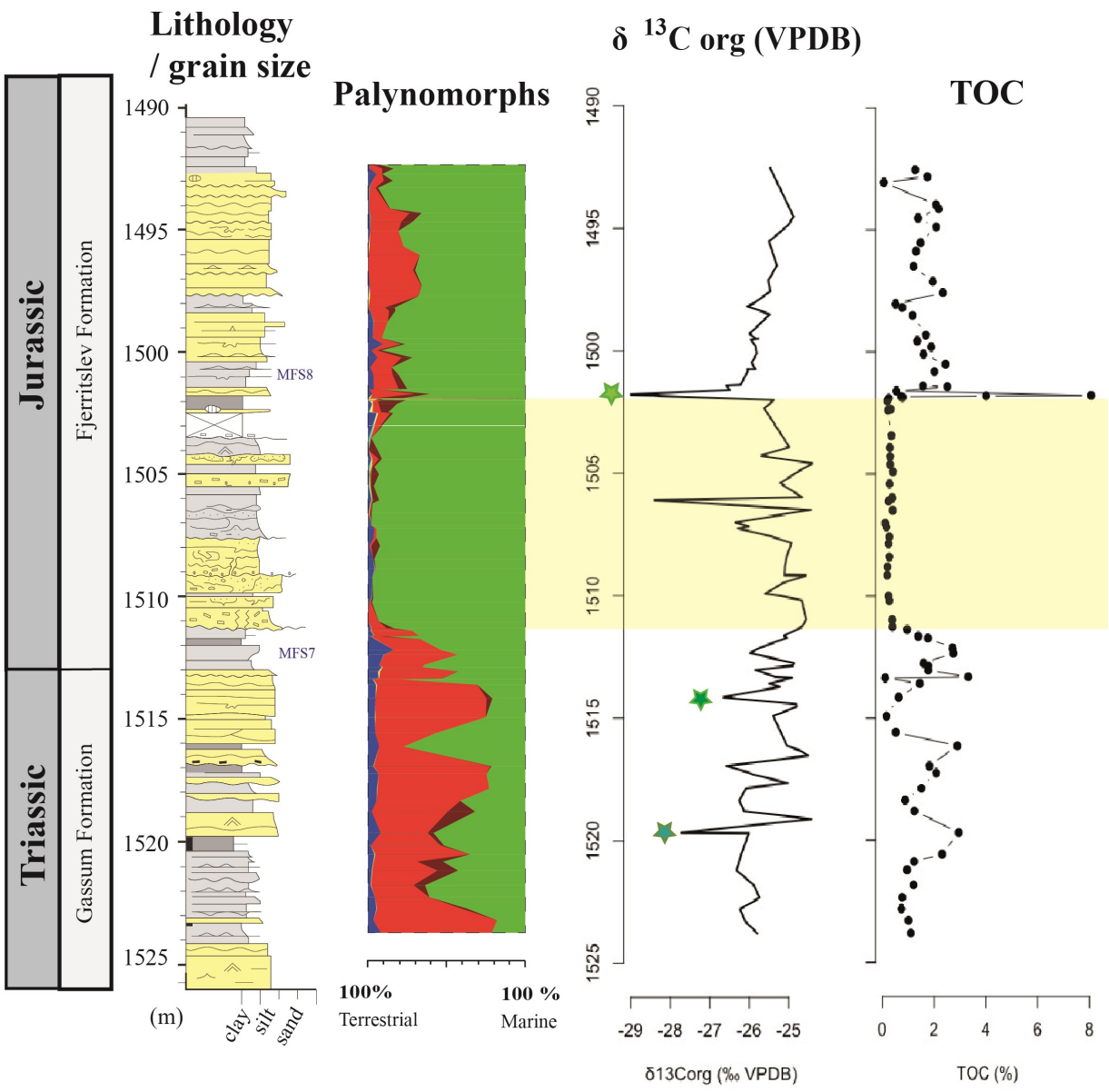

* **Suggested Spelae CIE**

Suggested Marshi CIE

Suggested Pre-Marshi CIE

Palynomorphs Legend:

- Acritarcs - marine
- Microalgae - freshwater
- Microalgae - freshwater (primarily Botryococcus ALBO)
- Dinoflagellate cysts - marine
- Miscellaneous microfossils
- Miscellaneous palynomorphs
- Spores and pollen

Figure 11. A stratigraphic illustration of the Stenlille 4 lithological variations (Lindström et al. 2019), combined with a schematic palynomorph, terrestrial versus marine assemblage chart after Lindström et al. (in prep). Including a combined chart with $\delta^{13}C_{org}$ data reported here, combined with a data gathered from GEUS. Lastly is a graph representing the TOC content for Stenlille 4 (data from GEUS). The yellow shaded emphasizes an area where dinoflagellate cysts are considerably absent as observed from the palynomorph chart (however this range coincides with the range of the gray siltstone interval from Fig 3).

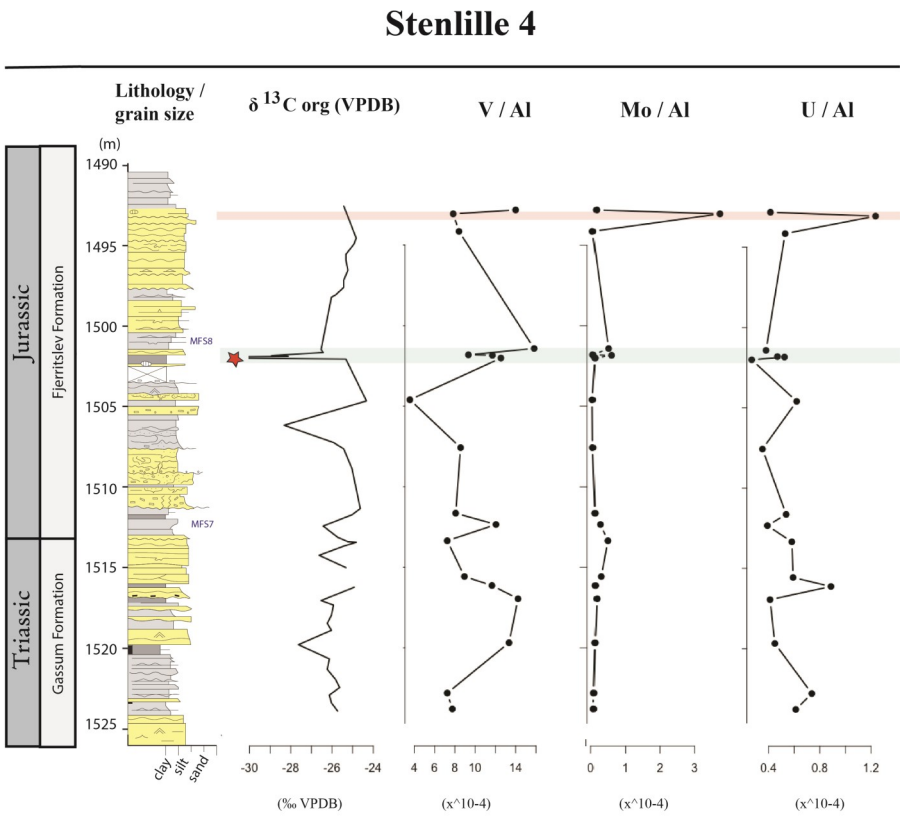

Figure 12. A stratigraphic illustration of Stenlille 4, showing stratigraphic trend of normalized values of V, Mo and U in regards to the Al content of ICP-MS values reported here. Including is the $\delta^{13}C_{org}$ values reported here without GEUS data. The red shaded area emphasizes the samples that had higher levels of normalized V, Mo and U. The green shaded area emphasizes the most negative CIE here.

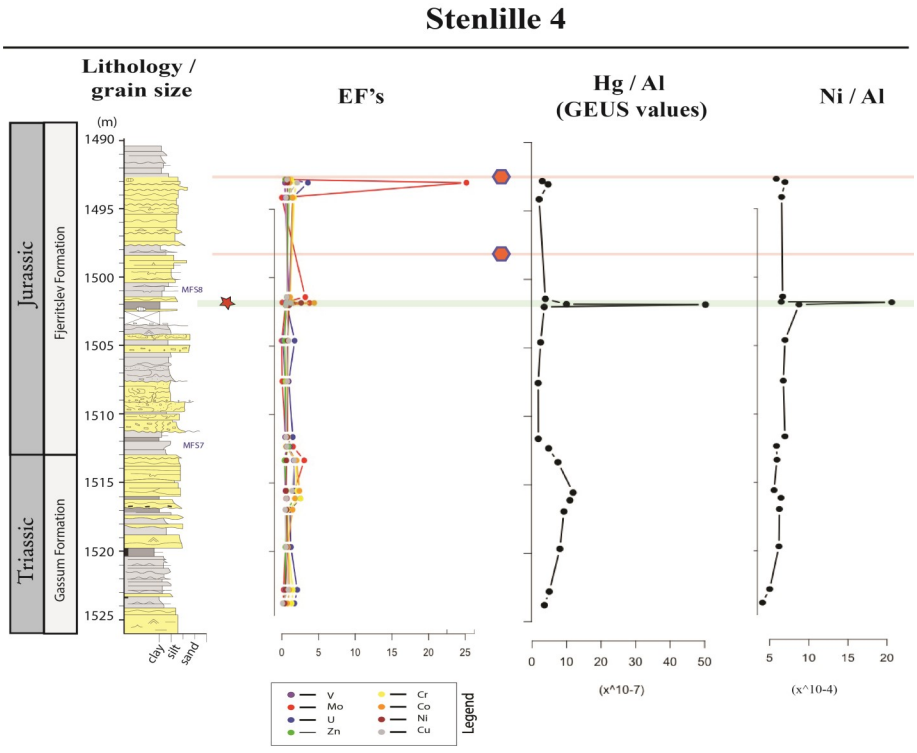

Figure 13. A chart that shows the relative distribution of EF's values of V, Mo, U, Zn, Cr, Co, Ni and Cu. Additionally reported normalized to Al, Hg and Ni content. Note that EF's are reffered to the average shale content. Based on ICP-MS values. The polygons refer to the high covarying interval of V, Mo and U observed from XRF data. The green shaded area and the star represent the location of the largest negative CIE excursion from this study. The stratigraphic chart is from Lindström et al. 2019.

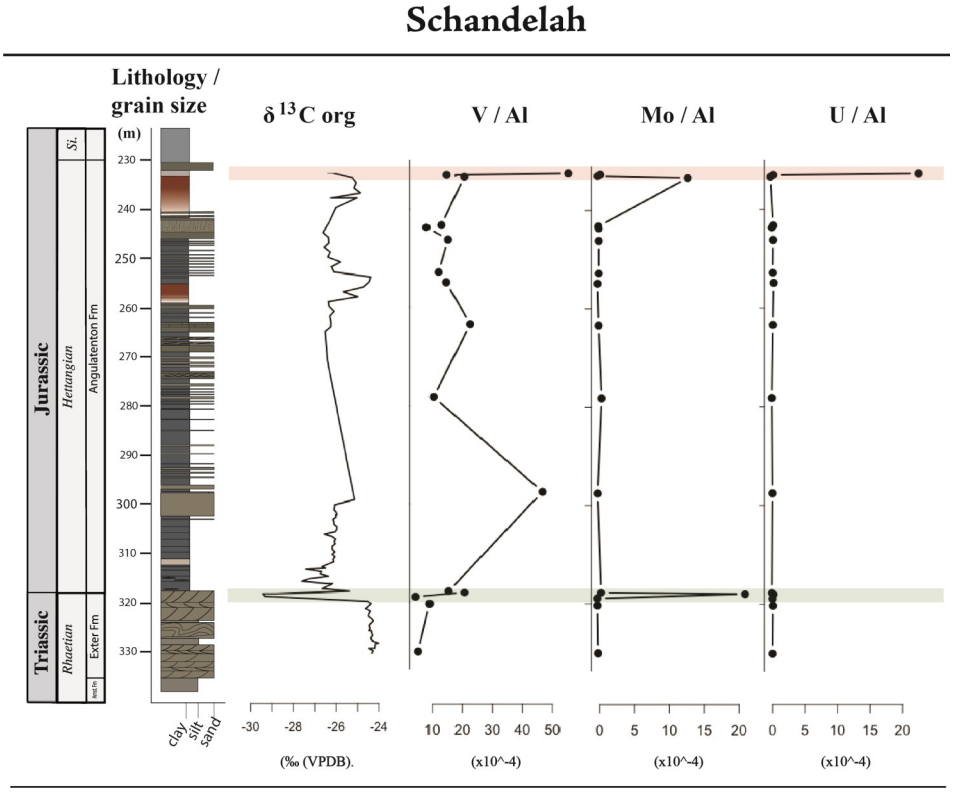

Figure 14. A stratigraphic illustration of Schandelah adjusted to the reported intervals reported herein, modified from van de Schootbrugge et al. (2018), including a graphic chart of $\delta^{13}C_{org}$ reported values from the same report. Then, V, Mo and U normalized to Al content of ICP-MS values reported here.

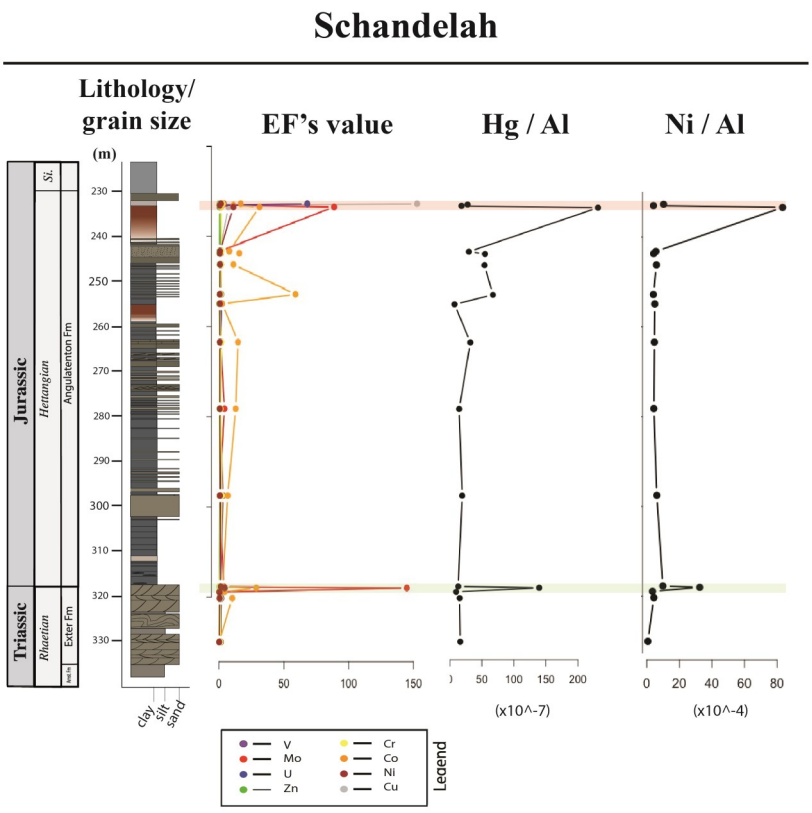

Figure 15. A chart that shows the relative distribution of EF's values of V, Mo, U, Zn, Cr, Co, Ni and Cu. Additionally reported normalized to Al, Hg and Ni content. Note that EF's are reffered to the average shale content. Based on ICP-MS values. The stratigraphic chart is modified from van de Schootbrugge et al. 2018.

and exposure to it, abrupt changes in the environment can influence these situations (Tribovillard et al, 2006), however remobilization as would follow from changes of oxygen availability occur at a relatively fine scale. In Stenlille and Schandelah, palynomorphs have been described by the presence of spores, pollen, dynoflaggellates, acritarchs and others, that indicates that both localities have not been subjected to significant post diagenic alterations. Van de Schootbrugge et al 2018, mentioned that the maturity of organic matter was high from well localities within the Lower Saxony Basin, possibly following an igneous intrusion around the Bramsche Massif of early Cretaceous or early-late Cretaceous age, however the Schandelah project was targeted around locality with low maturity of organic matter. So both localities were affected to a very limited low amount by regional diagenesis, as the palynomorphs are still preserved (the pollens would change in color with higher maturity).

6.2 Evaluation of the redox conditions

To evaluate the redox conditions of our cores we followed two approaches. The first one is to look at TOC-TE covariation and use the threshold set by Algeo and Maynard (2004) and the second one is to look at stratigraphc covariation of multi-elements. Following the first approach, we consider here only the relation of Algeo and Maynard (2004) for samples having < 10 % wt TOC, corresponding to their grey shale submember. In this case Mo, U, V and Zn should show a strong covariation with TOC in case of euxinic affinity. This is not observed in this study. That means that the samples of Stenlille 4 and Schandelah, mostly reflect oxic to dysoxic conditions. The EF's values that are reported here are considerably lower, suggesting that they are mainly controlled by the detrital fraction. Trace elements here, in general do not demonstrate intervals with covarying degree of high enrichments. The best approach in evaluating enrichments is using the covariation of V, Mo and U, those elements are least affected by detrital influences (Tribovillard et al. 2006). The sensitivity of gradients varies for the elements aswell, and U and V (including Cr) can accumulate under denitrifying conditions. On the other hand, Ni, Co, Cu, Zn Cd and Mo are enriched near only under sulfate-reducing conditions (Tribovillard). These elements allow suboxic environments to be distinguished from anoxic-euxinic ones (Tribovillard et al 2006).

This research concludes that there is no significant correlation of trace elemental enrichment covarying with the TOC content in Stenlille 4 except for weak insignificant negative correlation noted in normalized Cu and possibly in normalized Ni, that could however not be confirmed. The reason is because of only two enriched EFs values. Near all, Stenlille 4 samples exhibit low EF values in general and exhibit poor TOC-TE correlations, indicating that most of the trace elements mainly reside as part of the detrital fraction of the sediments. An exception is observed for the intervals that do show enrichment covarying amongst V, Mo and U at Stenlille 4 and are located at depths of 1492,54 m and 1498,18 m (XRF measurements). The comparison between the analytical techniques show that in the case of V, it can be observed that the XRF measurements do overestimate analysed concentrations, and thus indicating that the EF's values are also likely overestimated. However the concentration of reported values do show considerably high concentrations, and are not in such low concentrations that limitations of the XRF is a problem. The authigenic enrichment at these depths, with covarying observation of V, Mo and U imply that anoxic and/or euxinic conditions were met, either resulting from conditions at the sediment-water interface or within the water-column.

This granted further investigation, of the Stenlille 4 core, by looking at the intervals where those samples were taken. After looking at what can be observed from the core itself, and what is reported from detailed log reports that had previously been made by GEUS. Looking for absence or presence of any biofacies, would provide valuable information as indicators for the environmental conditions when these sediments were deposited. Biofacies demonstrate different levels of benthic O_2, and the presence of organic rich (often black if very rich in organic matter) laminated facies also demonstrate reduced environments. Closer look at depth interval of 1492,54 m showed bioturbation (fig 16 A), the samples are sampled from a silty grain-sized layer. And interestingly, when looking at the fractions of the major elements there, they show significant depletion in Fe and raised S contents. Suggested is that the enrichment observed at this interval, could have been affected by post remobilization, following change in oxygen availability, and most likely at the sediment-water interface. Additionally the depletion in Fe is significant, and indicates some remobilization of Fe, elsewhere. The second observation is within siltstone with sandy lenticular bedding, with no observed macrofossils and no bioturbation (Fig 16B). From the ICP-MS results, the samples that showed most enrichments and were detected in at least six different elements were at depths 1493,06 m and 1501,84 m, the former is within a fine grained sand layer with observed micro-joints, the latter is a sample that falls close to the largest negative carbon isotope excursion reported here. It is a silty layer with sandy lenticular lamination within (Fig 16C). At depth of 1513,35 m a low-grade enrichment is detected, mainly within Mo, main lithological composition laminated silt, and has burrowing observed within.

It has been demonstrated by Tribovillard et al. (2006) that when free H_2S is present, with reduction of elements to their lowest state, metal sulfides and oxyhydroxides can precipitate unlimited directly out of the water column at the sediment-water interface, leading to strong enrichment of U and V. Additionally, it was shown here before that there is no significant correlation of normalized V, Mo and U with TOC. Mo shows association with pyrite formation and organic matter that is rich in sulphur (Tribovillard et al. 2006), and here Mo shows no significant covariation with TOC in Stenlille 4, and therefore, where intervals with high authigenic enrichments in Mo occurs, are most likely accociated with formation of pyrite or at least sulphides. General enrichment of trace elements in Stenlille 4 and

Figure 16. Pictures from the Stenlille 4 core. Note the ruler for scale. A. Shows were the sample from depht of 1492,54 m was sampled from. B. Depth of sample from 1498,18 m. C. Depth of sample for 1501,84 m.

Schandelah, compared to average shale values demonstrate a general low level of enrichments. In Stenlille 4, the average EF‘s value of all ICP-MS measurements below or equal to 1 is for V, Zn, Ni, Cu and Mn. Above 1, the average enrichment is observed for Mo, (highest average EF‘s of 2,5), lower for U and Cr. For induvidual depth observations, two depth intervals show enrichments in more than seven elements, those depths are 1493,06 m and 1501,42 m and the latter has the most enriched individual elemental value of 25,27. In Schandelah a slightly more EF‘s values are observed on average. There, the elements that stay below EF‘s of 1 in averaged values is Zn, with value of 0,5, and has been mentioned earlier here that the Zn in Schandelah is significantly depleted in comparison to average shale values. Zn behaves as a micronutrient in oxic seawaters (Tribovillard et al. 2006), either the sedimentrary provenance source is for some reason depleted of Zn or as Schandelah is composed not dominantly of shales, but rather sandier intervals, this could be a reflection of lithology. Other succestions could be that bacterial decay was very active in releasing Zn^{2+} cations or $ZnCl^{+}$ ions to the water column, and since the sediments here are rather rich in S, then possibly Fe-Mn oxyhydroxide precipititation is not as dominant feature as in other shales. Other elements have slightly more enriched values than 1, and include V, U, Cr, Ni and Mn. Averaged EFs >10 are observed with Mo the highest (15,9), following Co and Cu. The individual elemental range of high EF‘s values is greater in Schandelah. Two depth intervals compose of EF‘s > 1 in more than 7 elements, and are located at depths of 232,7 m, 233,4 m and 318 m. Individual EF‘s values > 50 are found in U and Cu at depths of 232,7 m, Mo at 233,4 m, Co at 252,8 m and Mo at 318,0 m. In Schandelah, no strong covariation of U-V-Mo enrichments are detected that indicate euxinic levels of enrichment. In Stenille the same situation is observed, except for two intervals at 1492, 54 m and 1498,18 m. Further observation showed that the former interval had been bioturbated, with dysaerobic biofaces, reflected by the trace-fossils. That could imply post depostitional processes that have affected previously anoxic deposited sediments. In Stenlille 4, the variation in enrichment levels by individual elemental counts is more dominant in the Jurassic succession rather than the Triassic, and is observed from 1501,42 m (around the TJB). The covarying higher-end enriched intervals for V, Mo and U (XRF) are situated in Jurassic successions aswell. In Schandelah, there seems to be a a pattern for this variation in enrichment levels observed at the base of Jurassic as well, with enrichments detected in 8 elements, with different range of enrichments, and then additionally more dominated towards the base of the Hettangian, based on counts of individual EF‘s levels versus depths. An attempt of schematic classification of the accumulation behaviour was made (table 13 and 14) for each locality with Efs > 2 (including Appendix 4). Overview of the concentration of the major elements Si, Al, Ca, Fe and S (norm to 100% wt) can be viewed in table 11 and 12 for those same intervals.

6.3 The carbon isotope record of Stenlille 4

Van de Schootbrugge et al. (2008) emphasized that using bulk organic $\delta^{13}C$ records should be used in caution when addressing atmospheric and upper ocean pCO_2 conditions. Optimal would be to aquire $\delta^{13}C_{carb}$ records in association with organic carbon isotopic studies. Bulk organic carbon content can be influenced by regional recycling of respired CO_2 or by sulphur or methanogenic bacteria. The type of vegetations also can additionally modulate C-isotope excursions, as plants fractionate ^{13}C differently as well. Thus marine relative to terrestrial contribution of organic matter could also be an additional complicating factor, as the composition of the biomass gives different signatures, mostly in the perspective of terrestrial plant composition and phytoplankton communities. All the premention considerations could therefore add to the difference in the magnitude of isotopic excursions witnessed. But correlative peaks on peculiar stratigraphic level at different paleogeographic positions should avoid most of these caveats and reveal real perturbations of

the carbon cycle.

When evaluating the isotopic signal of all the 88 values obtained, the biggest change of the lower part occurs around depth interval of 1520 m, with a strong negative CIE. This CIE is correlated to the one called Pre-Marshi of Lindström et al. (2017) for Stenlille 1 based on lithological evidence and the position of MFS 7. Closely following, there is a large shift to more positive values, indicating that primary productivity was enhanced or at least was stabilitized. Then the variability of the signal becomes a more prominant feature, that could also be contributed to variations in lithology or in the orgin of the organic matter. Around depth 1513 m another CIE occurs. Its position just below MFS7 allow to correlate it as the Marshi CIE of Lindström et al. (2017). This level would thus correspond to the main extinction pulse. Latter a large CIE is observed and falls in the PRD palynozone close to the TJB boundary, here it is correlated to the Spelae CIE of Lindström et al. (2017). The lowest negative value of –29,0‰ above the gray siltstone interval collides with the top part of the *P. polymicroforatus* abundance interval (PRD zone of Lindström 2017), and is below the MFS8 maximum flooding surface. This biggest negative excursion could be correlated to the Spelae CIE in Stenlille 1 (Lindström et al. 2012; Lindström et al. 2019), which is close to the Triassic-Jurassic boundary. Van de Schootbrugge et al. (2018) also demonstrated a prominent CIE excursions at the Triassic- Jurassic boundary in Schandelah. This negative peak has been observed in other localities as the GSSP section, Kuh-joch (Hillebrandt et al. 2013), St Audrie‘s Bay (UK), (Hesselbo et al. 2002) and Mingolsheim, southern Germany (Quan et al. 2008) and other Triassic-Jurassic transition localities. Towards the Jurassic section, the trend gets more smoother, slowly shifting towards more positive values and seems to conform to the reapperance of the dinoflagellates (fig 11), and also where their numbers go down, the shift in the carbon isotopes seem to do follow the same trend.

6.4 Volcanogenic influence

The results of the regressions of TOC with the trace elements showed that their authigenic enrichment, does not correlate with the organic fraction. The detrital versus authigenic enrichments of V, Mo and U were evaluated for EF´s > 2 (table 13 and 14), and could be denoted to either recide in either authigenic sulphides or oxides. A possible exception is Ni, in consequence the authigenic enrichment has been attributed here to the organic fraction. For Ni it has been marked as an organic fraction, mainly based on the association of Ni with organic matter, however based only on two samples, this association could not be validated firmly.

High contents of Ni and Cu implicate 1) high flux of organic matter 2) reducing conditions are met (Tribovillard et al. 2006) or 3) high external input (weathering or volcanic input). When conditions become anoxic, Ni and additionally Cu are deposited largely by organometallic complexes (Tribovillard et al. 2006) and thus show strong correlation with TOC. Here, this relation was observed in Ni, however could not be validated as mentioned before. Additionally in this study, a negative correlation was observed in normalized Cu with TOC. High contents of Ni and Cu implicate either high OM flux or reducing conditions were met (Tribovillard et al. 2006). However, if the correlation to the organic TOC to matter of Ni and Cu is not observed or not clear, it is not possible to discriminate wheather the enrichments are a consequence of flux of organic matter or that the enrichments are a consequence of a reducing environment. In Stenlille 4, enrichments at corresponding depth intervals for Ni are observed at depth of 1501,84 m (one smaller EF of Ni at 1502,01 m). In Schandelah, higher enrichments in Ni are observed at 233,4 m and 318 m. When looking at normalized values, and stratigraphic distribution, Ni, Mo, Cu and Hg show co-occurring peaks at same intervals, at 233,4 m and 318 m, including rather low Al% wt values. At both localities, the Ni enrichments do not have a co-occurring substantial enrichments in V, Mo and U that would indicate euxinic or anoxic level of enrichments. When normalized to Al, Ni kept near constant ratio to Al both in Stenlille 4 and in Schandelah, and then except for significantly higher peaks, that are demonstrated with the EFs values mentioned above. The peaks at 1501,84 m in Stenlille 4 correspond stratigraphically to the 318 m peak in Schandelah. The Ni peaks thus are in conjuction to the Spelae CIE in Stenlille 4 and Schandelah. This is the top of the *P. polymicroforatus* abundance interval and the interval of the Spelae CIE. This could be explained by an additional input source of Ni. Correlation to volcanic activity of CAMP has been demonstrated by Lindström et al. (2019) by elevated concentrations of mercury in marine and terrestrial sediments across the TJB from the Danish Basin and northern Germany, with correlation to abnormalities detected in palynomorphs. Lindström et al. (2019) have measured, in their study Hg on a direct Hg analyzer, a method far more precise for Hg than ICP-MS. The Hg peak at the Marshi CIE as noticed by Lindström et al. (2019) have not been recovered in our ICP-MS data. This is perhaps due to sampling effect or a methodology effect (matrix effect in ICP-MS). However, this concludes that both core sections, Stenlille 4 and Schandelah, at this level see high levels of Ni. A second peak in Hg and Ni is seen in Schandelah at the top of the Hettangian (stratigraphically far above the last sample of Stenlille 4). After looking at reported mercury concentrations reported by GEUS for Stenlille, well nr 4, the elevated Ni concentration here coincides with elevated Hg concentrations reported by GEUS (Fig. 13). Additionally the biggest CIE excursion reported hereein falls close to that depth interval, and the reported $\delta^{13}C_{org}$ at this depth is -29,0‰. In Schandelah, a raised level of normalized Ni falls close to the TJB and a negative CIE excursion is reported there. Even if not straightforward (no peak at Marshi CIE), our dataset valids further testing on the accociation of Ni with volcanism or at least with prominent negative CIE excursions in future studies. This accociation can on the other hand, not be aknowledged in environments that have been affected by changes in redox conditions, as following consequence of reduced environments, would ”overwrite the signal” that would be demonstrated in

Ni otherwise. One consideration to include aswell is the strong correlation of the high normalized Ni peak (at 1501,84 in Stenlille 4) and higher TOC values around similar levels. The TOC content (GEUS data) is 0,72 (wt%) at this exact interval, however, just 5 cm above, the TOC content goes up to high ranging levels of 8,07 (wt %).

6.5 Additional discussion based on general observations

As mentioned by Tribovillard et al. (2006), using Al normalization on geochemical data, comes with some downsides, possibly resulting in spurious correleations when normalized and normalization itself can influence the results by increasing, decreasing or affecting the correlations between unmodified variables. Comparing the coefficient of variation of Al with to the coefficient of trace elements, and check if the difference is great could aid in discriminating weather that could be a problem. We have seen in part 5.3.1. here that if we exclude some outliers as for Mo, U and Cu, the difference between coefficient of variations of Al and of the trace elements was in a good range. However, Tribovillard et al. (2006) pointed out that there are some cases that normalizing to Al could not be possible. Those cases should be considered in instances were the detritial fraction is lower than 3-5%, and if there is an relative excess of aluminum compared to other detritial proxies as for an example Ti. Al could end up as being a scavanged product as hydroxide coatings of biogenic particles or that authigenic clay-mineral formation could result in excess aluminium (Tribovillard 2006). This is not the case here. Lastly, Tribovillard (2006) mentioned some problems that can arise when comparing to average shale values in the sense that they might not represent the local/regional sediments of studied area. Secondly, if there would be a diagenic component involved in the referented shale, that could lead to systematic underestimation of EFs in cases of some trace elements.

The XRF technology offers a way to determine the concentrations of elements in a fast and relatively easy way, without any rigorous or exhaustive preparations and destruction of samples. The downside of XRF is on the other hand that it is low in precision and it has high errors when dealing with the trace element concentrations. When addressing redox conditions of samples from sediments, it shows to have practical value, especially when dealing with great amount of samples. However, it is worth mentioning that the ICP-MS accuracy proved its value in this research when the normalization parameters of Al versus Ti were evaluated, with uncertainty that arose from XRF values in regards of Ti. Using the ICP -MS method on the other hand, excluded that uncertainty. The reduction of number of samples for the ICP-MS analysis involves disadvantages, as some samples that could provide information that is not detected with the XRF and its limitations, can be overlooked. The areas were enrichment is detected reliably by XRF, do provide however evaluable information. There seems to be an agreement amongst the techniques in the higher enrichment intervals. It could however not be evaluated, since they are few in numbers. For the major elements, employing the XRF shows to be useful, and resulting in good correlations between the XRF and ICP-MS at least for the major that were evaluated as of Al and Fe.

In comparison to average shale, both Stenlille and Schandelah reported lower values of Al and Fe. On the other hand, S results in generally higher levels, compared to average shale, and could be reflected by enhanced availability to organic matter, provided my marine productivity or terrestrial sources of organic matter. Other observations were made that showed some differences amongst Stenlille 4 and Schandelah. Cl showed a peculiar variation at both localities, especially at Stenlille 4. This could be from contamination resulting from salt diapirism from underlying or proximal successions or contact with brine fluids in general. It showed when working with the cores that they were covered with dried brine residues. However the change in Cl showed stratigraphic variations that could rather indicate variation amongst clay facies present. Zr and W showed a correlation to intervals based on lithology. This could be a result of a positive relationship with grain sizes and could be contributed by proximity to a terrigenous source, a factor that could also result as a consequence of its density or atomic caracteristics, that leads to those elements to be precipitated out of solution close to the input source, as it shows that the Schandelah core is more sandier and coarser grained than Stenlille. And noteable was that Zn was depleted in regards to comparion to average shale values in Schandelah, and on average rather enriched in Co.

7 Conclusion

The redox state during the accumulation of the sedimentary successions in Stenlille 4 and Schandelah, based on enrichments and covariation to organic matter and trace metals, was in near all cases ranging from oxic to suboxic. Euxinic level of enrichments was not observed. Both localities show more frequent fluctuations of enrichments among Jurassic succession in general. The variations of enrichments indicate different grades of redox conditions, varying from oxic to anoxic, most likely controlled by conditions at the sediment water interface, interlinked with differential rates in sedimentation or bacterial degradation or presence of varying sedimentary facies (grain size, lithology, carbonates, sulfides etc.). Most intervals showed no covarying agreement of enrichments within a suite of elements, and where relatively high enrichments occurs, it happens in unsystematic order, that can not be used to infer the redox gradient, and reflects only variations amongst varying facies that are present. The end of the *P. polymicroforatus* abundance interval show both in Stenlille 4 and in Schandelah weak indications toward more reducing conditions. The two others level within the Jurassic section (1493 m in Stenlille 4 and 232 - 233,4 in Schandelah) are not coresponding stratigraphically.

Correlation between the TOC content amongst V, U, Zn, Co, Cr and Mn showed no inferred correlation, indicating that where enrichments occurs amongst them, it is not controlled by accumulation of organic matter. Weak correlation was observed for Cu and Ni with higher enrichment levels, but in the latter

case it could not be validated, and in both cases, the correlation is made up of small population of samples that showed enrichments.

Nickel and mercury (GEUS data) showed a peculiar correlation to the largest negative CIE observed in Stenlille 4. The same is observed to occur around the biggest CIE observed in Schandelah. After being normalized to the Al content, in the case of Stenlille 4, both elements keep a near constant ratio except for the intervals falling close to the largest negative CIE. In Schandelah, the ratio of Ni and Hg shows similar pattern. The TOC correlation possibly demonstrated by Ni, in Stenlille 4 indicates that it resides in the organic fraction, but could not be validated since there are so few enriched Ni samples.

The organic carbon isotopic results from this study shows a covarying negative CIE around the TBJ that can be correlated to other TJB successions, including Stenlille 1 and other localities. Also the results here demonstrate other CIE intervals that could further increase correlations between successions from this interval in time. The isotopic signal demonstrate more intensity in variations during the Triassic interval, and towards the TJB boundary. The CIE excursion commenses relatively earlier than observed decrease in assemblages of marine palynomorphs is noted.

8 Aknowledgements

First of all, I would like to express my special thanks of gratitude to my supervisors Sylvain Richoz at Lund University and Sofie Lindström (GEUS) for providing me with the opportunity for this project. Especially in regards of providing me with sample material to work with. For their patient guidance and useful critiques during the process of this research. Additionally I would like to give special thanks to Gunver Krarup Pedersen (GEUS) for interesting discussions and contribution during the process. I would also like to thank Frans Lundberg and Isa Doverbratt at the Lund University for their assistance. My grateful thanks are extended to Mikael Calner for useful critiques and guidelines, as to other participants of the examination committee, Raimund Muscheler and my student opponent Jennie Lundqvist, for their time and contribution, it is really appreciated. Additionally I would like to give special credits to the contributions of all the teachers at the Lund University that I have steered along with, throughout my master's courses that have influenced and inspired me along the way and provided me with a solid foundations and tools to address a project as of this.

I would like to express special thanks to my family, especially my three kids that mean the world to me. For their endless patience for their mother's geological endeavours. To my husband, Ívar Atlason for his support, motivation and encouragement. I wish to thank all my good friends for their support, motivation and encouragement along the way. I would also like to pay my special regards and gratitude to my classmates that have sat beside me in countless study sessions throughout this project, for their perpetual encouragement, motivation and partitioning in sharing endless cups of coffee.

References

Adelson, J. M., Helz, G. R. & Miller, C. V., 2001: Reconstructing the rise of recent coastal anoxia; molybdenum in Chesapeake Bay sediments. *Geochim Cosmochim Acta 65*, 5233-5253.

Adriasola-Muñoz, Y., Littke, R. & Brix, M. R., 2007: Fluid systems and basin evolution of the western Lower Saxony Basin, Germany. *Geofluids 7*, 335-355.

Ahlberg, A., Olsson, I. & Simkevicius, P., 2003: Triassic-Jurassic weathering and clay mineral dispersal in basement areas and sedimentary basins of southern Sweden. *Sedimentary Geology 161*, 15-29.

Algeo, T.J. & Lyons, T.W., 2006: Mo-total organic carbon covariation in modern anoxic marine environments: implications for analysis of paleoredox and paleohydrographic conditions. *Palaeoceanography 21*, 1-23.

Algeo, T.J.. & Rowe, H., 2012: Paleoceanographic applications of trace-metal concentrations data. *Chem Geol, 324-325*, 6-18.

Algeo, T. J. & Maynard, J. B., 2004: Trace-element behavior and redox facies in core shales of Upper Pennsylvanian Kansas-type cyclothems. *Chemical Geology 206*, 289-318.

Anderson, D. M., Prell, W. L. & Barratt, N. J., 1989: Estimates of sea surface temperatures in the Coral Sea at the last glacial maximum, *Paleoceanography, 4,* 615-627.

Arndorff, L., 1993: Lateral relations of deltaic paleosols from the Lower Jurassic Rønne Formation on the Island of Bornholm, Denmark. *Paleogeography, Paleoclimatology, Paleoecology 100*, 235-250.

Barnes, C. E. & Cochran, J. K., 1990: Uranium removal in oceanic sediments and the oceanic U balance. *Earth planet Science Letter 97*, 94-101.

Berner, R. A., 1980: *Early Diagenesis - A Theoritcal Approach*. Princeton Series in Geochemistry, Princeton University Press, Princeton, 241 pp.

Berner, R. A., 1985: Sulphate reduction, organic matter decomposition and pyrite formation. *Philosophical Transactions of the Royal Society of London. Series A, Mathematical and Physical Sciences 315*, 25-38 pp.

Bertelsen, F., 1978: The Upper Triassic-Lower Jurassic Vinding and Gassum Formations of the Norweigan-Danish Basin. *Geological Survey of Denmark (Ser. B3)*, 26 pp.

Bertine, K. & Turekian, K., 1973: Molybdenum in marine deposits. *Geochim Cosmochim Acta 37*, 1415-1434.

Betz, D., Führer, F., Greiner, G. & Plein, E., 1987: Evolution of the Lower Saxony Basin. *Tectonophysics 137*, 127-170.

Blackburn, T. J., Olsen, P. E., Bowring, S. A., Mclean, N. M., Kent, D. V., Puffer, J., Mchone, G., Rasbury, E. T. & Et-Touhami, M., 2013: Zircon U-Pb geochronology links the end-Triassic extinction with the Central Atlantic Magmatic Province. *Science 340*, 941-945.

Blakey, R. C., 2014: Paleogeography and Paleotectonics of the Western Interior Seaway, Jurassic-Cretaceous of North America. *Search and Discovery, 30392,* 72 pp.

Blumenberg, M., Heunisch, C., Lückge, A. & Wiese, F., 2016: Photic zone euxinia in the central Rhaetian Sea prior the Triassic-Jurassic boundary. *Palaeogeography, Palaeoclimatology, Palaeoecology 461*, 55-64

Boland, D. D., Collins, R. N., Miller, C. J., Glover, C. J. & Waite, T. D., 2004: Effect of Solution and Solid-Phase Conditions on the Fe(II)-Accelerated Transformation of Ferrihydrite to Lepidocrocite and Goethite. *Environmental Science & Technology 48,* 5477-5485.

Bond, D. P. G. & Wignall, P. B., 2014: Large igneous provinces and mass extinctions: An update. *Geological Society of America Special Papers, 505*, 29-55.

Borch, T., Kretzschmar, R., Kappler, A., Cappellen, P. V., Ginder-Vogel, M., Voegelin, A. & Campbell, K., 2010: Biogeochemical Redox Processes and their Impact on Contaminant Dynamics. *Environmental Science &Technology 44*,15-23.

Bruland, K. W., 1983: Trace elements in seawater. *Chemical Oceanography 8***,** 157-220.

Brumsack, H.J., 1986: The inorganic geochemstry of Cretaceous black shales (DSDP Leg 41) In Comparison to modern upwelling sediments from the Gulf of California. *Summerhayes Cp, Shackleton (NJ) (eds) North Atlantic Paleoceanography 21***,** 447-462.

Brumsack, H.J, 1989: Geochemistry of recent TOC-rich sediments from the Gulf of California and the Black Sea. *Geologische Rundschau 78***,** 851-882.

Burdige, D. J., 2006: *Geochemistry of Marine Sediments*. Princeton University Press, 609 pp.

Calvert, S. E. 1983: Geochemistry of Namibian Shelf sediments. *In* E. Suess & J. Thiede (eds.): *Coastal Upwelling, Part A*, 337-375. Plenum, New York

Calvert, S. E. & Pedersen, T. F., 1993: Geochemistry of Recent oxic and anoxic marine sediments: implication for the geological record. *Marine Geology 113***,** 67-88.

Canfield, D. E., 1994: Factors influencing organic carbon preservation in marine sediments. *Chemical Geology 114***,** 315-329.

Cempel, M. & Nikel, G., 2006: Nickel: A Review of Its Sources and Environmental Toxicology. *Polish J. of Environ. Stud. 15***,** 375-382.

Collier, R. W., 1985: Molybdenum in the northeast Pacific Ocean. *Limnol. Oceanogr 30***,** 1351-1354.

Davies, J. H. F. L., Marzoli, A., Bertrand, H., Youbi, N., Ernesto, M. & Schaltegger, U., 2017: End-Triassic mass extinction started by intrusive CAMP activity. *Nature Communications 8*, 15596.

Descolas-Gros, C. & Fontugne, M., 1990: Stable carbon isotope fractionation by marine phytoplankton during photosynthesis. *Plant, Cell and Environment, 13(3),* 207-218.

Deuser, W. G., 1971: Organic-carbon budget of the Black Sea. *Deep-Sea Res. 18***,** 995-1004.

Duce, R. A., Liss, P. S., Merrill, J. T., Atlas, E. L., Buat-Menard, P., Hicks, B. B., Miller, J. M., Prospero, J. M., Arimoto, R., Church, T. M., Ellis, W., Galloway, J. N., Hansen, L., Jickells, T. D., Knap, A. H., Reinhardt, K. H., Schneider, B., Soudino, A., Tokos, J. J., Tsunogai, S., Wollast., R. & Zhou, M., 1991: The atmospheric input of trace species to the world ocean. *Global Biogeochemical Cycles 5***,** 193-259.

Dunne, J. P., Armstrong, R. A., Gnanadesikan, A. & Sarmiento, J. L., 2005: Emprical and mechanistic models for the particle export ratio. *Global Biogeochemical Cycles 19,* 1-16.

Dupont, C. L., Buck, K. N., Palenik, B. & Barbeau, K., 2010: Nickel utilization in phytoplankton assemblages from contrasting ocean regimes. *Deep-Sea Reservoir 57***,** 553-566.

Emerson, S. R. & Huested, S. S., 1991: Ocean anoxia and the concentrations of molybdenum and vanadium in seawater. *Marine Chemistry 34***,** 177-196.

Falkowski, P. G., Katz, M. E., Knoll, A. H., Quigg, A., Raven, J. A., Schofield, O. & Taylor, F. J. R., 2004: The Evolution of Modern Eukaryotic Phytoplankton. *Science magazine 305***,** 354-360.

Fogel, M. L. & Cifuentes, L. A., 1993: Isotope Fractionation during Primary Production. *In* M.H. Engel & S.A. Macko (eds): *Organic Geochemistry - Principles and Applications,* 73-98. Topics in Geobiology 11, Springer, Boston, MA.

Francois, R., 1988: A study on the regulation of the concentration of some trace metals (Rb, Sr, Zn, Pb, Cu, V, Cr, Ni, Mn and Mo) in Saanich Inlet sediments, British Columbia. *Marine Geology 83***,** 285-308.

Froelich, P. N., Klinkhammer, G. P., Bender, M. L., Luedtke, G. R., Heath, G. R., Cullen, D., Dauphin, P., Hammond, D., Hartman, B. & Maynard, V., 1979: Early oxidation of organic matter in pelagic sediments of the eastern equatorial Atlantic: suboxic diagenesis. Geochim. *Cosmochim. Acta 43***,** 1075-1090.

Fry, B. & Sherr, E. B., 1984: $\delta^{13}C$ measurements as indicators of carbon flow in marine and freshwater ecosystems. *Contrib. Mar. Sci. 27***,** 13-47.

Gobeil, C., Macdonald, R. W. & Sundby, B., 1997: Diagenetic seperation of cadmium and manganese in suboxic continental margin sediments. *Geochim Cosmochim Acta 61***,** 4647-4654.

Goldberg, S., Su, C. & Forster, H. S. 1998: Sorption of molybdeum on oxides, clay minerals and soils. *In* E. A. Jenne (eds): *Adsorption of Metals by Geomedia*, 401-426. Academic Press,

Goñi, M. A., Ruttenberg, K. C. & Eglinton, T. I., 1997: Sources and contribution of terrigenous or-

ganic carbon to surface sediments in the Gulf of Mexico. *Nature 389*, 275-278.
Hallam, A., 1981: *Facies Interpretation and the Stratigraphic Record.* Freeman, Oxford. 291 pp.
Hallam, A. & Wignall, P. B., 1999: Mass extinctions and sea-level changes. *Earth-Science Reviews 48*, 217-250.
Hallberg, R. O., 1974: Paleoredox conditions in the eastern Gotland basin during the recent centuries. *Merentutkimuslatosken Julk. Havsforskningsinst. Skr. 238*, 3-16.
Hastings, D. W., Emerson, S. R. & Mix, A. C., 1996: Vanadium in foraminiferal calcite as tracer for changes in the areal extent of reducing sediments. *Palaeoceanography II*, 665-678.
Hausinger, R. P., 1997: Metallocenter assembly in nickel-containing enzymes. *J. Biol. Inorg. Chem. 2*, 279-286.
Hautmann, M., 2004: Effect of end-Triassic CO2 maximum on carbonate sedimentation and marine mass extinction. *Facies 50*, 257-261.
Hautmann, M., 2012: Extinction: End-Triassic Mass Extinction. *Encyclopedia of Life Sciences*, 1-10. John Wiley & Sons.
Hedges, J. I. & Keil, R. G., 1995: Sedimentary organic matter preservation: an assessment and speculaticve synthesis. Marine Chemistry 49, 81-115.
Heimdal, T. H., Svensen, H. H., Ramezani, J., Lyer, K., Pereira, E., Rodrigues, R., Jones, M. T. & Callegaro, S., 2018: Large-scale sill emplacement in Brazil as a trigger for the end-Triassic crisis. *Scientific Reports, 8*, 1-12.
Helz, G. R., Miller, C. V., Charnock, J. M., Mosselmans, J. F. K., Pattrick, R. a. D., Carner, C. D. & Dj, D. J. V., 1996: Mechanisms of molybdenum removal from the sea and its concentration in black shales; EXAFS evidence. *Geochim Cosmochim Acta 60*, 3631-3642.
Herrmann, A. D., Kendall, B., Algeo, T. J., Gordon, G. W., Wasylenki, L. E. & Anbar, A. D., 2012: Anamolous molybdenum isotope trends in Upper Pennsylvanian euxinic facies: Significance for use of δ^{98}Mo as a global marine redox prox. *Chem Geol 324-325,* 387-398.
Hesselbo, S. P., Robinson, S. A., Surlyk, F. & Piasecki, S., 2002: Terrestrial and marine extinction at the Triassic-Jurassic boundary synchronized with major carbon-cycle perturbation: A link to initiation of massive volcanism? *Geology 30*, 251-254
Hillebrandt, A. V. & Krystyn, L., 2009: On the oldest Jurassic ammonites of Europe (Northern Calcareous Alps, Austria) and their global significance. *N. Jb. Geol. Paläont. 253*, 163-195.
Hillebrandt, A. V., Krystyn, L., Kürschner, W. M., Bonis, N. R., Schobben, M., Ruhl, M., Richoz, S., Urlichs, M., Bown, P. R., Kment, K., Mcroberts, C. A., Simms, M. J. & Tomasovych, A., 2013: The Global Stratotype Sections and Point (GSSP) for the base of the Kuhjoch (Karwendel Mountains, Northern Calcareous Alps, Tyrol, Austria). *Episodes 3/63,* 162-198
Holland, H. D., 1984: *The Chemical Evolution of the Atmosphere and Oceans.* Princeton University Press. 598 pp.
Huang, J.-H., Huang, F., Evans, L. & Glasauer, S., 2015: Vanadium: Global (bio)geochemistry. *Chemical Geology 417*, 68-89.
Huerta-Diaz, M. G. & Morse, J. W., 1992: Pyritization of trace metals in anoxic marine sediments. Geochim *Cosmochim Acta 56*, 2681-2702.
Jaraula, C., Grice, K. & Twitchett, R. J., 2013: Elevated ρCO^2 leading to End Triassic Extinction, photic zone euxinia and rising sea levels. *Geology 41*, 955-958.
Joseph, A., 2017: *Investigating Seafloors and Oceans - From Mud Volcanoes to Giant Squid*. (1st Edition). Elsevier Inc. 612 pp.
Kida, K., Shigematsu, T., Kijima, J., Numaguchi, M., Mochinaga, Y., Abe, N. & Morimura, S., 2001: Influence of Ni^{2+} and CO^{2+} on methanogenic activity and the amounts of coenzymes involved in methanogenesis. *J. Bioscience Bioeng. 91*, 590-595.
Kiessling, W., Aberhan, M., Brenneis, B. & Wagner, P. J., 2007: Extinction trajectories of benthic organisms across the Triassic-Jurassic boundary. *Palaeogeography, Palaeoclimatology, Palaeoecology 244*, 201-222.
Klinkhammer, G., 1980: Early diagenesis in sediments from the eastern equatorial Pacific II. Pore water metal results. *Earth and Planetary Science Letters 49*, 80-101.
Klinkhammer, G. P. & Palmer, M. R., 1991: Uranium in the oceans: where it goes and why? *Geochim Cosmochim Acta 55*, 1799-1806.
Laier, T. & Øbro, H., 2009: Environmental and safety monitoring of the natural gas underground storage at Stenlille, Denmark. *Geological Society, London, Special Publications 313*, 81-92.
Langmuir, D., 1978: Uranium solution-mineral equilibria at low temperatures with applications to sedimentary ore deposits. *Geochim Cosmochim Acta 42*, 547-569.
Legeleux, F., Reyss, J.-L., Bonte, P. & Organo, C., 1994: Concomitant enrichments of uranium, molybdenum and arsenic in suboxic continental margin sediments. *Oceanol Acta 1*, 417-429.
Levinton, J. S., 2008: *Marine Biology: Function, Biodiversity, Ecology*. Oxford University Press, New York. 423 pp.
Li, Y. H. & Schoonmaker, J. E., 2003: Chemical Composition and Mineralogy of Marine Sediments. *Treatise on Geochemistry 7*, 1-35.
Libes, S. M., 2009: *Introduction to Marine Biogeochemistr (second edition).* Academic Press. 928 pp.
Lindström, S., 2002: Lunnomidinium scaniense Lindstrom, gen. et sp nov., a new suessiacean dinoflagellate cyst from the Rhaetian of Scania, southern Sweden. *Palaeobotany and Palynology 120*, 247-261.
Lindström, S., 2016: Palynofloral patterns of terrestrial ecosystem change during the end-Triassic event - a review. *Geol. Mag. 153*, 223-251.

Lindström, S. & Erlström, M., 2006: The late Rhaetian transgression in southern Sweden: Regional (and global) recognition and relation to the Triassic-Jurassic boundary. *Palaeogeography, Palaeoclimatology, Palaeoecology 241*, 339-372.

Lindström, S., Pedersen, G. K., Schootbrugge, B. V. D., Hansen, K. H., Kuhlmann, N., Thein, J., Johansson, L., Petersen, H. I., Alwmark, C., Dybkjær, K., Weibel, R., Erlström, M., Nielsen, L. H., Oschmann, W. & Tegner, C., 2015: Intense and widespread seismicity during the end-Triassic mass extinction due to emplacement of a large igneous province. *Geology 43(5),* 387-390.

Lindström, S., Sanei, H., Schootbrugge, B. V. D., Pedersen, G. K., Lesher, C. E., Tegner, C., Heunisch, C., Dybkjær, K. & Outridge, P. M., 2019: Volcanic mercury and mutagenesis in land plants during the end-Triassic mass extinction. *Science Advances 5 (10),* 1-13.

Lindström, S., Schootbrugge, B. V. D., Dybkjær, K., Pedersen, G. K., Fiebig, J., Nielsen, L. H. & Richoz, S., 2012: No causal link between terrestrial ecosystem change and methane release during the end-Triassic mass extinction. *Geology 40*, 531-534.

Lindström, S., van de Schootbrugge, B., Hansen, K. H., Pedersen, G. K., Alsen, P., Thibault, N., Dybkjær, K., Bjerrum, C. J. & Nielsen, L. H., 2017: A new correlation of Triassic-Jurassic boundary successions in NW Europe, Nevada and Peru, and the Central Atlantic Magmatic Province: A time-line for the end-Triassic mass extinction. *Palaeogeography, Palaeoclimatology, Palaeoecology 478*, 80-102.

Lucas, S. G. & Tanner, L. H., 2007: The nonmarine Triassic-Jurassic boundary in the Newark Supergroup of eastern North America. *Earth-Science Reviews 84*, 1-20.

Luo, G., Richoz, S., van de Schootbrugge, B., Algeo, T.J., Xie, S., Ono, S. & Summons, R. E., 2018: Multiple sulfur-isotopic evidence for a shallowly stratified ocean following the Triassic-Jurassic boundary mass extinction. *Geochimica et Cosmochimica Acta 231,* 73-87.

Manspeizer, W., 1994: The breakup of Pangea and its impact on climate: Consequences of Variscan - Alleghanide orogenic collapse. *Geological Society of America Special Paper, 288,* 169-185.

Martin, J. M., Hogdahl, O. & Philippot, J. C., 1976: Rare earth element supply to the Ocean. *J. Geophys Res 81*, 3119-3124.

Martin, J.M. & Whitfield, M., 1983: The significance of the river input of chemical elements to the ocean. Trace metals in sea water. *Springer*, 265-296.

Martin, R. E., 1995: Cyclic and secular variation in microfossil biomineralization: clues to the biogeochemical evolution of Phanerozoic oceans. *Glob. Planet. Chang 11*, 1-23.

Marzoli, A., Callegaro, S., Corso, J. D., Davies, J. H. F. L., Chiaradia, M., Youbi, N., Bertrand, H., Reisberg, L., Merle, R. & Jourdan, F. 2018: The Central Atlantic Magmatic Province: A review. *In* L. H. Tanner (ed.): *The Late Triassic World,* 91-125. Springer International Publishing, Springer Cham, USA.

Mather, T. A., Pyle, D. M. & Oppenheimer, C. 2003a: Tropospheric volcanic aerosol, 139, 189-212. *In* A. Robock & C. Oppenheimer (eds.): *Volcanism and the Earth's Atmosphere.* Geophysical Monograph Series

McElwain, J. C., Beerling, D. J. & Woodward, F. I., 1999: Fossil plants and global warming at the Triassic-Jurassic boundary. *Science 285*, 1386 -1390.

McElwain, J. C., Popa, M. E., Hesselbo, S. P., Haworth, M. & Surlyk, F., 2007: Macroecological responses of terrestrial vegetation to climatic and atmospheric change across the Triassic/Jurassic boundary in East Greenland. *Paleobiology 33*, 547-573.

Mchone, G., 2003: Volatile Emissions from Central Atlantic Magmatic Province Basalts: Mass Assumptions and Environmental Consequences. *Geophysical monograph-American Geophysical Union, 136*, 241-254.

McLennan, S. M., 2001: Relationship between the trace element composition of sedimentary rocks and upper continental crust. *Geochemistry, Geophysics, Geosystems 2(4),* 1021.

McManus, J., Berelson, W. M., Klinkhammer, G. P., Hammond, D. E. & Holm, C., 2005: Authigenic uranium: relationship to oxygen penetration and organic carbon rain. *Geochim Cosmochim Acta 69*, 95-108.

McManus, J., Berelson, W.M., Severmann, S., Poulson, R.L., Hammond, D.E.,Klinkhammer, G.P. & Holm, G., 2006: Molybdenum and uranium geochemistry in continental margin sediments; Paleoproxy potential *Geochim Cosmochim Acta 70*, 4643-4662.

Metz, S. & Trefry, J. H., 2000: Chemical and mineralogical influences on concentrations of trace metals in hydrothermal fluids. *Geochim. Cosmochim. Acta 57*, 2267-2279.

Michelsen, O. & Nielsen, L. H., 1991: Structural development of the Fennoscandian Border Zone, offshore Denmark. *Marine and Petroleum Geology 10*, 124-134.

Moore, R.M., Webb, R., Tokarczyk, R. & Wever, R., 1996: Bromoperoxidase and iodoperoxidase enzymes and production of halgogenated methanes in marine diatom cultures. *J Geophys Res. 101*, 20899-20908.

Morford, J. L. & Emerson, S. R., 1999: The geochemistry of redox sensitive trace metals in sediments. *Geochim Cosmochim Acta 63*, 1735-1750.

Morford, J. L., Emerson, S. R., Breckel, E. J. & Kim, S. H., 2005: Diagenesis of oxyanions (V, U, Re, and Mo) in pore waters and sediments from a continental margin. *Geochimica et Cosmochimica Acta 69*, 5021-5032.

Morford, J. L., Martin, W. R. & Carney, M.C., 2009: Uranium diagenesis in sediments underlying

bottom waters with high oxygen content. *Geochim Cosmochim Acta 73*, 2920-2937.
Morse, J. W. & Luther III, G. W., 1999: Chemical influences on trace metal-sulfide interaction in anoxic sediments. *Geochim. Cosmochim. Acta 63*, 3373-3378.
Müller, P. J. & Suess, E., 1979: Productivity, sedimentation rate, and sedimentary organic matter in the ocean-I. Organic carbon preservation. *Deep-Sea Reservoir 26*, 1347-1362.
Muñoz, Y. A., Littke, R. & Brix, M. R., 2007: Fluid systems and basin evolution of the western Lower Saxony Basin, Germany. *Geofluids 7,* 335-355.
Neubert, N., Nägler, T.F. & Böttcher, M.E., 2008: Sulfidity controls molybdenum isotope fractionation into euxinic sediments: evidence from the modern Black Sea. *Geology 36*, 775-778.
Nadoll, P., Rehm, M., Duschl, F., Klemd, R., Kraemer, D. & Sośnicka, M., 2018: REY and Trace Element Chemistry of Fluorite from Post-Variscan Hydrothermal Veins in Paleozoic Units of the North German Basin. *Geosciences, 8(11*), 403.
Nalewajko, G., Lee, K. & Jack, T. R., 1995: Effects of vanadium on freshwater phytoplankton photosynthesis. *Water Air Soil Poll 81*, 93-105.
Nielsen, L. H., 2003: Late Triassic – Jurassic development of the Danish Basin and the Fennoscandian Border Zone, Southern Scandinavia. *GEUS Bulletin, 1*, 459 -526.
Nriagu, J. O., 1989: A global assessment of natural sources of atmospheric trace metals. *Nature 338*, 47-49.
Olsen, P. E., Kent, D.V., Sues, H.-D., Koeberl, C., Huber, H., Montanari, A., Rainforth, E. C., Fowell, S.J., Szajina, M.J. & Hartline, B.W., 2002: Ascent of dinosaurs linked to an iridiium anomaly at the Triassic-Jurassic boundary. *Science 296*, 1305-1307.
Oppenheimer, C., Francis, P. & Stix, J., 1998: Depletion rates of sulfur dioxide in tropospheric volcanic plumes. *Geophysical Research Letters 25*, 2671-2674.
Opsahl, S. & Benner, R., 1997: Distribution and cycling of terrigenous dissolved organic matter in the ocean. *Nature 386*, 480-482.
Paul, D., Skrzypek, G. & Fórizs, I., 2007: Normalization of measured stable isotopic compostitions to isotope reference scales - a review. *Rapid Communications in Mass Spectrometry, 21*, 3006-3014.
Peacock, C. L. & Sherman, D. M., 2007: Crystal-chemistry of Ni in ferromanganese crusts and nodules. *Am Miner 92*, 1087-1092.
Pedersen, T. F. & Calvert, S. E., 1990: Anoxia vs. productivity: what controls the formation of organic-rich sediments and sedimentary rocks? *American Association Petrology Geology Bulletin 74,* 454-466.
Percival, L.M.E., Ruhl, M., Hesselbo, S.P., Jenkyns, H.C., Mather, T.A. & Whiteside, J.H., 2017: Mercury evidence for pulsed volcanism during the end-Triassic mass extinction. *PNAS, 114 (30),* 7929-7934.
Peters, K. E., Sweeney, R. E. & Kaplan, I. R., 1978: Correlation of carbon and nitrogen stable isotopes in sedimentary organic matter. Limnol. *Oceanogr 23*, 598-604.
Petersen, H. I. & Lindström, S., 2012: Synchronous Wildfire Activity Rise and Mire Deforestation at the Triassic-Jurassic Boundary. *PLoS ONE 7(10), 1-15*.
Pilipchuk, M. F. & Volkov, I. I., 1974: Behaviour of molybdenum in processes of sediment formation and diagenesis. The Black Sea: Geology, Chemistry and Biology. *Am. Assoc. Petrol. Geol. Mem., 20,* 542-552.
Piper, D. Z. & Perkins, R. B., 2004: A modern vs. Permian black shales - the hydrography, primary productivity and water-column chemistry of deposition. *Chemical Geology 206*, 177-197.
Prange, A. & Kremling, K., 1985: Distribution of dissolved molybdenum, uranium and vanadium in Baltic Sea waters. *Marine Chemistry 16*, 259-274.
Premuzic, E. T., Benkovitz, C. M., Gaffney, J. S. & Walsh, J. J., 1982: The nature and distribution of organic matter in the surface sediments of the world oceans and seas. *Organic Geochemistry 4*, 63-77.
Preto, N., Kustatscher, E. & Wignall, P.B., 2010: Triassic climates - State of the art and perspectives. *Palaeogeography, Palaeoclimatology, Palaeoecology 290*, 1-10.
Pyle, D. M. & Mather, T. A., 2003: The importance of volcanic emissions for the global atmospheric mercury cycle. *Atmospheric Environment 37*, 5115-5124.
Quan, T. M., Schootbrugge, B. V. D., Field, M. P., Rosenthal, Y. & Falkowski, P. G., 2008: Nitrogen isotope and trace metal analyses from the Mingolsheim core (Germany): Evidence for redox variations across the Triassic-Jurassic boundary. *Global Biogeochemical Cycles 22(2),* 1-14.
Rampino, M. R., Rodriguez, S., Baransky, E. & Cai, Y., 2017: Global nickel anomaly links Siberian Traps eruptions and the latest Permian mass extinction. *Scientific Reports 7*, 1-6
Raup, D. M. & Sepkoski, J., 1982: Mass extinctions in the marine fossil record. *Science 215*, 1501-1503.
Richoz, S., Schootbrugge, B. V. D., Pross, J., Püttmann, W., Quan, T. M., Lindström, S., Heunisch, C., Fiebig, J., Maquil, R., Schouten, S., Hauzenberger, C. A. & Wignall, P. B., 2012: Hydrogen sulphide poisoning of shallow seas following the end-Triassic extinction. *Nature Geoscience 5*, 662-667.
Rickard, D. & Luther, G. W., 2007: Chemistry of Iron Sulfides. *Chem. Rev. 107*, 514-562.
Ridgwell, A., 2005: A Mid Mesozoic revolution in the regulation of ocean chemistry. *Marine Geology 217,* 339-357.
Romankevich, E. A., 1984: *Geochemistry of Organic Matter in the Ocean*. Springer, Berlin. 273 pp.

Rubin, K. H., 1997: Degassing of metals and metalloids from erupting seamount and mid-ocean ridge volcanoes: observations and predictions. *Geochim Cosmochim Acta 61 (17),* 3525-3542.

Ruhl, M., Bonis, N. R., Reichart, G. J., Damsté, J. S. S. & Kürschner, W. M., 2011: Atmopheric carbon injection linked to end-Triassic mass extinction. *Science 333,* 430-434.

Sadiq, M., 1988: Thermodynamic solubility relationships of inorganic vanadium in the marine environment. *Marine Chemistry 23*, 87-96.

Sanei, H., Grasby, S. E., Beauchamp, B. & Chen, Z., 2012: Mercury desposition through the Permo -Triassic Biotic Crisis. *Chem Geol. 351***,** 63-66.

Saunders, A. D., 2005: Large Igneous Provinces: Origin and Environmental Consequences. *Elements 1***,** 259-263.

Saunders, A. D., England, R. W., Reichow, M. K. & White, R. V., 2005: A mantle plume origin for the Siberian traps: uplift and extension in the West Siberian Basin, Russia. *Lithos 79***,** 407-424.

Sawlan, J. J. & Murray, J. W., 1983: Trace metal remobilization in the interstitial waters of red clay and hemipelagic marine sediments. *Earth planet Science Letter 64***,** 213-230.

Scheller, S., Geonrich, M., Boecher, R., Thauer, R. T. & Juan, B., 2012: The key nickel enzyme of methanogenesis catalyses the anaerobic oxidation of methane. *Nature 465***,** 606-608.

Schoeninger, M. J. & Deniro, M. J., 1984: Nitrogen and carbon isotopic composition of bone collagen from marine and terrestrial animals. *Geochimica et Cosmochimica Acta 48***,** 625-639.

Schoepfer, S. D., Shen, J., Wei, H., Tyson, R. V., Ingall, E. & Algeo, T. J., 2015: Total organic carbon, organic phosphorus, and biogenic barium fluxes as proxies for paleomarine productivity. *Earth-Science Reviews 149*, 23-52.

Schroeder, W. H. & Münthe, J., 1998: Atmospheric mercury - An overview. *Atmos. Environ, 32 (5),* 809-822.

Scott, C. & Lyons, T.W., 2012: Constraining molybdenum cycling and isotopic properties in euxinic versus non-euxinic sediments and sedimentary rocks. Refining the paleoproxies. *Chem Geol***,** 19-27.

Seralathan, P. & Hartmann, M., 1986: Molybdenum and vanadium in sediment cores from the NW -African continental margin and their relations to climatic and environmental conditions. *"Meteor.," Forshergebn. C, 40***,** 1-17.

Sharp, Z., 2009: *Principles of Stable Isotope Geochemistry (1st ed.)*. Pearson education, New Jersey. 314 pp.

Shaw, T. J., Gieskes, J. M. & Jahnke, R. A., 1990: Early diagenesis in differing depositional environments: The response of transition metals in pure water. *Geochim Cosmochim Acta 54***,** 1233-1246.

Smrzka, D., Zwicker, J., Bach, W., Feng, D., Himmler, T., Chen, D. & Peckmann, J., 2019: The behavior of trace elements in seawater, sedimentary pore water, and their incorporation into carbonate minerals: a review. *Facies 65 (4),* 1-47.

Stanley, S. M., 2007: An analysis of the history of marine animal diversity. *Paleobiology Memoirs 4***,** 1-55.

Svensen, H., Planke, S., Polozov, A. G., Schmidbauer, N., Corfu, F., Podladchikov, Y. Y. & Jamtveit, B., 2009: Siberian gas venting and the end-Permian environmental crisis. *Earth and Planetary Science Letters 277*, 490-500.

Swarzenski, P.W., Mckee, B.A., Skei, J.M. & Todd, J.F., 1999: Uranium biogeochemistry across the redox transition zone of a permanently stratified fjord: Framvaren, Norway. Marine *Chemistry 67***,** 181-198.

Tanner, L. H., Kyte, F. T., Richoz, S. & Krystyn, L., 2016: Distribution of iridium and associated geochemistry across the Triassic-Jurassic boundary in sections at Kuhjoch and Kendlbach, Northern Calcareous Alps, Austria. *Paleogeography, Paleoclimatology, Paleoecology 449*, 19-26

Tegner, C., Marzoli, A., Mcdonald, I., Youbie, N. & Lindström, S., 2020: Platinum-group elements link the end-Triassic mass extinction and the Central Atlantic Magmatic Province. *Scientific Reports, 10*, 3482.

Thibodeau, A.M. & Bergquist, B.A., 2017: Do mercury isotopes record the signature of massive volcanism in marine sedimentary records? *Geology, 45*, 95-96.

Thomazo, C., Pinti, D. L., Busigny, V., Ader, M., Hashizume, K. & Philippot, P., 2009: Biological activity and the Earth's surface evolution: Insights from carbon, sulfur, nitrogen and iron stable isotopes in the rock record. *General palaeontology (Palaeobiochemistry) 8***,** 665-678.

Thomson, J., Jarvis, I., Green, R. H., Green, D. A. & Clayton, T., 1998: Mobility and immobility of redox-sensitive elements in deep-sea turbidites during shallow burial. *Geochim Cosmochim Acta 62***,** 643-656.

Trefry, J. H. & Metz, S., 1989: Role of hydrothermal precipitates in the geochemical cycling of vanadium. *Nature 342*, 531-533.

Tribovillard, N., Algeo, T. J., Lyons, T. & Riboulleau, A., 2006: Trace metals as paleoredox and paleoproductivity proxies: An update. *Chemical Geology 232***,** 12-32.

Tyson, R.V., 2005: The "productivity versus preservation" controversy; cause, flaws and resolution, 17-33 pp, Society for Sedimentary Geology (SEPM-SSG*).* Special publication.

Vorlicek, T.P., Kahn, M.D., Kasuya, Y. & Helz, G.R., 2004: Capture of molybdenum in pyrite-forming sediments: role of ligand-induced reduction by polysulfides. *Geochim Cosmochim Acta 68***,** 547-556.

van de Schootbrugge, B., Tremolada, F., Rosenthal, Y., Bailey, T. R., Feist-Burkhardt, S., Brink-

huis, H., Pross, J., Kent, D. V. & Falkowski, P. G., 2007: End-Triassic calcification crisis and blooms of organic-walled ´disaster species´. *Palaeogeography, Palaeoclimatology, Palaeoecology 244*, 126-141.

van de Schootbrugge, B., Quan, T. M., Lindström, S., Püttmann, W., Heunisch, C., Pross, J., Fiebig, J., Petschick, R., Röhling, H.-G., Richoz, S., Rosenthal, Y. & Falkowski, P., 2009: Floral changes across the Triassic/Jurassic boundary linked to flood basalt volcanisms. *Nature Geoscience 2,* 589-594.

van de Schootbrugge, B., Richoz, S., Pross, J., Luppold, F. W., Hunze, S., Wonik, T., Blau, J., Meister, C., Van Der Weijst, C. M. H., Suan, G., Fraguas, A., Fiebig, J., Herrle, J. O., Guex, J., Little, C., Wignall, P. B., Püttmann, W. & Oschmann, W., 2018: The Schandelah Scientific Drilling Project: A 25-million year record of Early Jurassic palaeo-environmental change from northern Germany. *Newsletters on Stratigraphy 52*, 249-296.

Veevers, J.J., 1994: Pangea: Evolution of a supercontinent and its consewuences for Earth's paleoclimate and sedimentary environments. Pangea: Paleoclimate, Tectonics and Sedimentation During Accreation, Zenith and Breakup of a Supercontinent. *Geol. Soc. Am. Spec. Paper 288,* 13-23.

Vejbæk, O. V., 1997: Dybe strukturer i danske sedimentære bassiner. *Dansk Geologisk Forenings Nyheds- og Informationsskrift 4*, 1-31.

Vorlicek, T. P., Kahn, M. D., Kasuya, Y. & Helz, G. R., 2004: Capture of molybdenum in pyrite-forming sediments; role of ligand-induced reduction by polysulfides. *Geochim Cosmochim Acta 68*, 547-556.

Wanty, R. B. & Goldhaber, M. B., 1992: Thermodynamics and kinetics of reactions involving vanadium in natural systems: Accumulation of vanadium in sedimentary rocks. *Geochimica et Cosmochimica Acta 56*, 1471-1483.

Wedepohl, K. H., 1971: Environmental influences on the chemical compositions of shales and clays. *Phys. Chem. Earth 8*, 307-331.

Wedepohl, K. H., 1991: Chemical Composition and Fractionation of the Continental Crust. *Geologische Runschau 8*, 207-223.

Wehrli, B. & Stumm, W., 1989: Vanadyl in natural waters: adsorption and hydrolysis promote oxygenation. *Geochim Cosmochim Acta 53*, 69-77.

Whiteside, J. H., Olsen, P. G., Kent, D. V., Fowell, S. J. & Et-Touhami, M., 2007: Synchrony between the Central Atlantic magmatic province and the Triassic-Jurassic mass-extinction event? *Paleogeography, Paleoclimatology, Paleoecology 244*, 345-367.

Whitfield, M., 2002: Interactions between phytoplankton and trace metals in the oceans. *Adv. Mar. Biol. 41*, 3-120.

Winter, J. D., 2010: *Principles of Igneous and Metamorphic Petrology (2 ed.).* Prentice Hall. 702 pp.

Zhang, Y., Tobias, H. J., Sacks, G. L. & Brenna, J. T., 2012: Calibration and data processing in gas chromatography combustion isotope ratio mass spectrometry. *Drug Testing and Analysis 4 (12),* 912-922.

Zheng, Y., Anderson, R. F., Van Green, A. & Fleisher, M. Q., 2002: Remobilization of authigenic uranium in marine sediments by bioturbation. *Geochim Cosmochim Acta 66*, 1759-1772.

Ziegler, P. A., 1982: *Geological Atlas of Western and Central Europe.* The Hague: Shell Internationale Petroleum Maatschapij B.V. 371-372 pp.

Ziegler, P. A., 1987: Late Cretaceous and Cenozoic intra-plate compressional deformations in the Alpine foreland - a geodynamic model". . *Tectonophysics 137*, 389-420.

Zonneveld, K. a. F., Versteegh, G. J. M., Kasten, S., Eglinton, T. I., Emeis, K. C., Huguet, C., Koch, B. P., De Lange, G. J., Middelburg, J. J., Mollenhauer, G., Prahl, F. G., Rethemeyer, J. & Wakeham, S. G., 2010: Selective preservation of organic matter in marine environents; processes and impact on the sedimentary record. Biogeosciences 7, 483-511.

Appendix 1. XRF analysis

I. XRF analysis – Stenlille 4:

A. Results of bulk elemental concentration versus depth for Si, Al, Fe, S, K, Ca, Mg, V, Mn, Cr, Cu, Zn Ti, As, Rb, Sr, Y, Zr, Nb and Cl.

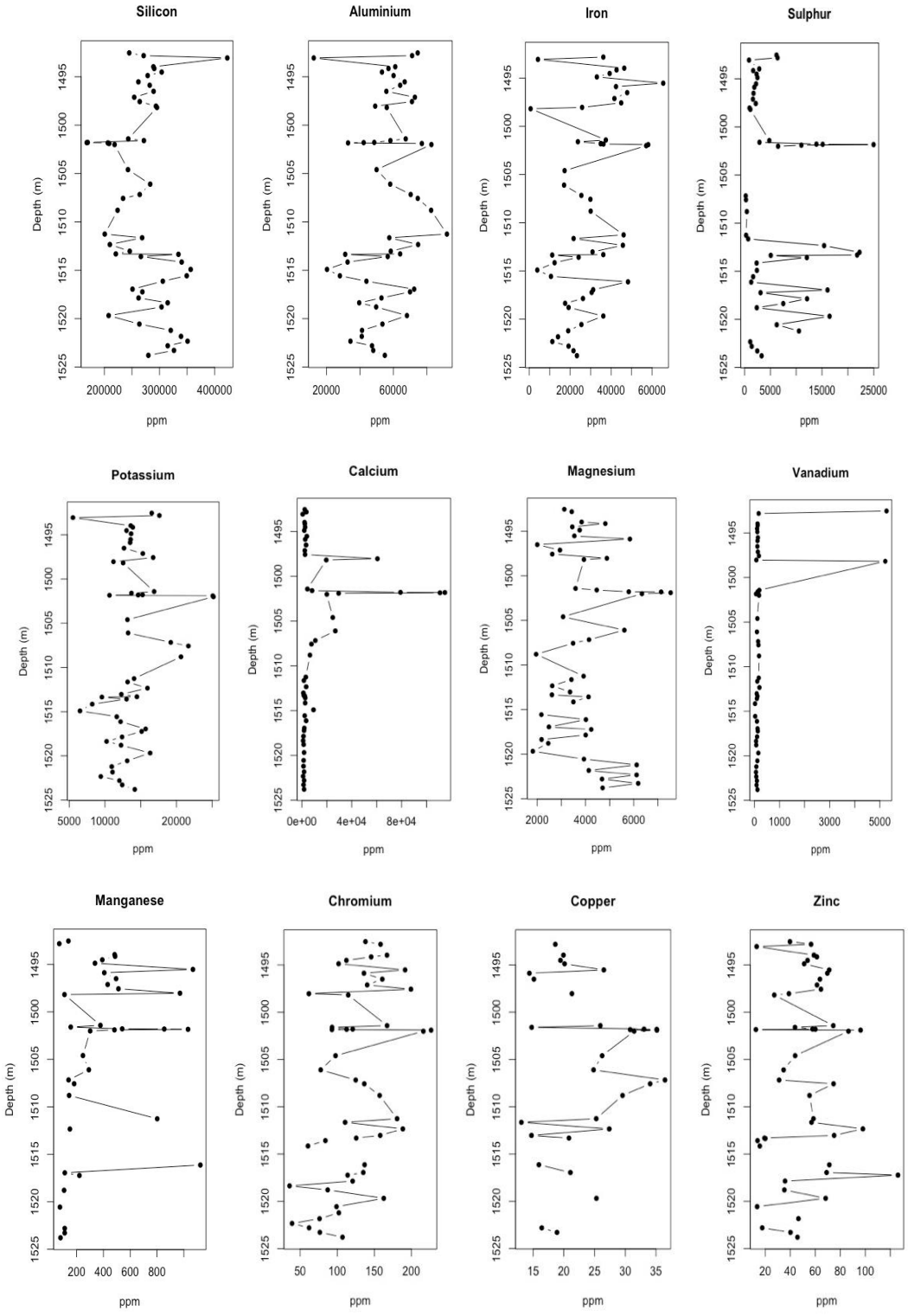

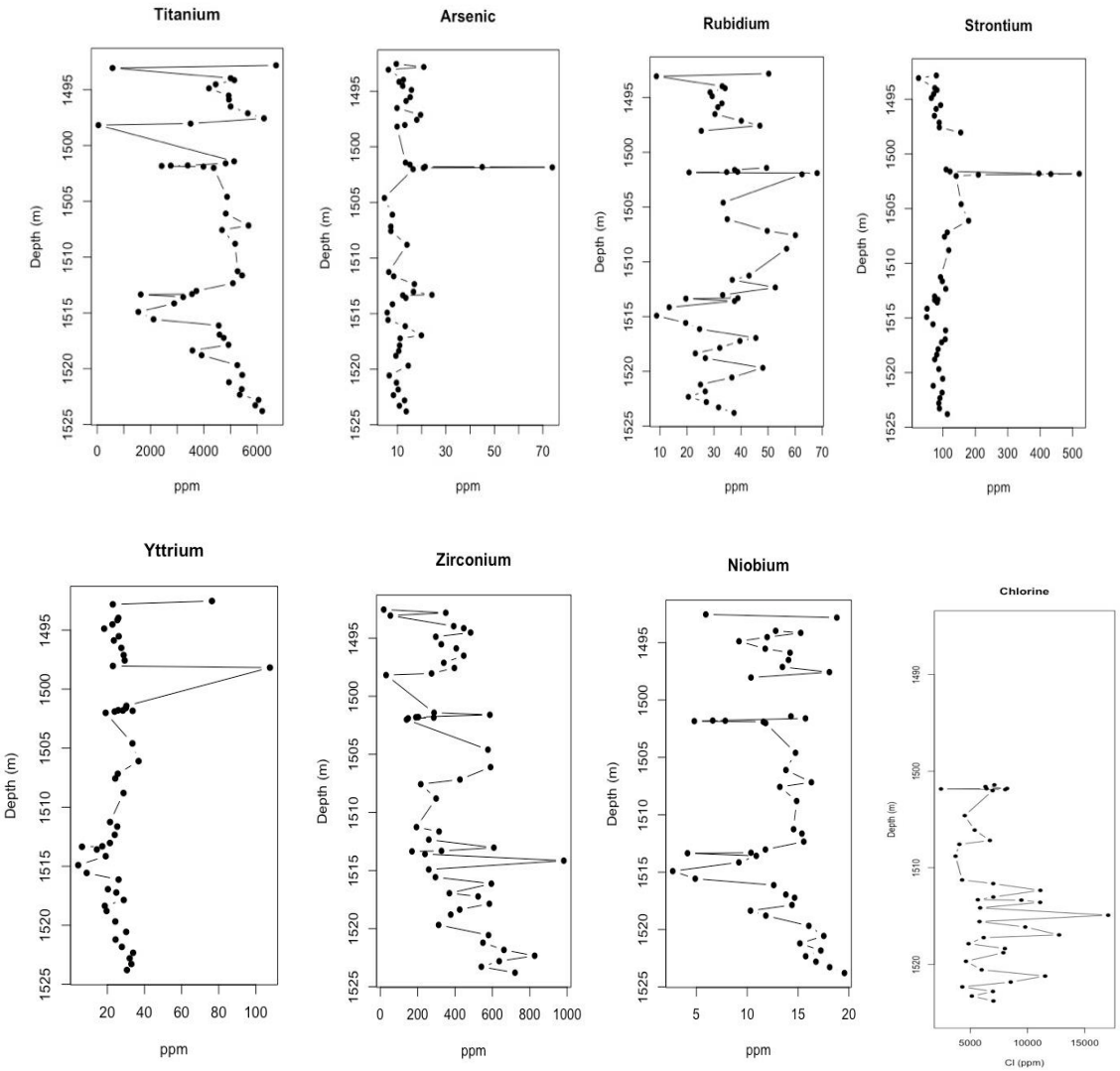
Titanium
Arsenic
Rubidium
Strontium
Yttrium
Zirconium
Niobium
Chlorine
Depth (m)
ppm
Cl (ppm)

B. Graphic histogram with the elemental distribution of the analysed variables as a series of bars, with frequency counts for Si, Al, Fe, K, Ca, Mg, S, V, Mn, Cr, Cu, Zn Ti, As, Rb, Sr, Y, Zr, Nb and Cl.

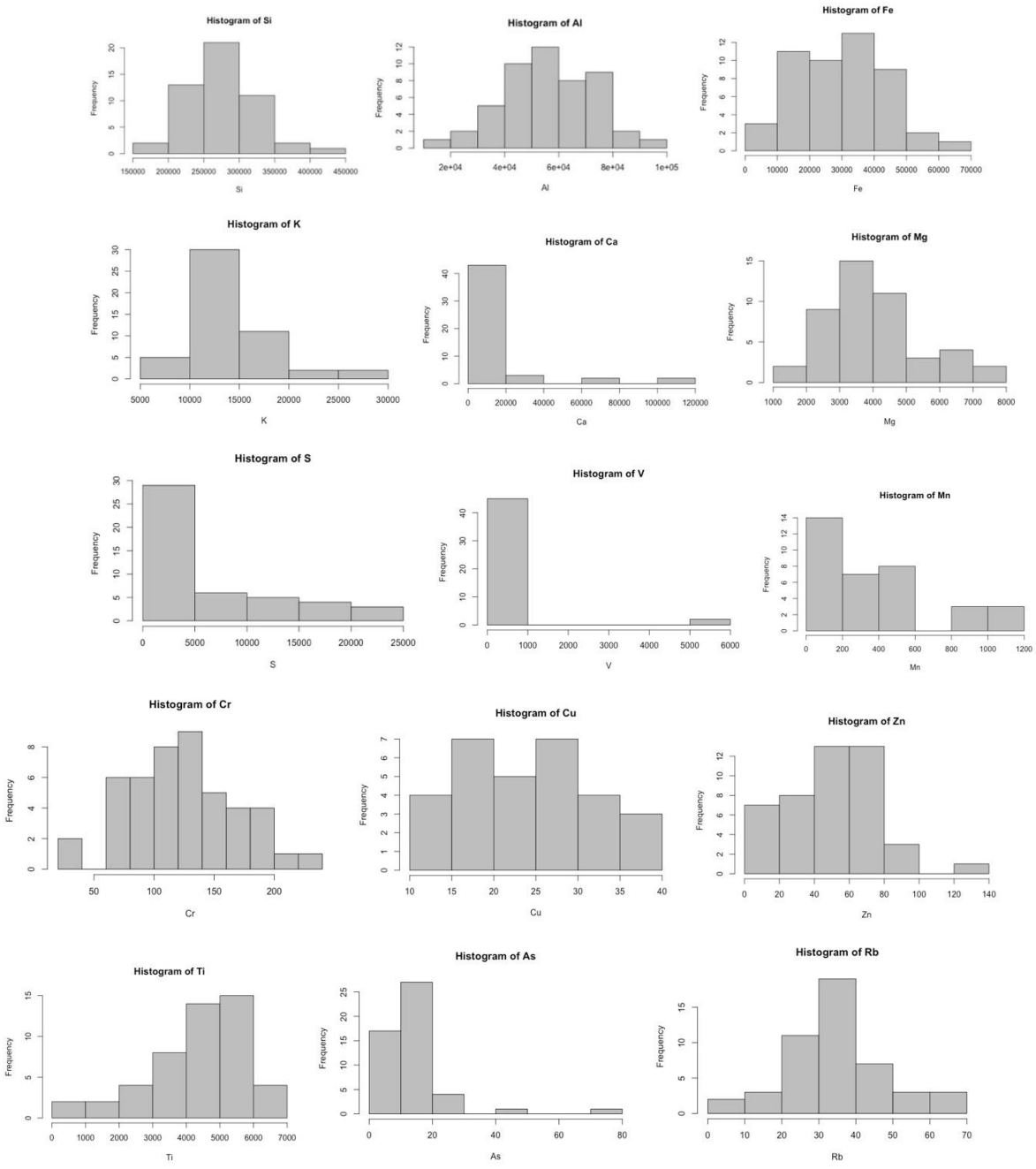

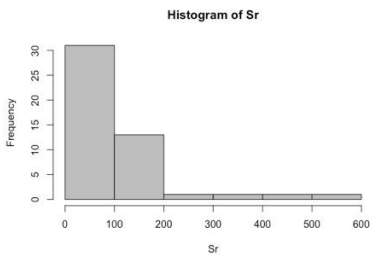
Histogram of Sr
Frequency
0
5
10
15
20
25
30
0
100
200
300
400
500
600
Sr

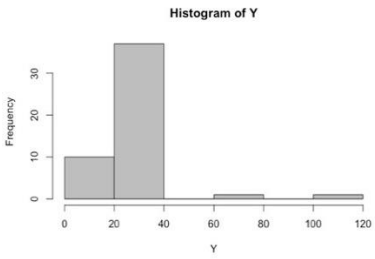
Histogram of Y
Frequency
0
10
20
30
0
20
40
60
80
100
120
Y

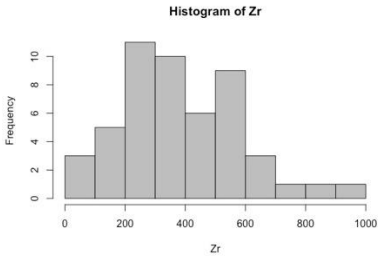
Histogram of Zr
Frequency
0
2
4
6
8
10
0
200
400
600
800
1000
Zr

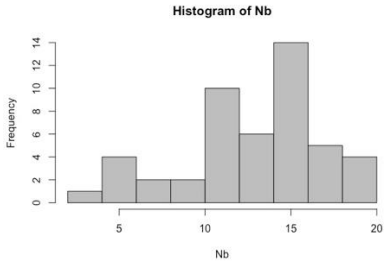
Histogram of Nb
Frequency
0
2
4
6
8
10
12
14
5
10
15
20
Nb

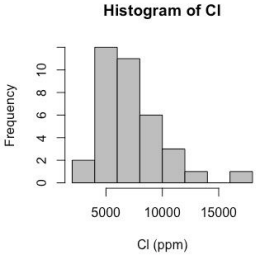
Histogram of Cl
Frequency
0
2
4
6
8
10
5000
10000
15000
Cl (ppm)

II. XRF analysis – Schandelah:

A. Results of bulk elemental concentration versus depth for Si, Al, Fe, K, Ca, Mg, S, V, Mn, Cr, Cu, Zn Ti, As, Rb, Sr, Y, Zr, Nb and Cl.

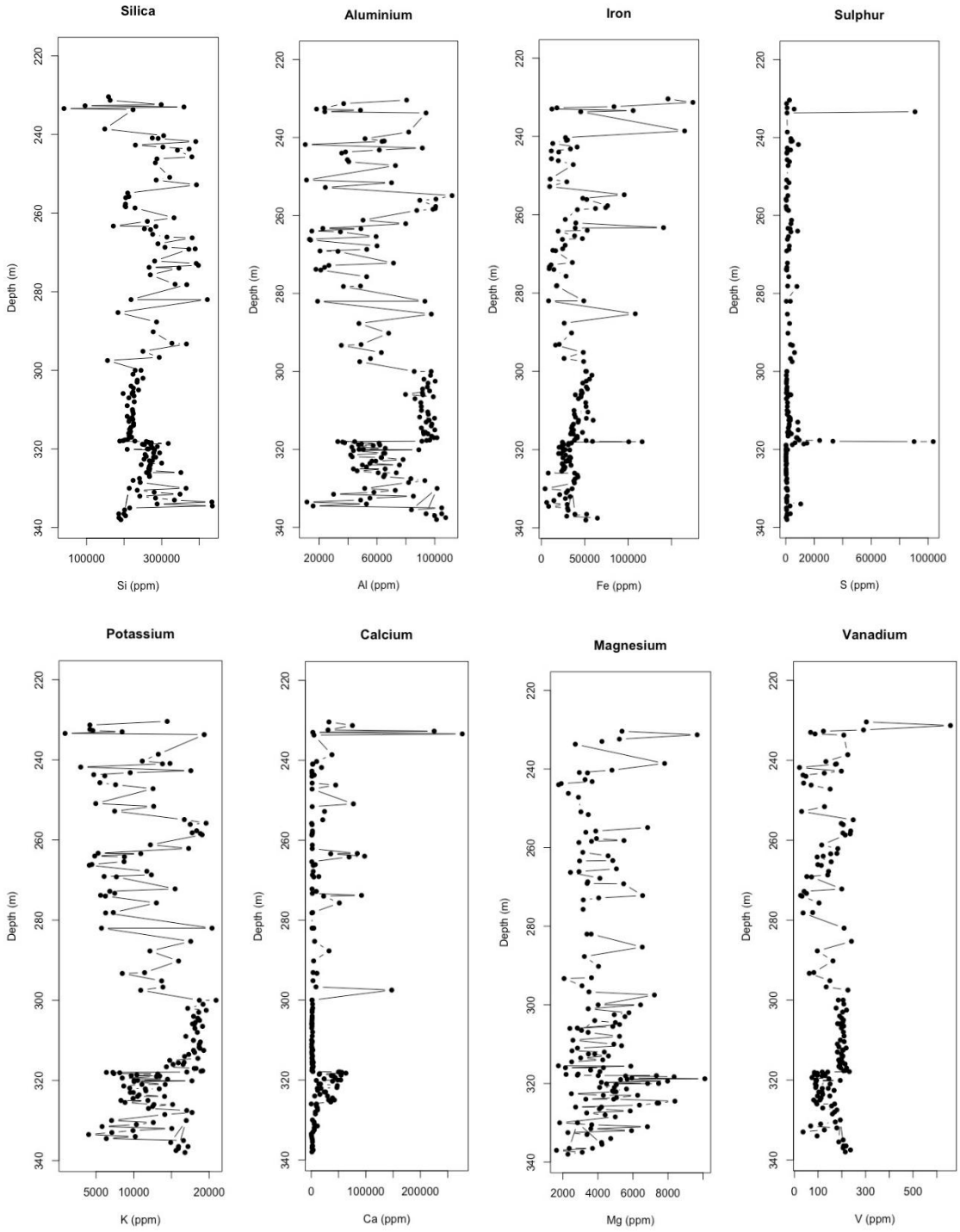

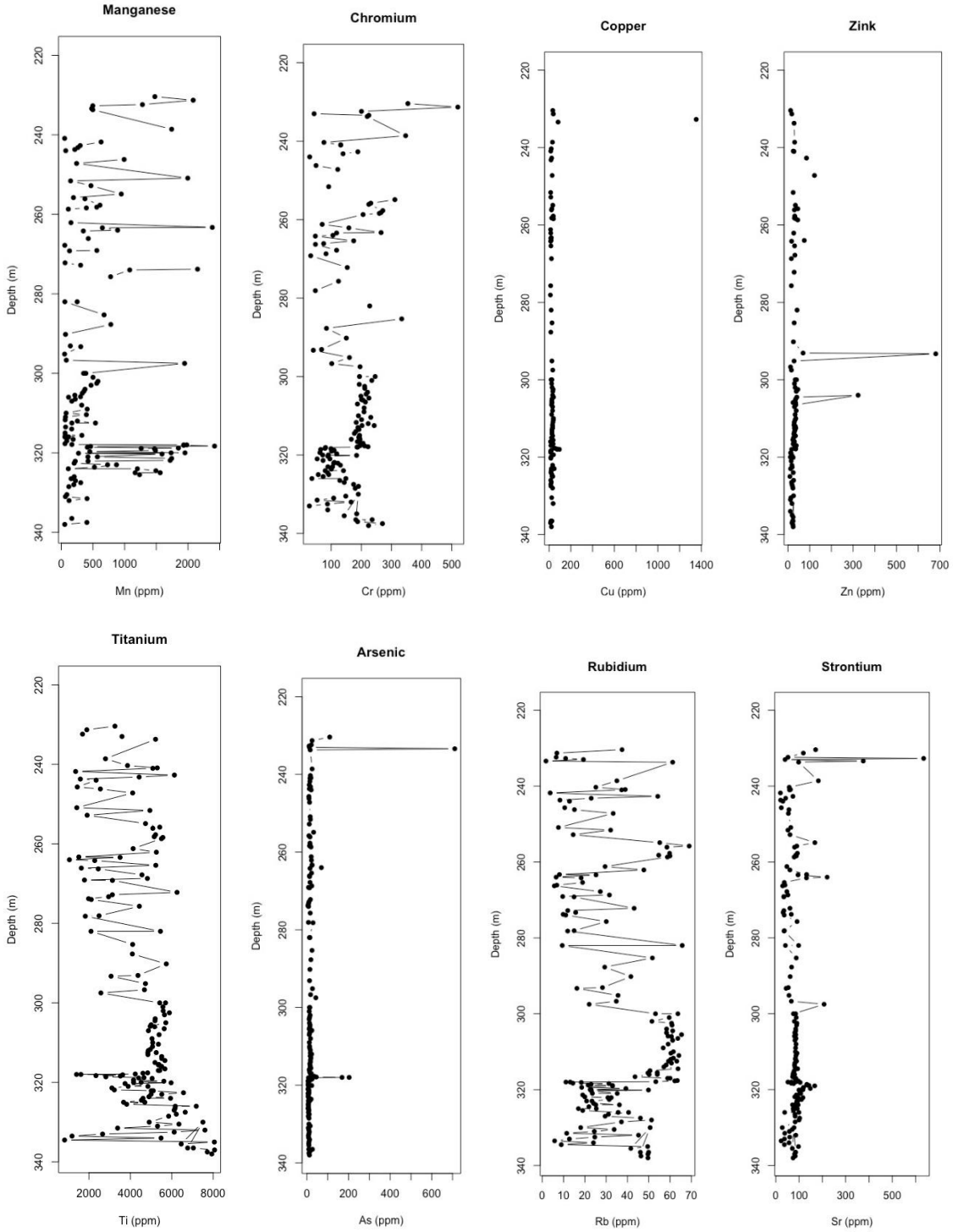
Manganese
Depth (m)
Mn (ppm)
Chromium
Cr (ppm)
Copper
Cu (ppm)
Zink
Zn (ppm)
Titanium
Ti (ppm)
Arsenic
As (ppm)
Rubidium
Rb (ppm)
Strontium
Sr (ppm)

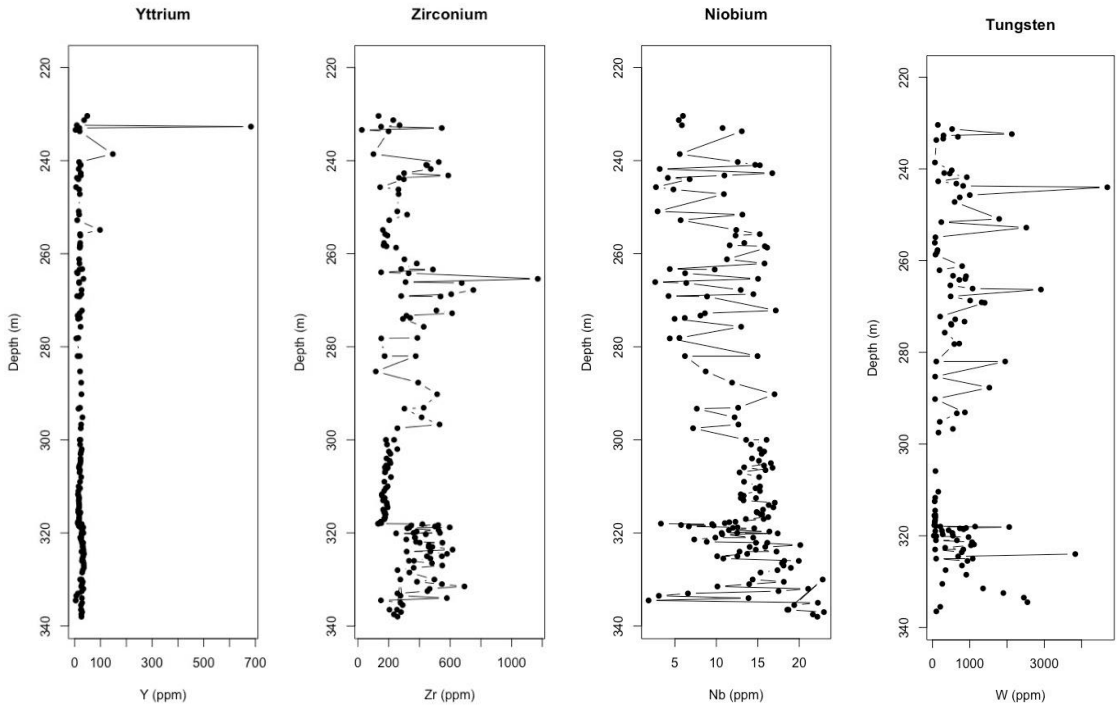
Yttrium
Zirconium
Niobium
Tungsten
Depth (m)
220
240
260
280
300
320
340
0 100 300 500 700
Y (ppm)
0 200 600 1000
Zr (ppm)
5 10 15 20
Nb (ppm)
0 1000 3000
W (ppm)

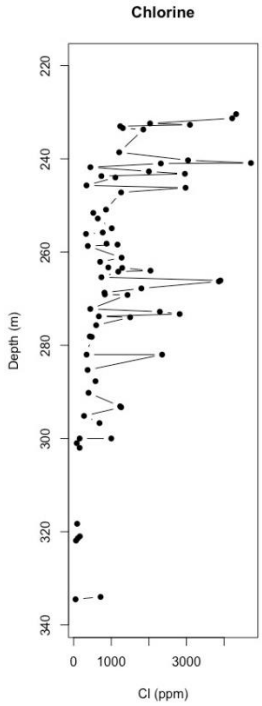
Chlorine
Depth (m)
220
240
260
280
300
320
340
0 1000 3000
Cl (ppm)

B. Graphic histogram with the elemental distribution of the analysed variables as a series of bars, with frequency counts for Si, Al, Fe, S, K, Ca, Mg, V, Mn, Cr, Cu, Zn Ti, As, Rb, Sr, Y, Zr, Nb and Cl.

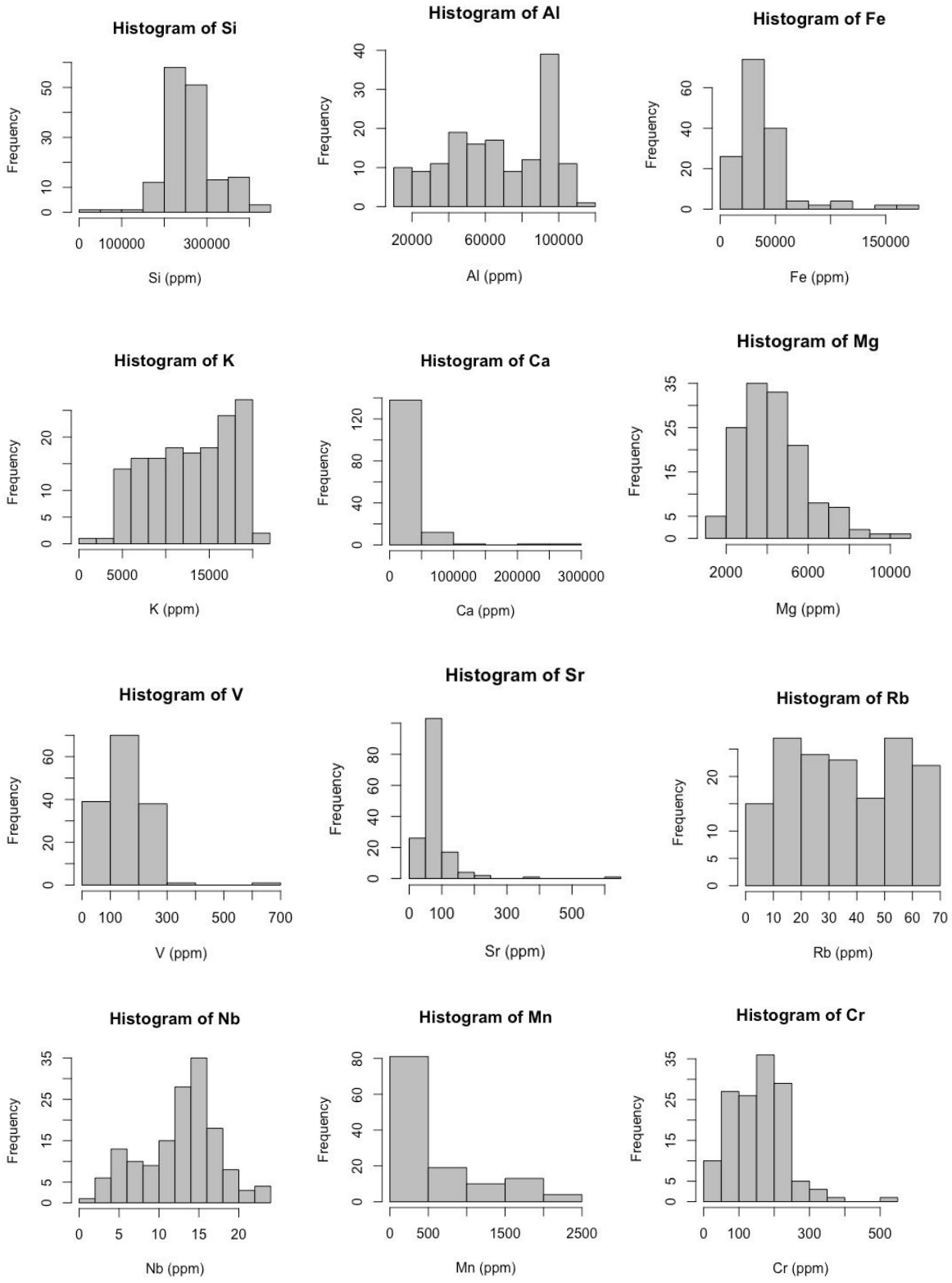

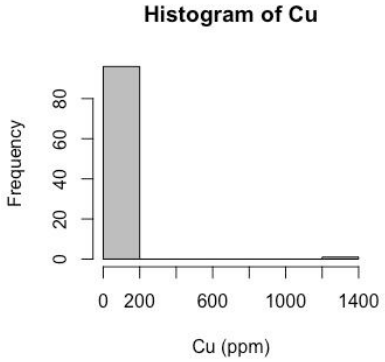
Histogram of Cu
Frequency
0
20
40
60
80
0
200
600
1000
1400
Cu (ppm)

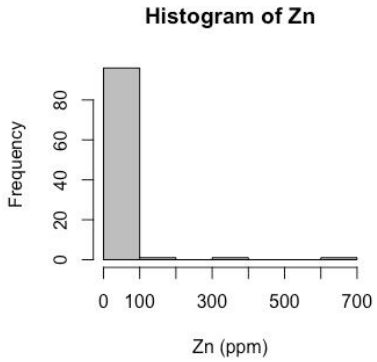
Histogram of Zn
Frequency
0
20
40
60
80
0
100
300
500
700
Zn (ppm)

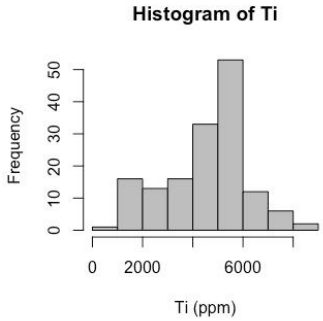
Histogram of Ti
Frequency
0
10
20
30
40
50
0
2000
6000
Ti (ppm)

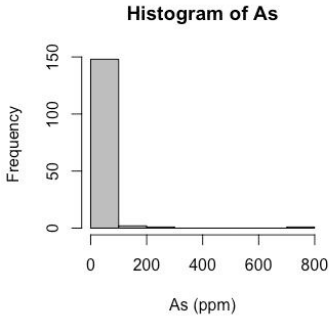
Histogram of As
Frequency
0
50
100
150
0
200
400
600
800
As (ppm)

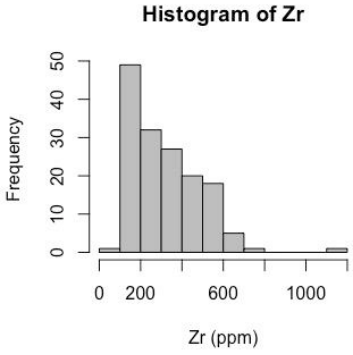
Histogram of Zr
Frequency
0
10
20
30
40
50
0
200
600
1000
Zr (ppm)

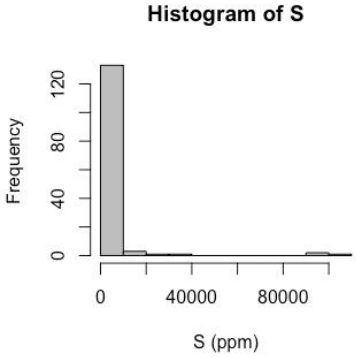
Histogram of S
Frequency
0
40
80
120
0
40000
80000
S (ppm)

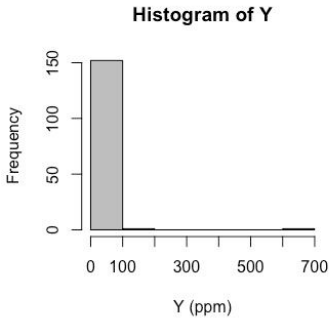
Histogram of Y
Frequency
0
50
100
150
0
100
300
500
700
Y (ppm)

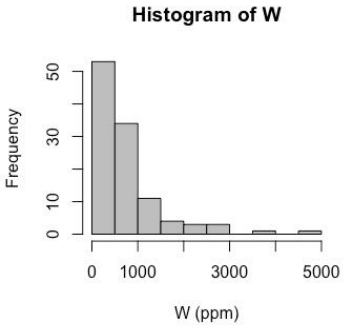
Histogram of W
Frequency
0
10
30
50
0
1000
3000
5000
W (ppm)

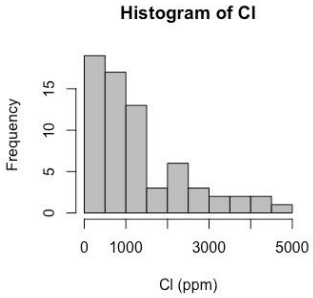
Histogram of Cl
Frequency
0
5
10
15
0
1000
3000
5000
Cl (ppm)

III. Results of reproductive analysis of a standard (2709a) from XRF measures

Element	Mean (ppm)	Standard deviation (ppm)	% St.dev from mean (±)	Standard error (ppm)	% of internal random error compared to mean value (±)
Al	71120,30	2030,11	2,85	364,62	1,28
Si	295125,08	4885,50	1,66	877,46	0,37
Fe	37445,22	226,56	0,61	40,69	0,64
S	1207,99	82,31	6,81	14,78	5,56
V	160,73	10,55	6,56	1,89	16,40
Cr	223,65	18,28	8,18	3,28	9,75
Cu	32,81	5,76	17,56	1,03	30,33
Mn	453,84	24,19	5,33	4,34	10,05
Ni	58,20	10,97	18,84	1,97	34,98
Zn	106,16	9,85	9,28	1,77	7,79
Ti	3198,86	70,90	2,22	12,73	1,83
Ca	19459,45	534,53	2,75	96,00	1,66
K	17503,88	415,52	2,37	74,63	1,23

IV. Iron and sulphur normalized to Al and S/Fe normalized to Al for both localities.

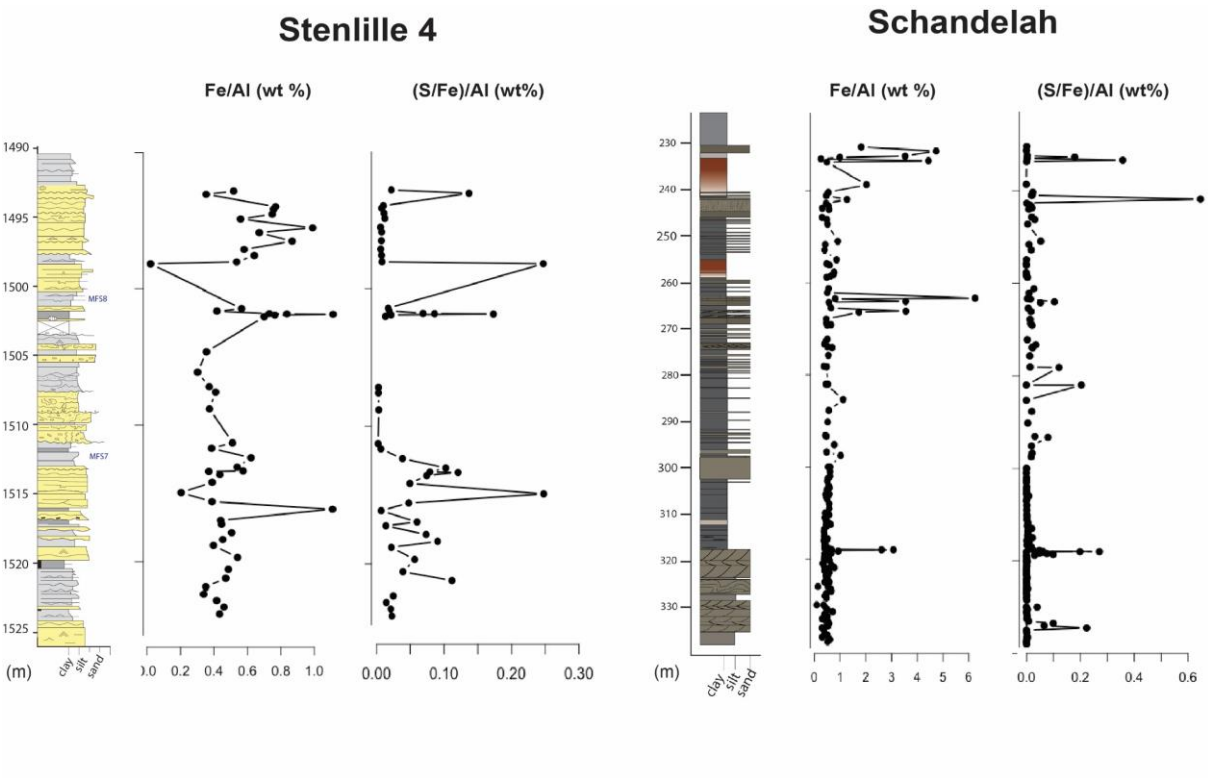

Appendix 2. ICP-MS analysis

A. Stenlille 4: Normalization of subsequent trace elements to Al

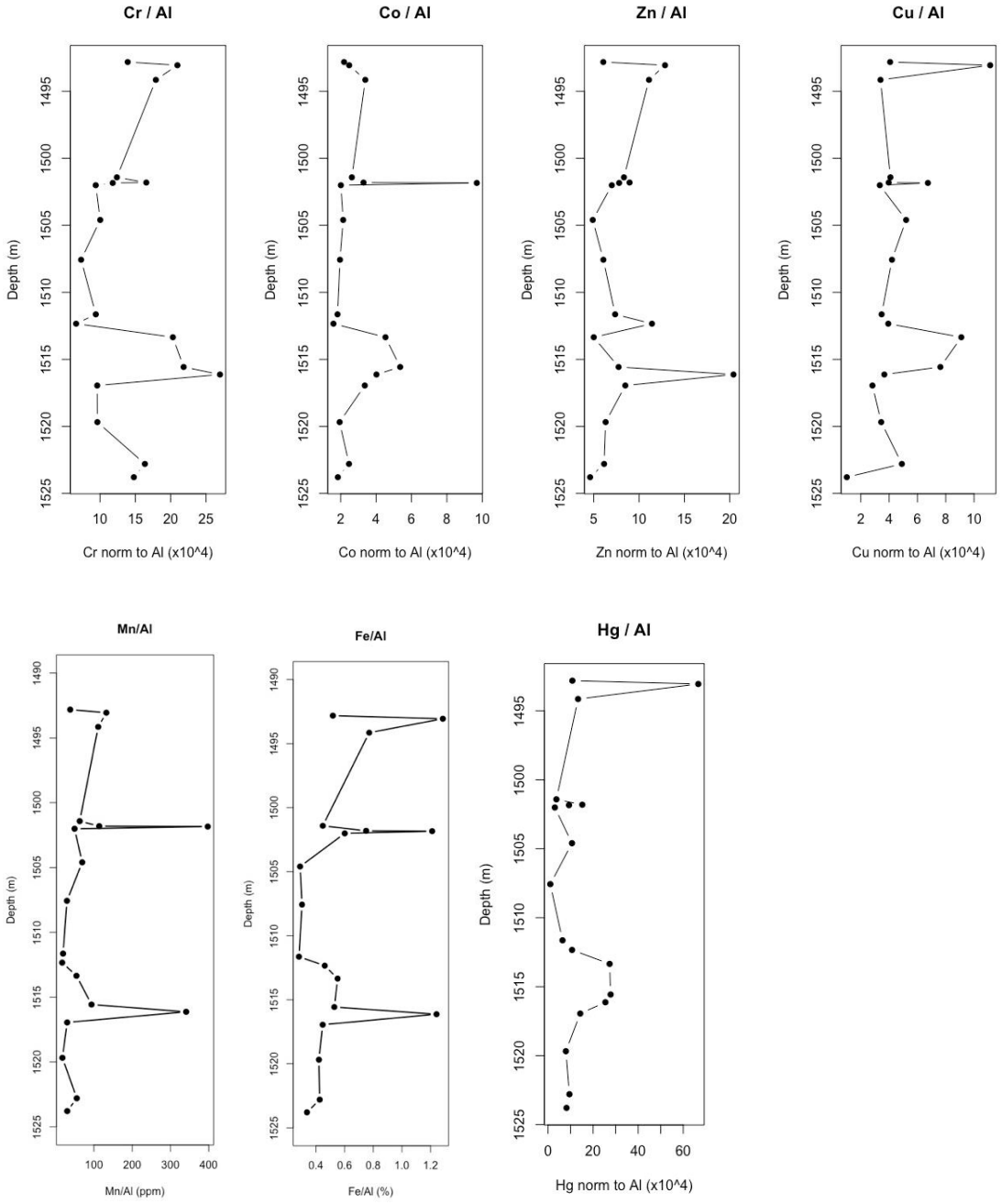

B. Schandelah: Normalization of subsequent trace elements to Al

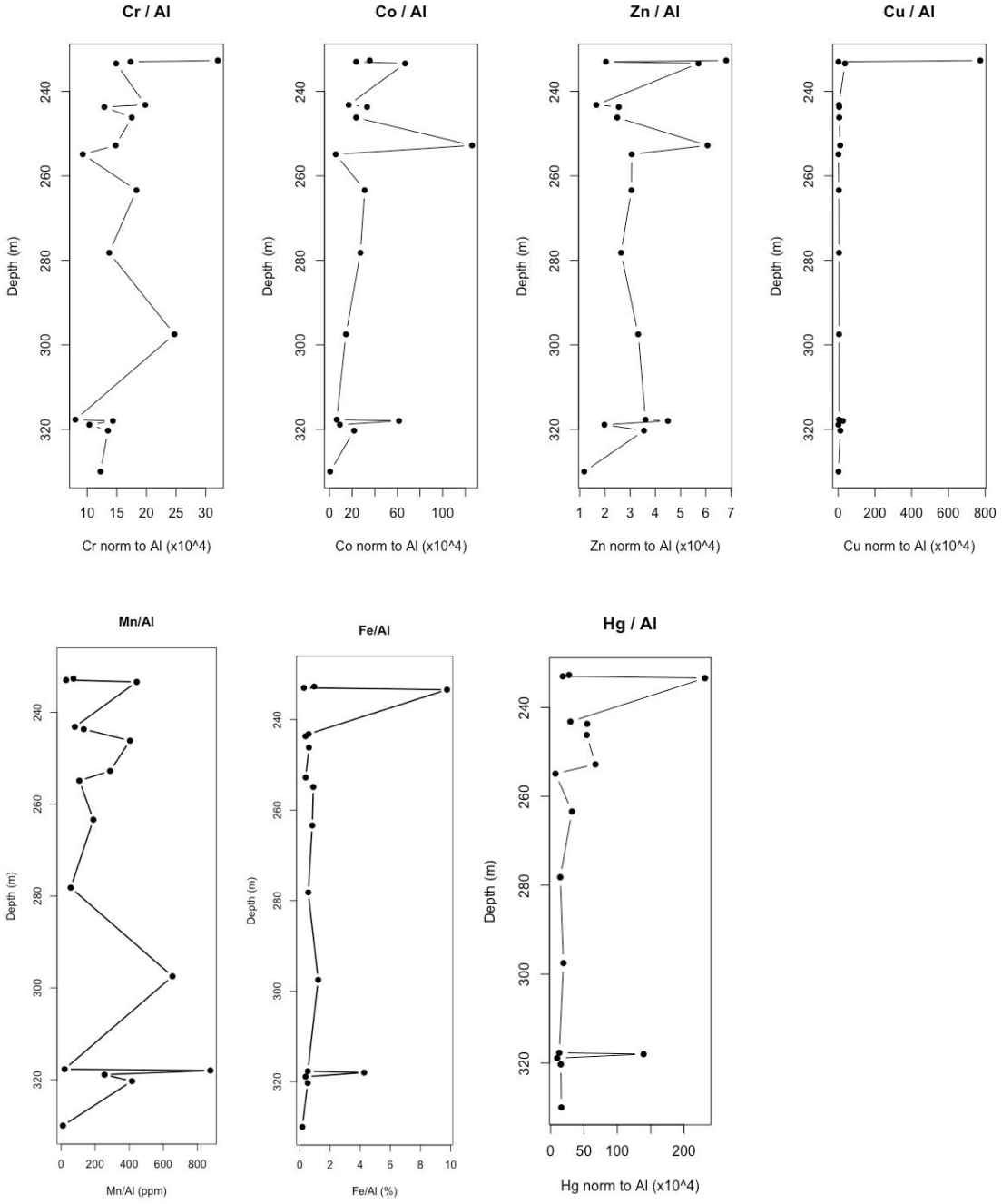

Appendix 3. ICP-MS analysis

a) ICP-MS analysis – Stenlille 4: Supplementary summary of 22 elements

Li (ppm)	Hf (ppm)	Er (ppm)	Be (ppm)	Ho (ppm)
Min. : 10.00	Min. :0.60	Min. :0.300	Min. :0.200	Min. :0.1000
1st Qu.: 32.65	1st Qu.:3.15	1st Qu.:2.425	1st Qu.:1.325	1st Qu.:0.8000
Median : 47.55	Median :4.10	Median :2.650	Median :2.100	Median :0.9500
Mean : 59.87	Mean :3.90	Mean :2.394	Mean :1.911	Mean :0.8556
3rd Qu.: 90.12	3rd Qu.:5.15	3rd Qu.:2.700	3rd Qu.:2.650	3rd Qu.:1.0000
Max. :159.00	Max. :6.40	Max. :3.500	Max. :3.000	Max. :1.3000
Cs (ppm)	**Eu (ppm)**	**Bi (ppm)**	**Se (ppm)**	**Ga (ppm)**
Min. :0.420	Min. :0.190	Min. :0.0600	Min. :0.2000	Min. : 3.00
1st Qu.:2.385	1st Qu.:1.167	1st Qu.:0.1650	1st Qu.:0.9000	1st Qu.:10.62
Median :3.935	Median :1.390	Median :0.2350	Median :1.0000	Median :15.80
Mean :3.918	Mean :1.302	Mean :0.2389	Mean :0.9944	Mean :15.72
3rd Qu.:5.732	3rd Qu.:1.468	3rd Qu.:0.3150	3rd Qu.:1.0000	3rd Qu.:21.05
Max. :6.890	Max. :2.270	Max. :0.4100	Max. :2.0000	Max. :25.70
Rb (ppm)	**Sm (ppm)**	**Nb (ppm)**	**Ba (ppm)**	**La (ppm)**
Min. : 20.20	Min. : 1.100	Min. : 0.200	Min. :157.0	Min. : 8.50
1st Qu.: 48.05	1st Qu.: 6.500	1st Qu.: 1.925	1st Qu.:255.2	1st Qu.:35.83
Median : 67.25	Median : 7.300	Median : 5.300	Median :269.0	Median :43.85
Mean : 68.01	Mean : 7.156	Mean : 8.483	Mean :268.1	Mean :41.06
3rd Qu.: 88.50	3rd Qu.: 8.300	3rd Qu.:15.700	3rd Qu.:280.5	3rd Qu.:49.15
Max. :128.00	Max. :12.800	Max. :22.400	Max. :403.0	Max. :68.30
Ce (ppm)	**Pr (ppm)**	**Nd (ppm)**	**Dy (ppm)**	**Yb (ppm)**
Min. : 19.10	Min. : 2.000	Min. : 7.10	Min. :0.600	Min. :0.400
1st Qu.: 77.35	1st Qu.: 8.625	1st Qu.:32.33	1st Qu.:4.300	1st Qu.:2.700
Median : 91.85	Median :10.500	Median :39.90	Median :4.950	Median :3.000
Mean : 84.09	Mean : 9.739	Mean :37.05	Mean :4.500	Mean :2.689
3rd Qu.: 94.58	3rd Qu.:11.550	3rd Qu.:43.38	3rd Qu.:5.175	3rd Qu.:3.100
Max. :127.00	Max. :16.600	Max. :64.00	Max. :6.800	Max. :3.800
Sr (ppm)	**Th (ppm)**			
Min. : 25.10	Min. : 2.20			
1st Qu.: 75.47	1st Qu.:11.40			
Median : 91.40	Median :13.45			
Mean :103.07	Mean :12.18			
3rd Qu.:104.75	3rd Qu.:15.18			
Max. :342.00	Max. :18.10			

b) ICP-MS analysis – Schandelah: Supplementary summary of 22 elements

Li (ppm)	Hf (ppm)	Er (ppm)	Be (ppm)	Ho (ppm)
Min. : 5.80	Min. :0.300	Min. : 0.300	Min. :0.200	Min. : 0.100
1st Qu.: 20.05	1st Qu.:0.875	1st Qu.: 1.425	1st Qu.:0.575	1st Qu.: 0.475
Median : 27.00	Median :2.150	Median : 1.850	Median :1.200	Median : 0.750
Mean : 38.29	Mean :2.744	Mean : 6.344	Mean :1.269	Mean : 2.775
3rd Qu.: 42.35	3rd Qu.:3.950	3rd Qu.: 2.600	3rd Qu.:1.500	3rd Qu.: 1.000
Max. :135.00	Max. :6.700	Max. :68.300	Max. :3.300	Max. :31.000
Cs (ppm)	**Eu (ppm)**	**Bi (ppm)**	**Se (ppm)**	**Ga (ppm)**
Min. : 0.320	Min. : 0.160	Min. :0.0500	Min. :0.500	Min. : 1.500
1st Qu.: 1.377	1st Qu.: 0.520	1st Qu.:0.1175	1st Qu.:0.675	1st Qu.: 5.550
Median : 1.940	Median : 1.065	Median :0.1400	Median :0.750	Median : 7.300
Mean : 2.882	Mean : 5.332	Mean :0.1650	Mean :1.019	Mean : 9.706
3rd Qu.: 3.115	3rd Qu.: 1.565	3rd Qu.:0.1900	3rd Qu.:1.050	3rd Qu.:10.825
Max. :10.300	Max. :63.000	Max. :0.4100	Max. :2.900	Max. :28.200
Rb (ppm)	**Y (ppm)**	**Ba (ppm)**	**La (ppm)**	**Ce (ppm)**
Min. : 4.40	Min. : 2.90	Min. : 60.0	Min. : 4.50	Min. : 10.90
1st Qu.: 26.12	1st Qu.: 12.05	1st Qu.:132.0	1st Qu.: 16.77	1st Qu.: 39.58
Median : 34.10	Median : 18.35	Median :180.0	Median : 29.85	Median : 64.95
Mean : 42.10	Mean : 71.58	Mean :238.4	Mean : 60.33	Mean : 182.36
3rd Qu.: 44.77	3rd Qu.: 24.60	3rd Qu.:259.8	3rd Qu.: 43.25	3rd Qu.: 88.70
Max. :115.00	Max. :817.00	Max. :641.0	Max. :509.00	Max. :1910.00
Pr (ppm)	**Nd (ppm)**	**Gd (ppm)**	**Dy (ppm)**	**Yb (ppm)**
Min. : 1.200	Min. : 4.40	Min. : 0.700	Min. : 0.70	Min. : 0.300
1st Qu.: 4.425	1st Qu.: 15.85	1st Qu.: 2.375	1st Qu.: 2.45	1st Qu.: 1.525
Median : 7.500	Median : 27.50	Median : 4.950	Median : 4.15	Median : 2.200
Mean : 24.869	Mean : 112.95	Mean : 24.069	Mean : 17.41	Mean : 4.162
3rd Qu.: 11.000	3rd Qu.: 43.27	3rd Qu.: 6.800	3rd Qu.: 5.70	3rd Qu.: 2.900
Max. :270.000	Max. :1280.00	Max. :283.000	Max. :200.00	Max. :33.000
Sr (ppm)	**Th (ppm)**			
Min. : 19.50	Min. : 1.700			
1st Qu.: 35.92	1st Qu.: 5.125			
Median : 67.75	Median : 9.700			
Mean :117.92	Mean : 9.144			
3rd Qu.:127.75	3rd Qu.:12.375			
Max. :623.00	Max. :15.700			

Appendix 4.

Table representing calculated values for EF‘s > 2 both from ICP-MS and XRF analysis, from both localities. The values are denoted to the sulphide fraction for Mo, U, V and for the organic fraction in Ni (more accurate would be to denote it to the authigenic fraction).

Stenlille 4	EF's > 2	c.p.t. Av.Sh.													Ni assumed in org. Fr.		
Depth	Mo	U	V	Ni	Al	V detr.	V org.	V sulf.	Mo detr.	Mo org.	Mo. Sulf.	U detr.	U. org.	U. Sulf	Ni detr.	Ni. org.	Ni. Sulf
XRF																	
1492,54	13,34	45,3	5269,0	x	74584,69	109,1	NO TOC C.	5159,9	1,09	No TOC c.	12,2	2,5	No TOC c.	42,8	x	x	x
1498,18	15,41	35,0	5217,2	x	56070,89	82,0	NO TOC C.	5135,2	0,82	No TOC c.	14,6	1,9	No TOC c.	33,1	x	x	x
1501,6	3,84	x	x	x	58255,48	x	x	x	0,85	No TOC c.	3,0	x	x	x	x	x	x
1522,33	x	3,1	x	x	34353,87	x	x	x	x	x	x	1,2	No TOC c.	2,0	x	x	x
ICP-MS																	
1493,06	3,88	1,3	x	x	10500	x	x	x	0,15	No TOC c.	3,7	0,4	No TOC c.	0,9	x	x	x
1501,42	3,89	x	x	x	80700	x	x	x	1,18	No TOC c.	2,7	x	x	x	x	x	x
1501,84	1,83	x	x	67,5	32200	x	x	x	0,47	No TOC c.	1,4	x	x	x	24,6	x	42,9
1513,35	1,18	x	x	x	25600	x	x	x	0,37	No TOC c.	0,8	x	x	x	x	x	x
1516,13	x	3,5	x	x	39300	x	x	x	x	x	x	x	x	x	x	x	x
1522,8	x	5,4	x	x	73000	x	x	x	x	x	x	x	x	x	x	x	x
								Av.sh						Av.Sh.			Av.Sh.
								(130/88900)						(3/88900)			(68/88900)

Schandelah	EF's > 2	c.p.t. Av.Sh.													Ni assumed in org. Fr.		
Depth	Mo	U	V	Ni	Al	V detr.	V org.	V sulf.	Mo detr.	Mo org.	Mo. Sulf.	U detr.	U. org.	U. Sulf	Ni detr.	Ni. org.	Ni. Sulf
XRF																	
230,4	x	3,2	303,2	x	80529	117,8	NO TOC c.	185,5	x	x	x	2,7	No TOC c.	0,5	x	x	x
231,3	x	x	657,5	80,18	36973	54,1	NO TOC c.	603,5	x	x	x	x	x	x	28,3	51,9	TOC CORR
232,4	x	x	291,3	x	23775	34,8	NO TOC c.	256,5	x	x	x	x	x	x	x	x	x
263,3	x	x	179,1	x	22571	33,0	NO TOC c.	146,1	x	x	x	x	x	x	x	x	x
263,4	x	x	153,0	x	48901	71,5	NO TOC c.	81,5	x	x	x	x	x	x	x	x	x
264	x	x	121,4	x	14934	21,8	NO TOC c.	99,5	x	x	x	x	x	x	x	x	x
266,1	x	x	99,0	x	13327	19,5	NO TOC c.	79,5	x	x	x	x	x	x	x	x	x
266,3	x	x	113,6	x	14049	20,5	NO TOC c.	93,0	x	x	x	x	x	x	x	x	x
317,9	8,83	x	x	x	91110	x	x	x	1,33	No TOC c.	7,50	x	x	x	x	x	x
ICP-MS																	
232,7	0,79	41,6	100,0	x	18100	26,5	NO TOC c.	73,5	0,26	No TOC c.	0,53	0,6	No TOC c.	41,0	x	x	x
233,4	15,7	x	x	102,0	12100	x	x	x	0,18	No TOC c.	15,52	x	x	x	9,3	92,7	TOC CORR
278,2	1,72	x	x	x	27700	x	x	x	0,41	No TOC c.	1,31	x	x	x	x	x	x
297,5	x	x	170,0	x	36400	53,2	NO TOC c.	116,8	x	x	x	x	x	x	x	x	x
317,7	5,53	x	x	x	100000	x	x	x	1,46	No TOC c.	4,07	x	x	x	x	x	x
318	53,2	x	x	83,9	25100	x	x	x	0,37	No TOC c.	52,83	x	x	x	19,2	64,7	TOC CORR
								Av.sh			Av.Sh.			Av.Sh.			Av.Sh.
								(130/88900)			(1,3/88900)			(3/88900)			(68/88900)

Appendix 5. $\delta^{13}C_{org}$ results for Stenlille 4

The table lists $\delta^{13}C_{org}$ values reported here (grey) and additionally previos reported GEUS values aquired from the same core section (orange).

Corrected depth	Values reported herein	GEUS values
1492,54	-25,5	
1494,52	-24,9	
1494,88	-25,0	
1495,53	-25,5	
1495,88	-25,4	
1496,51	-25,3	
1497,12	-25,5	
1497,57	-25,5	
1498,04	-25,9	
1498,18	-26,1	
1498,51		-25,48
1499,3		-25,99
1499,51		-25,83
1499,51		-25,77
1499,55		-25,96
1499,8		-25,84

1500,1		-25,81
1500,5		-25,94
1500,75		-25,84
1500,75		-25,97
1500,75		-26,05
1500,8		-26,03
1501,39		-26,22
1501,42	-26,6	
1501,6	-26,5	
1501,79	-29,0	
1501,81	-28,4	
1501,84	-28,2	
1502,01	-25,4	
1502,35		-25,62
1503,92		-24,99
1504,28		-25,69
1504,6	-24,4	
1504,9		-24,73
1505,4		-25,22
1505,98		-24,66
1506,1	-28,4	
1506,49		-24,44
1507,01		-26,35
1507,17	-26,0	
1507,25		-26,29
1507,57	-25,5	
1507,85		-24,93
1508,39		-25,05
1508,8	-25,1	
1509,15		-25,11
1509,17		-24,57
1509,48		-25,15
1509,92		-25,6
1510		-25,23
1510,18		-24,67
1510,97		-24,56
1511,26	-24,7	
1511,64	-25,1	
1511,71		-25,04
1512,14		-25,75
1512,34		-25,98
1512,75		-24,87
1512,85		-24,89
1513,03	-25,8	
1513,31	-25,3	
1513,35	-24,9	
1513,58	-25,5	
1513,72		-25,23
1514,15	-26,7	
1514,43		-24,81
1514,53		-24,8
1514,91	-25,4	
1516,13	-25,0	
1516,34		-24,68
1516,54		-24,51
1516,95	-26,6	
1517,23	-26,0	
1517,3		-25,91
1517,65		-25,02
1517,86	-26,1	
1518,36	-26,3	
1518,79	-26,1	
1519,12		-24,43
1519,68	-27,7	

1519,7		-26,01
1520,56	-26,2	
1521,21	-26,3	
1521,83	-25,9	
1522,33	-25,7	
1522,8	-26,2	
1523,28	-26,1	
1523,79	-25,8	
∑n	43	45
Average	-25,99	-25,37
Nr of outliers or removed values	3	
Corresponding Intervals and values for those 3:		
1501,90	-34,4	
1515,57	-43,1	
1512,34	-26,5	

Appendix 6. Comparison of XRF versus ICP-MS analytical methods

a) Stenlille 4

(ppm)	∑n	XRF Average	ICP-MS Average	Average difference	%Relative difference	% XRF Co.eff.V.	% ICP-MS Co.eff.V.	R2
Al	18	53836	62461	8625	16	36	43	0,91
Fe	18	30202	32200	1998	7	47	41	0,95
V	16	128	71	57	80	36	52	0,71
Mo	1	*3,48*	*3,30*	*0,18*	*5*	x	x	x
Zn	17,0	56,6	51,0	5,7	11	46	48	0,85
Cu	13	24,7	28,7	4,0	16	29	25	0,19
Ni	3	45,5	51,9	6,4	14	21	30	0
Mn	13	394	423	29	7	94	90	0,91
Cr	15	135	84	52	62	29	23	0,05

b) Schandelah

(ppm)	∑n	XRF average	ICP-MS average	Average difference	%Relative difference	% XRF Co.eff.V.	%ICP-MS Co.eff.V.	R2
Al	16	49102	43013	6090	14	50	58	0,95
Fe	16	38547	38256	291	0,76	87	92	0,98
V	15	118	71	47	66	58	70	0,77
Mo	3	26,1	24,8	1,3	5	104	101	0,99
U	1	*26,4*	*41,6*	*15,2*	x	x	x	x
Zn	4	24,1	37,5	13,3	55	48	33	0,7
Cu	10	170,3	169,9	0,3	0,18	245	255	0,94
Ni	4	94,3	65,6	28,7	44	32	54	0,32
Mn	13	869	1039	169	19	74	73	0,79
Cr	11	153	68	85	125	54	36	0,7

Appendix 7. XRF dataset for both localites.

a). Stenlille 4 – XRF data. reported in ppm.

Corrected depth	Sample	Ba	Ba Error	Sb	Sb Error	Sn	Sn Error	Cd	Cd Error	Ag	Ag Error	Bal	Bal Error
1492,54	538670	< LOD: 12.14		< LOD: 8.43		6.58	3.14	4.50	2.06	611662.81	985.26	< LOD: 1.69	
1492,82	538671	< LOD: 28.65		< LOD: 10.86		< LOD: 8.76		< LOD: 4.83		3.32	2.11	582581.88	1048.45
1493,06	538672	< LOD: 25.61		< LOD: 6.44		< LOD: 7.86		< LOD: 5.57		< LOD: 2.82		552714.88	1033.35
1493,97	538673	49.42	19.81	9.46	5.72	13.54	6.08	< LOD: 4.97		< LOD: 3.21		574601.38	1062.75
1494,15	538674	51.40	19.65	< LOD: 11.13		12.64	6.02	8.11	3.35	3.54	2.15	580408.69	1047.61
1494,52	538675	52.92	19.78	< LOD: 12.36		12.34	6.06	< LOD: 4.97		3.59	2.17	576355.81	1047.65
1494,88	538676	46.72	18.76	< LOD: 8.11		< LOD: 9.76		< LOD: 5.29		< LOD: 3.04		601142.63	996.95
1495,53	538677	82.85	21.41	< LOD: 9.13		< LOD: 9.65		< LOD: 7.20		< LOD: 4.07		575705.06	1107.61
1495,88	538678	46.84	19.56	< LOD: 11.96		11.32	5.98	5.54	3.30	3.37	2.14	581081.31	1061.16
1496,51	538679	80.00	20.35	9.14	5.83	10.64	6.16	< LOD: 5.06		4.29	2.23	580762.81	1054.33
1497,12	538680	36.35	19.20	< LOD: 8.31		< LOD: 8.74		< LOD: 4.81		4.51	2.13	602126.75	1006.25
1497,57	538681	45.56	20.20	< LOD: 7.65		10.73	6.17	< LOD: 5.06		< LOD: 3.30		587799.69	1051.35
1498,04	538682	71.08	20.96	< LOD: 7.96		< LOD: 14.56		< LOD: 4.81		< LOD: 3.40		548574.88	1120.89
1498,18	538683	10.10	5.63	< LOD: 8.86		< LOD: 4.88		3.93	2.14	573020.88	1049.72	< LOD: 2.72	
1501,42	538633	119.96	20.92	< LOD: 10.64		< LOD: 9.34		< LOD: 4.08		< LOD: 4.54		608350.88	1040.90
1501,6	538634	71.43	19.41	8.96	5.59	10.85	5.91	< LOD: 4.88		< LOD: 3.92		604559.13	1031.44
1501,79	538635	156.55	22.77	< LOD: 9.90		< LOD: 10.66		< LOD: 6.07		< LOD: 2.52		619118.63	1081.03
1501,81	538637	240.35	24.78	< LOD: 11.32		< LOD: 12.04		< LOD: 4.86		< LOD: 3.27		591504.75	1191.42
1501,84	538638	184.90	24.76	< LOD: 11.28		< LOD: 15.05		< LOD: 4.86		< LOD: 2.85		567199.56	1200.36
1501,9	538640	228.83	24.99	< LOD: 11.77		< LOD: 14.25		< LOD: 4.92		< LOD: 2.82		569146.19	1241.17
1502,01	538623	100.36	22.56	< LOD: 8.52		< LOD: 10.07		< LOD: 7.14		< LOD: 4.45		570851.69	1160.94
1504,6	538619	< LOD: 27.88		< LOD: 12.37		< LOD: 8.53		5.52	3.17	3.34	2.06	638120.38	936.39
1506,1	538642	81.45	20.13	< LOD: 9.59		< LOD: 9.09		< LOD: 5.02		< LOD: 2.22		584358.50	1079.88
1507,17	538643	162.91	20.83	< LOD: 10.20		< LOD: 13.12		< LOD: 7.09		< LOD: 3.79		591981.56	1070.66
1507,57	538644	153.91	20.72	< LOD: 7.69		< LOD: 12.88		< LOD: 4.53		< LOD: 3.90		618526.63	1014.31
1508,8	538611	61.27	18.86	< LOD: 8.14		13.22	5.79	5.01	3.17	< LOD: 3.07		623774.94	969.69
1511,26	538645	99.00	20.66	< LOD: 11.16		< LOD: 9.25		< LOD: 5.38		< LOD: 3.61		628347.31	1013.80
1511,64	538647	50.52	18.69	< LOD: 8.10		< LOD: 8.54		< LOD: 6.37		< LOD: 3.22		620036.88	981.05
1512,34	538603	220.90	23.64	< LOD: 8.67		< LOD: 12.09		< LOD: 4.58		< LOD: 2.57		614368.69	1096.80
1513,03	538648	89.89	20.86	< LOD: 11.07		< LOD: 9.44		5.61	3.49	< LOD: 3.37		613481.81	1032.71
1513,31	538649	138.57	20.61	< LOD: 12.07		< LOD: 12.44		< LOD: 4.67		< LOD: 2.23		630950.25	1005.69
1513,35	538650	< LOD: 37.60		< LOD: 7.40		< LOD: 7.68		6.90	3.12	< LOD: 2.98		592271.94	986.58
1513,58	538651	84.53	19.87	< LOD: 8.29		< LOD: 8.99		< LOD: 5.07		< LOD: 3.21		605998.19	1031.96
1514,15	538652	< LOD: 28.22		< LOD: 7.07		< LOD: 10.36		< LOD: 4.87		< LOD: 3.10		588128.81	1039.58
1514,91	538653	42.13	18.04	< LOD: 8.10		< LOD: 8.27		< LOD: 5.66		< LOD: 2.97		580567.88	1007.44
1515,57	538654	50.39	17.53	< LOD: 11.63		8.99	5.38	4.82	2.98	3.36	1.94	585842.38	991.62
1516,13	538655	135.11	22.00	< LOD: 14.25		< LOD: 14.49		< LOD: 6.39		< LOD: 3.46		564260.44	1129.91
1516,95	538656	146.36	21.41	< LOD: 12.62		< LOD: 9.55		< LOD: 6.34		< LOD: 3.42		590462.13	1103.12
1517,23	538657	117.25	20.20	< LOD: 10.93		< LOD: 9.08		< LOD: 5.12		< LOD: 3.72		593970.81	1076.62
1517,86	538658	79.00	19.79	< LOD: 7.46		< LOD: 13.35		< LOD: 6.64		< LOD: 3.24		618107.63	1013.99
1518,36	538659	83.41	19.05	< LOD: 8.79		< LOD: 12.67		< LOD: 6.84		< LOD: 3.48		594744.56	1031.40
1518,79	538660	68.28	19.30	9.25	5.57	8.86	5.86	< LOD: 4.90		< LOD: 2.36		596153.63	1015.54
1519,68	538661	73.00	20.30	< LOD: 8.03		< LOD: 8.70		< LOD: 4.01		< LOD: 3.03		640588.56	977.28
1520,56	538662	129.83	20.42	< LOD: 8.67		< LOD: 11.03		< LOD: 4.41		< LOD: 3.93		620203.00	1016.10
1521,21	538664	79.44	19.59	< LOD: 7.66		< LOD: 13.33		< LOD: 6.49		< LOD: 3.18		572978.50	1073.04
1521,83	538665	89.48	19.33	< LOD: 8.32		< LOD: 13.20		< LOD: 6.55		3.58	2.11	573816.63	1067.84
1522,33	538666	33.02	17.97	< LOD: 7.83		< LOD: 11.10		< LOD: 6.47		< LOD: 2.81		575063.88	1040.54
1522,8	538667	79.60	19.10	< LOD: 8.24		< LOD: 11.14		< LOD: 4.77		< LOD: 3.09		584558.31	1052.98
1523,28	538668	92.29	19.63	< LOD: 8.41		< LOD: 8.85		< LOD: 6.80		< LOD: 3.05		569587.69	1079.68
1523,79	538669	87.01	20.00	< LOD: 10.84		< LOD: 11.89		< LOD: 6.37		< LOD: 2.50		603418.88	1041.89

Corrected depth	Sample	Mo	Mo Error	Nb	Nb Error	Th	Th Error	Zr	Zr Error	Y	Y Error	Sr	Sr Error	U	U Error
1492,54	538670	13.34	1.28	5.93	2.98	269.75	3.66	18.52	1.30	76.34	2.09	< LOD: 2.12		45.29	1.18
1492,82	538671	< LOD: 3.44		18.81	1.36	5.81	3.07	350.49	4.24	22.92	1.39	79.70	2.16	< LOD: 1.50	
1493,06	538672	< LOD: 1.50		< LOD: 1.50		< LOD: 2.80		53.92	1.81	< LOD: 1.50		24.87	1.30	< LOD: 1.50	
1493,97	538673	< LOD: 3.61		12.80	1.32	< LOD: 4.42		392.82	4.58	25.91	1.39	74.97	2.14	< LOD: 1.50	
1494,15	538674	< LOD: 1.96		15.26	1.34	< LOD: 4.70		446.67	4.89	25.38	1.38	81.74	2.21	< LOD: 1.54	
1494,52	538675	< LOD: 1.99		11.96	1.30	< LOD: 4.95		483.18	5.09	22.72	1.32	71.55	2.09	< LOD: 2.32	
1494,88	538676	< LOD: 2.97		9.19	1.22	< LOD: 3.87		296.90	3.84	18.27	1.23	64.22	1.95	< LOD: 1.50	
1495,53	538677	< LOD: 2.42		11.77	1.37	< LOD: 4.86		326.36	4.37	26.12	1.45	93.01	2.46	< LOD: 1.50	
1495,88	538678	< LOD: 2.31		14.21	1.33	< LOD: 3.71		406.44	4.66	23.49	1.35	79.04	2.19	< LOD: 1.50	
1496,51	538679	< LOD: 1.99		14.06	1.36	< LOD: 6.36		446.47	4.98	27.51	1.42	73.92	2.16	< LOD: 1.50	
1497,12	538680	< LOD: 1.81		13.46	1.31	< LOD: 4.58		339.70	4.19	28.76	1.42	88.68	2.27	< LOD: 1.50	
1497,57	538681	< LOD: 2.58		18.08	1.40	< LOD: 4.75		396.36	4.64	29.31	1.50	89.04	2.32	< LOD: 1.50	
1498,04	538682	< LOD: 2.07		10.37	1.28	< LOD: 5.79		274.38	3.86	22.97	1.31	154.92	2.98	< LOD: 1.50	
1498,18	538683	15.41	1.33	< LOD: 4.63		416.53	4.64	31.00	1.43	107.59	2.46	< LOD: 1.78		34.95	1.06
1501,42	538633	3.48	1.88	14.30	1.37	< LOD: 4.70		287.63	4.00	30.23	1.54	109.87	2.58	< LOD: 1.82	
1501,6	538634	3.84	2.06	15.73	1.36	< LOD: 4.08		586.53	5.73	29.93	1.46	121.98	2.66	< LOD: 1.50	
1501,79	538635	< LOD: 2.44		6.61	1.30	< LOD: 5.12		203.43	3.73	25.86	1.47	396.02	5.06	< LOD: 1.51	
1501,81	538637	< LOD: 3.15		7.84	1.38	< LOD: 4.88		190.52	3.90	28.32	1.56	520.46	6.14	< LOD: 2.71	
1501,84	538638	< LOD: 3.07		4.80	1.34	< LOD: 4.35		286.13	4.44	33.60	1.56	432.79	5.47	< LOD: 2.54	
1501,9	538640	< LOD: 1.92		11.59	1.44	5.37	3.41	149.21	3.35	23.90	1.65	209.22	3.82	< LOD: 1.62	
1502,01	538623	< LOD: 1.75		11.81	1.35	5.60	3.16	140.64	3.02	19.06	1.47	140.94	2.97	< LOD: 1.50	
1504,6	538619	< LOD: 3.52		14.75	1.32	< LOD: 5.95		576.01	5.51	33.49	1.43	156.25	2.91	< LOD: 1.82	
1506,1	538642	< LOD: 2.14		13.81	1.37	< LOD: 3.99		590.10	5.79	36.81	1.53	179.27	3.22	2.67	1.53
1507,17	538643	< LOD: 1.99		16.31	1.38	< LOD: 6.06		426.27	4.84	25.59	1.46	113.32	2.60	< LOD: 2.28	
1507,57	538644	< LOD: 1.74		13.21	1.33	< LOD: 6.13		216.65	3.45	24.21	1.47	104.97	2.50	< LOD: 2.66	
1508,8	538611	< LOD: 1.74		14.86	1.32	< LOD: 4.52		298.66	3.89	28.69	1.46	118.14	2.55	< LOD: 2.24	
1511,26	538645	< LOD: 1.73		14.56	1.37	< LOD: 4.62		193.45	3.34	21.43	1.40	92.65	2.41	< LOD: 2.39	
1511,64	538647	< LOD: 1.76		15.38	1.32	5.47	3.05	314.38	4.00	25.30	1.36	98.26	2.36	< LOD: 2.25	
1512,34	538603	< LOD: 2.90		15.56	1.45	6.63	3.33	259.56	4.01	23.96	1.55	108.79	2.71	< LOD: 1.72	
1513,03	538648	< LOD: 3.13		11.79	1.32	< LOD: 5.65		607.81	5.88	21.36	1.36	74.50	2.15	< LOD: 2.18	
1513,31	538649	< LOD: 3.39		10.37	1.31	< LOD: 6.69		327.39	4.26	17.26	1.34	84.68	2.31	< LOD: 2.46	
1513,35	538650	< LOD: 1.50		4.13	1.08	< LOD: 3.09		169.59	2.84	6.32	1.00	74.67	1.99	< LOD: 1.50	
1513,58	538651	< LOD: 2.45		10.89	1.26	5.47	3.01	239.28	3.53	14.31	1.24	82.45	2.20	< LOD: 1.50	
1514,15	538652	< LOD: 3.40		9.18	1.26	< LOD: 3.97		982.02	7.73	19.09	1.23	51.27	1.81	< LOD: 1.50	
1514,91	538653	< LOD: 1.51		2.68	1.05	< LOD: 3.03		259.28	3.41	4.28	1.00	49.87	1.68	< LOD: 1.50	
1515,57	538654	< LOD: 1.59		4.89	1.10	< LOD: 3.17		295.15	3.68	8.84	1.03	69.48	1.94	< LOD: 1.50	
1516,13	538655	< LOD: 2.32		12.61	1.40	< LOD: 6.32		594.48	6.12	26.02	1.44	108.22	2.67	< LOD: 2.24	
1516,95	538656	< LOD: 1.98		13.80	1.37	6.77	3.26	369.58	4.57	20.27	1.42	107.18	2.57	< LOD: 2.50	
1517,23	538657	< LOD: 2.13		14.66	1.38	< LOD: 4.96		523.48	5.49	24.80	1.45	95.95	2.44	< LOD: 2.09	
1517,86	538658	< LOD: 2.13		14.40	1.36	< LOD: 3.87		583.56	5.74	28.82	1.45	85.22	2.28	< LOD: 2.06	
1518,36	538659	< LOD: 1.88		10.32	1.26	< LOD: 5.36		424.74	4.70	18.60	1.24	81.05	2.18	< LOD: 1.50	
1518,79	538660	< LOD: 1.81		11.83	1.26	< LOD: 3.81		376.77	4.34	19.55	1.25	74.76	2.08	< LOD: 1.50	
1519,68	538661	< LOD: 1.84		16.06	1.37	< LOD: 4.66		312.13	4.11	24.26	1.45	87.41	2.31	< LOD: 2.60	
1520,56	538662	< LOD: 2.15		17.53	1.41	< LOD: 7.15		579.10	5.78	30.12	1.48	99.54	2.47	< LOD: 1.50	
1521,21	538664	< LOD: 2.00		15.18	1.32	< LOD: 4.20		549.33	5.37	24.38	1.31	70.25	2.04	< LOD: 1.50	
1521,83	538665	< LOD: 2.13		17.24	1.36	< LOD: 6.73		661.70	6.05	27.81	1.37	97.52	2.37	< LOD: 1.50	
1522,33	538666	< LOD: 2.22		15.75	1.33	< LOD: 3.93		826.17	6.74	33.85	1.39	90.75	2.24	3.14	1.39
1522,8	538667	< LOD: 2.12		16.76	1.37	< LOD: 5.18		636.42	5.94	32.00	1.43	87.46	2.27	< LOD: 1.85	
1523,28	538668	< LOD: 2.03		18.11	1.38	4.94	3.21	540.90	5.40	32.92	1.45	89.40	2.29	< LOD: 1.84	
1523,79	538669	< LOD: 2.28		19.56	1.43	< LOD: 7.39		721.01	6.54	30.53	1.49	113.71	2.61	< LOD: 2.52	

Corrected depth	Sample	Rb	Rb Error	Bi	Bi Error	Au	Au Error	Se	Se Error	As	As Error	Pb	Pb Error
1492,54	538670	< LOD: 9.44		< LOD: 4.28		< LOD: 1.79		18.03	3.02	9.56	2.55	< LOD: 30.51	
1492,82	538671	50.20	1.24	< LOD: 9.78		< LOD: 4.90		< LOD: 1.99		20.86	3.09	7.60	2.56
1493,06	538672	8.71	1.00	< LOD: 12.59		< LOD: 4.19		< LOD: 1.58		6.27	2.16	< LOD: 1.93	
1493,97	538673	33.02	1.06	< LOD: 11.18		< LOD: 4.59		< LOD: 1.87		12.48	3.08	12.18	2.74
1494,15	538674	34.09	1.07	< LOD: 9.85		< LOD: 4.75		< LOD: 1.99		10.70	2.81	5.47	2.53
1494,52	538675	28.55	1.00	< LOD: 9.71		< LOD: 4.55		< LOD: 1.99		12.20	2.95	8.97	2.61
1494,88	538676	29.33	1.00	< LOD: 10.65		< LOD: 4.47		< LOD: 1.89		15.79	2.96	8.88	2.52
1495,53	538677	32.90	1.11	< LOD: 10.20		< LOD: 5.10		< LOD: 2.26		15.27	3.25	9.91	2.90
1495,88	538678	31.42	1.04	< LOD: 13.30		< LOD: 4.74		< LOD: 1.92		13.56	2.99	8.32	2.62
1496,51	538679	30.34	1.04	< LOD: 9.94		< LOD: 4.94		< LOD: 2.16		9.84	2.95	8.49	2.70
1497,12	538680	40.08	1.13	< LOD: 9.63		< LOD: 4.78		< LOD: 1.81		19.55	3.11	9.77	2.61
1497,57	538681	46.96	1.24	< LOD: 10.44		< LOD: 4.92		< LOD: 1.93		17.98	3.40	17.66	2.94
1498,04	538682	25.30	1.00	< LOD: 9.73		< LOD: 4.74		< LOD: 1.95		13.06	2.92	8.40	2.53
1498,18	538683	< LOD: 10.29		< LOD: 4.51		< LOD: 1.93		12.35	2.93	9.89	2.58	< LOD: 31.66	
1501,42	538633	49.42	1.28	< LOD: 10.99		< LOD: 5.30		< LOD: 2.44		13.34	3.74	31.80	3.36
1501,6	538634	37.64	1.12	< LOD: 11.04		< LOD: 4.72		< LOD: 1.98		15.16	2.95	5.80	2.50
1501,79	538635	38.70	1.19	< LOD: 10.69		< LOD: 5.32		< LOD: 2.19		21.41	3.89	29.71	3.34
1501,81	538637	34.66	1.19	< LOD: 12.60		< LOD: 5.91		< LOD: 2.42		44.99	5.08	53.82	4.09
1501,84	538638	20.77	1.00	< LOD: 11.60		< LOD: 5.91		< LOD: 3.22		73.89	5.76	67.22	4.35
1501,9	538640	68.10	1.61	< LOD: 10.97		< LOD: 5.68		< LOD: 2.55		20.74	3.61	11.40	3.11
1502,01	538623	62.52	1.46	< LOD: 10.07		< LOD: 5.21		< LOD: 2.16		16.47	3.13	6.51	2.75
1504,6	538619	33.40	1.03	< LOD: 16.04		< LOD: 4.40		< LOD: 1.85		4.61	2.31	< LOD: 2.34	
1506,1	538642	34.87	1.10	13.70	7.49	< LOD: 4.92		< LOD: 1.95		7.94	2.77	5.76	2.49
1507,17	538643	49.66	1.28	< LOD: 15.89		< LOD: 4.95		< LOD: 2.01		7.31	2.58	< LOD: 3.39	
1507,57	538644	60.06	1.39	< LOD: 14.09		< LOD: 4.80		< LOD: 1.97		7.32	2.57	< LOD: 3.63	
1508,8	538611	56.83	1.31	< LOD: 13.28		< LOD: 4.55		< LOD: 1.83		13.93	2.72	< LOD: 3.54	
1511,26	538645	42.95	1.22	< LOD: 9.83		< LOD: 4.91		< LOD: 2.00		6.44	3.14	16.12	2.95
1511,64	538647	36.73	1.08	< LOD: 10.41		< LOD: 4.57		< LOD: 1.92		8.46	3.00	14.95	2.72
1512,34	538603	52.66	1.39	< LOD: 10.72		< LOD: 7.12		< LOD: 2.38		17.01	3.73	21.55	3.28
1513,03	538648	33.21	1.07	< LOD: 12.56		< LOD: 5.01		< LOD: 2.97		16.63	3.56	23.69	3.08
1513,31	538649	38.81	1.16	< LOD: 9.91		< LOD: 5.17		< LOD: 2.01		24.25	3.86	27.94	3.23
1513,35	538650	19.62	1.00	< LOD: 8.23		< LOD: 4.37		< LOD: 1.65		12.24	2.58	5.13	2.18
1513,58	538651	37.58	1.10	< LOD: 9.51		< LOD: 4.72		< LOD: 1.81		13.47	3.17	16.54	2.76
1514,15	538652	13.43	1.00	12.51	7.32	< LOD: 4.79		< LOD: 1.86		7.97	2.78	7.43	2.45
1514,91	538653	8.79	1.00	< LOD: 8.97		< LOD: 4.24		< LOD: 1.60		5.79	2.77	15.84	2.48
1515,57	538654	19.54	1.00	< LOD: 9.39		< LOD: 4.44		< LOD: 1.58		6.13	3.03	23.24	2.73
1516,13	538655	24.66	1.00	< LOD: 10.74		< LOD: 5.27		< LOD: 2.25		13.22	3.13	7.08	2.77
1516,95	538656	45.46	1.25	< LOD: 10.46		< LOD: 4.99		< LOD: 2.16		19.88	3.81	28.20	3.27
1517,23	538657	39.56	1.17	< LOD: 11.06		< LOD: 5.10		< LOD: 2.09		11.12	3.77	33.70	3.40
1517,86	538658	32.12	1.06	< LOD: 11.05		< LOD: 4.84		< LOD: 2.01		10.91	3.44	23.92	3.07
1518,36	538659	23.09	1.00	< LOD: 11.49		< LOD: 4.74		< LOD: 1.86		10.56	2.94	11.22	2.58
1518,79	538660	26.79	1.00	< LOD: 13.43		< LOD: 4.79		< LOD: 1.83		9.38	2.95	13.65	2.62
1519,68	538661	48.04	1.26	< LOD: 12.52		< LOD: 4.81		< LOD: 2.14		14.48	3.49	22.63	3.09
1520,56	538662	36.59	1.12	< LOD: 14.34		< LOD: 5.12		< LOD: 2.08		6.62	2.81	6.72	2.59
1521,21	538664	24.99	1.00	< LOD: 15.09		< LOD: 4.61		< LOD: 1.82		9.64	2.98	13.65	2.64
1521,83	538665	26.74	1.00	< LOD: 14.17		< LOD: 4.77		< LOD: 1.88		10.32	2.60	< LOD: 3.45	
1522,33	538666	20.53	1.00	11.56	7.31	< LOD: 4.48		< LOD: 1.73		8.36	2.47	< LOD: 2.83	
1522,8	538667	27.16	1.00	< LOD: 16.38		< LOD: 4.76		< LOD: 1.86		12.95	2.77	< LOD: 3.55	
1523,28	538668	31.69	1.03	< LOD: 10.50		< LOD: 4.71		< LOD: 1.87		10.82	2.78	5.48	2.44
1523,79	538669	37.40	1.13	< LOD: 17.55		< LOD: 5.06		< LOD: 2.12		13.62	2.81	< LOD: 4.11	

Corrected depth	Sample	W	W Error	Zn	Zn Error	Cu	Cu Error	Ni	Ni Error	Co	Co Error	Fe	Fe Error	Mn	Mn Error
1492,54	538670	38.28	6.13	39.74	9.14	< LOD: 25.09		< LOD: 73.82		34380.86	212.61	< LOD: 50.31		138.48	18.30
1492,82	538671	< LOD: 32.46		56.63	6.69	18.60	8.91	< LOD: 25.87		< LOD: 75.94		36197.81	221.66	70.59	34.64
1493,06	538672	< LOD: 28.90		13.12	5.22	< LOD: 11.09		< LOD: 23.71		< LOD: 30.79		4270.50	76.50	< LOD: 47.52	
1493,97	538673	< LOD: 42.54		58.92	6.93	19.93	9.12	< LOD: 26.33		< LOD: 85.19		46419.88	257.62	483.72	42.34
1494,15	538674	< LOD: 32.61		61.27	6.89	< LOD: 13.34		< LOD: 26.19		< LOD: 82.17		42664.27	244.37	486.94	42.39
1494,52	538675	< LOD: 40.96		53.84	6.77	19.44	9.07	< LOD: 25.89		< LOD: 79.14		39292.00	233.45	391.40	41.06
1494,88	538676	< LOD: 30.99		51.10	6.47	20.11	8.78	< LOD: 25.12		< LOD: 71.80		33039.96	208.98	336.80	39.65
1495,53	538677	< LOD: 42.85		71.16	7.53	26.50	9.76	< LOD: 28.62		< LOD: 100.67		65464.32	327.63	1067.83	51.71
1495,88	538678	< LOD: 32.57		69.62	7.10	14.38	8.97	< LOD: 26.13		< LOD: 82.19		42384.62	244.91	406.32	41.33
1496,51	538679	< LOD: 33.94		63.74	7.12	15.12	9.18	< LOD: 26.92		< LOD: 87.35		47858.35	265.19	494.38	43.05
1497,12	538680	< LOD: 32.59		61.35	6.83	< LOD: 13.02		< LOD: 25.75		< LOD: 80.33		41613.19	238.73	431.54	40.97
1497,57	538681	< LOD: 33.62		64.55	7.07	< LOD: 13.60		< LOD: 27.21		< LOD: 84.45		44926.74	254.53	511.96	43.20
1498,04	538682	< LOD: 34.75		38.92	6.40	21.31	9.18	< LOD: 26.45		< LOD: 67.20		25832.40	191.05	971.20	51.77
1498,18	538683	40.17	6.28	27.23	9.07	< LOD: 25.30		< LOD: 72.02		31452.89	205.56	679.65	45.79	109.27	19.43
1501,42	538633	< LOD: 34.24		74.41	7.37	25.94	9.47	< LOD: 27.71		< LOD: 80.55		37439.38	233.79	377.48	42.38
1501,6	538634	< LOD: 32.80		43.76	6.55	14.76	9.07	< LOD: 26.75		< LOD: 65.42		23778.25	181.36	155.98	38.21
1501,79	538635	< LOD: 39.14		57.82	7.16	33.05	9.85	< LOD: 42.28		< LOD: 79.23		35037.28	235.18	539.93	46.10
1501,81	538637	< LOD: 38.52		60.11	7.52	35.12	10.44	40.04	20.73	< LOD: 82.99		34919.00	245.71	853.80	53.43
1501,84	538638	< LOD: 45.98		12.52	6.15	30.80	10.24	39.77	20.46	< LOD: 82.93		36292.45	248.54	1031.31	55.57
1501,9	538640	< LOD: 38.36		96.22	8.55	35.14	10.69	53.83	21.58	< LOD: 108.27		58140.71	327.60	482.25	46.54
1502,01	538623	< LOD: 39.62		86.56	7.87	31.44	9.86	< LOD: 37.19		< LOD: 96.46		57142.40	305.53	301.02	40.45
1504,6	538619	< LOD: 30.81		43.88	6.28	26.23	8.97	< LOD: 24.92		< LOD: 55.64		17287.78	150.61	247.02	38.76
1506,1	538642	< LOD: 32.80		34.69	6.29	24.83	9.39	< LOD: 27.08		< LOD: 57.17		17032.21	154.61	291.08	41.58
1507,17	538643	< LOD: 33.45		31.10	6.29	36.46	9.69	< LOD: 27.69		< LOD: 67.79		25478.46	189.95	139.80	38.25
1507,57	538644	< LOD: 33.57		74.63	7.34	34.05	9.52	< LOD: 28.16		< LOD: 72.39		29889.36	205.49	181.30	38.53
1508,8	538611	< LOD: 31.58		55.41	6.60	29.55	9.03	< LOD: 25.66		< LOD: 69.52		30022.07	198.90	143.78	36.16
1511,26	538645	< LOD: 33.33		58.53	7.01	25.27	9.45	< LOD: 30.78		< LOD: 86.34		46114.63	263.29	801.26	48.81
1511,64	538647	< LOD: 31.07		57.01	6.64	13.07	8.71	< LOD: 25.50		< LOD: 86.07		21684.40	169.93	< LOD: 50.42	
1512,34	538603	< LOD: 43.52		98.07	8.44	27.39	10.17	56.69	21.01	< LOD: 91.46		45769.50	274.86	149.63	40.24
1513,03	538648	< LOD: 33.55		75.08	7.33	14.73	9.25	< LOD: 27.49		< LOD: 73.96		30927.09	208.95	< LOD: 51.86	
1513,31	538649	< LOD: 33.58		19.39	5.99	20.82	9.39	< LOD: 28.15		< LOD: 79.48		36191.96	230.85	< LOD: 51.96	
1513,35	538650	< LOD: 29.42		20.06	5.41	< LOD: 12.41		< LOD: 23.35		< LOD: 44.99		11231.78	118.21	< LOD: 47.23	
1513,58	538651	< LOD: 32.11		13.83	5.64	< LOD: 19.18		< LOD: 26.23		< LOD: 65.22		24133.36	181.33	< LOD: 53.15	
1514,15	538652	< LOD: 31.79		15.66	5.68	< LOD: 12.38		< LOD: 25.04		< LOD: 49.81		12391.79	130.58	< LOD: 53.95	
1514,91	538653	< LOD: 28.68		< LOD: 7.41		< LOD: 11.32		< LOD: 23.50		< LOD: 30.49		3946.83	73.58	< LOD: 47.08	
1515,57	538654	< LOD: 29.22		< LOD: 9.46		< LOD: 11.39		< LOD: 23.35		< LOD: 44.00		10628.39	115.70	< LOD: 50.97	
1516,13	538655	< LOD: 40.16		71.25	7.64	15.93	9.68	< LOD: 28.27		< LOD: 91.56		48256.55	277.62	1123.47	54.97
1516,95	538656	< LOD: 34.49		69.05	7.38	21.06	9.51	< LOD: 28.42		< LOD: 75.73		31243.65	214.47	111.58	38.27
1517,23	538657	< LOD: 34.87		126.11	8.59	< LOD: 13.81		< LOD: 27.30		< LOD: 74.34		30509.74	210.57	220.64	40.19
1517,86	538658	< LOD: 33.05		35.80	6.39	< LOD: 20.97		< LOD: 27.05		< LOD: 69.26		26251.82	192.07	< LOD: 76.05	
1518,36	538659	< LOD: 31.67		< LOD: 10.16		< LOD: 13.25		< LOD: 25.58		< LOD: 57.21		17536.88	154.45	< LOD: 53.80	
1518,79	538660	< LOD: 31.13		35.28	6.05	< LOD: 12.98		< LOD: 25.68		< LOD: 58.61		19249.56	159.35	106.34	36.39
1519,68	538661	< LOD: 32.93		68.29	7.17	25.30	9.34	< LOD: 27.52		< LOD: 78.27		36201.43	228.12	< LOD: 83.39	
1520,56	538662	< LOD: 33.16		13.50	5.77	< LOD: 18.75		< LOD: 27.34		< LOD: 68.59		25497.49	191.09	75.37	37.45
1521,21	538664	< LOD: 31.17		< LOD: 8.07		< LOD: 13.29		< LOD: 26.08		< LOD: 59.06		19034.64	159.15	< LOD: 51.40	
1521,83	538665	< LOD: 32.01		46.54	6.49	< LOD: 19.85		< LOD: 26.15		< LOD: 51.96		14055.06	138.40	< LOD: 61.45	
1522,33	538666	< LOD: 29.81		< LOD: 11.09		< LOD: 15.50		< LOD: 24.56		< LOD: 46.99		11294.71	121.53	< LOD: 49.24	
1522,8	538667	< LOD: 31.83		17.57	5.74	16.40	9.00	< LOD: 25.71		< LOD: 59.36		19213.15	161.68	110.92	37.26
1523,28	538668	< LOD: 31.69		40.16	6.32	18.88	9.08	< LOD: 26.45		< LOD: 62.88		21628.53	171.25	110.89	37.11
1523,79	538669	< LOD: 35.60		45.77	6.80	< LOD: 13.73		< LOD: 26.98		< LOD: 65.27		23300.56	181.11	79.52	37.00

Corrected depth	Sample	Cr	Cr Error	V	V Error	Ti	Ti Error	Ca	Ca Error	K	K Error	Al	Al Error
1492,54	538670	138.09	23.70	5268.98	60.46	< LOD: 27.57		2229.74	134.26	16546.07	194.29	74584.69	791.66
1492,82	538671	158.42	19.86	166.97	27.34	6709.66	71.18	3529.11	162.83	17610.62	207.53	71224.95	823.84
1493,06	538672	< LOD: 15.14		< LOD: 14.50		573.79	17.11	649.39	57.29	5518.89	80.63	12414.02	380.33
1493,97	538673	167.11	21.45	122.98	26.54	5006.15	65.70	2109.41	141.99	13606.87	195.15	61146.68	764.08
1494,15	538674	145.77	20.68	127.06	25.54	5142.69	64.06	2324.34	140.83	13899.22	190.87	57091.06	697.37
1494,52	538675	112.40	20.36	104.74	23.73	4444.44	58.84	2554.99	141.67	13017.43	182.68	53198.95	693.86
1494,88	538676	101.85	18.69	113.93	22.08	4190.83	54.46	1899.09	122.20	13655.13	177.80	60142.42	699.58
1495,53	538677	191.49	24.90	135.72	28.75	4931.69	70.25	3918.23	188.68	13588.08	211.83	66790.50	832.61
1495,88	538678	136.02	20.74	121.10	25.25	4941.25	63.09	2615.32	144.71	13518.06	189.02	64081.79	750.22
1496,51	538679	160.76	21.65	116.48	26.23	5004.75	65.46	3313.49	162.05	12665.16	189.38	55828.46	730.37
1497,12	538680	140.39	20.90	133.74	26.63	5646.70	67.51	2311.67	145.50	15298.33	201.23	72891.38	787.12
1497,57	538681	199.38	22.32	175.92	29.28	6256.83	74.00	2498.94	155.75	16739.95	218.03	71150.39	813.58
1498,04	538682	61.82	20.21	74.64	22.18	3502.37	55.37	60604.30	500.89	11189.27	163.91	49144.43	861.93
1498,18	538683	114.81	23.96	5217.20	61.77	42.86	19.40	19540.19	297.24	12542.31	171.41	56070.89	753.27
1501,42	538633	167.22	18.94	194,13	24.48	5136.00	61.09	4423.53	166.95	16877.09	199.33	67403.05	783.33
1501,6	538634	93.07	16.97	127,13	21.27	4817.90	54.90	8120.04	189.54	13704.93	167.76	58255.48	714.04
1501,79	538635	120.90	20.37	119,09	23.93	3396.03	59.03	79087.68	593.50	15260.62	196.18	48593.64	964.33
1501,81	538637	112.69	21.19	113,1	23.36	2758.49	58.29	114702.45	724.76	14636.14	195.35	42277.54	1055.54
1501,84	538638	92.90	22.00	62,55	22.55	2415.65	56.20	110776.08	718.29	10628.30	173.58	32926.52	969.62
1501,9	538640	226.59	22.47	165,1	26.92	3984.49	64.31	29477.40	416.95	25084.61	272.75	77055.61	1077.69
1502,01	538623	216.15	23.10	183,03	27.38	4369.95	65.68	19993.05	354.68	25174.99	273.96	82771.81	1032.22
1504,6	538619	97.76	16.07	115,62	20.92	4872.38	54.75	24755.31	299.27	13142.63	158.34	49993.84	673.57
1506,1	538642	77.69	16.70	99,22	20.86	4824.30	54.78	26797.10	310.08	13233.11	159.01	58139.32	781.66
1507,17	538643	124.94	17.79	144,58	23.84	5675.56	62.34	10781.29	225.77	19204.79	204.89	70383.19	805.35
1507,57	538644	136.51	17.64	157,92	23.10	4681.21	57.55	7637.57	205.48	21667.95	220.09	74622.96	798.73
1508,8	538611	157.24	18.21	181,46	24.21	5172.95	60.47	6434.39	192.23	20635.03	214.52	82597.04	822.31
1511,26	538645	180.69	20.47	169,74	26.10	5267.86	65.24	3095.48	154.31	14071.20	193.39	92049.43	895.94
1511,64	538647	110.61	16.15	112,27	21.45	5435.10	56.92	1578.56	108.20	13164.52	161.26	57586.16	684.94
1512,34	538603	188.49	19.56	197,88	25.58	5089.53	63.78	3384.61	160.53	15941.07	204.74	74818.66	874.34
1513,03	538648	157.98	17.35	89,96	19.56	3720.88	48.87	1192.46	103.59	12290.88	163.68	58465.00	731.59
1513,31	538649	125.64	18.46	117,71	21.47	3554.42	51.44	1514.77	119.39	14464.72	185.43	64071.05	782.57
1513,35	538650	< LOD: 31.47		< LOD: 18,46		1633.42	28.34	2238.69	97.83	9568.47	120.20	31224.43	528.08
1513,58	538651	84.03	16.24	96,52	18.26	3224.17	44.44	2646.91	124.64	13022.13	161.95	56641.47	724.54
1514,15	538652	60.57	13.32	22,81	14.62	2884.42	37.18	2595.27	103.87	8217.89	114.58	32636.35	534.47
1514,91	538653	< LOD: 17.23		< LOD: 19,41		1543.77	25.92	9301.52	151.00	6503.98	91.80	20327.54	483.94
1515,57	538654	< LOD: 29.90		28,48	13.12	2112.09	31.28	2214.48	97.48	11650.69	131.20	28041.54	492.60
1516,13	538655	136.96	21.42	99,99	24.53	4560.29	61.17	3365.23	156.25	12185.39	181.94	43905.75	688.88
1516,95	538656	135.12	18.00	121,8	22.16	4588.60	55.85	1922.19	127.27	15694.60	186.75	72463.67	841.75
1517,23	538657	114.05	18.03	132,69	22.46	4747.40	56.94	1712.03	122.16	15129.77	184.73	69988.55	779.94
1517,86	538658	120.79	16.74	105,03	21.34	4925.07	55.54	1255.93	103.66	12388.76	160.81	52909.20	675.38
1518,36	538659	35.76	15.37	64,55	17.28	3571.44	43.81	1002.47	86.85	10228.98	135.58	39593.96	585.07
1518,79	538660	87.17	15.10	70,91	18.22	3916.27	46.46	1406.40	97.46	12248.48	148.88	49727.53	651.46
1519,68	538661	162.79	18.10	153,24	23.50	5258.01	60.35	1735.22	128.15	16318.67	194.47	68137.89	778.48
1520,56	538662	99.09	16.61	115,33	21.69	5440.10	57.79	1379.03	105.54	13108.11	164.10	53487.53	669.62
1521,21	538664	102.16	15.96	74,8	19.73	4941.42	52.65	1269.27	94.79	10944.84	143.77	41280.53	634.10
1521,83	538665	76.20	14.88	61,38	18.98	5422.39	52.75	1742.15	97.13	11057.62	137.50	41125.14	592.09
1522,33	538666	39.07	14.41	72,66	18.41	5346.85	51.08	972.39	79.57	9421.77	124.02	34353.87	546.22
1522,8	538667	62.08	15.75	97,13	20.96	6052.19	58.00	1753.66	103.05	12024.31	148.87	47242.37	616.91
1523,28	538668	76.60	16.81	84,29	22.01	5931.68	59.65	1304.67	101.24	12407.63	156.49	47998.82	654.20
1523,79	538669	107.17	16.65	120,15	22.59	6191.56	61.57	1733.70	113.83	14167.49	169.59	54909.77	705.07

Corrected depth	Sample	P	P Error	Si	Si Error	Cl	Cl Error	S	S Error	Mg	Mg Error
1492,54	538670	< LOD: 182.39		245143.47	914.93	< LOD: 35.63		6198.78	96.47	3122.96	1164.71
1492,82	538671	< LOD: 203.47		271238.56	984.20	< LOD: 38.84		6399.57	102.97	3432.66	1291.91
1493,06	538672	< LOD: 214.52		422826.50	1197.08	< LOD: 30.02		872.54	44.71	< LOD: 2238.86	
1493,97	538673	< LOD: 201.60		288904.75	1008.54	< LOD: 37.62		2856.30	73.40	3841.39	1281.96
1494,15	538674	< LOD: 194.29		290420.50	978.90	< LOD: 35.10		1684.00	58.52	4822.81	1226.51
1494,52	538675	< LOD: 204.95		303931.19	1020.74	< LOD: 36.03		2344.72	66.81	3454.26	1223.79
1494,88	538676	< LOD: 184.77		278527.78	966.52	< LOD: 35.61		2508.29	65.94	3759.50	1138.85
1495,53	538677	< LOD: 196.88		261701.84	979.62	< LOD: 38.76		2237.99	69.56	3538.73	1361.01
1495,88	538678	< LOD: 193.45		282233.81	982.06	< LOD: 35.82		1901.34	61.79	5839.52	1270.90
1496,51	538679	< LOD: 208.60		289236.06	1011.03	< LOD: 37.05		1748.32	62.71	2002.21	1238.40
1497,12	538680	< LOD: 189.60		254148.39	931.55	< LOD: 36.19		1633.26	59.61	2942.73	1183.80
1497,57	538681	< LOD: 206.81		264156.47	969.46	< LOD: 38.05		2186.87	67.91	2624.74	1265.83
1498,04	538682	< LOD: 240.86		293531.66	1109.58	< LOD: 47.95		970.48	71.90	4884.92	1801.26
1498,18	538683	< LOD: 215.42		295401.00	1028.92	< LOD: 38.46		1138.84	59.50	3935.09	1360.00
1501,42	538633	< LOD: 193.77		243356.97	928.13	7104.72	69.13	4798,33	91.06	3590.19	1271.55
1501,6	538634	< LOD: 2163.69		271705.91	1028.09	6326.28	64.65	2901,52	141.70	4466.18	1213.28
1501,79	538635	< LOD: 239.55		169813.66	925.18	8216.74	91.59	13915,03	183.25	5793.80	2157.03
1501,81	538637	< LOD: 249.63		168171.83	982.92	6416.49	89.60	15127,91	206.88	7135.26	2645.46
1501,84	538638	< LOD: 262.48		206399.09	1041.41	2439.82	62.95	24973,03	256.18	< LOD: 3716.72	
1501,9	538640	< LOD: 228.42		208728.63	969.69	8050.79	86.53	11004,22	155.33	7527.85	1974.28
1502,01	538623	< LOD: 210.03		218567.72	946.92	6952.20	76.71	6495,8	117.68	6339.59	1740.78
1504,6	538619	< LOD: 2061.70		242838.80	967.30	4513.84	56.08	< LOD: 179,29		3072.29	1205.88
1506,1	538642	< LOD: 2312.07		283104.19	1100.29	5384.61	64.87	< LOD: 201,51		5611.32	1390.75
1507,17	538643	< LOD: 200.32		264104.13	979.77	6712.93	68.57	238,73	52.27	4145.46	1304.14
1507,57	538644	< LOD: 182.23		233976.67	910.44	4046.83	53.49	284,62	49.64	3486.48	1219.57
1508,8	538611	< LOD: 177.59		224039.67	876.94	3711.68	51.18	453,7	50.34	1954.42	1145.31
1511,26	538645	< LOD: 169.96		200794.91	850.99	4285.19	54.81	308,72	47.51	3921.20	1209.50
1511,64	538647	< LOD: 191.72		268490.16	967.09	7004.08	66.76	712,21	52.49	3418.37	1133.28
1512,34	538603	< LOD: 202.96		210014.53	890.45	11128.67	90.98	15404,62	159.43	2623.33	1368.68
1513,03	538648	< LOD: 2212.55		246047.00	964.98	7013.05	68.12	22253,61	218.69	3359.70	1218.37
1513,31	538649	< LOD: 195.74		220833.95	882.75	5660.17	62.11	21789,9	183.72	< LOD: 2743.04	
1513,35	538650	< LOD: 208.74		334309.84	1049.91	9463.38	76.44	5084,95	88.22	2609.95	1097.43
1513,58	538651	< LOD: 206.73		266275.97	969.40	11107.98	88.02	12064,7	136.85	4125.67	1270.41
1514,15	538652	< LOD: 2197.58		340148.97	1163.09	5859.69	60.02	2351,51	140.52	3499.28	1068.50
1514,91	538653	< LOD: 221.19		356450.19	1096.64	17057.37	111.65	2403,46	73.33	< LOD: 1694.94	
1515,57	538654	< LOD: 201.84		349279.47	1068.06	5804.41	57.99	1674,59	58.62	2173.43	1040.07
1516,13	538655	< LOD: 2338.48		305956.47	1117.29	9806.42	83.07	1301,16	146.46	4018.83	1330.15
1516,95	538656	< LOD: 211.18		251068.17	956.10	12766.75	97.66	16065,53	161.78	2486.47	1322.03
1517,23	538657	< LOD: 2134.53		268931.28	1028.40	6169.07	64.33	3111,08	141.86	4239.25	1202.14
1517,86	538658	< LOD: 2124.09		262049.52	998.79	4849.75	56.22	12108,46	175.62	4009.16	1158.42
1518,36	538659	< LOD: 207.87		314781.56	1038.56	8022.16	70.84	7502,48	104.43	2180.12	1110.92
1518,79	538660	< LOD: 203.39		303632.16	1027.56	7888.47	71.52	2379,03	69.82	2458.89	1136.62
1519,68	538661	< LOD: 187.44		207834.88	854.83	4620.14	56.41	16462,96	157.00	1817.47	1189.25
1520,56	538662	< LOD: 2093.66		263489.69	1004.72	5989.77	61.79	6239,02	150.89	3936.10	1143.27
1521,21	538664	< LOD: 2354.02		320348.94	1121.94	11542.36	88.81	10535,93	182.01	6122.08	1258.17
1521,83	538665	< LOD: 2231.45		338970.75	1156.39	8533.25	73.34	< LOD: 270,72		4134.63	1123.46
1522,33	538666	< LOD: 2218.41		350845.94	1170.19	4299.98	51.67	1106,31	136.59	6118.09	1128.04
1522,8	538667	< LOD: 2131.37		314866.19	1089.68	6980.12	64.80	1399,91	133.03	4684.97	1118.05
1523,28	538668	< LOD: 2248.35		326163.78	1134.30	5133.58	58.03	2477,59	145.43	6184.10	1213.59
1523,79	538669	< LOD: 2206.74		279801.59	1060.90	7020.92	69.05	3314,49	146.45	4708.55	1218.19

b) Schandelah – XRF data. Reported in ppm.

Current depth (m)	Ba	Ba Error	Sb	Sb Error	Sn	Sn Error	Cd	Cd Error	Ag	Ag Error	Bal	Bal Error	Mo	Mo Error	Nb	Nb Error	Th	Th Error	Zr	Zr Error	Y	Y Error	Sr	Sr Error	U	U Error
230,4	170.02	29.89	< LOD: 11.38		< LOD: 11.85		< LOD: 6.05		< LOD: 3.61		544739.75	1522.02	< LOD: 2.42		5.97	1.67	< LOD: 4.81		134.32	3.69	48.77	2.12	171.16	4.03	3.22	2.01
231,3	172.95	31.34	< LOD: 13.60		< LOD: 13.73		< LOD: 6.20		< LOD: 6.97		522339.19	1661.94	< LOD: 4.80		5.47	1.70	7.33	4.17	229.89	4.77	36.64	1.88	118.45	3.53	< LOD: 3.04	
232,4	37.03	23.52	< LOD: 8.98		< LOD: 9.43		< LOD: 5.83		< LOD: 4.69		544565.25	1166.94	< LOD: 2.01		5.84	1.29	< LOD: 5.29		270.93	4.10	8.34	1.08	52.43	2.00	< LOD: 1.50	
232,7	174.86	28.05	< LOD: 11.54		< LOD: 13.63		< LOD: 5.69		< LOD: 4.43		531818.38	1460.59	< LOD: 2.51		< LOD: 2.84		< LOD: 6.35		150.97	4.01	682.57	6.67	634.68	7.40	26.40	2.62
233	< LOD: 27.52		9.95	5.19	< LOD: 8.14		9.06	3.09	5.36	2.02	558019.75	1042.29	< LOD: 3.52		10.75	1.20	< LOD: 5.50		545.46	5.12	18.17	1.15	39.83	1.56	< LOD: 1.50	
233,4	134.92	33.19	< LOD: 15.92		< LOD: 16.06		< LOD: 6.94		< LOD: 5.25		457774.59	1908.74	17.69	2.37	< LOD: 1.50		6.82	4.17	25.61	2.92	3.43	1.30	375.52	6.25	< LOD: 2.34	
233,7	61.22	20.69	< LOD: 7.84		< LOD: 9.36		< LOD: 7.52		< LOD: 4.50		600342.44	1060.33	< LOD: 1.75		13.07	1.35	7.71	3.13	199.66	3.38	19.27	1.44	98.06	2.46	< LOD: 2.20	
238,6	181.40	30.04	< LOD: 11.41		< LOD: 16.88		< LOD: 6.07		< LOD: 6.38		528209.75	1650.25	< LOD: 2.51		5.58	1.97	< LOD: 5.19		101.30	3.51	147.69	3.36	182.86	4.35	5.34	2.19
240,3	< LOD: 42.23		< LOD: 8.30		< LOD: 12.18		< LOD: 4.83		4.56	2.14	577518.81	1029.73	< LOD: 2.90		12.58	1.25	< LOD: 3.57		525.77	5.17	17.06	1.21	57.92	1.86	< LOD: 1.50	
240,9	44.46	19.45	< LOD: 9.70		< LOD: 8.85		< LOD: 5.66		< LOD: 3.17		593318.25	1030.80	< LOD: 1.98		14.68	1.32	< LOD: 6.42		444.73	4.81	23.13	1.36	63.03	1.96	< LOD: 1.50	
241	< LOD: 41.81		< LOD: 7.35		< LOD: 8.51		< LOD: 4.72		< LOD: 3.44		584623.06	1027.31	< LOD: 2.51		15.25	1.30	< LOD: 6.01		449.05	4.76	22.40	1.32	59.11	1.88	< LOD: 1.50	
241,8	< LOD: 26.03		< LOD: 7.34		< LOD: 8.37		7.71	3.15	< LOD: 3.01		551059.56	1013.12	< LOD: 1.89		3.16	1.10	< LOD: 3.28		473.96	4.74	15.53	1.05	19.93	1.24	< LOD: 1.50	
242,7	45.30	19.99	< LOD: 8.42		< LOD: 9.08		5.58	3.37	< LOD: 3.25		604529.56	1026.55	< LOD: 1.81		16.75	1.36	5.13	3.06	300.39	3.97	23.45	1.44	73.64	2.11	< LOD: 1.50	
243,2	< LOD: 28.93		< LOD: 8.38		< LOD: 8.81		< LOD: 6.72		3.29	2.12	574274.25	1058.06	< LOD: 2.90		10.97	1.29	< LOD: 6.84		587.45	5.66	23.92	1.32	42.50	1.69	< LOD: 1.50	
243,7	< LOD: 24.26		< LOD: 7.47		< LOD: 7.89		8.37	2.98	3.35	1.91	560389.00	994.84	< LOD: 2.89		4.15	1.05	< LOD: 2.96		267.38	3.37	8.87	1.00	20.85	1.21	< LOD: 1.50	
244	< LOD: 27.32		< LOD: 9.51		< LOD: 8.75		5.12	3.23	4.69	2.13	583148.69	953.40	< LOD: 2.61		6.78	1.15	< LOD: 5.59		298.82	3.74	14.41	1.07	30.78	1.44	< LOD: 1.50	
245,7	< LOD: 23.94		7.66	4.92	10.91	5.23	6.86	2.91	5.31	1.93	557248.31	983.56	< LOD: 1.74		2.71	1.02	< LOD: 2.83		144.73	2.51	5.66	1.00	23.75	1.24	< LOD: 1.50	
246,2	< LOD: 27.30		< LOD: 7.95		< LOD: 7.63		5.02	3.23	3.75	2.11	587737.69	998.93	< LOD: 2.36		4.82	1.14	< LOD: 3.26		263.61	3.55	17.43	1.13	56.64	1.81	< LOD: 1.50	
247,2	< LOD: 33.02		< LOD: 7.29		< LOD: 8.18		< LOD: 5.60		< LOD: 3.89		581487.88	1036.72	< LOD: 1.89		10.91	1.25	< LOD: 4.31		264.62	3.65	19.79	1.28	54.19	1.83	< LOD: 1.50	
250,9	< LOD: 28.18		< LOD: 9.89		< LOD: 8.99		< LOD: 6.70		4.71	2.19	564771.19	1021.11	< LOD: 1.63		2.91	1.11	< LOD: 3.20		256.35	3.53	15.56	1.09	64.50	1.93	< LOD: 1.50	
251,6	< LOD: 27.41		8.42	5.32	9.17	5.61	5.20	3.11	< LOD: 2.99		588427.06	1008.23	< LOD: 1.70		13.14	1.24	< LOD: 4.01		319.95	3.91	17.33	1.21	52.26	1.76	< LOD: 1.50	
252,8	147.45	18.67	< LOD: 7.89		< LOD: 8.32		6.18	3.09	5.54	2.06	534840.44	1012.36	< LOD: 2.42		5.69	1.10	< LOD: 4.80		204.00	3.05	9.95	1.00	61.21	1.81	< LOD: 1.50	
254,9	102.29	25.24	< LOD: 9.63		< LOD: 12.50		< LOD: 5.13		< LOD: 4.15		524213.84	1373.53	< LOD: 2.06		12.40	1.65	8.53	3.57	162.38	3.53	98.17	2.46	167.86	3.53	< LOD: 2.97	
255,8	134.39	21.27	< LOD: 7.95		< LOD: 9.47		< LOD: 5.87		< LOD: 3.04		606968.38	1070.82	< LOD: 1.76		15.24	1.39	6.06	3.14	177.88	3.26	20.84	1.52	90.19	2.41	< LOD: 1.50	
256,1	59.03	20.96	< LOD: 9.61		< LOD: 9.46		< LOD: 5.90		< LOD: 4.13		623846.13	1015.31	< LOD: 1.75		12.32	1.35	5.60	3.10	192.25	3.32	21.70	1.46	80.74	2.27	< LOD: 1.50	
257,7	107.52	23.05	< LOD: 10.84		< LOD: 14.91		< LOD: 4.59		< LOD: 2.91		587439.06	1150.81	< LOD: 1.87		13.37	1.43	8.26	3.30	169.72	3.34	21.14	1.54	92.81	2.55	< LOD: 1.50	
258,2	< LOD: 47.71		< LOD: 8.34		< LOD: 9.90		6.09	3.66	< LOD: 3.54		589278.63	1122.00	< LOD: 1.81		11.61	1.36	7.71	3.19	166.88	3.22	20.41	1.47	85.66	2.39	< LOD: 1.50	
258,4	66.10	21.45	< LOD: 8.09		< LOD: 12.75		< LOD: 5.58		< LOD: 3.72		601668.25	1080.04	< LOD: 1.78		15.85	1.40	8.13	3.18	185.52	3.33	21.29	1.49	88.27	2.39	< LOD: 1.50	
258,7	54.97	19.82	< LOD: 7.46		10.68	6.03	< LOD: 4.96		< LOD: 3.95		609920.81	1008.11	< LOD: 1.73		16.13	1.34	7.81	3.06	248.46	3.60	19.55	1.39	79.05	2.17	< LOD: 2.30	
261,2	48.55	18.91	< LOD: 8.19		8.88	5.78	8.42	3.25	5.93	2.14	560737.13	1035.89	< LOD: 1.67		11.28	1.22	< LOD: 5.42		302.45	3.79	17.15	1.19	47.54	1.69	< LOD: 1.50	
262,1	65.69	19.87	< LOD: 8.57		< LOD: 9.02		5.73	3.34	< LOD: 3.23		583826.50	1058.30	< LOD: 2.76		15.81	1.33	5.13	3.09	382.90	4.47	18.53	1.35	60.80	1.94	< LOD: 1.50	
263,3	111.32	29.01	< LOD: 15.04		< LOD: 17.82		< LOD: 5.81		< LOD: 4.28		560599.88	1424.43	< LOD: 3.48		4.38	1.54	< LOD: 4.78		281.44	4.92	29.30	1.65	132.30	3.48	< LOD: 1.61	
263,4	48.56	20.53	< LOD: 10.80		< LOD: 11.79		< LOD: 5.14		< LOD: 3.44		567572.00	1078.17	< LOD: 3.44		9.80	1.28	< LOD: 6.59		487.84	5.21	18.67	1.28	95.66	2.40	< LOD: 1.50	
264	729.97	27.49	< LOD: 11.80		< LOD: 16.88		< LOD: 4.88		< LOD: 3.90		560817.56	1151.12	< LOD: 1.81		< LOD: 1.83		< LOD: 4.48		151.19	3.27	8.99	1.11	220.47	3.82	< LOD: 1.50	
264,2	39.99	19.93	< LOD: 7.55		12.65	6.13	< LOD: 5.94		3.28	2.18	588529.31	1006.36	< LOD: 2.38		6.23	1.16	< LOD: 3.45		329.76	4.08	11.25	1.11	131.90	2.67	< LOD: 1.50	
265,4	38.09	20.01	< LOD: 12.69		< LOD: 12.45		< LOD: 6.39		< LOD: 3.27		601353.38	1037.80	< LOD: 4.80		15.03	1.42	< LOD: 6.24		1169.54	9.05	33.90	1.50	36.48	1.67	< LOD: 2.13	
266,1	57.58	20.11	< LOD: 10.97		< LOD: 8.00		5.72	3.37	< LOD: 3.25		601785.50	964.72	< LOD: 3.47		2.62	1.16	< LOD: 4.97		310.01	4.01	17.07	1.13	39.87	1.65	< LOD: 1.50	
266,3	92.13	19.06	< LOD: 8.14		< LOD: 8.57		4.97	3.17	< LOD: 4.04		559712.13	1010.30	< LOD: 3.36		6.37	1.20	< LOD: 3.68		675.29	6.08	17.37	1.13	29.60	1.47	< LOD: 1.50	
267,8	28.82	19.06	< LOD: 11.19		< LOD: 8.72		< LOD: 4.80		< LOD: 3.13		592410.00	1004.50	< LOD: 3.67		12.94	1.29	< LOD: 4.82		750.82	6.39	26.70	1.36	47.60	1.72	< LOD: 2.09	
268,7	29.11	18.99	< LOD: 10.51		< LOD: 8.69		< LOD: 4.82		< LOD: 3.92		585737.06	1025.24	< LOD: 2.07		14.47	1.32	5.04	3.20	606.63	5.72	25.74	1.37	52.19	1.81	< LOD: 1.50	
269,1	64.51	18.00	< LOD: 9.45		< LOD: 8.22		< LOD: 4.54		4.54	2.01	548079.75	1023.53	< LOD: 1.71		4.23	1.09	< LOD: 3.13		281.54	3.58	9.72	1.00	34.53	1.47	< LOD: 1.50	
269,2	28.17	18.08	< LOD: 7.88		< LOD: 8.31		8.18	3.12	3.80	2.01	553439.06	1028.22	< LOD: 3.24		8.88	1.18	< LOD: 3.70		537.24	5.09	18.91	1.14	34.61	1.49	< LOD: 1.50	
272,2	78.06	20.07	< LOD: 11.33		< LOD: 9.11		< LOD: 5.00		3.88	2.19	578567.00	1086.35	< LOD: 3.92		17.17	1.40	< LOD: 6.90		510.91	5.33	28.11	1.47	60.94	1.99	< LOD: 2.64	
272,8	53.14	18.39	< LOD: 11.34		< LOD: 8.43		< LOD: 4.63		3.32	2.03	542856.69	1057.98	< LOD: 2.85		8.62	1.19	< LOD: 3.55		612.78	5.54	19.13	1.15	34.98	1.50	< LOD: 1.50	
273,3	< LOD: 24.52		< LOD: 9.34		10.68	5.33	9.60	3.01	4.28	1.94	548567.44	1001.28	< LOD: 1.53		8.08	1.10	< LOD: 4.52		315.76	3.65	11.51	1.00	31.60	1.38	< LOD: 1.50	
273,8	< LOD: 28.08		< LOD: 8.50		< LOD: 12.33		5.00	3.31	< LOD: 4.28		602926.13	979.42	< LOD: 1.74		6.19	1.17	< LOD: 3.26		340.34	4.08	20.11	1.16	66.57	1.96	< LOD: 1.50	
274	< LOD: 40.45		< LOD: 8.77		9.48	5.61	4.93	3.10	5.32	2.06	581475.81	979.70	< LOD: 1.60		4.96	1.12	< LOD: 3.13		292.79	3.67	13.51	1.04	36.27	1.51	< LOD: 1.50	
275,7	38.04	20.67	< LOD: 11.72		< LOD: 10.87		< LOD: 5.23		< LOD: 3.37		572105.88	1065.17	< LOD: 1.93		12.99	1.30	< LOD: 4.99		427.81	4.73	22.72	1.31	91.41	2.30	< LOD: 2.32	
278,1	< LOD: 36.40		< LOD: 7.73		11.20	5.49	4.59	3.01	4.18	1.99	582306.00	989.16	< LOD: 2.26		5.54	1.13	< LOD: 3.81		386.95	4.25	13.79	1.07	36.95	1.52	< LOD: 1.50	
278,2	145.27	19.14	< LOD: 7.78		< LOD: 8.52		< LOD: 5.98		< LOD: 3.07		559285.13	1042.01	< LOD: 2.10		4.38	1.11	< LOD: 3.09		151.87	2.73	6.33	1.00	35.67	1.51	< LOD: 1.50	
282	75.70	20.66	< LOD: 8.87		10.51	6.24	< LOD: 5.06		< LOD: 3.60		606656.69	1038.07	< LOD: 1.72		14.97	1.35	< LOD: 4.56		173.79	3.15	19.77	1.45	98.04	2.44	< LOD: 1.50	
282	218.94	18.81	< LOD: 7.81		8.92	5.52	8.07	3.10	5.09	2.03	526491.00	1057.51	< LOD: 1.98		6.21	1.12	< LOD: 3.22		375.78	4.16	11.28	1.00	41.42	1.58	< LOD: 1.50	
285,3	95.81	24.49	<LOD: 14.25		14.44	7.37	<LOD: 6.50		<LOD: 4.77		572624.63	1268.70	<LOD: 1.98		8.71	1.44	<LOD: 5.03		116.18	3.03	20.66	1.59	87.89	2.63	<LOD: 1.50	
287,7	<LOD: 35.64		<LOD: 11.00		10.98	6.35	8.33	3.55	5.29	2.32	581017.75	1032.95	<LOD: 3.17		11.90	1.28	<LOD: 4.57		391.85	4.49	25.19	1.34	67.77	2.02	<LOD: 1.50	
290,2	36.18	20.71	<LOD: 7.91		<LOD: 13.08		<LOD: 5.26		<LOD: 3.56		586476.25	1067.88	<LOD: 2.90		17.02	1.39	5.59	3.25	515.38	5.37	26.13	1.44	61.79	2.00	<LOD: 1.50	
293,1	81.55	19.58	<LOD: 8.42		12.93	5.98	5.59	3.29	<LOD: 3.18		573851.50	1042.49	<LOD: 3.47		12.63	1.27	<LOD: 4.54		427.39	4.65	20.57	1.28	53.81	1.82	<LOD: 1.50	
293,3	71.34	19.22	11.07	5.56	<LOD: 8.73		6.31	3.25	<LOD: 3.14		550051.81	1051.15	<LOD: 1.67		7.64	1.17	<LOD: 3.53		302.68	3.80	14.60	1.16	44.36	1.65	<LOD: 1.50	
295,16	46.88	20.42	<LOD: 11.98		<LOD: 9.29		<LOD: 7.45		4.55	2.25	606090.38	1028.46	<LOD: 2.90		12.20	1.34	<LOD: 3.71		414.48	4.79	30.07	1.47	56.90	1.95	<LOD: 1.50	
296,7	43.11	19.29	<LOD: 11.30		8.86	5.88	<LOD: 4.86		<LOD: 3.15		588355.69	1041.81	<LOD: 2.03		12.66	1.31	<LOD: 5.96		530.81	5.37	24.98	1.38	66.77	2.03	<LOD: 1.50	
297,5	127.57	24.70	<LOD: 13.21		<LOD: 12.27		<LOD: 5.01		<LOD: 4.17		571552.00	1221.74	<LOD: 1.98		7.19	1.33	<LOD: 5.06		256.96	4.07	23.54	1.39	207.40	3.69	<LOD: 1.50	
300	104.37	22.54	<LOD: 9.43		<LOD: 10.09		<LOD: 4.53		<LOD: 2.69		584503.81	1129.67	<LOD: 1.98		13.59	1.41	5.20	3.23	235.25	3.77	22.20	1.50	75.78	2.28	<LOD: 2.19	
300	108.03	23.22	<LOD: 8.78		<LOD: 9.27		<LOD: 4.61		<LOD: 3.99		585232.94	1153.35	<LOD: 1.87		16.06	1.45	8.40	3.28	182.50	3.40	19.63	1.53	85.24	2.42	<LOD: 1.87	
301	125.57	23.08	<LOD: 8.72		10.69	6.89	<LOD: 4.61		<LOD: 2.66		588366.50	1144.93	<LOD: 1.92		14.19	1.44	8.55	3.32	189.47	3.49	20.90	1.54	87.81	2.48	<LOD: 1.96	
302	153.70	23.33	<LOD: 9.82		<LOD: 12.65		<LOD: 5.90		<LOD: 2.58		568155.38	1193.92	<LOD: 2.90		15.26	1.47	5.15	3.32	256.38	4.01	27.16	1.59	79.92	2.39	<LOD: 1.99	
302,5	129.73	22.76	<LOD: 9.63		<LOD: 14.73		<LOD: 4.46		<LOD: 2.53		578636.06	1156.13	<LOD: 1.89		15.77	1.45	8.37	3.29	201.78	3.54	25.11	1.58	90.68	2.48	<LOD: 2.10	
303	144.86	22.46	<LOD: 13.66		10.53	6.68	<LOD: 4.47		<LOD: 2.53		588892.56	1134.75	<LOD: 1.89		15.47	1.44	<LOD: 4.83		211.56	3.60	22.74	1.55	89.45	2.46	<LOD: 1.50	
305	98.32	22.12	<LOD: 8.66		<LOD: 9.91		<LOD: 4.41		<LOD: 2.48		586028.13	1123.79	<LOD: 1.83		16.58	1.42	5.78	3.18	211.78	3.54	21.93	1.50	81.69	2.33	<LOD: 1.50	
305,9	69.20	20.51	<LOD: 8.82		<LOD: 9.29		<LOD: 5.10		<LOD: 3.14		645671.75	949.42	<LOD: 1.68		13.35	1.32	6.78	3.04	176.24	3.14	16.38	1.39	80.26	2.22	<LOD: 1.52	
306,5	111.06	21.68	<LOD: 13.59		<LOD: 9.70		<LOD: 7.76		<LOD: 4.30		597198.50	1074.39	<LOD: 1.75		15.93	1.39	8.95	3.15	180.23	3.24	20.59	1.48	86.66	2.34	<LOD: 1.50	
304	92.48	21.74	<LOD: 8.17		<LOD: 13.38		<LOD: 4.36		<LOD: 4.60		603714.88	1070.62	<LOD: 1.76		14.30	1.38	<LOD: 4.65		186.12	3.31	22.46	1.49	85.45	2.35	<LOD: 1.50	
304,5	116.24	21.78	<LOD: 12.44		<LOD: 9.74		<LOD: 5.24		<LOD: 3.47		598188.38	1096.17	<LOD: 1.84		15.14	1.42	8.37	3.24	206.39	3.52	22.76	1.53	85.69	2.38	<LOD: 2.10	
305,5	114.07	21.32	<LOD: 9.07		<LOD: 9.57		<LOD: 5.05		<LOD: 3.40		606692.81	1059.13	<LOD: 1.75		15.75	1.38	6.46	3.12	183.89	3.28	18.50	1.46	85.89	2.34	<LOD: 1.50	
306	93.29	20.43	<LOD: 11.79		12.64	6.19	<LOD: 5.08		<LOD: 2.84		616637.19	1027.58	<LOD: 1.73		16.78	1.37	5.00	3.07	195.16	3.32	17.38	1.41	82.67	2.27	<LOD: 1.50	
307	95.43	20.37	<LOD: 8.73		<LOD: 9.12		<LOD: 6.45		<LOD: 2.57		629639.06	993.21	<LOD: 1.68		12.80	1.32	5.79	3.05	176.45	3.16	18.88	1.42	82.35	2.26	<LOD: 1.50	
308	96.54	21.33	<LOD: 9.00		<LOD: 14.28		<LOD: 5.28		<LOD: 3.41		597364.88	1082.70	<LOD: 1.81		15.16	1.39	8.08	3.18	214.83	3.53	25.35	1.53	87.02	2.36	<LOD: 1.50	
309	122.94	20.93	<LOD: 13.55		<LOD: 12.88		<LOD: 5.17		<LOD: 3.86		620732.63	1030.17	<LOD: 1.75		13.34	1.37	<LOD: 4.62		172.18	3.20	20.73	1.46	85.12	2.35	<LOD: 1.50	
310	62.36	19.60	<LOD: 11.09		<LOD: 8.90		4.99	3.29	<LOD: 3.79		618787.25	1008.87	<LOD: 1.67		15.27	1.33	6.14	3.03	194.10	3.25	15.29	1.36	84.37	2.25	<LOD: 1.50	
310,4	39.47	20.41	<LOD: 8.81		11.22	6.23	<LOD: 5.09		<LOD: 3.33		593438.31	1054.64	<LOD: 2.98		14.73	1.33	8.71	3.06	181.09	3.17	20.80	1.43	91.24	2.33	<LOD: 1.50	
311	96.16	19.88	<LOD: 12.04		12.10	6.01	<LOD: 4.92		<LOD: 2.60		612419.25	1016.38	<LOD: 1.64		15.26	1.32	5.23	2.99	170.05	3.06	14.29	1.36	86.70	2.27	<LOD: 1.50	
311,7	51.85	19.55	<LOD: 12.83		<LOD: 13.14		<LOD: 6.44		<LOD: 3.91		632624.88	975.17	<LOD: 1.62		12.95	1.30	6.31	3.00	155.93	2.96	12.88	1.33	84.79	2.25	<LOD: 1.50	
312	85.18	20.97	<LOD: 12.98		10.82	6.33	<LOD: 7.59		<LOD: 3.22		593231.63	1081.51	<LOD: 1.69		13.30	1.33	6.03	3.06	156.81	3.04	15.15	1.39	84.33	2.30	<LOD: 1.50	
312,5	96.80	22.20	<LOD: 9.68		<LOD: 11.65		<LOD: 5.47		<LOD: 2.60		595941.75	1111.98	<LOD: 1.83		12.95	1.39	4.96	3.18	168.54	3.25	17.48	1.47	86.87	2.42	<LOD: 1.50	
312,5	58.11	20.16	<LOD: 8.68		<LOD: 9.17		<LOD: 5.04		3.45	2.20	604738.06	1035.53	<LOD: 1.67		14.78	1.33	8.58	3.06	174.63	3.12	16.71	1.39	89.19	2.31	<LOD: 1.50	
313	80.76	20.77	<LOD: 10.69		<LOD: 9.34		<LOD: 7.14		<LOD: 3.46		612949.63	1055.84	<LOD: 1.71		13.28	1.34	4.97	3.07	163.23	3.10	15.64	1.41	81.99	2.28	<LOD: 1.50	
313,5	67.36	20.09	<LOD: 10.40		12.49	6.13	<LOD: 4.98		<LOD: 3.27		609378.75	1019.91	<LOD: 1.65		17.05	1.34	7.37	3.02	186.46	3.17	16.50	1.35	80.67	2.19	<LOD: 1.50	
314	54.04	20.26	<LOD: 8.11		11.27	6.18	<LOD: 5.76		<LOD: 3.09		609163.25	1024.96	<LOD: 1.64		16.32	1.34	7.81	3.03	189.06	3.19	17.48	1.36	82.14	2.21	<LOD: 1.50	
314,5	72.74	19.79	<LOD: 11.29		11.33	6.03	<LOD: 4.95		4.03	2.17	625644.44	989.28	<LOD: 1.68		16.88	1.35	8.83	3.08	193.61	3.25	17.35	1.39	93.80	2.35	<LOD: 1.50	
315	33.83	19.27	<LOD: 12.37		9.23	5.90	<LOD: 4.86		4.21	2.14	614852.19	1000.05	<LOD: 1.59		15.63	1.30	10.24	3.01	164.08	2.97	14.15	1.28	79.56	2.15	<LOD: 1.50	
315,5	<LOD: 28.17		<LOD: 10.25		<LOD: 8.59		5.23	3.18	<LOD: 3.09		627455.63	970.20	<LOD: 1.60		14.86	1.30	7.23	2.97	169.59	3.01	13.60	1.29	76.36	2.12	<LOD: 1.69	
315,6	66.06	20.50	<LOD: 10.67		10.48	6.22	6.31	3.45	3.94	2.24	608736.94	1037.44	<LOD: 1.65		14.92	1.35	6.93	3.05	175.88	3.14	22.12	1.40	77.51	2.19	<LOD: 1.50	
316	37.07	19.25	<LOD: 11.39		12.16	5.91	5.08	3.25	<LOD: 3.15		627532.06	964.68	<LOD: 2.41		15.35	1.30	5.37	2.93	179.51	3.06	18.43	1.34	80.97	2.16	<LOD: 1.50	
316	33.64	19.37	<LOD: 7.33		<LOD: 8.83		<LOD: 6.12		<LOD: 2.45		626197.38	977.32	<LOD: 1.60		15.53	1.31	4.58	2.92	178.33	3.05	17.71	1.31	73.65	2.08	<LOD: 1.50	
316,6	<LOD: 30.10		<LOD: 7.64		<LOD: 13.19		<LOD: 3.97		<LOD: 4.18		617513.13	1000.40	<LOD: 1.64		16.26	1.33	7.53	3.00	177.04	3.09	17.49	1.30	72.33	2.08	<LOD: 2.13	
317	64.34	20.26	<LOD: 10.54		9.39	6.15	<LOD: 4.02		3.87	2.22	603259.75	1046.50	<LOD: 1.67		13.56	1.32	7.62	3.03	169.45	3.06	16.99	1.38	81.79	2.22	<LOD: 2.22	
317	61.65	20.33	<LOD: 8.72		10.28	6.18	<LOD: 4.70		<LOD: 3.73		602637.81	1030.13	<LOD: 3.00		15.71	1.32	9.62	3.04	173.26	3.07	17.23	1.37	85.98	2.24	<LOD: 1.50	
317,6	<LOD: 42.71		<LOD: 7.31		<LOD: 8.79		<LOD: 4.87		<LOD: 2.22		617579.81	984.67	<LOD: 1.64		12.30	1.25	<LOD: 4.29		148.47	2.80	12.79	1.30	86.08	2.20	<LOD: 1.50	
317,7	94.73	21.88	<LOD: 13.68		<LOD: 9.86		<LOD: 7.72		3.96	2.37	598955.19	1088.10	4.17	1.79	11.55	1.33	<LOD: 4.58		148.24	2.99	18.17	1.48	96.44	2.46	<LOD: 1.50	
317,9	68.35	21.67	<LOD: 9.28		10.00	6.55	<LOD: 4.42		<LOD: 3.50		591086.75	1126.57	8.83	1.89	11.02	1.34	<LOD: 4.64		152.45	3.07	11.81	1.40	87.89	2.39	<LOD: 2.36	
318	100.13	27.49	<LOD: 16.12		<LOD: 12.88		<LOD: 5.53		<LOD: 3.31		481510.84	1486.70	56.46	2.60	<LOD: 2.08		<LOD: 4.06		133.59	3.20	15.43	1.42	52.38	2.15	<LOD: 1.72	
318	628.58	32.67	<LOD: 12.91		<LOD: 17.74		<LOD: 6.07		<LOD: 6.45		474305.84	1637.86	65.42	2.84	3.31	1.46	<LOD: 7.99		131.27	3.38	14.01	1.51	67.15	2.51	<LOD: 2.53	
318,1	<LOD: 28.17		<LOD: 10.71		<LOD: 12.18		<LOD: 4.94		3.83	2.16	601943.69	988.80	<LOD: 2.29		9.49	1.25	<LOD: 4.61		419.57	4.65	27.34	1.30	104.70	2.42	<LOD: 1.50	
318,3	33.04	21.29	<LOD: 8.15		<LOD: 9.68		<LOD: 5.97		<LOD: 4.54		570338.25	1093.31	<LOD: 2.72		5.74	1.23	<LOD: 3.70		522.28	5.39	18.78	1.22	66.48	2.05	<LOD: 1.50	
318,4	<LOD: 28.71		<LOD: 8.32		<LOD: 8.73		7.89	3.28	4.24	2.13	584235.50	1035.09	<LOD: 2.97		9.66	1.23	<LOD: 5.79		347.20	4.19	15.74	1.22	76.70	2.11	<LOD: 1.50	
318,6	982.06	23.87	<LOD: 7.26		<LOD: 10.60		<LOD: 4.91		<LOD: 3.16		558002.25	1090.01	<LOD: 2.10		6.68	1.22	<LOD: 3.76		501.19	5.19	17.81	1.23	133.39	2.74	<LOD: 2.12	
318,8	<LOD: 44.46		<LOD: 7.82		10.36	6.26	<LOD: 5.16		<LOD: 3.33		585925.44	1080.51	<LOD: 2.15		12.55	1.35	<LOD: 5.95		597.09	5.86	33.05	1.44	134.06	2.81	<LOD: 2.36	
318,9	<LOD: 28.54		<LOD: 12.07		<LOD: 12.69		7.99	3.28	4.00	2.12	596720.06	1018.09	<LOD: 1.76		12.00	1.27	<LOD: 6.11		332.66	4.11	25.72	1.33	142.47	2.78	<LOD: 1.50	
319	<LOD: 41.83		10.24	5.69	<LOD: 8.96		5.20	3.31	5.22	2.20	579555.38	1051.39	<LOD: 2.93		14.57	1.31	5.02	3.10	320.90	4.09	27.51	1.36	167.13	3.03	<LOD: 2.13	
319,7	<LOD: 33.98		<LOD: 7.30		15.38	5.97	7.04	3.28	4.88	2.15	584603.94	1031.56	<LOD: 1.82		16.40	1.33	<LOD: 4.63		382.04	4.41	28.65	1.39	148.26	2.83	<LOD: 2.17	
320	<LOD: 30.45		<LOD: 12.02		<LOD: 9.92		<LOD: 4.99		<LOD: 3.32		581652.25	1081.15	<LOD: 1.88		10.64	1.30	<LOD: 5.69		362.03	4.44	28.60	1.38	116.89	2.63	<LOD: 1.50	
320	<LOD: 29.86		<LOD: 8.65		13.34	6.15	<LOD: 5.02		3.81	2.20	587347.94	1046.98	<LOD: 2.93		12.51	1.32	<LOD: 4.80		533.37	5.38	33.87	1.42	111.66	2.53	<LOD: 1.50	
320,1	37.29	19.19	<LOD: 12.65		9.95	5.87	<LOD: 5.19		<LOD: 3.11		630009.75	978.15	<LOD: 1.71		17.40	1.36	<LOD: 4.54		248.88	3.61	27.09	1.44	99.58	2.39	2.68	1.51
320,3	128.90	19.90	<LOD: 8.43		<LOD: 12.14		<LOD: 6.61		<LOD: 3.19		588316.19	1016.18	<LOD: 2.66		10.71	1.27	<LOD: 6.47		441.65	4.77	27.38	1.32	102.98	2.40	<LOD: 1.50	
321	132.37	19.20	<LOD: 8.52		11.61	5.78	7.53	3.21	5.31	2.11	593582.44	1014.27	<LOD: 3.33		14.45	1.30	<LOD: 5.87		371.71	4.32	25.68	1.34	107.20	2.43	<LOD: 1.50	
321	348.20	20.44	<LOD: 10.94		9.59	5.83	6.90	3.25	<LOD: 3.11		582197.06	1039.15	<LOD: 2.73		9.88	1.23	<LOD: 3.65		370.78	4.29	21.36	1.24	103.25	2.38	<LOD: 1.50	
321,4	<LOD: 29.09		<LOD: 8.44		9.15	5.94	6.77	3.31	4.66	2.16	605577.94	1000.01	<LOD: 2.01		7.33	1.22	<LOD: 4.70		314.68	4.03	24.30	1.27	88.35	2.27	<LOD: 1.50	
321,9	<LOD: 30.50		<LOD: 8.02		<LOD: 9.27		<LOD: 5.11		<LOD: 3.66		596786.69	1011.05	<LOD: 2.12		8.84	1.26	<LOD: 6.18		377.45	4.43	27.92	1.33	81.63	2.19	<LOD: 1.50	
322,1	<LOD: 29.05		<LOD: 11.72		<LOD: 8.91		4.97	3.29	<LOD: 3.19		587007.13	1047.85	<LOD: 3.00		16.15	1.36	<LOD: 4.85		549.42	5.46	32.58	1.44	116.78	2.58	<LOD: 1.91	
322,1	<LOD: 29.23		<LOD: 8.44		10.86	5.99	<LOD: 4.92		4.72	2.17	587971.50	1031.28	<LOD: 2.24		14.78	1.33	<LOD: 6.73		402.51	4.59	28.36	1.39	95.15	2.35	<LOD: 1.50	
322,6	<LOD: 32.65		<LOD: 12.38		<LOD: 8.72		6.02	3.24	<LOD: 3.51		603742.75	1002.19	<LOD: 3.26		20.13	1.38	6.36	3.16	461.27	4.90	30.79	1.41	110.20	2.49	<LOD: 1.50	
323	<LOD: 26.86		<LOD: 10.89		17.26	5.84	6.82	3.20	4.19	2.08	598741.50	993.13	<LOD: 2.95		15.90	1.32	<LOD: 4.60		460.33	4.83	31.57	1.36	94.10	2.29	<LOD: 1.50	
323	<LOD: 29.20		<LOD: 8.52		<LOD: 13.60		<LOD: 5.20		<LOD: 3.29		586478.19	1065.53	<LOD: 2.56		14.02	1.36	<LOD: 3.78		484.04	5.18	30.89	1.41	90.44	2.35	<LOD: 1.85	
323,6	<LOD: 28.15		<LOD: 8.16		9.15	5.76	5.51	3.19	4.04	2.09	581434.25	1044.75	<LOD: 2.79		14.76	1.35	<LOD: 3.82		616.03	5.82	33.65	1.43	88.09	2.27	<LOD: 2.40	
324	48.12	19.89	<LOD: 8.00		<LOD: 12.76		<LOD: 5.99		<LOD: 2.19		613725.56	1005.49	<LOD: 3.27		17.26	1.37	5.29	3.08	317.11	4.08	26.45	1.39	71.89	2.10	<LOD: 1.50	
324	<LOD: 28.85		9.31	5.81	<LOD: 11.68		<LOD: 5.05		4.52	2.23	598529.50	981.93	<LOD: 2.87		12.80	1.31	<LOD: 4.64		471.15	4.94	34.21	1.41	95.97	2.33	<LOD: 1.50	
324,5	<LOD: 28.27		<LOD: 7.47		12.08	6.05	6.31	3.34	4.09	2.18	587802.75	1038.19	<LOD: 2.05		13.72	1.32	<LOD: 3.72		579.48	5.58	36.12	1.44	88.15	2.25	<LOD: 1.50	
325	<LOD: 27.82		<LOD: 12.53		11.42	5.94	5.14	3.27	<LOD: 4.08		600082.00	1009.03	<LOD: 3.24		10.10	1.28	<LOD: 3.67		546.07	5.39	32.82	1.38	74.91	2.10	<LOD: 1.50	
325	<LOD: 46.65		<LOD: 11.60		<LOD: 8.97		<LOD: 6.67		<LOD: 3.21		581731.44	1065.21	<LOD: 1.92		12.54	1.31	<LOD: 4.29		448.76	4.85	32.90	1.41	92.14	2.31	<LOD: 1.98	
325,5	<LOD: 26.86		<LOD: 8.11		<LOD: 8.53		5.61	3.17	<LOD: 3.06		605141.88	980.93	<LOD: 1.86		10.84	1.25	<LOD: 5.21		471.48	4.87	29.84	1.32	76.17	2.08	<LOD: 1.50	
326	<LOD: 23.01		<LOD: 7.10		13.38	5.07	10.44	2.86	3.93	1.83	556457.06	1021.86	<LOD: 2.54		19.95	1.26	<LOD: 3.09		364.89	3.92	28.20	1.27	38.28	1.47	<LOD: 1.50	
326	56.90	20.65	<LOD: 12.47		13.05	6.32	<LOD: 4.13		<LOD: 3.35		592245.81	1066.41	<LOD: 1.93		18.19	1.42	5.68	3.19	332.08	4.29	32.31	1.51	99.39	2.47	<LOD: 1.94	
326,5	<LOD: 27.85		<LOD: 7.34		10.47	5.93	<LOD: 4.87		<LOD: 3.17		591959.94	1025.04	<LOD: 1.97		17.92	1.39	<LOD: 6.26		481.43	5.08	34.91	1.47	82.22	2.21	<LOD: 1.71	
327	32.56	20.40	<LOD: 7.77		<LOD: 10.22		<LOD: 4.05		<LOD: 3.32		589142.44	1071.85	<LOD: 2.16		18.11	1.43	<LOD: 3.93		548.54	5.64	35.19	1.52	82.99	2.29	<LOD: 1.83	
327,5	<LOD: 36.85		<LOD: 8.35		10.27	5.90	6.00	3.26	3.98	2.13	595713.63	1020.07	<LOD: 1.83		18.99	1.38	10.16	3.15	362.66	4.31	35.38	1.51	102.68	2.40	<LOD: 1.85	
328	56.59	20.31	<LOD: 11.33		9.47	6.16	<LOD: 5.10		<LOD: 3.28		608140.13	1050.27	<LOD: 1.81		17.37	1.40	<LOD: 4.68		257.79	3.78	31.25	1.54	99.78	2.47	<LOD: 1.50	
328,5	<LOD: 27.13		<LOD: 8.21		8.75	5.77	7.60	3.23	5.80	2.13	601656.13	1000.05	<LOD: 1.76		15.33	1.32	8.06	3.06	334.89	4.09	29.00	1.39	83.11	2.17	<LOD: 1.62	
330	<LOD: 24.27		<LOD: 7.44		8.20	5.24	6.86	2.94	<LOD: 2.80		564100.19	1032.07	<LOD: 2.71		14.38	1.21	<LOD: 3.23		497.11	4.73	21.12	1.15	28.01	1.35	<LOD: 1.50	
330,5	<LOD: 27.65		<LOD: 10.64		14.72	5.73	<LOD: 4.66		<LOD: 3.03		631737.00	960.63	<LOD: 1.84		18.14	1.37	<LOD: 5.52		384.48	4.46	31.43	1.43	70.68	2.06	<LOD: 1.50	
331	<LOD: 35.27		<LOD: 12.12		<LOD: 8.78		<LOD: 6.70		<LOD: 3.10		604459.19	1013.04	<LOD: 3.26		13.96	1.33	<LOD: 4.76		546.56	5.42	28.27	1.37	58.46	1.91	<LOD: 1.58	
331,5	81.28	19.11	<LOD: 9.70		<LOD: 9.29		<LOD: 3.90		<LOD: 2.47		573095.38	1030.17	<LOD: 2.16		10.13	1.27	<LOD: 3.78		692.92	6.23	25.46	1.28	38.46	1.63	<LOD: 1.50	
332	55.12	20.04	<LOD: 10.05		<LOD: 12.47		<LOD: 4.37		<LOD: 2.21		603482.00	1049.52	<LOD: 2.03		21.08	1.45	6.45	3.25	466.65	5.07	33.72	1.54	86.08	2.29	<LOD: 1.94	
332,5	<LOD: 26.18		8.06	5.34	8.63	5.63	7.96	3.16	6.25	2.10	606278.63	946.48	<LOD: 3.61		17.50	1.31	6.34	3.03	452.24	4.70	27.79	1.30	59.99	1.86	<LOD: 1.50	
333	<LOD: 27.08		<LOD: 7.88		<LOD: 11.78		<LOD: 4.62		<LOD: 2.97		585536.44	1016.58	<LOD: 1.60		6.57	1.15	<LOD: 3.18		257.28	3.48	12.33	1.04	37.52	1.54	<LOD: 1.50	
333,5	<LOD: 24.02		<LOD: 9.76		<LOD: 7.79		7.89	2.94	5.78	1.94	539454.94	991.38	<LOD: 2.92		3.06	1.04	<LOD: 2.98		276.85	3.43	6.19	1.00	23.15	1.25	<LOD: 1.50	
334	45.23	19.41	<LOD: 8.42		9.65	5.93	5.98	3.29	<LOD: 3.95		596521.63	1030.37	<LOD: 3.04		13.88	1.33	<LOD: 3.73		578.44	5.61	27.82	1.37	56.91	1.90	<LOD: 1.50	
334,5	58.55	18.05	<LOD: 10.46		<LOD: 8.25		6.63	3.08	6.24	2.06	526490.00	1017.97	<LOD: 2.76		1.82	1.02	<LOD: 3.18		149.98	2.62	3.87	1.00	37.06	1.48	<LOD: 1.50	
335	79.85	19.28	<LOD: 11.32		10.29	5.85	<LOD: 4.83		<LOD: 3.10		617749.88	1000.88	<LOD: 1.71		22.25	1.40	8.39	3.08	276.39	3.76	28.74	1.45	97.44	2.35	<LOD: 1.50	
335,5	37.04	18.49	<LOD: 9.54		9.00	5.65	6.66	3.15	<LOD: 3.03		654455.25	903.13	<LOD: 2.15		19.40	1.34	6.09	2.98	290.65	3.78	24.35	1.34	71.07	2.02	<LOD: 1.50	
330	80.11	20.18	<LOD: 8.99		10.47	6.11	<LOD: 5.13		<LOD: 3.23		618401.19	1016.10	<LOD: 1.79		22.83	1.44	8.16	3.14	275.87	3.84	26.79	1.47	78.60	2.19	<LOD: 1.50	
336,5	70.15	19.48	<LOD: 8.38		<LOD: 8.82		<LOD: 4.88		3.22	2.12	638719.19	958.88	<LOD: 1.75		18.56	1.38	7.30	3.08	254.31	3.67	24.48	1.41	84.76	2.25	<LOD: 1.77	
336,5	84.65	21.04	<LOD: 11.77		<LOD: 10.69		<LOD: 4.76		<LOD: 3.38		622387.81	1025.12	<LOD: 1.77		18.70	1.42	7.94	3.14	205.28	3.41	25.29	1.47	85.06	2.31	<LOD: 1.75	
337	75.27	19.32	<LOD: 8.32		<LOD: 11.36		<LOD: 4.84		<LOD: 3.07		638145.19	966.27	<LOD: 1.75		22.98	1.43	6.96	3.09	280.17	3.83	28.91	1.47	80.80	2.20	<LOD: 1.77	
337,5	89.81	22.31	<LOD: 8.63		<LOD: 13.54		<LOD: 4.44		<LOD: 4.82		609834.69	1077.53	<LOD: 1.88		21.65	1.50	8.08	3.26	234.38	3.74	25.72	1.50	83.62	2.36	<LOD: 1.95	
338	116.12	20.96	<LOD: 10.48		10.33	6.27	<LOD: 7.17		<LOD: 3.17		625873.94	1019.52	<LOD: 1.81		22.19	1.47	5.60	3.16	257.87	3.82	26.12	1.50	74.34	2.20	<LOD: 1.50	

Current depth (m)	Rb	Rb Error	Bi	Bi Error	Au	Au Error	Se	Se Error	As	As Error	Pb	Pb Error	W	W Error	Zn	Zn Error	Cu	Cu Error	Ni	Ni Error	Co	Co Error	Fe	Fe Error	Mn	Mn Error
230,4	37.47	1.49	< LOD: 12.35		< LOD: 8.87		< LOD: 3.50		109.47	5.88	< LOD: 4.33		144.64	34.56	12.22	8.02	34.99	12.73	65.61	25.52	< LOD: 159.71		146010.80	692.62	1477.16	63.27
231,3	6.87	1.00	< LOD: 13.53		< LOD: 10.11		< LOD: 5.31		24.85	3.83	< LOD: 4.68		526.85	44.15	17.66	9.93	39.84	13.76	80.18	27.11	< LOD: 176.58		174728.70	846.22	2081.92	72.23
232,4	6.53	1.00	< LOD: 9.93		53.44	8.18	< LOD: 17.48		21.11	2.76	< LOD: 2.72		2128.59	56.40	< LOD: 16.07		< LOD: 20.90		< LOD: 30.04		< LOD: 113.79		83765.68	397.21	1281.46	54.54
232,7	10.98	1.00	< LOD: 13.10		< LOD: 8.60		< LOD: 6.91		10.74	3.12	< LOD: 3.75		296.65	34.55	< LOD: 12.41		1353.03	29.40	89.32	23.50	176.45	46.65	17873.02	184.28	497.74	54.76
233	19.34	1.00	< LOD: 12.00		14.87	5.02	< LOD: 4.75		11.81	2.44	< LOD: 2.23		682.23	32.95	< LOD: 9.93		< LOD: 11.89		< LOD: 24.29		59.30	32.53	12125.41	122.63	< LOD: 47.62	
233,4	1.74	1.00	< LOD: 13.21		< LOD: 11.01		< LOD: 4.83		710.64	15.54	113.45	6.66	288.68	41.13	< LOD: 13.66		83.43	14.84	137.33	27.91	< LOD: 235.98		105848.43	639.19	480.07	55.39
233,7	61.25	1.42	< LOD: 10.02		< LOD: 5.40		< LOD: 2.13		15.87	2.76	< LOD: 2.66		102.83	25.44	28.34	6.57	< LOD: 13.71		< LOD: 28.75		< LOD: 86.61		45334.96	259.64	497.69	43.49
238,6	35.05	1.53	< LOD: 12.96		< LOD: 12.23		< LOD: 3.59		24.98	3.78	< LOD: 4.49		66.28	34.22	30.98	8.68	31.73	13.31	125.85	27.51	< LOD: 171.16		165202.30	789.70	1742.24	67.85
240,3	25.17	1.00	< LOD: 10.31		11.72	4.91	< LOD: 3.54		16.58	3.12	13.19	2.67	516.50	31.52	< LOD: 10.40		20.79	8.97	< LOD: 25.12		< LOD: 84.10		27819.94	189.65	< LOD: 74.14	
240,9	38.99	1.12	< LOD: 10.60		7.06	4.62	< LOD: 3.63		19.20	2.85	< LOD: 3.45		315.93	28.83	24.68	6.92	16.34	8.95	< LOD: 25.87		< LOD: 71.50		30187.50	201.94	53.69	34.78
241	37.28	1.08	< LOD: 13.31		9.77	4.82	< LOD: 4.44		14.79	2.81	3.93	2.43	464.26	30.84	27.83	7.27	< LOD: 13.03		< LOD: 25.07		< LOD: 68.97		28826.89	194.02	< LOD: 55.47	
241,8	3.72	1.00	< LOD: 9.47		24.16	5.54	< LOD: 6.72		14.48	3.05	15.43	2.62	920.69	36.47	< LOD: 10.34		< LOD: 11.77		< LOD: 24.49		51.70	33.56	13125.24	128.33	629.24	44.62
242,7	54.26	1.31	< LOD: 9.80		< LOD: 5.22		< LOD: 2.32		11.48	3.25	18.56	2.95	153.01	25.93	85.46	7.88	24.50	9.19	< LOD: 26.44		< LOD: 81.55		41232.44	240.10	299.73	39.36
243,2	22.99	1.00	< LOD: 9.85		12.32	5.17	< LOD: 3.81		17.40	2.94	4.19	2.49	640.46	33.90	< LOD: 10.22		18.16	9.15	< LOD: 26.27		< LOD: 74.63		33524.11	213.50	263.65	38.82
243,7	8.31	1.00	< LOD: 10.51		21.94	5.19	< LOD: 7.94		11.90	2.26	< LOD: 1.96		821.99	33.99	< LOD: 9.77		< LOD: 13.48		< LOD: 22.73		< LOD: 50.00		11446.32	115.82	213.91	35.73
244	12.79	1.00	< LOD: 8.66		118.12	9.88	< LOD: 47.93		20.49	2.51	< LOD: 2.37		4690.33	68.74	< LOD: 19.57		< LOD: 13.90		< LOD: 25.60		550.80	42.53	19979.18	154.59	70.98	32.73
245,7	10.54	1.00	< LOD: 8.17		22.57	5.29	< LOD: 9.15		9.63	2.20	< LOD: 1.99		1001.23	35.54	< LOD: 10.28		< LOD: 12.06		< LOD: 22.49		< LOD: 45.61		11562.92	114.95	< LOD: 45.75	
246,2	15.12	1.00	< LOD: 10.19		10.57	4.99	< LOD: 5.16		10.04	2.53	< LOD: 4.51		732.08	33.79	< LOD: 10.07		< LOD: 19.57		< LOD: 24.94		< LOD: 57.99		19509.16	158.14	992.21	50.18
247,2	33.32	1.04	< LOD: 14.39		12.44	5.07	< LOD: 3.83		12.68	3.18	16.86	2.85	593.44	33.64	122.17	9.44	29.17	9.21	< LOD: 26.09		98.87	52.07	36752.12	222.06	242.49	37.53
250,9	7.59	1.00	< LOD: 9.31		45.10	6.92	< LOD: 17.40		15.76	3.47	26.79	3.05	1789.04	47.16	< LOD: 13.33		< LOD: 13.72		< LOD: 24.86		116.41	31.46	10139.21	116.20	1996.36	63.99
251,6	32.11	1.00	< LOD: 13.94		< LOD: 8.70		< LOD: 3.39		16.78	2.85	5.88	2.40	236.19	26.41	23.97	6.47	15.34	8.61	< LOD: 24.83		< LOD: 68.05		29308.31	192.82	148.02	35.42
252,8	14.53	1.00	< LOD: 8.24		65.42	7.51	< LOD: 21.41		11.47	2.33	< LOD: 2.22		2516.90	51.77	< LOD: 14.74		16.74	8.76	< LOD: 24.17		242.26	30.95	9583.16	107.42	469.05	40.68
254,9	55.17	1.52	< LOD: 11.50		< LOD: 6.11		< LOD: 2.74		32.11	3.68	< LOD: 3.64		79.11	28.06	34.30	7.41	34.95	11.00	69.21	22.31	< LOD: 124.45		95526.77	454.19	947.18	52.42
255,8	69.02	1.53	< LOD: 10.21		< LOD: 5.28		< LOD: 2.14		9.78	2.74	< LOD: 3.03		< LOD: 34.03		45.21	6.73	25.84	9.63	< LOD: 44.63		< LOD: 89.75		47764.88	271.84	193.23	39.22
256,1	58.56	1.40	< LOD: 9.91		< LOD: 5.06		< LOD: 2.12		14.83	2.73	< LOD: 2.69		63.21	24.37	29.77	6.52	22.71	9.44	< LOD: 28.21		< LOD: 91.90		52282.11	282.28	374.46	41.31
257,7	59.80	1.49	< LOD: 10.65		< LOD: 9.77		< LOD: 2.51		14.58	3.01	< LOD: 3.24		134.95	28.13	31.44	7.17	39.25	10.46	31.16	20.71	< LOD: 110.27		76343.28	372.04	611.50	46.01
258,2	54.70	1.39	< LOD: 10.24		< LOD: 6.03		< LOD: 3.51		15.29	2.81	< LOD: 2.93		118.54	26.66	29.90	6.86	24.21	9.75	< LOD: 28.97		< LOD: 113.22		74114.55	355.71	560.10	43.72
258,4	59.99	1.43	< LOD: 10.26		< LOD: 5.25		< LOD: 2.20		12.78	3.11	8.23	2.85	< LOD: 36.51		36.21	6.68	40.71	10.02	< LOD: 41.67		< LOD: 99.18		62386.25	317.38	396.73	41.49
258,7	58.78	1.35	< LOD: 9.76		< LOD: 5.05		< LOD: 2.14		19.51	2.84	< LOD: 2.85		81.31	24.19	44.95	6.73	< LOD: 19.26		< LOD: 26.67		< LOD: 81.21		41495.54	239.79	112.28	35.49
261,2	29.50	1.00	< LOD: 8.88		11.76	5.09	< LOD: 4.83		20.68	2.71	< LOD: 2.37		795.63	34.73	< LOD: 11.40		14.81	8.75	< LOD: 24.99		133.44	45.72	27540.62	186.23	< LOD: 72.02	
262,1	47.71	1.23	< LOD: 9.81		< LOD: 5.47		< LOD: 3.55		21.63	3.14	7.61	2.62	188.09	26.34	26.65	6.61	16.15	9.02	< LOD: 26.48		< LOD: 79.90		39701.59	234.29	153.51	36.31
263,3	8.08	1.00	< LOD: 11.72		16.38	6.65	< LOD: 6.24		24.45	3.56	< LOD: 3.97		551.42	42.28	< LOD: 15.61		21.43	12.29	43.61	24.61	< LOD: 156.43		140858.88	679.67	2383.25	73.54
263,4	25.25	1.00	< LOD: 10.35		17.29	5.70	< LOD: 8.41		24.50	3.20	4.76	2.62	900.33	38.21	< LOD: 14.90		16.33	9.33	< LOD: 26.94		< LOD: 112.11		39002.70	237.81	649.44	45.74
264	6.51	1.00	< LOD: 9.97		19.93	6.20	< LOD: 7.87		69.48	5.15	39.32	3.77	878.36	41.19	75.26	9.98	19.73	10.15	< LOD: 29.68		< LOD: 96.44		52895.88	307.15	889.82	51.75
264,2	18.27	1.00	< LOD: 11.90		13.01	5.21	< LOD: 6.40		14.94	4.15	56.70	3.70	720.07	34.49	16.86	7.63	15.01	8.85	< LOD: 25.12		< LOD: 59.59		19312.61	159.64	348.92	40.12
265,4	18.94	1.00	< LOD: 15.69		9.65	5.12	< LOD: 4.01		22.15	3.50	14.01	2.92	479.21	32.73	30.63	7.78	17.64	9.58	< LOD: 27.61		< LOD: 80.64		38250.73	235.69	< LOD: 77.31	
266,1	6.86	1.00	< LOD: 9.04		19.39	5.80	< LOD: 8.27		12.59	2.38	< LOD: 2.26		1076.43	39.81	< LOD: 11.64		< LOD: 12.67		< LOD: 25.65		< LOD: 85.55		47300.80	258.04	426.97	40.60
266,3	5.66	1.00	< LOD: 10.36		72.56	8.36	< LOD: 26.63		12.97	2.46	< LOD: 2.41		2909.15	57.85	< LOD: 16.21		< LOD: 13.02		< LOD: 25.96		132.53	44.18	24259.06	177.17	< LOD: 48.71	
267,8	27.27	1.00	< LOD: 13.55		8.63	4.82	< LOD: 3.25		14.99	3.64	33.22	3.22	486.78	30.97	32.17	7.38	< LOD: 16.04		< LOD: 25.35		< LOD: 66.89		27400.19	187.45	55.87	34.07
268,7	31.55	1.02	< LOD: 11.42		19.05	5.71	< LOD: 7.08		23.27	3.18	7.66	2.61	1010.09	38.74	15.65	8.43	22.61	9.25	< LOD: 25.80		< LOD: 66.50		24565.64	180.44	< LOD: 51.51	
269,1	9.60	1.00	< LOD: 12.06		24.13	5.84	< LOD: 12.25		7.86	2.21	< LOD: 2.11		1318.77	40.49	< LOD: 11.50		< LOD: 11.76		< LOD: 23.81		< LOD: 66.89		13247.72	128.01	561.59	43.35
269,2	14.94	1.00	< LOD: 15.15		30.32	6.09	< LOD: 12.19		12.61	2.32	< LOD: 2.09		1400.71	41.73	< LOD: 12.26		< LOD: 14.15		< LOD: 24.39		< LOD: 54.36		16388.38	141.66	131.18	35.17
272,2	43.16	1.20	< LOD: 12.94		< LOD: 7.77		< LOD: 2.29		16.79	2.82	< LOD: 2.65		205.22	27.39	28.69	6.86	< LOD: 13.71		< LOD: 27.12		< LOD: 79.47		35705.41	225.78	60.15	35.46
272,8	11.97	1.00	< LOD: 14.55		12.22	4.91	< LOD: 3.19		9.90	2.57	< LOD: 3.36		609.56	32.20	< LOD: 9.37		< LOD: 11.95		< LOD: 24.45		< LOD: 77.43		11133.12	119.24	305.70	39.73
273,3	15.69	1.00	< LOD: 8.42		17.34	5.05	< LOD: 7.44		7.61	2.13	< LOD: 1.96		859.94	33.97	< LOD: 10.10		< LOD: 13.06		< LOD: 22.95		85.80	28.67	9257.19	104.04	< LOD: 44.59	
273,8	9.80	1.00	16.46	6.29	8.11	4.77	< LOD: 6.31		4.83	2.57	6.36	2.38	497.31	31.00	< LOD: 9.22		< LOD: 13.03		< LOD: 24.69		< LOD: 62.99		8930.63	110.61	2150.38	66.78
274	11.04	1.00	< LOD: 9.20		11.07	4.71	< LOD: 3.19		7.90	2.48	3.57	2.20	508.42	30.52	< LOD: 8.94		< LOD: 11.52		< LOD: 23.73		< LOD: 50.90		14398.03	134.63	1080.97	51.70
275,7	30.08	1.01	< LOD: 14.29		< LOD: 6.83		< LOD: 3.21		15.84	2.67	< LOD: 2.46		329.37	28.95	15.58	6.71	15.41	9.02	< LOD: 26.07		< LOD: 70.86		28451.27	198.01	779.28	47.58
278,1	14.96	1.00	< LOD: 10.27		18.53	5.17	< LOD: 4.16		7.35	2.30	< LOD: 2.21		717.94	33.76	< LOD: 9.92		13.02	8.57	< LOD: 24.27		< LOD: 56.73		17812.27	148.33	< LOD: 44.56	
278,2	11.93	1.00	< LOD: 9.48		13.47	5.00	< LOD: 6.43		29.38	2.93	< LOD: 2.30		586.17	32.35	< LOD: 9.71		< LOD: 12.97		< LOD: 24.80		< LOD: 55.83		17391.31	148.65	< LOD: 69.67	
282	65.74	1.45	< LOD: 10.11		< LOD: 5.09		< LOD: 2.23		12.37	2.90	4.83	2.62	101.99	24.98	41.96	6.86	19.68	9.25	< LOD: 27.23		< LOD: 88.34		48888.13	268.35	251.56	38.65
282	9.39	1.00	< LOD: 9.40		46.37	6.87	< LOD: 17.83		14.37	2.53	< LOD: 2.34		1950.30	47.26	< LOD: 13.42		< LOD: 11.91		< LOD: 24.52		239.38	30.19	8299.90	102.03	57.12	33.89
285,3	51.73	1.49	< LOD: 10.82		< LOD: 7.41		< LOD: 2.70		24.48	3.36	< LOD: 3.49		71.76	28.77	28.87	7.31	27.74	10.83	< LOD: 40.20		< LOD: 143.94		108313.95	494.31	675.90	47.47
287,7	29.33	1.00	< LOD: 9.49		33.78	6.57	< LOD: 14.29		19.03	2.90	< LOD: 4.20		1525.37	45.11	< LOD: 13.34		16.76	9.32	< LOD: 26.59		353.50	47.57	26301.80	188.04	782.32	47.32
290,2	41.63	1.18	< LOD: 10.30		< LOD: 4.92		< LOD: 2.17		14.55	2.72	< LOD: 2.60		69.37	24.18	25.23	6.37	< LOD: 20.77		< LOD: 27.17		< LOD: 77.27		34780.03	223.27	67.65	35.88
293,1	28.29	1.00	< LOD: 10.34		21.29	5.64	< LOD: 7.99		12.77	3.55	30.45	3.18	869.78	37.41	69.64	9.09	< LOD: 12.56		< LOD: 25.69		< LOD: 87.14		20608.63	164.26	144.39	36.72
293,3	16.27	1.00	< LOD: 8.84		7.63	4.96	< LOD: 5.44		< LOD: 7.07		93.46	4.35	653.23	36.55	680.48	16.35	< LOD: 13.12		< LOD: 24.10		< LOD: 55.14		16318.42	143.94	307.56	39.28
295,16	35.60	1.11	< LOD: 14.88		< LOD: 5.63		< LOD: 3.67		26.55	3.25	3.92	2.59	195.64	27.11	28.35	6.85	26.43	9.47	< LOD: 27.08		< LOD: 106.23		48331.30	268.43	53.13	34.97
296,7	34.78	1.08	< LOD: 16.97		9.20	5.03	< LOD: 6.29		17.57	2.77	< LOD: 2.55		547.35	32.74	11.86	7.32	< LOD: 13.53		< LOD: 26.58		< LOD: 69.38		26159.79	189.63	80.04	35.86
297,5	22.04	1.00	< LOD: 10.52		< LOD: 7.41		< LOD: 2.57		42.88	3.69	< LOD: 4.79		160.41	28.35	15.95	6.74	34.65	10.34	< LOD: 29.37		< LOD: 93.50		48704.57	296.83	1946.38	66.62
300	53.19	1.39	< LOD: 10.36		< LOD: 5.15		< LOD: 2.24		14.23	2.92	< LOD: 2.97		< LOD: 34.82		33.45	6.61	19.03	9.81	< LOD: 29.64		< LOD: 112.72		51892.23	291.54	388.53	43.22
300	63.71	1.52	< LOD: 10.60		< LOD: 5.38		< LOD: 2.38		12.33	2.89	< LOD: 3.20		< LOD: 35.42		39.26	6.82	27.11	10.12	< LOD: 42.24		< LOD: 95.11		51059.73	291.01	352.85	43.04
301	59.62	1.49	< LOD: 10.75		< LOD: 5.35		< LOD: 2.24		11.12	2.91	< LOD: 3.89		< LOD: 48.26		30.14	6.73	24.04	10.07	< LOD: 29.85		< LOD: 100.63		58262.54	316.78	501.43	45.60
302	51.52	1.40	< LOD: 10.67		< LOD: 5.50		< LOD: 2.38		15.40	3.06	< LOD: 3.89		< LOD: 36.10		33.17	6.77	28.36	10.27	< LOD: 30.27		< LOD: 99.43		55465.47	309.06	579.79	47.39
302,5	60.73	1.48	< LOD: 10.62		< LOD: 6.73		< LOD: 2.27		12.86	3.10	5.86	2.80	< LOD: 35.39		45.53	6.93	37.76	10.24	< LOD: 44.60		< LOD: 94.86		51731.61	291.65	560.36	46.50
303	60.94	1.48	< LOD: 11.42		< LOD: 5.29		< LOD: 2.17		10.84	3.03	5.48	2.76	< LOD: 34.80		38.39	6.74	35.02	10.14	< LOD: 30.72		< LOD: 92.11		47706.81	278.32	470.78	45.19
305	58.37	1.42	< LOD: 10.25		< LOD: 5.04		< LOD: 2.17		14.32	2.94	< LOD: 4.70		< LOD: 34.61		35.52	6.63	26.92	9.81	< LOD: 28.95		< LOD: 89.47		46159.29	269.17	333.07	42.11
305,9	59.07	1.37	< LOD: 9.80		< LOD: 5.16		< LOD: 2.14		23.70	4.09	39.54	3.52	79.95	24.35	23.45	6.28	27.97	9.37	< LOD: 27.74		< LOD: 85.89		45922.73	257.35	303.78	39.50
306,5	63.67	1.45	< LOD: 10.17		< LOD: 5.01		< LOD: 1.94		13.38	3.38	18.55	3.02	< LOD: 33.75		36.09	6.46	23.50	9.51	< LOD: 28.19		< LOD: 87.05		45696.81	261.96	221.00	39.27
304	58.40	1.41	< LOD: 9.97		< LOD: 5.00		< LOD: 2.19		12.29	3.00	5.62	2.71	< LOD: 37.65		322.98	12.14	32.75	9.78	< LOD: 28.54		< LOD: 92.46		51809.21	283.80	375.22	41.99
304,5	61.26	1.46	< LOD: 10.42		< LOD: 7.14		< LOD: 2.24		14.93	3.00	< LOD: 5.64		< LOD: 35.09		40.76	6.73	41.31	10.12	< LOD: 37.47		< LOD: 94.51		53126.54	291.77	358.13	42.15
305,5	65.41	1.47	< LOD: 10.06		< LOD: 5.07		< LOD: 2.07		11.06	2.83	< LOD: 3.86		< LOD: 34.20		32.61	6.43	24.84	9.55	< LOD: 28.40		< LOD: 88.50		47183.89	267.56	214.54	39.05
306	60.67	1.40	< LOD: 9.87		< LOD: 5.07		< LOD: 1.99		20.50	3.28	10.76	2.76	< LOD: 33.73		35.46	6.42	24.96	9.40	< LOD: 27.78		< LOD: 81.82		39165.07	239.13	115.77	37.05
307	61.24	1.41	< LOD: 9.82		< LOD: 4.84		< LOD: 2.05		11.45	2.64	< LOD: 2.66		< LOD: 33.03		30.20	6.25	32.73	9.47	< LOD: 27.30		< LOD: 83.91		42712.34	249.52	166.87	37.76
308	59.12	1.41	< LOD: 10.21		< LOD: 5.02		< LOD: 2.11		17.29	3.18	8.12	2.77	< LOD: 41.88		38.14	6.64	32.29	9.77	< LOD: 38.33		< LOD: 91.59		51120.80	281.46	322.95	40.87
309	56.81	1.39	< LOD: 9.88		< LOD: 5.14		< LOD: 2.10		11.73	3.12	10.10	2.84	< LOD: 33.27		33.07	6.35	24.13	9.50	< LOD: 39.73		< LOD: 91.48		51531.41	282.93	409.86	42.45
310	61.58	1.39	< LOD: 9.73		< LOD: 4.83		< LOD: 2.00		13.07	2.79	< LOD: 3.71		< LOD: 31.99		36.11	6.24	40.57	9.50	< LOD: 27.00		< LOD: 79.03		37633.78	229.55	76.88	35.48
310,4	60.40	1.38	< LOD: 9.86		< LOD: 9.76		< LOD: 2.30		13.12	3.28	17.82	2.99	156.01	26.35	32.76	6.72	39.92	9.57	< LOD: 27.28		< LOD: 124.86		53637.69	279.19	396.95	40.24
311	64.18	1.41	< LOD: 11.94		< LOD: 4.66		< LOD: 1.91		16.54	2.83	< LOD: 4.17		< LOD: 32.44		29.13	6.13	36.31	9.41	< LOD: 26.85		< LOD: 79.08		38103.35	230.85	66.98	35.43
311,7	61.59	1.39	< LOD: 9.68		< LOD: 4.93		< LOD: 2.06		16.25	2.86	< LOD: 3.69		73.54	23.83	27.94	6.33	31.33	9.30	< LOD: 26.90		< LOD: 92.75		39297.97	235.13	62.03	34.95
312	60.33	1.41	< LOD: 9.84		< LOD: 4.85		< LOD: 2.74		22.67	3.26	7.55	2.74	< LOD: 42.14		33.85	6.42	32.88	9.60	< LOD: 32.66		< LOD: 90.80		51836.54	280.05	254.93	38.99
312,5	59.27	1.45	< LOD: 10.30		< LOD: 5.16		< LOD: 2.21		17.28	3.23	6.24	2.83	< LOD: 34.82		36.07	6.68	32.49	9.99	< LOD: 29.18		< LOD: 99.79		59710.90	315.23	540.07	45.27
312,5	63.19	1.41	< LOD: 9.89		< LOD: 5.17		< LOD: 2.16		16.12	2.86	< LOD: 4.98		59.83	24.10	29.83	6.37	30.26	9.36	< LOD: 27.39		< LOD: 83.31		42849.56	246.76	168.20	36.92
313	60.68	1.42	< LOD: 9.90		< LOD: 5.09		< LOD: 2.09		19.12	3.37	13.56	2.89	< LOD: 33.57		32.46	6.35	27.15	9.52	< LOD: 28.08		< LOD: 85.00		42372.57	252.01	< LOD: 83.33	
313,5	58.16	1.34	< LOD: 9.74		< LOD: 4.82		< LOD: 2.05		16.84	2.94	5.14	2.53	< LOD: 31.96		29.53	6.03	26.99	9.20	< LOD: 27.20		< LOD: 88.15		36940.43	225.77	68.55	35.04
314	57.11	1.33	< LOD: 9.68		< LOD: 4.68		< LOD: 1.98		17.26	2.87	< LOD: 3.65		< LOD: 31.97		27.40	6.00	27.24	9.21	< LOD: 26.77		< LOD: 76.71		35514.35	221.11	165.26	37.28
314,5	63.76	1.41	< LOD: 9.93		< LOD: 5.20		< LOD: 2.10		13.90	2.74	< LOD: 3.71		72.10	24.36	34.72	6.53	33.30	9.40	< LOD: 26.99		< LOD: 91.09		34836.91	220.15	< LOD: 67.47	
315	50.61	1.24	< LOD: 9.62		< LOD: 4.69		< LOD: 1.82		15.85	3.16	14.84	2.75	< LOD: 31.55		25.78	5.87	23.04	8.92	< LOD: 26.16		< LOD: 76.84		37015.84	223.40	60.56	34.42
315,5	54.02	1.29	< LOD: 9.49		< LOD: 5.05		< LOD: 1.99		15.74	2.86	4.89	2.46	77.46	23.82	22.71	6.12	28.67	9.07	< LOD: 25.76		< LOD: 76.54		34852.18	217.06	63.50	34.45
315,6	49.63	1.27	< LOD: 9.75		< LOD: 5.11		< LOD: 2.09		18.98	2.78	< LOD: 2.58		50.87	23.93	24.59	6.24	38.02	9.56	< LOD: 26.90		< LOD: 87.06		47397.02	262.52	325.42	40.00
316	54.04	1.28	< LOD: 9.59		< LOD: 4.98		< LOD: 2.34		13.79	2.89	7.39	2.55	77.04	23.69	30.00	6.26	26.04	8.99	< LOD: 25.95		< LOD: 107.41		36793.39	221.85	57.70	34.11
316	50.20	1.24	< LOD: 12.24		< LOD: 4.50		< LOD: 1.82		11.15	2.61	< LOD: 3.87		< LOD: 30.93		26.99	5.87	14.23	8.70	< LOD: 25.82		< LOD: 73.66		33826.38	212.66	117.17	35.90
316,6	43.57	1.18	< LOD: 9.59		< LOD: 5.01		< LOD: 1.98		13.09	2.67	< LOD: 2.97		72.20	23.85	24.07	6.18	37.64	9.37	< LOD: 26.35		< LOD: 115.32		41351.55	239.66	188.66	37.06
317	58.87	1.36	< LOD: 9.79		< LOD: 6.13		< LOD: 2.21		21.05	3.46	18.18	2.95	61.16	24.43	38.26	6.59	28.56	9.30	< LOD: 27.10		< LOD: 84.10		41448.73	242.03	< LOD: 51.48	
317	60.05	1.36	< LOD: 9.78		< LOD: 4.90		< LOD: 1.91		16.58	3.18	13.63	2.76	< LOD: 32.65		32.47	6.13	17.24	8.97	< LOD: 27.20		< LOD: 80.17		40049.32	235.21	87.47	35.34
317,6	63.45	1.36	< LOD: 11.89		< LOD: 4.86		< LOD: 1.94		20.83	3.27	15.78	2.76	63.65	23.12	30.74	6.16	< LOD: 11.82		< LOD: 25.53		< LOD: 89.61		38107.74	224.14	< LOD: 55.47	
317,7	62.25	1.44	< LOD: 9.95		< LOD: 6.56		< LOD: 2.30		34.34	5.12	74.22	4.38	47.96	25.15	34.06	6.65	52.06	10.21	< LOD: 29.48		< LOD: 91.63		51590.72	281.56	58.98	35.54
317,9	53.33	1.37	< LOD: 10.01		< LOD: 5.91		< LOD: 3.70		44.95	5.79	96.86	4.90	90.23	26.20	35.74	6.90	71.62	10.71	37.92	20.06	< LOD: 139.96		58952.74	309.45	168.39	37.79
318	11.11	1.00	< LOD: 10.57		21.24	7.36	< LOD: 16.25		168.76	8.78	136.05	6.39	1143.24	48.36	< LOD: 14.79		76.47	12.63	81.47	23.81	157.18	88.90	100741.13	498.77	1932.76	66.77
318	13.11	1.00	< LOD: 11.65		< LOD: 11.14		< LOD: 5.08		203.02	10.11	169.55	7.31	212.12	35.06	16.91	8.13	95.48	13.75	110.34	25.50	< LOD: 146.96		116174.86	582.90	1980.73	70.18
318,1	18.33	1.00	< LOD: 9.42		47.17	7.16	< LOD: 13.92		7.56	2.23	< LOD: 2.26		2058.07	49.94	< LOD: 14.48		< LOD: 15.77		< LOD: 25.42		174.78	44.41	24289.53	179.36	1932.43	62.14
318,3	14.40	1.00	< LOD: 13.68		16.47	5.68	< LOD: 9.23		16.93	2.92	< LOD: 4.91		901.40	38.18	< LOD: 11.31		20.50	9.46	< LOD: 26.83		< LOD: 76.78		34635.91	224.55	2418.90	69.13
318,4	31.30	1.01	< LOD: 9.27		14.73	5.29	< LOD: 5.72		25.07	3.35	14.05	2.74	734.52	34.88	< LOD: 16.35		16.05	8.95	< LOD: 26.22		< LOD: 72.99		31458.54	205.07	463.06	41.66
318,6	22.93	1.00	< LOD: 11.62		16.04	5.51	< LOD: 7.26		19.05	3.08	7.62	2.58	834.75	36.61	< LOD: 11.01		< LOD: 13.51		< LOD: 26.40		< LOD: 66.91		25526.52	185.41	412.42	42.40
318,8	21.52	1.00	< LOD: 10.26		7.71	4.89	< LOD: 4.39		11.71	2.60	< LOD: 2.54		431.90	31.20	< LOD: 13.34		16.02	9.21	< LOD: 26.32		< LOD: 74.79		30904.93	211.12	1848.39	62.98
318,9	32.95	1.02	< LOD: 9.35		< LOD: 7.67		< LOD: 2.96		5.71	2.30	< LOD: 2.32		252.98	26.86	12.26	6.29	< LOD: 12.11		< LOD: 25.00		< LOD: 64.14		24103.43	178.29	1261.59	54.30
319	33.06	1.04	< LOD: 9.67		< LOD: 4.99		< LOD: 3.55		7.78	2.32	< LOD: 2.30		76.05	23.67	14.71	5.86	< LOD: 15.98		< LOD: 25.40		< LOD: 64.82		24744.22	182.29	1472.04	57.36
319,4	18.53	1.00	< LOD: 10.37		10.08	4.91	< LOD: 5.24		7.77	2.27	< LOD: 2.19		534.17	31.95	< LOD: 10.57		40.79	9.46	< LOD: 25.47		< LOD: 81.56		20453.60	165.36	1486.79	58.06
319,7	39.28	1.11	< LOD: 12.44		< LOD: 7.23		< LOD: 4.02		6.56	2.33	< LOD: 2.37		273.69	27.25	19.69	6.54	< LOD: 13.07		< LOD: 25.24		86.63	44.08	24559.32	179.19	451.38	41.83
320	22.93	1.00	< LOD: 11.42		< LOD: 5.18		< LOD: 2.06		6.64	2.31	< LOD: 2.30		35.91	23.78	11.03	5.81	< LOD: 13.80		< LOD: 26.29		< LOD: 69.97		27488.24	198.93	1952.45	64.99
320	22.49	1.00	< LOD: 9.89		< LOD: 7.27		< LOD: 3.83		7.70	2.37	< LOD: 2.37		549.31	32.22	< LOD: 13.47		18.21	9.14	< LOD: 26.32		< LOD: 81.21		26230.71	190.02	1733.25	61.17
320,1	49.87	1.26	< LOD: 10.64		< LOD: 5.42		< LOD: 2.10		23.15	3.25	10.63	2.67	102.17	24.60	23.89	6.25	< LOD: 18.92		< LOD: 26.46		< LOD: 73.61		32685.58	211.01	272.32	39.05
320,3	23.05	1.00	< LOD: 9.50		18.47	5.60	< LOD: 9.71		8.47	2.26	< LOD: 2.23		966.80	37.88	< LOD: 15.51		16.80	9.02	< LOD: 25.57		< LOD: 82.09		25549.94	184.33	1590.26	58.49
321	35.21	1.05	< LOD: 13.71		14.32	5.13	< LOD: 4.98		7.77	2.33	< LOD: 2.32		655.89	33.65	14.72	7.47	< LOD: 12.22		< LOD: 25.56		< LOD: 71.23		22883.74	172.58	421.31	41.62
321	23.55	1.00	< LOD: 14.87		< LOD: 4.82		< LOD: 1.89		5.40	2.21	< LOD: 2.16		92.56	23.50	< LOD: 12.48		< LOD: 17.51		< LOD: 25.34		< LOD: 58.82		19907.16	161.03	570.78	44.62
321,4	19.00	1.00	< LOD: 9.15		22.45	5.83	< LOD: 8.33		9.99	2.28	< LOD: 2.17		1061.35	39.54	< LOD: 18.78		< LOD: 14.02		< LOD: 25.93		< LOD: 108.65		27883.86	195.39	1742.65	60.57
321,9	19.99	1.00	< LOD: 9.35		27.02	6.04	< LOD: 10.63		9.91	2.28	< LOD: 2.23		1114.91	40.45	< LOD: 19.12		< LOD: 15.43		< LOD: 26.43		< LOD: 74.80		32903.66	213.08	1718.48	59.77
322,1	30.84	1.02	< LOD: 11.80		< LOD: 4.87		< LOD: 2.08		5.73	2.29	< LOD: 2.31		< LOD: 34.42		18.11	5.90	< LOD: 15.53		< LOD: 25.82		< LOD: 66.37		24891.20	183.91	423.24	42.38
322,1	32.41	1.04	< LOD: 10.86		26.65	5.96	< LOD: 8.59		9.22	2.38	< LOD: 2.39		1031.73	39.55	< LOD: 12.67		33.07	9.48	< LOD: 26.66		77.88	50.54	33756.12	214.08	221.06	37.54
322,6	31.45	1.02	< LOD: 9.96		< LOD: 9.27		< LOD: 3.15		6.87	2.45	< LOD: 2.53		340.18	28.60	19.29	6.77	< LOD: 13.18		< LOD: 26.12		86.32	48.56	30836.05	202.66	204.43	37.28
323	23.34	1.00	< LOD: 9.49		18.59	5.41	< LOD: 7.27		7.29	2.30	< LOD: 2.32		826.74	35.80	< LOD: 11.60		21.83	8.94	< LOD: 25.14		< LOD: 69.31		28336.42	191.96	730.86	45.63
323	20.83	1.00	< LOD: 14.85		< LOD: 5.13		< LOD: 2.68		6.84	2.27	< LOD: 2.24		71.09	24.22	12.01	5.99	47.47	9.87	< LOD: 26.94		< LOD: 74.94		32487.70	215.87	872.23	50.16
323,6	24.08	1.00	11.89	7.22	13.74	5.34	< LOD: 5.13		20.18	2.72	< LOD: 2.34		785.77	35.79	< LOD: 12.15		18.95	9.17	< LOD: 26.18		< LOD: 87.85		24035.98	179.86	523.83	43.90
324	36.24	1.09	< LOD: 9.75		< LOD: 4.67		< LOD: 1.90		7.24	2.35	< LOD: 2.36		< LOD: 31.30		24.46	5.87	17.97	9.03	< LOD: 26.23		< LOD: 75.70		34218.26	218.33	112.07	36.28
324	25.15	1.00	< LOD: 10.73		83.75	9.07	< LOD: 39.61		14.45	2.46	< LOD: 2.52		3830.57	64.31	< LOD: 18.32		< LOD: 15.05		< LOD: 26.31		206.36	44.78	25304.89	180.35	1201.18	52.13
324,5	21.89	1.00	< LOD: 10.50		12.37	5.17	< LOD: 6.76		7.83	2.30	< LOD: 2.28		688.01	34.20	< LOD: 10.34		26.15	9.25	< LOD: 25.91		< LOD: 67.99		27294.23	191.55	1493.02	57.37
325	16.97	1.00	< LOD: 10.38		20.32	5.79	< LOD: 10.66		7.09	2.31	< LOD: 2.34		1079.09	39.42	< LOD: 11.73		35.01	9.45	< LOD: 25.68		< LOD: 66.79		25031.54	183.51	1561.62	58.38
325	25.38	1.00	< LOD: 14.39		< LOD: 5.04		< LOD: 2.03		6.69	2.30	< LOD: 2.27		98.49	24.19	9.12	5.85	27.51	9.20	< LOD: 25.82		< LOD: 66.57		26165.40	188.76	1166.20	53.88
325,5	19.00	1.00	< LOD: 9.22		19.24	5.50	< LOD: 7.89		7.44	2.25	< LOD: 2.22		937.65	36.97	< LOD: 11.02		< LOD: 12.09		< LOD: 25.26		< LOD: 64.15		23582.28	174.60	1235.74	53.33
326	35.66	1.00	< LOD: 11.87		< LOD: 4.01		< LOD: 1.50		5.74	2.00	< LOD: 1.78		< LOD: 27.75		< LOD: 6.22		< LOD: 10.71		< LOD: 21.93		< LOD: 37.08		7894.31	96.61	< LOD: 41.17	
326	40.54	1.18	< LOD: 10.10		< LOD: 5.01		< LOD: 2.09		7.96	2.45	< LOD: 2.50		< LOD: 32.78		26.09	6.07	16.48	9.28	< LOD: 27.89		< LOD: 80.57		38261.34	236.73	204.92	38.85
326,5	31.09	1.03	< LOD: 12.28		15.15	5.40	< LOD: 5.78		9.64	2.41	< LOD: 2.43		790.87	36.08	16.78	7.97	21.08	9.18	< LOD: 26.00		< LOD: 81.13		41483.10	239.98	156.46	36.00
327	29.52	1.04	< LOD: 15.76		< LOD: 4.88		< LOD: 1.97		7.42	2.46	< LOD: 2.51		< LOD: 33.32		17.97	5.96	17.02	9.34	< LOD: 27.45		< LOD: 84.29		42168.89	250.57	224.02	39.11
327,5	46.11	1.19	< LOD: 9.95		< LOD: 7.95		< LOD: 4.00		11.10	2.66	< LOD: 3.63		351.20	28.63	20.84	6.81	17.78	8.90	< LOD: 25.82		< LOD: 77.94		38777.70	228.56	307.02	38.51
328	51.32	1.30	< LOD: 12.04		< LOD: 5.97		< LOD: 2.04		6.73	2.53	< LOD: 2.66		< LOD: 33.37		22.95	6.02	33.02	9.57	< LOD: 27.30		< LOD: 79.80		37371.64	233.55	198.73	38.74
328,5	37.19	1.08	< LOD: 9.61		12.34	5.30	< LOD: 5.95		10.04	2.79	7.05	2.57	906.81	36.44	< LOD: 11.83		< LOD: 14.10		< LOD: 25.75		92.59	52.02	38081.00	223.93	120.09	34.60
330	18.06	1.00	< LOD: 14.38		< LOD: 4.04		< LOD: 1.99		< LOD: 3.14		< LOD: 2.03		< LOD: 28.02		< LOD: 6.10		< LOD: 10.94		< LOD: 22.93		< LOD: 30.53		4235.12	74.83	< LOD: 43.73	
330,5	33.77	1.05	< LOD: 15.92		< LOD: 7.81		< LOD: 2.49		15.80	2.82	< LOD: 3.58		263.46	27.42	13.53	6.48	24.66	9.08	< LOD: 26.03		< LOD: 82.35		30441.35	203.02	88.68	35.59
331	24.45	1.00	< LOD: 9.90		< LOD: 4.78		< LOD: 1.91		6.75	2.43	< LOD: 2.44		< LOD: 30.99		11.43	5.43	< LOD: 16.55		< LOD: 25.61		< LOD: 69.56		28699.18	197.12	65.45	35.47
331,5	11.48	1.00	< LOD: 14.92		32.77	6.44	< LOD: 13.84		9.22	2.40	< LOD: 2.35		1356.19	43.45	< LOD: 20.09		< LOD: 13.85		< LOD: 26.03		< LOD: 63.17		21103.96	168.29	407.41	42.25
332	45.21	1.22	< LOD: 11.08		< LOD: 4.68		< LOD: 1.96		11.51	2.89	6.12	2.58	< LOD: 32.52		18.53	5.91	38.17	9.63	< LOD: 26.83		< LOD: 75.62		33145.95	216.72	123.91	37.28
332,5	24.67	1.00	< LOD: 9.38		39.00	6.73	< LOD: 17.04		9.64	2.28	< LOD: 2.28		1901.04	47.07	< LOD: 14.51		< LOD: 12.36		< LOD: 25.04		125.33	45.20	27611.42	184.93	< LOD: 48.73	
333	12.75	1.00	< LOD: 9.38		< LOD: 4.35		< LOD: 1.61		7.30	2.29	< LOD: 2.11		< LOD: 29.71		< LOD: 6.83		< LOD: 11.67		< LOD: 24.41		< LOD: 50.72		14421.25	135.98	< LOD: 49.91	
333,5	5.79	1.00	< LOD: 9.24		54.35	7.14	< LOD: 21.62		8.22	2.20	< LOD: 2.12		2451.09	49.92	< LOD: 14.08		< LOD: 11.57		< LOD: 23.38		114.23	25.24	6095.29	85.66	< LOD: 40.57	
334	24.04	1.00	< LOD: 10.62		< LOD: 4.80		< LOD: 1.93		12.71	3.10	13.41	2.71	< LOD: 31.82		11.15	5.54	< LOD: 12.36		< LOD: 26.14		< LOD: 71.68		29715.68	201.37	< LOD: 49.49	
334,5	8.93	1.00	< LOD: 7.87		58.55	7.37	< LOD: 24.66		10.33	2.56	< LOD: 3.49		2546.56	51.29	< LOD: 14.45		< LOD: 11.76		< LOD: 24.08		122.10	28.25	8379.78	99.94	< LOD: 44.19	
335	49.51	1.23	< LOD: 10.84		< LOD: 4.56		< LOD: 1.87		8.99	2.64	< LOD: 3.62		< LOD: 30.90		19.33	5.65	< LOD: 16.90		< LOD: 25.64		< LOD: 70.32		30155.67	200.64	< LOD: 51.66	
335,5	41.60	1.13	< LOD: 9.44		< LOD: 8.98		< LOD: 2.12		9.65	2.53	< LOD: 3.52		208.63	26.11	23.87	6.43	< LOD: 11.78		< LOD: 24.85		< LOD: 70.31		30898.56	200.02	< LOD: 59.73	
330	50.67	1.28	< LOD: 10.05		< LOD: 4.77		< LOD: 1.98		9.84	2.66	< LOD: 3.98		< LOD: 32.14		25.77	6.00	< LOD: 12.57		< LOD: 27.47		< LOD: 77.58		35435.49	223.84	< LOD: 52.89	
336,5	46.08	1.22	< LOD: 9.84		< LOD: 5.21		< LOD: 2.21		9.03	2.76	5.42	2.55	103.31	24.63	23.78	6.30	27.42	9.21	< LOD: 26.83		< LOD: 80.71		38651.37	232.07	< LOD: 56.52	
336,5	49.95	1.29	< LOD: 10.09		< LOD: 4.95		< LOD: 2.05		26.36	3.66	18.42	3.04	< LOD: 33.09		21.35	5.99	17.96	9.24	< LOD: 27.70		< LOD: 91.30		52152.82	280.73	166.91	37.27
337	49.63	1.26	< LOD: 12.54		< LOD: 4.78		< LOD: 1.94		14.98	2.99	8.00	2.59	< LOD: 31.42		18.48	5.71	13.98	8.87	< LOD: 26.37		< LOD: 71.32		29226.27	200.51	< LOD: 51.18	
337,5	46.36	1.29	< LOD: 10.44		< LOD: 5.36		< LOD: 2.32		9.79	2.70	< LOD: 2.94		< LOD: 41.13		23.05	6.30	< LOD: 13.22		< LOD: 33.77		< LOD: 101.44		64613.36	327.81	404.82	42.22
338	49.64	1.30	< LOD: 11.87		< LOD: 5.07		< LOD: 2.17		12.26	3.21	12.33	2.92	< LOD: 33.67		24.12	6.16	22.38	9.48	< LOD: 39.59		< LOD: 91.44		51238.02	280.76	55.40	35.66

Current depth (m)	Cr	Cr Error	V	V Error	Ti	Ti Error	Ca	Ca Error	K	K Error	Al	Al Error	P	P Error	Si	Si Error	Cl	Cl Error	S	S Error	Mg	Mg Error
230,4	354.34	37.80	303.23	39.50	3253.42	82.61	32556.67	561.55	14435.46	275.97	80529.41	1236.84	4726.96	183.30	158373.02	898.95	4320.11	67.69	2594.07	93.02	5371.75	2378.82
231,3	519.96	42.32	657.54	45.01	1894.14	80.67	75493.24	832.11	4176.21	176.17	36973.11	1112.47	2635.03	186.78	162767.89	988.60	4215.30	73.47	558.80	80.49	9664.41	3182.79
232,4	200.44	28.72	291.30	28.30	1686.45	54.58	30794.66	465.30	4174.89	138.62	23775.04	676.45	< LOD: 235.73		298691.97	1092.37	2031.02	46.85	901.84	63.82	5222.36	1782.94
232,7	< LOD: 85.17		122.48	41.49	< LOD: 124.03		225303.61	1117.08	4577.17	133.06	18211.48	1380.22	93008.95	654.64	95976.29	899.28	3093.20	83.88	5872.46	184.95	< LOD: 10975.89	
233	43.33	14.18	68.41	16.43	3594.98	41.66	2952.01	109.89	8455.83	116.02	48593.71	626.74	< LOD: 2224.86		359234.50	1182.57	1237.53	34.81	< LOD: 234.23		4226.22	1100.84
233,4	224.87	35.48	87.28	25.60	< LOD: 111.95		276760.78	1410.23	886.31	126.05	23904.86	1888.42	< LOD: 325.86		39891.29	700.26	1307.24	77.60	90808.25	588.18	< LOD: 8534.86	
233,7	219.63	20.90	208.36	26.70	5217.45	65.89	5103.93	192.70	19344.68	228.40	93961.14	952.83	< LOD: 194.86		223718.30	918.60	1852.55	43.87	854.28	57.40	2706.27	1300.94
238,6	346.93	41.47	224.96	40.61	2797.52	83.62	37946.41	613.51	13254.93	273.14	81985.53	1321.01	8805.09	212.85	148446.95	895.76	1210.12	47.69	1071.12	77.31	7806.10	2730.06
240,3	75.95	18.25	132.88	21.00	3861.89	51.30	9863.95	211.67	11131.41	157.36	51757.20	699.52	< LOD: 2311.67		305173.97	1093.06	3041.60	48.15	3562.50	148.66	4798.19	1300.71
240,9	131.60	18.58	177.07	23.81	5299.19	60.40	2704.31	137.69	14803.31	183.52	65037.78	739.50	< LOD: 206.94		275021.38	964.48	4714.03	55.60	4585.72	85.80	2933.67	1196.66
241	131.59	17.80	173.15	23.02	5085.59	58.26	2706.03	134.66	13812.53	174.98	63528.26	734.12	< LOD: 209.41		290552.13	992.35	2318.31	42.82	3701.13	78.79	3402.20	1202.54
241,8	< LOD: 20.64		21.62	12.14	1353.51	27.56	18849.35	234.13	2962.58	72.65	10406.93	439.78	< LOD: 249.79		390717.69	1139.51	444.63	28.68	8845.52	115.44	< LOD: 1746.37	
242,7	188.40	20.77	198.01	27.87	6128.06	70.58	1327.33	133.81	17570.33	216.42	91424.00	914.27	< LOD: 192.08		229990.86	915.73	2001.15	43.70	1009.57	57.27	3264.64	1254.50
243,2	139.39	18.83	126.14	21.93	4424.35	55.14	1451.26	106.75	9532.32	150.39	61641.77	718.26	< LOD: 2188.93		303197.22	1070.67	2958.69	45.68	3372.24	141.01	3665.71	1172.50
243,7	< LOD: 29.87		36.55	12.60	1582.62	28.51	5538.56	132.03	4692.73	87.58	38273.68	561.62	< LOD: 224.61		373005.19	1103.39	737.43	30.37	970.09	49.82	1904.21	1071.92
244	28.76	15.86	48.50	16.07	2344.41	37.57	1270.71	85.45	6157.36	110.00	35597.36	548.47	< LOD: 217.81		341925.44	1054.77	1109.88	32.94	738.69	47.68	1751.40	1071.60
245,7	< LOD: 19.65		39.06	12.28	1433.42	27.09	1694.18	82.42	5506.94	92.72	39543.30	551.94	< LOD: 222.01		380346.44	1100.03	341.42	26.70	965.51	47.95	< LOD: 1438.29	
246,2	49.80	17.35	70.68	17.67	2549.80	42.67	44797.26	397.90	7588.11	124.99	40482.79	711.37	< LOD: 223.19		287256.44	1044.39	2975.46	52.52	2546.84	81.54	2306.82	1454.32
247,2	121.80	20.11	150.85	23.03	4110.88	55.64	1593.15	120.71	12559.14	177.04	72789.09	788.17	< LOD: 206.07		283157.16	985.59	1260.92	36.76	1606.74	60.12	2884.76	1196.61
250,9	< LOD: 23.53		< LOD: 21.11		1410.26	34.45	77278.68	503.99	4958.58	100.78	11267.23	567.27	< LOD: 247.94		321265.31	1125.86	859.38	40.77	623.86	67.88	3022.72	1720.44
251,6	91.73	18.35	126.86	22.47	4943.52	57.37	1821.58	118.49	12643.13	168.53	70103.58	748.03	< LOD: 201.75		285387.41	973.13	520.60	30.68	2242.43	64.15	3446.33	1156.00
252,8	< LOD: 25.52		30.68	15.64	1910.61	35.59	24409.48	272.74	7463.34	112.39	24290.34	555.21	< LOD: 262.18		392565.84	1148.90	641.05	33.04	443.82	51.65	< LOD: 3045.63	
254,9	311.20	30.83	247.82	35.42	4732.14	80.92	21123.88	408.32	16704.09	257.51	111964.73	1266.84	4591.40	179.96	209451.66	952.63	1011.40	43.14	1471.74	73.07	6834.67	1994.62
255,8	231.35	21.36	197.75	27.66	5421.03	68.27	827.70	130.81	19595.93	232.71	100811.91	960.25	< LOD: 186.45		212570.00	887.62	772.87	35.64	156.26	45.82	3873.04	1272.10
256,1	224.84	21.83	205.72	27.36	5085.91	66.83	1562.43	142.57	17489.83	224.55	89650.84	868.55	355.23	122.35	204275.28	840.74	327.72	30.44	434.46	46.72	3306.74	1205.74
257,7	271.24	26.36	237.25	32.00	5217.53	76.22	2336.07	180.09	18337.92	256.99	100618.27	1014.99	< LOD: 183.73		203651.31	877.26	< LOD: 44.04		283.73	48.16	3915.82	1391.41
258,2	265.09	26.20	204.54	31.55	5153.60	75.25	2277.90	176.67	17748.56	250.09	100400.96	1004.57	< LOD: 178.47		202594.98	864.13	873.96	36.46	478.55	50.53	5484.51	1412.13
258,4	259.65	23.89	235.14	30.21	5569.92	73.41	1653.98	155.10	18839.45	243.40	98726.27	986.90	< LOD: 184.94		204140.25	874.92	1166.35	38.97	747.74	54.76	3628.86	1338.41
258,7	205.72	20.22	214.45	26.66	5502.40	66.23	1132.54	131.02	19072.53	223.10	87559.00	895.63	< LOD: 191.90		228942.56	914.14	376.12	32.78	1899.82	66.23	2909.04	1243.10
261,2	70.18	18.32	115.19	21.52	4133.65	52.80	2020.05	119.29	12205.53	163.70	50378.58	676.54	< LOD: 212.83		332873.56	1057.96	1274.23	36.72	4031.02	82.38	3134.48	1210.28
262,1	158.61	20.51	183.08	25.68	5256.17	63.90	1894.20	137.77	17280.81	210.25	79892.47	853.42	< LOD: 205.88		261849.28	960.58	703.21	34.45	3631.10	80.70	4579.16	1305.73
263,3	265.53	38.45	179.14	33.02	1508.21	67.71	84461.13	823.64	5269.50	179.82	22571.48	910.92	2011.98	179.99	171302.53	989.98	920.58	47.59	1584.30	91.64	4845.46	2806.94
263,4	117.97	20.86	153.02	23.79	3503.91	56.56	35681.52	412.70	10932.32	171.35	48901.27	783.46	< LOD: 222.88		284550.78	1047.20	1290.35	41.72	3024.59	85.27	2948.01	1529.24
264	105.77	25.13	121.35	28.83	1053.27	59.07	97764.77	704.11	4819.88	134.16	14933.95	735.34	< LOD: 253.69		254001.69	1089.59	2042.45	55.13	8310.70	148.12	< LOD: 5114.76	
264,2	47.52	17.51	96.08	18.57	2276.84	44.31	69375.34	503.42	8757.60	136.91	34698.20	752.71	< LOD: 230.96		270320.84	1059.90	1185.27	44.60	3600.29	99.60	< LOD: 3497.70	
265,4	174.67	19.29	155.18	24.02	5229.12	61.50	1111.08	101.84	8709.14	148.04	59406.81	704.72	< LOD: 2049.33		276042.09	1024.89	738.46	31.54	1877.40	128.46	5051.74	1171.46
266,1	75.03	20.44	98.99	20.01	1629.37	41.64	7468.88	199.51	4445.79	113.55	13327.27	427.32	< LOD: 206.45		313903.81	1001.36	3902.95	48.05	1146.68	52.72	2917.55	1169.43
266,3	47.84	16.86	113.59	18.30	2447.00	41.08	3717.26	126.05	4097.00	94.21	14048.91	419.60	< LOD: 2275.52		381100.81	1197.21	3860.77	47.40	< LOD: 197.86		2428.32	1074.98
267,8	117.89	17.91	144.08	21.85	4560.59	54.85	3682.67	143.20	11729.06	160.95	60025.98	698.08	< LOD: 2150.16		289993.03	1035.88	1800.92	38.70	2471.42	133.99	4109.79	1172.47
268,7	82.90	17.71	140.50	22.19	4823.75	56.19	2235.91	120.14	12338.90	163.17	52934.40	658.81	< LOD: 2173.72		308718.25	1083.09	819.33	32.18	2211.29	134.65	3415.66	1139.08
269,1	< LOD: 22.15		52.56	15.01	1780.30	33.57	13848.31	212.05	6067.96	103.55	20608.91	479.60	< LOD: 232.40		389138.25	1129.45	829.77	30.95	608.23	47.39	3381.48	1183.71
269,2	32.14	15.55	72.40	17.34	3133.05	42.13	4756.14	136.17	7699.84	118.40	33029.50	535.19	< LOD: 2267.88		372245.06	1182.77	1431.50	34.37	< LOD: 202.16		5467.09	1157.64
272,2	153.34	19.89	199.73	26.42	6256.02	68.50	1582.02	128.95	15483.23	197.70	71453.08	793.18	< LOD: 2107.87		281291.56	1044.64	442.10	31.51	1160.44	130.42	6549.21	1276.27
272,8	< LOD: 33.08		41.03	16.61	3129.83	41.04	9297.39	174.74	6820.96	107.23	26738.59	538.73	< LOD: 2408.35		391938.22	1275.93	2291.42	42.92	< LOD: 208.85		4042.24	1178.67
273,3	< LOD: 20.36		51.07	15.04	2948.77	37.13	2037.96	92.19	7475.44	107.55	23760.36	487.38	< LOD: 223.24		397730.59	1132.76	2818.10	43.58	794.35	49.63	3160.81	1114.04
273,8	< LOD: 32.79		26.35	16.13	1979.87	41.32	92150.93	562.64	5597.93	108.95	17766.03	651.06	< LOD: 236.38		266424.47	1087.82	669.22	42.31	361.91	70.50	< LOD: 2605.52	
274	< LOD: 36.41		32.36	14.99	2109.97	35.60	22779.92	270.74	6237.83	105.49	21105.72	508.76	< LOD: 234.31		345855.72	1093.46	1502.23	37.83	717.79	53.31	< LOD: 1842.71	
275,7	124.25	20.31	103.94	24.13	4434.54	61.70	51539.23	476.54	13004.40	180.96	52868.82	844.72	< LOD: 225.78		269687.13	1045.29	597.64	39.32	2073.87	81.51	3151.86	1653.67
278,1	47.54	15.19	77.15	15.91	2486.78	37.29	2704.94	108.65	7284.45	114.33	48632.59	607.50	< LOD: 205.55		335608.78	1044.47	429.31	27.76	1300.55	51.87	< LOD: 2356.30	
278,2	< LOD: 25.75		36.82	15.58	1821.86	34.43	1237.62	81.89	6271.53	105.93	36784.96	558.97	< LOD: 223.52		366737.06	1103.84	480.70	28.54	7809.93	103.03	< LOD: 1606.84	
282	227.81	22.54	209.55	28.68	5454.46	70.10	1635.82	152.47	20383.58	242.58	93173.98	933.76	< LOD: 189.31		218378.59	896.40	343.41	33.02	365.98	49.73	3367.99	1289.27
282	< LOD: 21.07		< LOD: 23.79		2097.34	35.85	4735.14	125.77	5717.92	96.11	18935.87	457.50	< LOD: 217.74		421484.31	1169.73	2352.66	40.18	3223.37	71.34	3611.84	1117.88
285,3	333.89	31.36	240.50	35.33	4110.02	78.95	6270.70	270.00	17552.88	281.96	97625.88	1096.07	< LOD: 185.07		183660.22	865.76	370.48	34.49	1121.54	61.84	6531.33	1665.28
287,7	84.35	19.47	96.86	22.53	4095.36	56.51	32654.45	376.16	12143.02	169.94	47533.14	757.68	< LOD: 223.71		286315.34	1050.48	579.76	37.00	2647.16	82.23	3224.06	1488.38
290,2	150.24	20.09	162.63	25.93	5737.15	66.31	4441.26	171.91	15943.20	199.87	68085.36	783.27	LOD: 2131.03		277388.38	1047.05	395.84	31.97	1516.33	134.48	4028.80	1231.20
293,1	68.27	17.38	82.02	20.85	4368.41	52.70	3410.73	136.37	11436.72	153.40	49023.83	655.23	< LOD: 211.12		327177.41	1065.70	1236.05	36.22	3291.22	75.86	3627.18	1191.82
293,3	40.73	16.70	62.75	18.34	3067.79	43.96	10481.27	198.20	8479.95	127.47	35341.43	605.82	< LOD: 243.20		365873.44	1127.12	1262.51	37.20	4672.98	89.69	2064.54	1246.17
295,16	160.55	21.10	149.62	25.65	4729.19	63.13	3272.97	160.48	13696.53	194.90	63058.84	759.70	< LOD: 201.58		250066.53	936.44	275.47	29.58	6128.44	97.45	3086.68	1250.02
296,7	101.92	18.38	134.08	22.45	4680.48	56.76	8724.75	204.24	13868.94	176.28	55531.25	694.25	LOD: 2208.09		293487.59	1065.89	686.46	32.39	3304.90	140.87	3485.23	1214.71
297,5	195.72	26.65	225.50	29.68	2574.80	69.82	147462.58	868.31	10923.42	190.74	48060.00	1199.49	< LOD: 240.15		155731.50	1005.98	< LOD: 69.81		4480.78	137.83	7225.11	3011.59
300	193.99	23.61	185.16	29.14	5419.47	71.59	1682.16	152.39	18702.01	238.83	85763.66	933.81	< LOD: 198.09		244915.06	975.80	999.53	38.69	747.88	56.54	4009.19	1372.20
300	245.78	22.91	205.67	29.67	5701.29	73.43	1388.83	152.43	20915.10	252.61	97537.97	976.73	< LOD: 189.25		229470.69	934.59	158.16	32.51	720.67	55.22	6434.05	1412.59
301	234.66	24.04	208.43	30.52	5573.08	74.63	2457.47	173.37	19188.09	247.99	97111.74	1013.40	< LOD: 191.14		223602.08	948.88	81.48	32.70	373.16	52.19	3444.28	1384.65
302	193.14	24.88	176.01	30.31	5586.38	74.74	2710.07	175.47	17159.88	235.75	92511.66	963.11	< LOD: 198.06		250184.61	979.04	157.44	31.97	672.93	53.99	5767.16	1419.31
302,5	210.98	23.93	219.76	30.30	5886.19	74.72	1795.05	156.44	19611.23	244.77	100298.50	1020.51	< LOD: 194.20		234985.64	965.23	< LOD: 46.40		480.70	53.08	4929.65	1408.08
303	211.47	21.92	203.27	28.21	5648.95	70.47	1698.89	148.82	18623.90	231.81	95336.26	951.54	< LOD: 187.14		234517.66	942.82	< LOD: 45.85		455.02	50.19	5539.10	1344.45
305	198.46	21.97	206.96	28.08	5713.44	70.06	1367.79	141.13	18733.65	229.65	96429.45	978.46	< LOD: 191.54		238278.77	962.07	< LOD: 45.04		722.76	54.94	5235.54	1366.72
305,9	200.70	20.08	182.20	25.84	4959.16	63.95	1493.13	136.86	17790.21	220.53	79763.02	819.37	< LOD: 255.57		197270.80	830.74	< LOD: 39.33		2977.10	72.42	2819.79	1172.78
306,5	213.61	21.61	208.00	27.76	5635.02	69.12	1478.26	143.08	19125.04	230.66	98977.30	947.83	< LOD: 184.12		226246.81	909.72	< LOD: 42.50		1340.41	59.98	3060.61	1249.93
304	220.65	21.78	190.57	27.61	5199.21	67.90	1779.47	149.89	17936.37	227.86	94896.77	941.24	< LOD: 178.59		218298.81	899.72	< LOD: 41.85		914.26	54.84	3814.09	1275.48
304,5	215.84	21.90	199.31	27.62	5190.73	67.79	1741.84	148.98	18504.13	230.99	91598.57	922.07	< LOD: 181.40		224591.66	908.25	< LOD: 44.37		624.60	51.06	4993.21	1310.96
305,5	225.20	20.05	204.09	26.07	5004.32	64.07	1189.25	133.53	18180.29	220.93	91469.40	909.72	< LOD: 180.03		223818.52	904.78	< LOD: 41.68		377.09	47.78	4848.74	1277.39
306	205.62	19.04	191.51	25.21	5172.66	62.84	907.36	119.63	18034.76	211.83	91853.95	871.56	< LOD: 174.02		221158.16	882.73	< LOD: 38.77		3572.47	77.17	2393.95	1140.20
307	187.07	19.43	198.32	24.81	4872.15	61.15	989.72	124.17	18110.61	214.10	86286.29	846.15	< LOD: 169.85		212503.69	865.57	< LOD: 38.93		348.76	45.09	3437.54	1157.73
308	209.30	21.90	206.80	27.80	5388.57	68.65	2536.55	160.85	18432.52	229.79	90347.68	906.38	< LOD: 183.93		227006.63	902.73	< LOD: 40.85		1211.72	57.31	5231.06	1310.60
309	208.88	21.01	209.42	26.85	5046.36	65.73	1877.19	146.15	16906.38	217.96	90691.79	884.04	< LOD: 169.26		208167.53	861.42	< LOD: 38.46		1077.78	54.04	2569.71	1168.30
310	190.37	18.41	193.73	24.38	5079.42	60.80	814.37	116.47	17919.05	206.91	90802.49	862.14	< LOD: 169.71		222145.73	879.30	< LOD: 39.40		892.82	51.35	4906.69	1184.66
310,4	231.32	23.05	209.83	29.13	5355.26	70.67	2130.33	161.05	18838.02	237.45	95130.90	964.04	< LOD: 184.79		222822.06	904.75	< LOD: 42.57		1752.67	65.28	5347.41	1366.58
311	200.73	18.77	181.04	24.36	5070.81	60.89	862.17	119.64	18690.62	212.16	95558.95	888.03	< LOD: 172.28		224446.05	886.43	< LOD: 38.45		1009.39	53.45	2828.32	1146.19
311,7	183.00	19.51	187.45	24.94	4963.66	61.65	889.90	121.52	18663.75	216.39	89544.90	840.00	< LOD: 174.44		208128.63	841.50	< LOD: 37.86		2386.16	65.53	2516.87	1115.72
312	222.80	21.85	218.21	27.05	4866.94	65.37	1504.85	145.35	18778.27	232.49	99841.59	977.82	< LOD: 180.94		221202.09	905.02	< LOD: 41.16		3138.26	77.66	4361.98	1315.20
312,5	242.54	22.90	202.96	28.62	4843.88	68.70	2945.40	178.03	17927.36	235.98	95684.24	967.92	< LOD: 181.69		214373.38	897.45	< LOD: 41.33		3222.93	78.63	3811.64	1331.01
312,5	202.26	20.76	206.05	26.44	5250.45	65.18	1618.49	141.36	19278.51	225.60	96140.94	912.14	< LOD: 189.66		223306.89	885.84	< LOD: 40.26		2190.13	66.69	3456.04	1234.20
313	188.74	19.99	181.35	25.18	4847.87	62.02	985.31	126.36	18065.93	216.42	94041.14	900.42	< LOD: 176.24		212831.86	867.41	< LOD: 37.78		8404.20	111.22	4598.03	1238.53
313,5	192.10	19.32	198.28	25.27	5514.90	63.87	1274.65	125.88	17291.70	206.46	97987.39	918.15	< LOD: 183.31		225186.17	898.01	< LOD: 39.49		2417.77	69.01	3009.75	1190.01
314	181.83	18.86	204.40	24.82	5517.82	62.89	2572.63	143.18	16736.76	199.75	97594.12	914.41	< LOD: 180.69		225161.61	895.67	< LOD: 38.80		2390.93	68.47	4273.66	1218.74
314,5	176.97	19.02	199.28	24.83	5669.31	63.27	1258.33	125.45	18503.60	208.19	90712.05	832.98	< LOD: 166.78		218060.34	857.23	< LOD: 36.42		1787.87	59.60	2498.52	1089.20
315	194.06	18.55	186.47	24.23	5188.62	61.00	2258.97	134.24	14770.09	188.01	100030.98	919.21	< LOD: 181.44		214613.45	866.45	< LOD: 37.70		8729.74	113.52	LOD: 1709.94	
315,5	191.65	18.51	202.25	24.51	5377.75	61.88	1461.96	124.38	16680.27	198.99	92161.32	872.54	< LOD: 185.92		216841.02	875.12	< LOD: 37.52		2385.94	67.57	1738.28	1124.69
315,6	193.69	21.37	191.64	26.91	5353.45	66.71	3873.98	173.52	15906.69	208.33	93584.64	919.07	< LOD: 184.25		216728.63	881.32	< LOD: 38.65		1255.23	57.45	5875.45	1310.70
316	195.56	19.07	213.65	24.97	5490.62	62.99	1884.02	133.59	16546.42	200.25	92351.84	877.31	< LOD: 185.69		212314.00	861.90	< LOD: 37.62		3903.95	80.49	2141.89	1150.00
316	166.61	18.15	193.91	24.05	5512.63	61.30	1980.79	127.05	15218.38	185.89	95249.34	850.61	< LOD: 167.65		215160.30	846.55	< LOD: 35.27		1618.66	56.88	4311.29	1119.32
316,6	186.99	20.12	187.33	26.23	5670.07	66.44	3755.84	163.59	14331.47	192.93	97844.23	899.34	< LOD: 179.89		213273.38	858.83	< LOD: 37.29		1597.09	58.96	3578.85	1180.72
317	205.53	20.30	219.90	26.18	5351.83	65.00	1820.04	140.91	18268.19	218.62	99462.98	946.66	< LOD: 190.28		217271.91	880.97	< LOD: 39.38		7942.37	110.75	4109.26	1277.13
317	196.62	19.93	195.26	26.00	5424.05	64.88	2617.33	151.25	18019.78	213.60	101564.16	955.02	< LOD: 186.41		219958.20	889.59	< LOD: 39.85		7513.34	109.00	LOD: 1788.21	
317,6	196.41	19.03	216.10	24.27	4836.40	59.38	1272.46	126.20	19142.23	214.36	96488.91	891.06	< LOD: 177.88		209443.94	838.98	< LOD: 37.57		9363.50	115.21	2868.62	1169.36
317,7	211.09	21.81	207.93	26.71	4607.11	63.86	2193.62	156.07	18925.92	231.89	94357.06	957.04	< LOD: 200.73		202185.95	847.89	< LOD: 40.93		23794.31	193.97	2179.45	1341.00
317,9	222.20	22.40	231.59	27.08	4236.56	63.22	3195.44	172.18	17042.70	226.41	91109.56	983.95	< LOD: 203.12		197014.34	847.16	< LOD: 43.54		33112.16	237.95	2824.57	1433.18
318	187.72	30.60	140.57	25.78	1396.90	52.56	49904.61	600.19	6373.28	173.02	32884.34	1085.53	< LOD: 295.83		228556.56	1002.87	< LOD: 70.74		90175.61	498.05	4016.04	2665.72
318	185.67	32.66	117.39	31.84	1608.73	65.06	52729.52	634.55	7228.18	187.77	44598.55	1266.45	< LOD: 299.71		188277.47	950.71	< LOD: 62.39		103607.11	553.53	7337.08	3026.04
318,1	81.22	18.87	84.45	21.30	3628.03	53.65	56197.87	467.97	8136.35	137.50	36238.32	704.69	< LOD: 219.38		258910.22	1006.53	< LOD: 44.58		< LOD: 81.18		5579.61	1629.63
318,3	79.47	21.26	96.57	20.44	2336.93	48.29	63571.19	527.41	7353.46	141.95	37617.54	793.85	LOD: 2508.38		264967.91	1111.30	92.12	34.93	6500.43	186.41	8347.25	1866.96
318,4	99.26	18.57	122.54	20.99	3516.91	50.51	15337.77	261.26	13185.13	172.91	61419.04	778.98	< LOD: 212.83		272474.44	977.97	< LOD: 41.35		14839.70	152.98	LOD: 1928.73	
318,6	65.20	18.61	84.31	26.81	2814.47	57.10	14734.21	242.99	10400.60	147.69	49317.21	719.12	LOD: 2480.46		317512.59	1136.30	< LOD: 41.65		12622.54	192.32	5933.70	1417.68
318,8	109.40	19.93	96.98	23.81	4656.26	62.01	54671.23	482.25	9668.47	155.28	47188.47	821.52	LOD: 2401.58		248875.05	1062.40	< LOD: 47.84		4589.80	170.10	10102.15	1805.80
318,9	109.23	18.10	129.94	21.92	4401.88	55.71	36952.59	378.52	13440.55	169.49	62018.06	844.67	< LOD: 208.73		254196.55	1002.78	< LOD: 44.73		136.63	53.06	5664.28	1530.99
319	101.33	19.35	117.07	24.07	5052.64	62.25	40825.68	411.08	13020.27	173.21	57409.98	813.96	< LOD: 211.46		271552.81	1020.10	< LOD: 43.01		147.58	53.33	5293.53	1539.52
319,4	62.75	17.92	74.32	21.16	4153.50	54.19	44009.53	400.95	8475.84	133.76	42644.32	734.86	LOD: 2342.05		288202.38	1121.02	< LOD: 43.89		< LOD: 202.11		7975.87	1574.72

319,7	118.56	18.19	145.57	23.88	5618.43	62.36	23612.09	311.84	14481.14	177.53	65752.62	796.84	< LOD: 208.43		275106.44	993.72	< LOD: 47.03		299.72	50.47	4193.45	1353.70
320	90.78	19.91	93.49	23.21	4156.46	59.05	54065.39	476.80	10524.43	159.57	50639.34	827.52	< LOD: 223.12		261750.98	1038.89	< LOD: 48.62		112.03	56.94	6835.29	1731.77
320	71.69	20.11	90.72	23.69	4518.63	60.89	48368.92	454.38	10046.89	156.87	47589.50	784.65	LOD: 2308.21		265144.91	1082.40	< LOD: 49.04		< LOD: 201.34		7463.19	1619.82
320,1	184.22	19.10	193.34	25.72	5969.07	66.21	9350.28	223.75	17721.19	205.23	88984.00	886.61	< LOD: 178.11		208183.92	870.85	< LOD: 38.69		1280.86	58.80	4489.02	1247.90
320,3	88.81	19.21	91.90	22.75	3743.08	55.55	39122.57	401.66	10045.31	152.92	43743.09	741.93	< LOD: 223.58		280707.88	1048.73	< LOD: 45.54		173.45	53.97	5051.72	1551.74
321	95.86	17.94	150.55	22.82	4846.66	57.12	14003.67	241.73	14172.90	171.53	65491.11	751.09	< LOD: 208.20		278406.41	982.41	164.07	29.44	267.49	46.60	4095.39	1249.63
321	53.53	17.47	88.27	21.82	3895.31	52.63	16957.77	257.55	11079.96	149.37	64549.88	744.53	< LOD: 200.93		294494.13	1011.49	< LOD: 38.27		263.00	45.85	4934.38	1252.37
321,4	73.04	19.12	92.32	20.86	3106.99	50.80	47775.48	441.39	8669.26	143.90	41798.48	721.07	< LOD: 209.13		255788.23	997.26	110.23	31.62	134.29	52.75	5628.46	1556.75
321,9	110.72	20.55	90.04	22.13	3225.40	53.64	47046.79	452.03	9461.51	155.09	42896.89	749.19	< LOD: 212.34		258995.17	1012.30	61.48	32.13	89.63	53.59	4830.34	1592.47
322,1	108.41	17.99	117.53	22.48	5107.39	58.75	17921.70	276.68	11534.35	159.34	63217.32	757.72	LOD: 2173.32		283907.06	1060.47	< LOD: 38.83		< LOD: 185.16		4907.59	1280.79
322,1	122.19	19.85	142.67	23.99	5009.32	60.69	11152.92	235.73	13380.73	179.46	62907.96	778.44	< LOD: 217.01		278308.19	1003.52	< LOD: 41.80		162.30	46.18	5031.31	1348.72
322,6	130.63	18.67	167.40	25.19	6567.52	67.14	11822.18	232.08	11608.23	162.19	78081.53	816.89	< LOD: 192.64		253071.59	942.42	< LOD: 38.01		134.83	43.33	2481.19	1183.02
323	104.52	18.72	116.62	23.55	5518.42	62.04	23946.13	315.40	9944.42	150.39	59154.16	753.78	< LOD: 198.46		267293.59	975.88	< LOD: 40.42		188.77	46.57	4304.16	1315.53
323	89.06	19.76	103.15	23.76	5000.40	61.58	26382.53	342.29	9540.98	152.92	56522.83	767.81	< LOD: 204.20		275313.31	1015.10	< LOD: 41.17		150.10	47.77	6264.69	1434.83
323,6	100.41	17.97	119.40	22.23	4899.10	57.33	15872.14	256.58	10706.93	152.45	55096.22	712.66	LOD: 2244.82		299926.56	1092.17	< LOD: 38.39		534.16	133.40	5056.94	1279.13
324	140.81	19.65	149.52	25.53	5941.94	66.45	6411.37	192.57	14086.20	186.26	75557.32	800.23	< LOD: 178.01		245518.11	934.37	< LOD: 37.71		244.73	44.44	3307.07	1171.36
324	80.04	18.93	97.53	22.63	4613.84	57.84	29820.41	350.54	10497.56	154.36	49919.28	726.59	< LOD: 209.26		270027.75	991.75	< LOD: 42.35		165.58	49.77	4897.04	1410.41
324,5	87.77	19.56	112.62	23.13	4535.21	58.80	39106.87	401.03	9907.43	151.62	52724.81	778.63	LOD: 2246.99		267019.53	1057.25	< LOD: 42.92		< LOD: 193.79		8392.58	1549.28
325	57.14	18.81	81.48	20.87	3670.95	52.51	42460.20	409.51	8299.68	137.59	43700.48	710.53	LOD: 2205.54		265677.94	1048.00	< LOD: 42.79		< LOD: 190.89		7462.94	1489.61
325	91.91	19.15	108.11	23.09	4697.32	58.90	31866.90	362.43	11873.94	163.54	65678.68	827.34	< LOD: 203.71		268246.28	1000.23	< LOD: 42.99		216.75	50.61	7380.99	1492.46
325,5	73.41	18.01	91.10	20.22	3821.52	51.19	35809.84	367.22	8840.58	137.55	46291.34	724.78	< LOD: 207.23		266896.41	1006.35	< LOD: 41.98		187.63	50.44	6368.87	1477.45
326	35.99	13.47	94.95	19.39	7185.34	57.10	158.12	68.43	12678.66	137.13	60842.96	678.35	< LOD: 207.75		351084.28	1068.17	< LOD: 34.82		301.24	41.86	2723.66	1072.19
326	148.62	20.62	169.50	26.73	6171.91	69.17	9543.75	229.04	15154.37	195.27	73363.93	820.62	< LOD: 192.81		259608.92	970.53	< LOD: 40.00		264.41	46.97	4198.22	1286.67
326,5	128.64	20.59	156.99	26.85	6160.45	69.50	9651.23	229.79	12508.94	180.28	65368.91	773.97	< LOD: 198.58		266521.25	964.94	< LOD: 38.29		286.93	45.56	4082.10	1275.67
327	143.29	21.31	119.39	27.15	6118.37	71.00	11370.71	252.11	11951.69	180.73	64645.08	806.13	LOD: 2158.09		267464.69	1049.73	< LOD: 40.17		< LOD: 184.60		5843.47	1352.29
327,5	174.34	20.18	179.16	27.60	6651.64	71.96	11651.36	250.54	17023.65	207.08	83454.81	878.61	< LOD: 195.79		240901.38	925.34	< LOD: 39.18		793.94	54.36	3355.25	1293.84
328	190.58	19.70	169.40	26.48	6220.84	68.91	7574.39	212.44	17734.55	209.73	93130.94	903.47	< LOD: 184.14		223914.03	899.25	< LOD: 38.19		339.12	47.48	4407.27	1260.65
328,5	179.66	19.49	160.36	25.61	5850.42	66.16	7692.96	208.61	14116.79	187.75	81912.17	857.59	< LOD: 237.16		242877.20	923.78	< LOD: 37.55		777.94	52.29	4986.42	1296.21
330	< LOD: 17.40		< LOD: 23.03		4911.23	44.45	< LOD: 76.03		7056.75	95.90	51520.48	606.24	< LOD: 200.26		364850.31	1106.29	< LOD: 32.72		890.69	46.77	1810.28	978.72
330,5	148.31	18.03	172.34	24.81	6347.25	65.66	5189.25	166.27	12594.93	168.41	72666.48	746.89	< LOD: 180.87		234895.08	890.88	< LOD: 35.69		1167.24	52.33	3642.24	1112.83
331	108.20	17.87	110.65	22.31	5313.15	58.42	5475.66	161.91	10347.43	148.99	57889.95	696.69	LOD: 1990.17		279989.91	1033.54	< LOD: 36.30		< LOD: 172.92		6823.97	1183.95
331,5	53.45	16.17	68.61	17.86	3383.90	44.72	11302.88	203.42	5798.08	107.41	29987.08	528.81	LOD: 2259.24		348861.09	1164.79	< LOD: 34.83		< LOD: 190.02		3589.34	1159.43
332	166.00	19.32	178.70	27.43	7604.36	74.50	5489.32	180.94	15041.72	190.07	85204.07	872.38	< LOD: 187.47		241755.92	939.99	< LOD: 38.38		1088.27	55.96	5917.17	1287.71
332,5	87.75	17.95	126.29	23.36	6119.17	62.46	5643.18	163.87	9900.28	146.85	55152.52	660.39	< LOD: 194.56		283600.28	960.86	< LOD: 34.39		435.41	44.14	2280.86	1094.38
333	27.77	14.21	36.76	14.71	2656.15	36.43	3248.80	112.64	7093.06	109.45	48713.27	585.09	< LOD: 191.08		333832.50	1049.85	< LOD: 31.57		671.00	43.32	3371.51	1015.62
333,5	< LOD: 18.07		< LOD: 20.57		1179.95	22.71	336.83	47.32	4014.44	74.03	11557.53	391.13	< LOD: 245.43		433653.84	1181.49	< LOD: 31.97		708.89	44.08	LOD: 2305.93	
334	88.55	18.37	95.80	22.84	5482.19	60.26	624.91	89.69	10196.83	151.80	52724.24	683.69	LOD: 2210.55		287787.00	1053.95	715.96	32.01	10492.19	171.21	4727.05	1206.79
334,5	< LOD: 19.38		< LOD: 25.99		820.19	22.98	1245.36	72.79	6363.91	96.35	15807.80	429.23	< LOD: 247.63		434808.16	1174.05	50.18	23.72	2976.91	67.52	LOD: 2331.18	
335	184.65	18.21	205.59	27.43	8060.43	74.90	2209.57	135.16	16593.27	194.50	104797.68	941.91	< LOD: 179.51		214770.48	878.86	< LOD: 37.86		402.51	46.82	4204.74	1191.31
335,5	143.22	17.66	186.84	24.83	6457.18	65.63	2327.69	129.07	14897.49	182.30	83862.12	770.08	< LOD: 163.88		201205.00	803.51	< LOD: 33.48		574.64	44.12	4228.40	1064.95
330	189.92	18.92	193.54	27.51	7506.52	73.98	2257.52	140.43	16969.36	201.88	101606.53	898.32	< LOD: 173.86		213649.75	859.16	< LOD: 35.66		317.13	44.16	2831.62	1124.63
336,5	181.75	19.39	207.33	26.89	6769.80	70.56	1910.21	132.34	15938.45	198.03	93999.67	856.57	< LOD: 167.77		199516.70	824.45	< LOD: 34.84		966.43	50.90	2357.56	1085.87
336,5	235.83	21.60	217.68	30.47	7045.84	78.27	2631.25	161.90	17196.27	221.66	104796.40	970.39	< LOD: 173.10		185732.02	817.92	< LOD: 37.14		3173.45	75.52	3687.09	1245.03
337	187.59	17.49	205.34	26.74	8069.85	73.56	1612.86	121.95	15906.74	185.91	99901.38	872.81	< LOD: 164.96		203783.50	840.06	< LOD: 35.04		706.86	48.07	1629.56	1037.48
337,5	270.03	23.60	236.39	33.18	7718.93	86.06	3644.33	186.86	15603.79	225.04	107576.82	1029.03	< LOD: 171.80		186198.48	842.09	< LOD: 38.78		238.79	46.37	3101.08	1293.69
338	223.89	21.60	214.63	31.19	7936.20	82.44	1254.03	135.80	16793.28	218.85	101258.98	947.11	< LOD: 175.44		191389.03	834.60	< LOD: 36.69		835.04	52.26	2281.27	1186.41

Tidigare skrifter i serien ”Examensarbeten i Geologi vid Lunds universitet”:

551. Ahrenstedt, Viktor, 2018: The Neoproterozoic Visingsö Group of southern Sweden: Lithology, sequence stratigraphy and provenance of the Middle Formation. (45 hp)
552. Berglund, Marie, 2018: Basaltkuppen - ett spel om mineralogi och petrologi. (15 hp)
553. Hernnäs, Tove, 2018: Garnet amphibolite in the internal Eastern Segment, Sveconorwegian Province: monitors of metamorphic recrystallization at high temperature and pressure during Sveconorwegian orogeny. (45 hp)
554. Halling, Jenny, 2019: Characterization of black rust in reinforced concrete structures: analyses of field samples from southern Sweden. (45 hp)
555. Stevic, Marijana, 2019: Stratigraphy and dating of a lake sediment record from Lyngsjön, eastern Scania - human impact and aeolian sand deposition during the last millennium. (45 hp)
556. Rabanser, Monika, 2019: Processes of Lateral Moraine Formation at a Debris-covered Glacier, Suldenferner (Vedretta di Solda), Italy. (45 hp)
557. Nilsson, Hanna, 2019: Records of environmental change and sedimentation processes over the last century in a Baltic coastal inlet. (45 hp)
558. Ingered, Mimmi, 2019: Zircon U-Pb constraints on the timing of Sveconorwegian migmatite formation in the Western and Median Segments of the Idefjorden terrane, SW Sweden. (45 hp)
559. Hjorth, Ingeborg, 2019: Paleomagnetisk undersökning av vulkanen Rangitoto, Nya Zeeland, för att bestämma dess utbrottshistoria. (15 hp)
560. Westberg, Märta, 2019: Enigmatic worm-like fossils from the Silurian Waukesha Lagerstätte, Wisconsin, USA. (15 hp)
561. Björn, Julia, 2019: Undersökning av påverkan på hydraulisk konduktivitet i förorenat område efter in situ-saneringsförsök. (15 hp)
562. Faraj, Haider, 2019: Tolkning av georadarprofiler över grundvattenmagasinet Verveln - Gullringen i Kalmar län. (15 hp)
563. Bjermo, Tim, 2019: Eoliska avlagringar och vindriktningar under holocen i och kring Store Mosse, södra Sverige. (15 hp)
564. Langkjaer, Henrik, 2019: Analys av Östergötlands kommande grundvattenresurser ur ett klimtperspektiv - med fokus på förstärkt grundvattenbildning. (15 hp)
565. Johansson, Marcus, 2019: Hur öppet var landskapet i södra Sverige under Atlantisk tid? (15 hp)
566. Molin, Emmy, 2019: Litologi, sedimentologi och kolisotopstratigrafi över krita–paleogen-gränsintervallet i borrningen Limhamn-2018. (15 hp)
567. Schroeder, Mimmi, 2019: The history of European hemp cultivation. (15 hp)
568. Damber, Maja, 2019: Granens invandring i sydvästa Sverige, belyst genom pollenanalys från Skottenesjön. (15 hp)
569. Lundgren Sassner, Lykke, 2019: Strandmorfologi, stranderosion och stranddeposition, med en fallstudie på Tylösand sandstrand, Halland. (15 hp)
570. Greiff, Johannes, 2019: Mesozoiska konglomerat och Skånes tektoniska utveckling. (15 hp)
571. Persson, Eric, 2019: An Enigmatic Cerapodian Dentary from the Cretaceous of southern Sweden. (15 hp)
572. Aldenius, Erik, 2019: Subsurface characterization of the Lund Sandstone – 3D model of the sandstone reservoir and evaluation of the geoenergy storage potential, SW Skåne, South Sweden. (45 hp)
573. Juliusson, Oscar, 2019: Impacts of subglacial processes on underlying bedrock. (15 hp)
574. Sartell, Anna, 2019: Metamorphic paragenesis and P-T conditions in garnet amphibolite from the Median Segment of the Idefjorden Terrane, Lilla Edet. (15 hp)
575. Végvári, Fanni, 2019: Vulkanisk inverkan på klimatet och atmorsfärcirkulationen: En litterarurstudie som jämför vulkanism på låg respektive hög latitud. (15 hp)
576. Gustafsson, Jon, 2019: Petrology of platinum-group element mineralization in the Koillismaa intrusion, Finland. (45 hp)
577. Wahlquist, Per, 2019: Undersökning av mindre förkastningar för vattenuttag i sedimentärt berg kring Kingelstad och Tjutebro. (15 hp)
578. Gaitan Valencia, Camilo Esteban, 2019: Unravelling the timing and distribution of Paleoproterozoic dyke swarms in the eastern Kaapvaal Craton, South Africa. (45 hp)
579. Eggert, David, 2019: Using Very-Low-Frequency Electromagnetics (VLF-EM) for geophysical exploration at the Albertine Graben, Uganda - A new CAD approach for 3D data blending. (45 hp)
580. Plan, Anders, 2020: Resolving temporal links between the Högberget granite and the Wigström tungsten skarn deposit in Bergslagen (Sweden) using trace elements and U-Pb LA-ICPMS on complex zircons.

(45 hp)

581. Pilser, Hannes, 2020: A geophysical survey in the Chocaya Basin in the central Valley of Cochabamba, Bolivia, using ERT and TEM. (45 hp)
582. Leopardi, Dino, 2020: Temporal and genetical constraints of the Cu-Co Vena-Dampetorp deposit, Bergslagen, Sweden. (45 hp)
583. Lagerstam Lorien, Clarence, 2020: Neck mobility versus mode of locomotion – in what way did neck length affect swimming performance among Mesozoic plesiosaurs (Reptilia, Sauropterygia)? (45 hp)
584. Davies, James, 2020: Geochronology of gneisses adjacent to the Mylonite Zone in southwestern Sweden: evidence of a tectonic window? (45 hp)
585. Foyn, Alex, 2020: Foreland evolution of Blåisen, Norway, over the course of an ablation season. (45 hp)
586. van Wees, Roos, 2020: Combining luminescence dating and sedimentary analysis to derive the landscape dynamics of the Velická Valley in the High Tatra Mountains, Slovakia. (45 hp)
587. Rettig, Lukas, 2020: Implications of a rapidly thinning ice-margin for annual moraine formation at Gornergletscher, Switzerland. (45 hp)
588. Bejarano Arias, Ingrid, 2020: Determination of depositional environment and luminescence dating of Pleistocene deposits in the Biely Váh valley, southern foothills of the Tatra Mountains, Slovakia. (45 hp)
589. Olla, Daniel, 2020: Petrografisk beskrivning av Prekambriska ortognejser i den undre delen av Särvskollan, mellersta delen av Skollenheten, Kaledonska orogenen. (15 hp)
590. Friberg, Nils, 2020: Är den sydatlantiska magnetiska anomalin ett återkommande fenomen? (15 hp)
591. Brakebusch, Linus, 2020: Klimat och väder i Nordatlanten-regionen under det senaste årtusendet. (15 hp)
592. Boestam, Max, 2020: Stränder med erosion och ackumulation längs kuststräckan Trelleborg - Abbekås under perioden 2007-2018. (15 hp)
593. Agudelo Motta, Laura Catalina, 2020: Methods for rockfall risk assessment and estimation of runout zones: A case study in Gothenburg, SW Sweden. (45 hp)
594. Johansson, Jonna, 2020: Potentiella nedslagskratrar i Sverige med fokus på Östersjön och östkusten. (15 hp)
595. Haag, Vendela, 2020: Studying magmatic systems through chemical analyses on clinopyroxene - a look into the history of the Teno ankaramites, Tenerife. (45 hp)
596. Kryffin, Isidora, 2020: Kan benceller bevaras över miljontals år? (15 hp)
597. Halvarsson, Ellinor, 2020: Sökande efter nedslagskratrar i Sverige, med fokus på avtryck i berggrunden. (15 hp)
598. Jirdén, Elin, 2020: Kustprocesser i Arktis – med en fallstudie på Prins Karls Forland, Svalbard. (15 hp)
599. Chonewicz, Julia, 2020: The Eemian Baltic Sea hydrography and paleoenvironment based on foraminiferal geochemistry. (45 hp)
600. Paradeisis-Stathis, Savvas, 2020: Holocene lake-level changes in the Siljan Lake District – Towards validation of von Post's drainage scenario. (45 hp)
601. Johansson, Adam, 2020: Groundwater flow modelling to address hydrogeological response of a contaminated site to remediation measures at Hjortsberga, southern Sweden. (15 hp)
602. Barrett, Aodhan, 2020: Major and trace element geochemical analysis of norites in the Hakefjorden Complex to constrain magma source and magma plumbing systems. (45 hp)
603. Lundqvist, Jennie, 2020: "Man fyller det med information helt enkelt": en fenomenografisk studie om studenters upplevelse av geologisk tid. (45 hp)
604. Zachén, Gabriel, 2020: Classification of four mesosiderites and implications for their formation. (45 hp)
605. Viðarsdóttir, Halla Margrét, 2020: Assessing the biodiversity crisis whitin the Triassic-Jurassic boundary interval using redox sensitive trace metals and stable carbon isotope geochemistry. (45 hp)

LUNDS UNIVERSITET

Geologiska institutionen
Lunds universitet
Sölvegatan 12, 223 62 Lund